

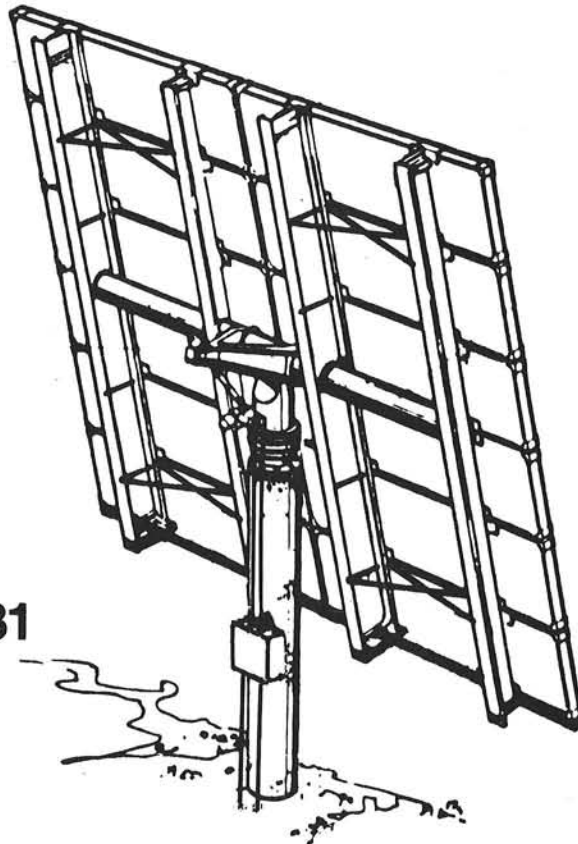
**UNLIMITED RELEASE**

*When printing a copy of any digitized SAND  
Report, you are required to update the  
markings to current standards.*

Final Report

# **Second Generation Heliostat Development**

for SOLAR CENTRAL RECEIVERS



**March 31, 1981**

**Detail Design Report  
Volume I - Appendices II**

**SAND 81-8175**

**FINAL REPORT  
SECOND GENERATION HELIOSTAT DEVELOPMENT  
FOR SOLAR CENTRAL RECEIVERS**

**VOLUME I  
DETAIL DESIGN REPORT**

**(APPENDIX II)**

**MARCH 31, 1981**

**BOEING ENGINEERING & CONSTRUCTION  
(A Division of The Boeing Company)  
P.O. Box 3707  
SEATTLE, WASHINGTON 98124**

**PREPARED FOR  
SANDIA NATIONAL LABORATORIES  
LIVERMORE, CALIFORNIA  
UNDER CONTRACT 83-2729C**

## ABSTRACT

Trade Studies, Design Analysis, and Test Procedures prepared by Ford Aerospace and Communications Corporation for Boeing Engineering and Construction Company, submitted during period 24 July through 24 October, 1980.

## TABLE OF CONTENTS

Report E-1	Azimuth Drive Trade Studies and Design Analysis
Report E-2	Elevation Drive Trade Studies
Report E-3	Elevation Actuator Trade Studies
Report E-4	Cost Trade-Plastic vs. Bronze Nut for Elevation Actuator
Report E-5	Gimbal Housing and Torque-Tube/Arms Assembly Structural Analysis
Report E-6	Elevation Drive Design Analysis
Report E-7	Elevation Bearing Design Analysis
Report E-8	Pointing Error Analysis
Report E-9	Combined Structural Compliances
Report E-10	Actuator Screw/Nut Test Procedures
Report E-11	Azimuth Drive/Bearing Test Procedures
Report E-12	Gimbal/Actuator Drive Assembly Test Procedures
Report E-13	Drive Motor Trade Studies
Report E-14	Electrical Drive Control Configuration
Report E-15	Sensor Selection
Report E-16	Hall Effect Sensor Evaluation





REPORT E-1

AZIMUTH DRIVE TRADE STUDIES AND DESIGN ANALYSIS

FOR

GIMBAL/ACTUATOR DRIVE ASSEMBLY

FOR

BOEING SECOND GENERATION HELIOSTAT

JUNE 27, 1980

Reference: FACC TM21



**Ford Aerospace &  
Communications Corporation**

## TABLE OF CONTENTS

## Section

- 1.0 Introduction
- 2.0 Conclusion
- 3.0 Discussion of Three Designs
  - 3.1 Worm Gear Actuator Per Drawing 1133-104
  - 3.2 Planetary Actuator Per Drawing 1133-102
  - 3.3 Differential Planetary Per Drawing 1133-102
- 4.0 Drawings of Three Designs
  - 4.1 E-1133-104
  - 4.2 E-1133-103
  - 4.3 E-1133-102
- 5.0 Calculations

Data prepared by Winsmith, "Evaluation of Azimuth Drive", with Ford Aerospace & Communications Corporation.

## 1.0 INTRODUCTION

Three different types of rotary drive and bearing assemblies are investigated. These drives are designed and sized to meet load and life requirements for an azimuth actuation system for the second generation heliostat program as defined in Document WDL-SW-528522 of Ford Aerospace and Communication Division.

The general arrangements of these actuators are shown on Drawings E-1133-104, E-1133-103, and E-1133-102.

A structural analysis of the actuator per E-1133-102 is included in this report. The other two actuator types are only briefly examined although they are sized to meet applicable load-life specifications.

## 2.0 CONCLUSIONS

The actuator design considered the most suitable for the applications is the one shown on Drawing E-1133-102. It consists of a small worm gear drive as the first reduction stage and of a differential planetary as the final reduction.

## 3.0 DISCUSSION OF THE THREE DESIGNS

### 3.1 Worm Gear Actuator Per Drawing E-1133-104.

This design consists of a 3-stage worm gear speed reducer of the following ratios: last stage 58:1, intermediate stage 30:1, and first stage 30:1 for an overall gear ratio of 52200:1. The design shown is such that the output gear is stationary while the entire housing rotates about the central axis. A large angular contact type bearing is used to support radial, axial, and moment loads. All other bearings used to support internal gearing are of the tapered roller type. Overall efficiency is estimated to be 11.8% which would require a drive motor of .127 HP.

The same principle of design could also be arranged such that the housing is stationary. The output worm gear could then serve as a mounting base for the mirror support structure, and the output seal would not be submersed in oil.

Although this basic design is entirely feasible and proven (it is a very common gear box for clarifier drives in the water treatment industry) it is relatively heavy and requires either a very complex housing casting, or separate housings for each of the three reduction stages. For these reasons, it is not recommended.

### 3.2 Planetary Actuator Per Drawing E-1133-103.

This design consists of four reduction stages: One worm gear stage of 30:1 gear ratio, the second planetary stage of 12.375:1 gear ratio, the third planetary stage of 12.375:1 ratio, and the final planetary stage of 11.375:1 gear ratio for an overall gear ratio of 52260:1. The output ring gear serves on the inner race of an angular contact bearing which is capable of supporting all radial, axial, and moment loads. The seals for the output ring gear are subjected to static oil pressure since the oil level is about 5 inches higher than the seal. Overall efficiency is estimated to be 60% requiring a drive motor of .025 HP.

Although overall efficiency of this gear drive system is comparatively high, it is achieved through an expensive gear train using many components. Only proven principles of construction are utilized resulting in an assembly with a high probability of successful operations. However, because of the relatively high expense of manufacturing, this design is not recommended.

### 3.3 DIFFERENTIAL PLANETARY PER DRAWING E-1133-102

Principle of operation of this gear drive is as follows: A primary worm gear drive of 71:1 reduction ratio drives the sun gear of the final planetary gear assembly which consists of three planet gears, one sun gear, and two ring gears. The number of teeth of the individual gears are: sun gear = 16, planet gears = 82, stationary ring gear = 179, output ring gear = 182. Gear ratio of this planetary is 739.375:1 for an overall reduction ratio of 52495:1.

In order for a planetary gear set of 3 equally spaced planet gears to be assembled, the sum of the number of teeth of sun gear and ring gear must be a multiple of 3. This condition is met for both ring gears since the difference in the number of teeth of the ring gears is also 3. Therefore, it is possible to use the same planet gear to mesh with both ring gears as long as both ring gears are modified to properly mesh with the planet. All planet gears are identical since no "timing" of the planets is required.

The ring gears also serve a dual purpose of providing inner and outer race configuration of the required azimuth bearing. A 4-point contact configuration with 45 degrees contact angle was selected to support radial, axial, and moment loads.

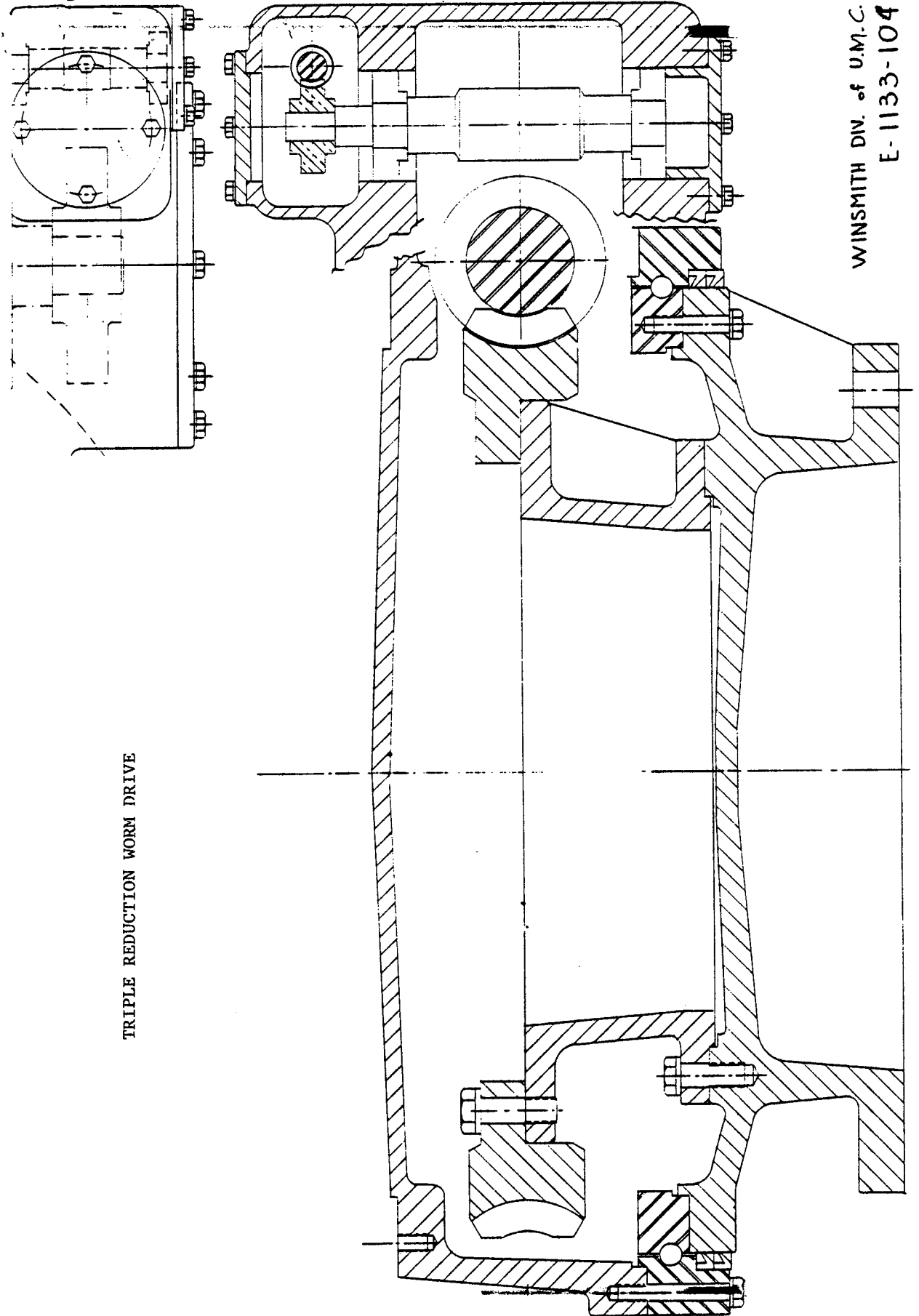
Lubrication of primary and final gear reduction is by separate oil baths. The primary worm gear is lubricated by a synthetic lubricant, Mobil SHC 626, which is proven to be an excellent worm gear lubricant with long life capability. Dual seals on the lower output shaft will prevent loss of lubricant. The planetary gear stage can be lubricated with the same fluid. There is no shaft seal below the oil level, only an O-ring is used as a dust seal and it is located above the oil level. The filler plug is arranged such that it is not possible to overfill. No vent will be used which should minimize accumulation of water.

Overall efficiency of this gear drive is estimated to be 21.7% requiring a .07 HP drive motor.

In comparison to the two other designs, this drive system consists of fewer, simply manufactured components. Differential planetaries and worm gear boxes are widely used in the industry resulting in a high level of confidence that this proposed design can successfully operate over a long period of time while providing the specified performance characteristics.

- 4.0 DRAWINGS OF THREE DESIGNS
- 4.1 Drawing #E-1133-104  
Triple Reduction Worm Drive
- 4.2 Drawing #E-1133-103  
Triple Stage Planetary Plus Worm Drive
- 4.3 Drawing #E-1133-102  
Differential Planetary Plus Worm Drive

WINSMITH DIV. of U.M.C.  
E-1133-104

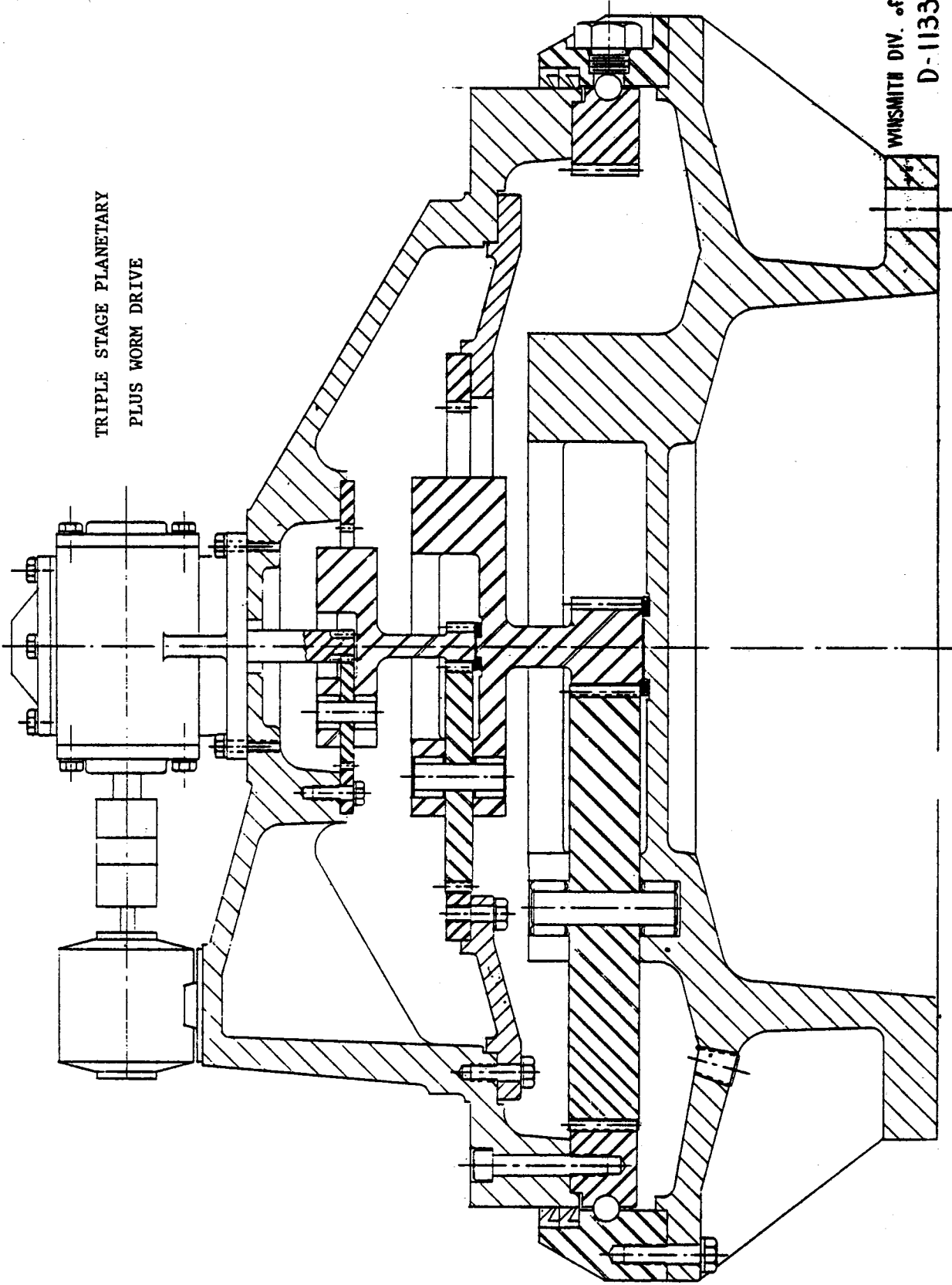


TRIPLE REDUCTION WORM DRIVE

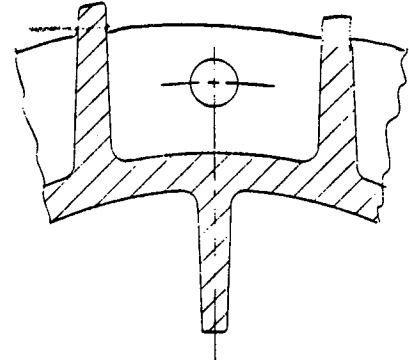
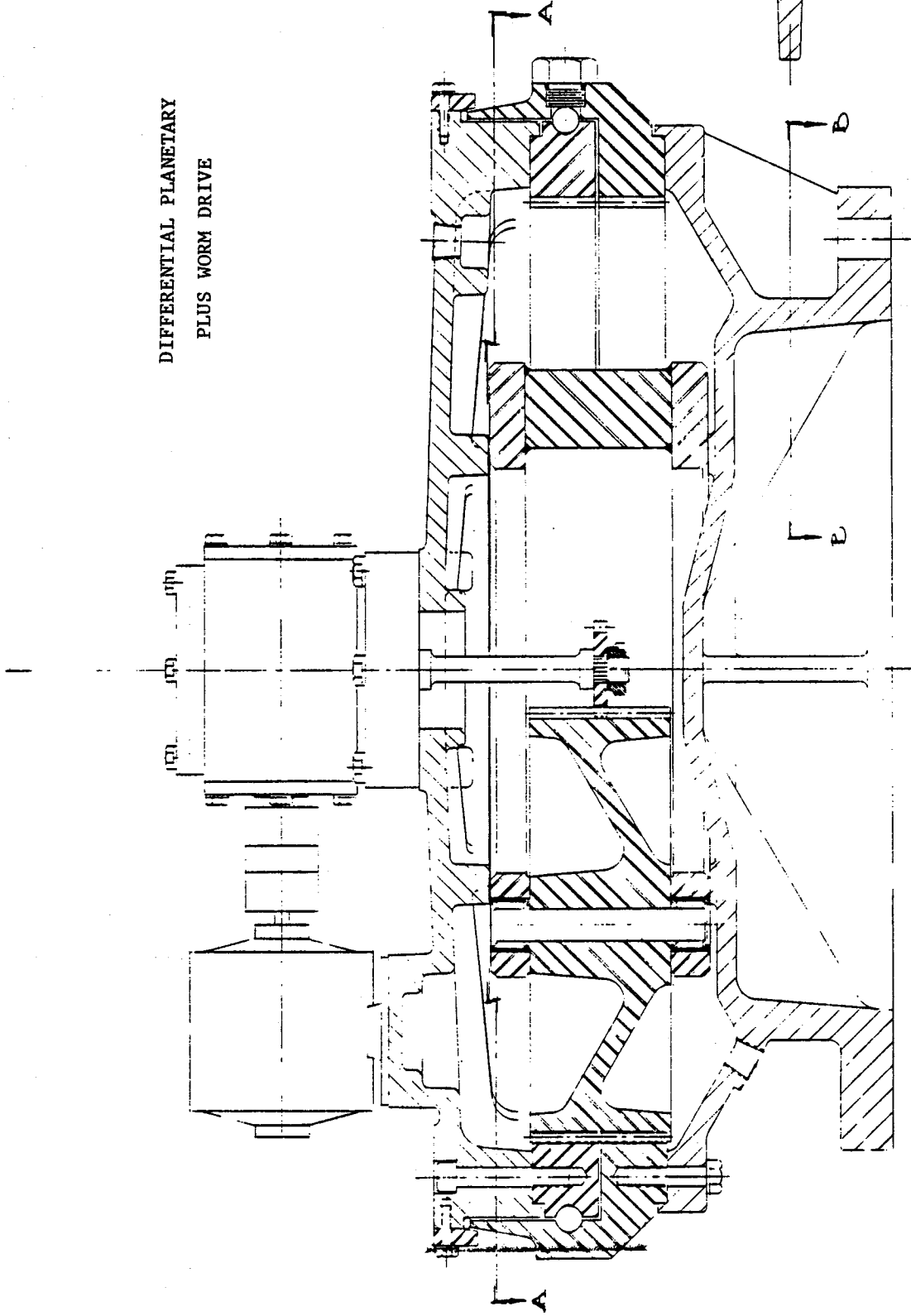


WINSMITH DIV. of U.M.C.  
D-1133-103

TRIPLE STAGE PLANETARY  
PLUS WORM DRIVE



DIFFERENTIAL PLANETARY  
PLUS WORM DRIVE



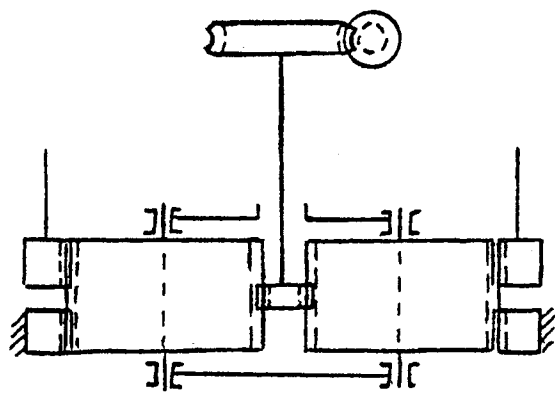
SECTION C-C

SECTION BB  
WINSMITH DIV. of U.M.C.  
E-1133-102

5.0 CALCULATIONS

Input worm gear drive :

71 : 1 gear ratio  
 45.9 % efficiency  
 .22 input HP capacity



Output planetary gear drive :

Nº of sun gear teeth = 16  
 Nº of planet teeth = 82  
 Nº of stationary ring teeth = 179  
 Nº of output ring teeth = 182  
 Gear ratio = 739.375  
 Efficiency = 47.259

$$\text{Output speed} = \frac{1800}{71 \times 739.375} = \frac{1800}{52495.625} = \underline{\underline{.0342885717 \text{ rpm}}}$$

$$\text{Output HP} = \frac{2300 \times .0342885717}{5252} = \underline{\underline{.01502}}$$

$$\text{Input HP} = \frac{.01502}{.459 \times .47259} = \underline{\underline{.06922}}$$

# Worm Gear Set

<i>N<sup>o</sup> of Starts</i>	1.	
<i>N<sup>o</sup> of Teeth</i>	71.	
<i>Center Distance</i>	1.523721631	
<i>Normal Pressure Angle (deg.)</i>	28.	
<i>Lead Angle (deg.)</i>	3.39	
<i>P.D. Worm</i>	.5854003873	
<i>P.D. Gear</i>	2.462042875	
<i>D.P. Normal</i>	28.88839057	
<i>D.P. Axial</i>	28.83784061	
<i>C.P. Normal</i>	.1087493139	
<i>C.P. Axial</i>	0.108939941	
<i>Worm O.D.</i>	.6738258708	
<i>Worm Root Dia.</i>	.5466700255	
<i>Gear Throat Dia.</i>	2.491518036	
<i>Gear Base Circle</i>	2.17301472	
<i>E. P. D. Worm</i>	.6143755484	
<i>Theor. Pin Dia.</i>	.0616019602	
<i>Theor. Dim. over Pins</i>	.7054051616	
<i>Actual Pin Dia.</i>	0.0674	
<i>Actual Dim. over Pins</i>	.7235533419	
<i>Helix Angle at E. P. D.</i>	3.227846519	
<i>Worm Root Radius</i>	.0150693327	
	0.85	



# HELICAL GEAR SET

Center Distance

01/13/14

Final Design

	PINION	PLANET
<i>No of Teeth</i>	16.	82.
<i>N. D. P.</i>	10.	10.
<i>N. P. A. (deg.)</i>	25.	25.
<i>Helix Angle (deg.)</i>	0.	0.
<i>T. D. P.</i>	10.	10.
<i>P. D.</i>	1.6	8.2
<i>O. P. D.</i>	1.6	8.2
<i>Add. Incr.</i>	0.025	-0.025
<i>Addendum</i>	0.12	0.07
<i>Dedendum</i>	0.09	0.14
<i>O. D.</i>	1.84	8.34
<i>Root Dia.</i>	1.42	7.92
<i>T. P. A.</i>	25.	25.
<i>O. T. P. A.</i>	25.	25.
<i>Base Circle</i>	1.450092459	7.431723854
<i>T. I. F. Dia.</i>	1.493345781	8.017781791
<i>Deg. of Roll</i>	6.709084557	21.98402456
<i>Top Land</i>	.0455289039	.0671495835
<i>Cont. Length</i>	.2282162283	0.159689535
<i>E. P. D.</i>	1.647034122	8.149266642
<i>Theor. Pin Dia.</i>	.1836578068	0.171180195
<i>Act. Pin Dia.</i>	0.1875	0.173
<i>" F "</i>	.8674697804	4.111177664
<i>Dim. Over Pins</i>	1.922439561	8.395355329

# HELICAL GEAR SET

Center Distance

900

0.000

Food Machinery

	PINION		RING	
<i>Nº of Teeth</i>	82.		182.	
<i>N. D. P.</i>	10.		10.	
<i>N. P. A. (deg.)</i>	25.		25.	
<i>Helix Angle (deg.)</i>	0.		0.	
<i>T. D. P.</i>	10.		10.	
<i>P. D.</i>	8.2		18.2	
<i>O. P. D.</i>	8.036		17.836	
<i>Add. Incr.</i>	-0.025		0.125	
<i>Addendum</i>	0.07		0.22	
<i>Dedendum</i>	0.14		-0.01	
<i>O. D.</i>	8.34		17.76	
<i>Root Dia.</i>	7.92		18.18	
<i>T. P. A.</i>	25.		25.	
<i>O. T. P. A.</i>	22.36120203		22.36120203	
<i>Base Circle</i>	7.431723854		16.49480172	
<i>T. I. F. Dia.</i>	7.961213836		18.1253053	
<i>Deg. of Roll</i>	21.98402456		26.22050239	
<i>Top Land</i>	.0671495835		.0742944175	
<i>Cont. Length</i>	.3637994898		.1011790965	
<i>E. P. D.</i>	8.149266642		17.95162501	
<i>Theor. Pin Dia.</i>	0.171180195		.1686199379	
<i>Act. Pin Dia.</i>	0.173		0.17	
<i>" F "</i>	4.111177664		8.940411265	
<i>Dim. Over Pins</i>	8.395355329		17.71082253	



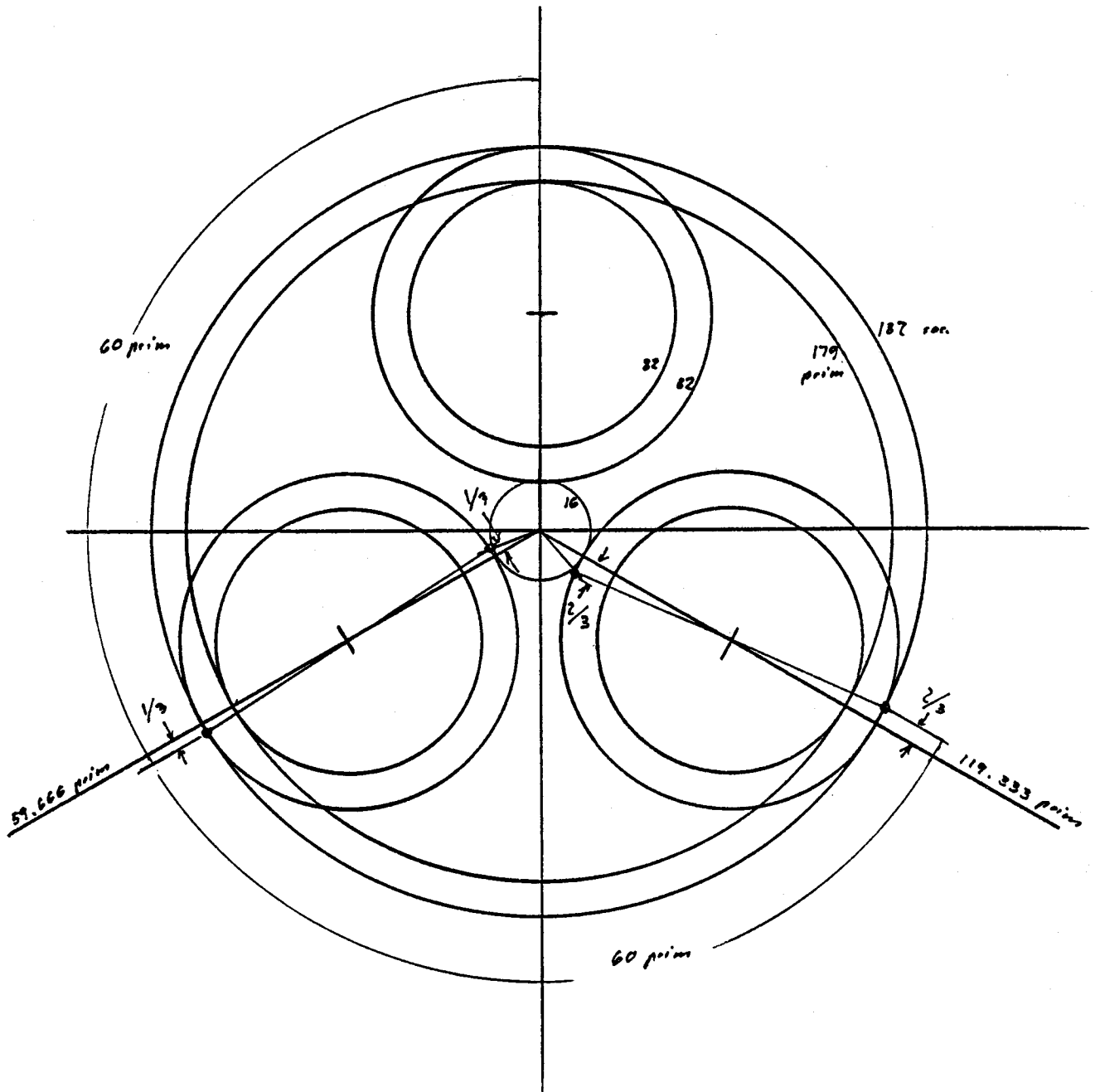
# HELICAL GEAR SET

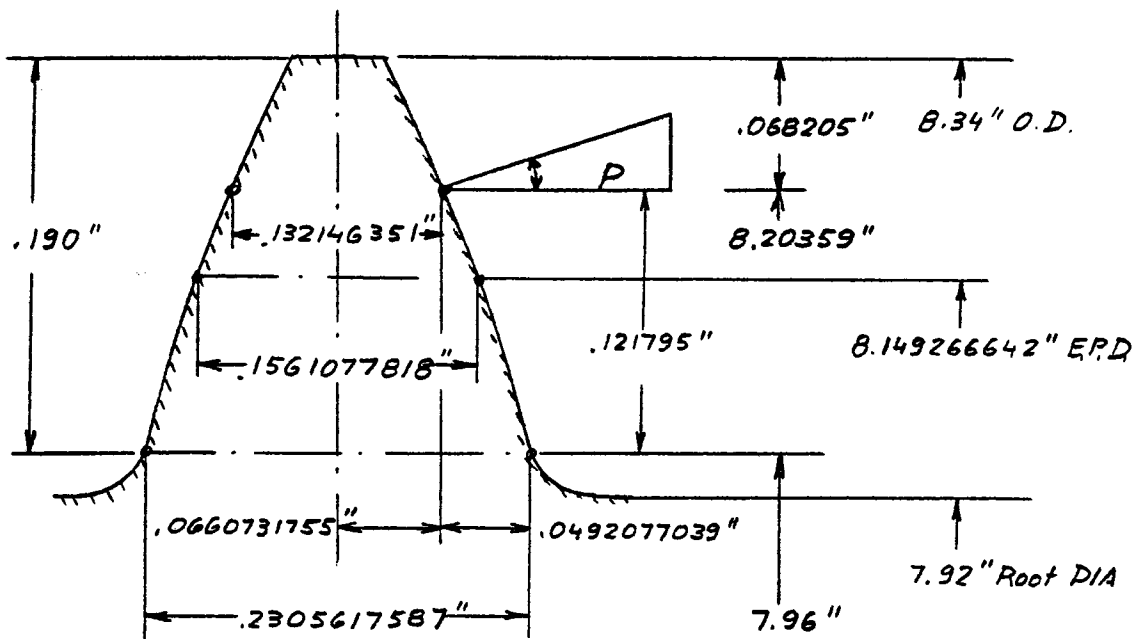
Center Distance

0.12 z

Full Addendum

	PINION		RING
N <sup>o</sup> of Teeth	82.		179.
N.D.P.	10.		10.
N.P.A. (deg.)	25.		25.
Helix Angle (deg.)	0.		0.
T.D.P.	10.		10.
P.D.	8.2		17.9
O.P.D.	8.284536083		18.08453608
Add. Incr.	-0.025		-0.025
Addendum	0.07		0.07
Dedendum	0.14		0.14
O.D. <i>W.D</i>	8.34		17.76
Root Dia.	7.92		18.18
T.P.A.	25.		25.
O.T.P.A.	26.22576402		26.22576402
Base Circle	7.431723854		16.22290939
T.I.F. Dia.	7.97628528		18.13960029
Deg. of Roll	21.98402456		28.66554305
Top Land	.0671495835		0.068065068
Cont. Length	.0619177389		.3821794068
E.P.D.	8.149266642		17.95196661
Theor. Pin Dia.	0.171180195		.1743260008
Act. Pin Dia.	0.173		0.175
" F "	4.111177664		8.937501766
Dim. Over Pins	8.395355329		17.69931528





Base Circle = 7.431723854"

Position of highest point of single tooth contact is :

$$\frac{.19 \times (\text{cont. ratio} - 1)}{\text{cont. ratio}} = \frac{.19 \times .56}{1.56} = .068205"$$

Limit torque = 7800 ft. lbs  $\times$  12 = 93600 in. lbs.

$$P = \frac{93600 \times 2}{3 \times 18.08453608} = 3450.5 \text{ lbs}$$

$$\text{Section Modulus} = \frac{b \times h^2}{6} = \frac{1 \times .2305617587^2}{6} = .0088597874 \text{ in}^3$$

$$\text{Bending stress due to } P = \frac{3450.5 \times .121795}{.0088597874} = \underline{\underline{47434 \text{ psi}}}$$

**REQUIREMENT 4. Strength**

Resistance to tooth breakage is a function of gear design. The behavior of the material must be known and must be consistent under repeated loads and in the presence of high stress concentrations, due to a sudden sectional change.

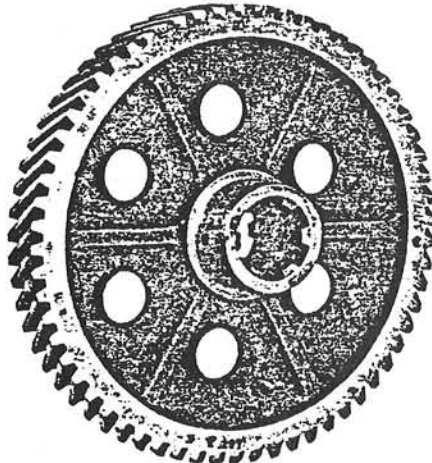
Using the patented Meehanite® process, which incorporates the concept of constitutional carbide control in relation to casting section, it is possible to achieve uniform solidity and uniform physical properties regardless of variations in gear size or dimensions.

FIGURE 5

SPECIFICATIONS FOR MEEHANITE METAL

	General Engineering Types			Nodular S Types		Air Hardened
	GC	GA	GM	SP-80	SH-100	AQ
Tensile Strength (psi, Min.)	40,000	50,000	55,000	80/100,000	100/170,000	65,000
Modulus of Elasticity (psi)	17,000,000	20,000,000	22,000,000	24,000,000	24,000,000	22,000,000
Compression Strength (psi)	150,000	175,000	200,000	160/200,000	200/340,000	200,000
Specific Compressive Stresses**	95,000	105,000	110,000	115,000	120,000	115,000
Shear Strength (psi)	40,000	48,000	55,000	70/90,000	90/160,000	55,000
Fatigue Strength	17,500	22,000	25,000	39,000	43,000	22,000
Impact Strength	4.5	7.2	8.0	$\frac{3}{8}$ " bar 45-65 unnotched	$\frac{3}{8}$ " bar 35-50 unnotched	8.0
*Damping Capacity (per cent)	28.	24.	21.	12	8	20
Brinell Hardness (Min. "as cast")	>195	>207	>217	207/267	263/550	"as cast" up to 280 heat treated up to 550

\*Energy dissipated first cycle at 20,000 psi Torsional stress  
\*\*According to Hertz formula



The high modulus values are indicative of the excellent elastic properties which may be used in design.

Another important Meehanite property is its ability to withstand the effect of sudden changes of section due to design. This quality designated solidity is related to the correct selection and processing of the metal to assure property uniformity throughout the section.

Meehanite castings exhibit a high degree of freedom from notch sensitivity. Notch sensitivity relates to the effect of key ways, grooves, sharp fillets, or defective machine finish as stress raisers, with reduced resistance to failure under static and particularly under dynamic loadings.

Local pressure angle at "P" :

$$\cos \bar{\Phi} = \frac{7.431723854}{8.20359} \quad \bar{\Phi} = \underline{\underline{25.054^\circ}}$$

Compressive stress due to  $P \times \tan \bar{\Phi}$  :

$$\bar{\sigma}_c = \frac{3450.5 \times \tan 25.054}{.2305617587 \times 1} = \underline{\underline{6995 \text{ psi}}}$$

Bending stress due to  $P \times \tan \bar{\Phi}$

$$\bar{\sigma}_B = \frac{3450.5 \times \tan 25.054 \times .0660731755}{.0088597874} = \underline{\underline{12029 \text{ psi}}}$$

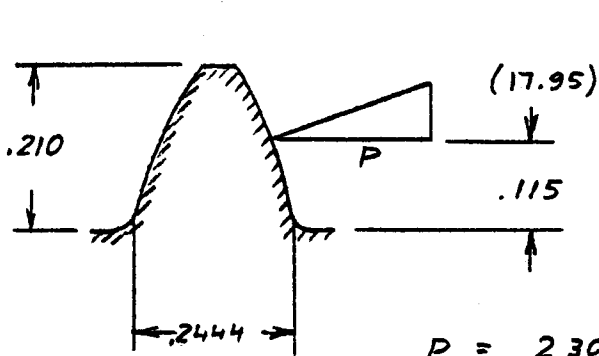
Average stress concentration factor for bending stresses in the root of gear teeth is about 3.0. For limit load condition a stress concentration factor of 2.0 will allow for some stress redistribution without local yielding of a magnitude affecting the operating quantities of this gear drive

Maximum tensile stresses are :

$$\begin{array}{rcl} + 2 \times 47434 & = & 94868 \\ - 2 \times 12029 & = & 24058 \\ - 6995 & = & \underline{\underline{6995}} \\ & & \underline{\underline{63815 \text{ psi tensile}}} \end{array}$$

Maximum compressive stresses are

$$\begin{array}{rcl} + 2 \times 47434 & = & 94868 \\ + 2 \times 12029 & = & 24058 \\ + 6995 & = & \underline{\underline{6995}} \\ & & \underline{\underline{125921 \text{ psi compressive}}} \end{array}$$



$$B.C. = 7.431723854$$

$$EPD = 8.149266642$$

$$t_1 = .1561077818$$

$$D_2 = 7.92$$

$$t_2 = .2444087636$$

$$P = \frac{2300 \times 12 \cdot 2}{17.836 \cdot 3} = 1032 \text{ lbs}$$

Deflection of a cantilever beam is :

$$f = \frac{P \cdot l^3}{3 \cdot E \cdot I}$$

$$I = \frac{b \times h^3}{12} = \frac{1.25 \times 2.444^3}{12} = .0015207$$

$$f = \frac{1032 \times .115^3}{3 \times 29 \times 10^6 \times .0015207} = .00001186''$$

Combined deformations of a cylinder in a groove is :

$$y = \frac{2(1-\nu^2)}{E} p (1 - 2 \ln \frac{b}{2})$$

$$b = 2.15 \sqrt{\frac{P}{E} \frac{D_1 \cdot D_2}{D_1 - D_2}}$$

$$b = 2.15 \sqrt{\frac{1032 / \cos 25^\circ}{1.25 \times 29 \times 10^6} \frac{1.7327 \times 3.7824}{3.7824 - 1.7327}} = .02154''$$

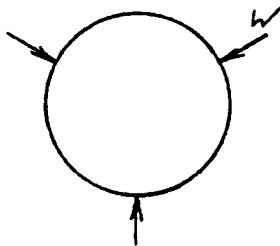
$$D_1 = \text{base circle ring gear} = \frac{t \cdot 25}{2} = \frac{16.2229 \cdot t \cdot 25}{2} = 3.7824$$

$$D_2 = \text{base circle planet} = \frac{t \cdot 25}{2} = \frac{7.4317 \cdot t \cdot 25}{2} = 1.7327$$

$$y = \frac{2(1 - .26^2)}{29 \times 10^6} \times \frac{1138}{1.25} \left(1 - 2 \ln \frac{.02154}{2}\right) = .000589''$$

Total deflection due to bending and compression :

$$2 \times .000589 + 4 \times .00001186 = \underline{\underline{.001225''}}$$



Carrier deflection :

$$\text{Separating Load} = 2 \times 1032 \times \tan 25^\circ = \underline{\underline{962.5 \text{ lbs}}}$$

$$\text{Radial displacement : } x = \frac{WR^3}{2IE} \left[ \frac{1}{S^2} \left( \frac{\theta}{2} + \frac{SC}{2} \right) - \frac{1}{\theta} \right]$$

$$W = 962.5 \text{ lbs}$$

$$R = 4.9''$$

$$E = 24 \times 10^6 \text{ psi}$$

$$I = \frac{2 \times .68 \times 2^3}{12} = .90667 \text{ in}^4$$

$$S = \sin \theta = \sin 30^\circ$$

$$C = \cos \theta = \cos 30^\circ$$

(Roark, page 158)

$$\theta = \frac{2\pi \cdot 30}{360} = \frac{\pi}{6} = 30^\circ$$

$$x = \frac{962.5 \times 4.9^3}{2 \times 24 \times 10^6 \times .90667} \left[ \frac{1}{\sin^2 30} \left( \frac{\pi}{12} + \frac{\sin 30 \times \cos 30}{2} \right) - \frac{6}{\pi} \right] = \underline{\underline{8.75 \times 10^{-6}''}}$$

This small value of radial deflection can be neglected.

Angular deflection due to elastic deflection of planetary carrier is also very small (about .00014") and will be neglected.

Angular rotational compliance due to elastic deformation is :

$$\frac{2 \times .001225}{17.95 \times 2300 \times 12} = \underline{\underline{.495 \times 10^{-8} \text{ radians / in. lbs}}}$$

Backlash (total)	Ring Gear betw. pins	$\Delta$	Planet Gear over pins	$\Delta$
0	17.71082	.00000	8.39535	.00000
.002	17.71320	.00238	8.39322	.00213
.004	17.71558	.00476	8.39109	.00426
.006	17.71795	.00713	8.38895	.00640
.008	17.72033	.00951	8.38681	.00854
.010	17.72270	.01188	8.38467	.01068

Total permissible backlash =  $\frac{17.836 \times \pi \times .07}{360} = \underline{\underline{.01089"}}$

The following maximum backlash values are assumed :

.004 at worm gear mesh resulting in

$$\frac{.004 \times 1.6}{2.462} = .0026" \text{ backlash on pinion}$$

.004" between pinion and planet

.004" between planet and each ring gear

Total free play of output ring gear is :

$$\begin{aligned} \text{play between planet and stationary ring gear} &= .004" \\ \text{play between planet and output ring gear} &= \frac{.004"}{.008"} \end{aligned}$$

$$\frac{.008 \times 360}{17.836 \times \pi} = \underline{\underline{.0514"}}$$

Actual maximum installed free play of output ring gear will be less than this value because of out of roundness of various components.



Total approach of two races separated by a ball is :

$$\delta_N = 7.8107 \times 10^{-6} (C_{\delta_o} + C_{\delta_i}) \left( \frac{P_o^2}{d} \right)^{1/3}$$

$$\frac{d}{E} \cos 45 = \frac{.5}{21.1} \cos 45 = .0168$$

from chart 56 :  $C_{\delta_o} \sim C_{\delta_i} = 1.345$

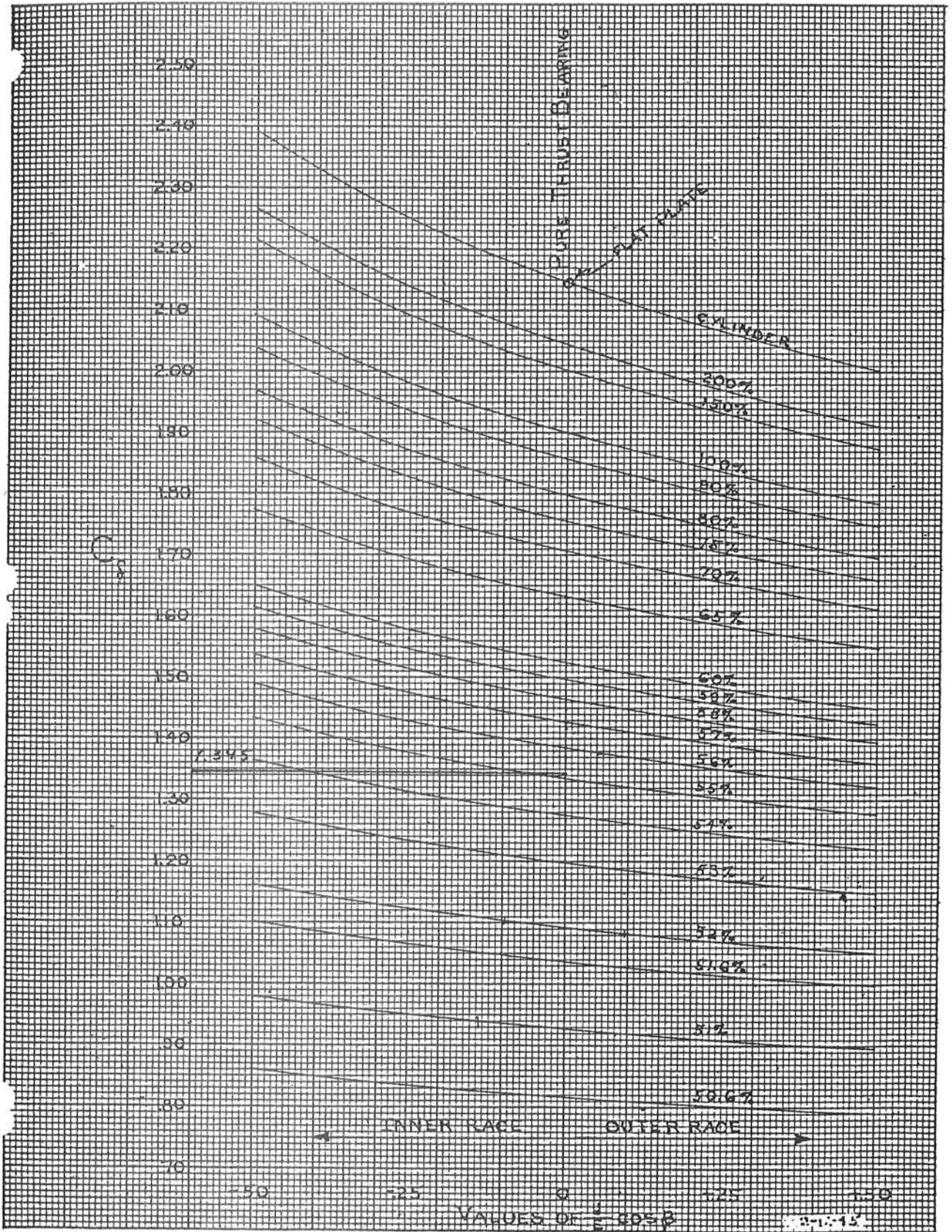
$$\delta_N = 7.8107 \times 10^{-6} \times 2.69 \times \frac{1}{\sqrt[3]{.5}} \times P_o^{2/3} = 26.47 \times 10^{-6} \times P_o^{2/3}$$

Ball #	Position°	Position"	$\delta_N$ $\times 10^{-3}$	P lbs	Moment in. lbs
1	0	10.550	2.27845	798.6	8 425.2
2	5.4545	10.502	2.26809	793.2	8 330.2
3	16.363	10.122	2.18602	750.5	7 596.6
4	21.818	9.794	2.11518	714.3	6 995.8
5	27.273	9.377	2.02512	669.2	6 275.1
6	32.727	8.875	1.91671	616.2	5 468.8
7	38.182	8.293	1.79101	556.6	4 939.8
8	43.636	7.635	1.64891	491.7	3 754.1
9	49.090	6.909	1.49212	423.2	2 923.9
10	54.545	6.119	1.32150	352.7	2 158.2
11	60.000	5.275	1.13923	282.3	1 489.1
12	65.454	4.383	.94658	213.8	937.1
13	70.909	3.450	.74509	149.3	515.1
14	76.364	2.487	.53711	91.4	227.3
15	81.818	1.501	.32417	42.8	64.2
16	87.273	.502	.10841	8.3	4.2

60 104.7

Total overturning moment required to cause a  $2.27845 \times 10^{-3}$ " deflection is

$$4 \times 60 104.7 = 240 418.8 \text{ in. lbs}$$



Limit permanent deformation =  $.001 \times .5 = .0005''$  on flat plate

$$\frac{h}{d} = K \left( \frac{P}{d^2} \right)^n$$

$h = .0005$

$d = .50$

$K = 575 \times 10^{-10}$  for steel of 50 Rockwell "C"

$n = 1.21$  "

$$P = \sqrt[n]{\frac{h \cdot d^{2n-1}}{K}} = \sqrt[1.21]{\frac{.0005 \cdot .5^{1.42}}{575 \times 10^{-10}}} = 798.6 \text{ lbs}$$

$$\delta_N = 26.47 \times 10^{-6} \times 798.6^{2/3} = 2.27845 \times 10^{-3}''$$

$$\text{Angular deflection} = \frac{2.27845 \times 10^{-3}}{10.55} = .215966 \times 10^{-3} \text{ rad}$$

$$\text{Moment compliance} = \frac{.215966 \times 10^{-3}}{240418.8} = \underline{\underline{.0898 \times 10^{-8} \text{ rad/in. lbs}}}$$

Maximum load of highest loaded ball at 23500 ft-lbs of overturning moment is

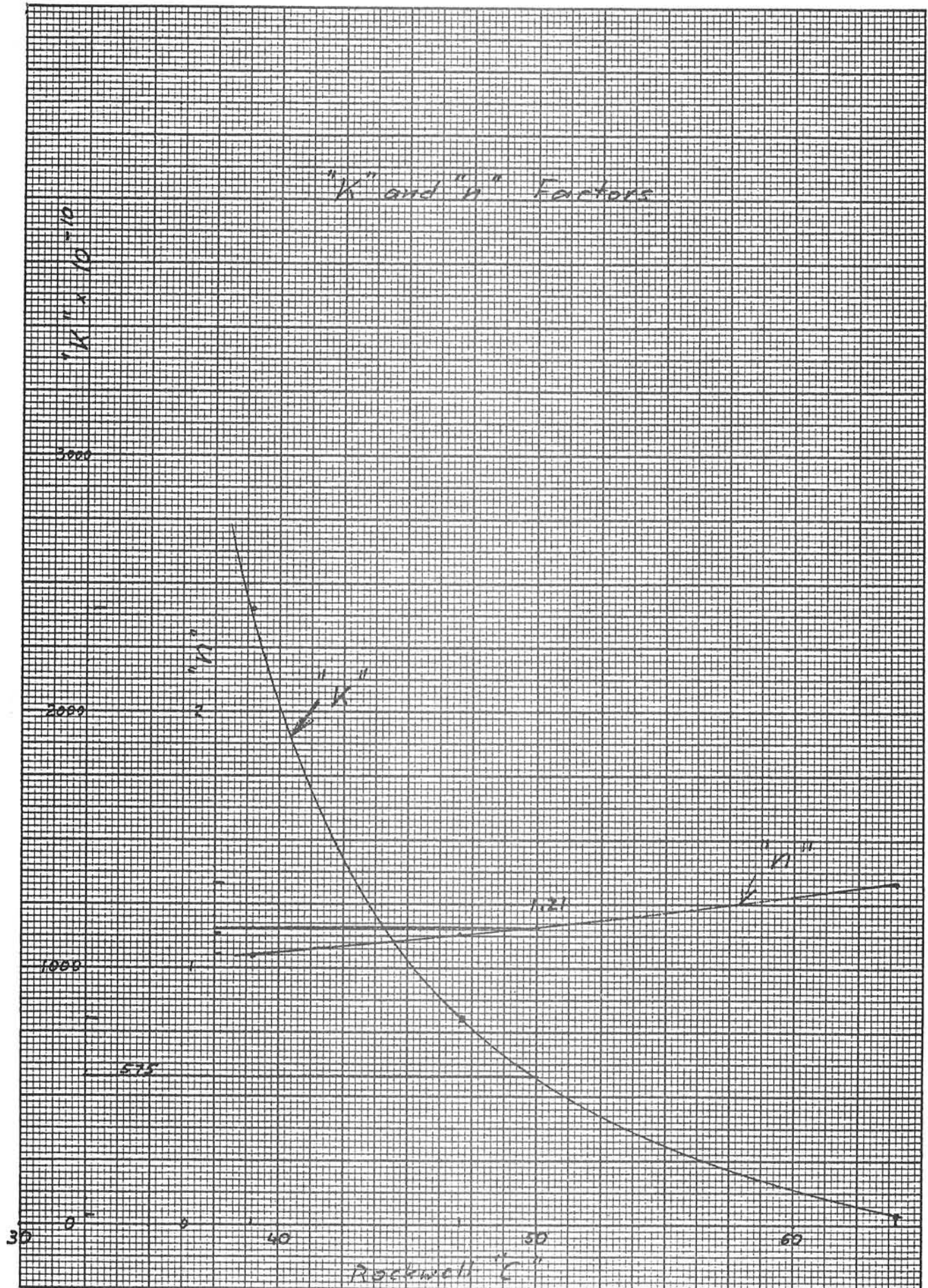
$$\frac{798.6 \times 23500 \times 12}{240418.8} = \underline{\underline{936.7 \text{ lbs}}}$$

Mean compressive stress between maximum loaded ball and inner race is:

$$S_m = 15079 f_s \left( \frac{P_0}{d^2} \right)^{1/3}$$

$$S_m = 15079 \times 1.3 \left( \frac{936.7}{.5^2} \right)^{1/3} = \underline{\underline{304464 \text{ psi}}}$$

Bearing dimensions : pitch DIA = 21.1 "  
 ball DIA = .5 "  
 race curvature = 55 %  
 number of balls = 66 load balls



	Sun	Planet	Ring	Arm
Train locked	+1	0	+1	+1
Arm locked	+ 179/16	- 179/82	-1	0
Results	1 + 179/16	- 179/82	0	+1

$$\text{Gear ratio planet / sun} = \frac{179/82}{1 + 179/16} = 5.5831$$

Total number of planet revolutions :

$$\frac{1 \times 364 \times 739.375 \times 30}{5.5831} = 1.4461 \times 10^6$$

For 1% failure rate the life adjustment factor is .21

Adjusted number of revolutions is :

$$\frac{1.4461 \times 10^6}{.21} = \underline{\underline{6.886 \times 10^6}}$$

Mean effective output torque = 7200 in·lbs

Ring gear operating pitch diameter = 17.836

Bearing reaction due to output torque :

$$\frac{7200 \times 2 \times 1.30}{17.836 \times 3 \times 3.40} = 102.9 \text{ lbs}$$

Mean effective input torque =  $\frac{600 \times 12}{739.375 \times .4726} = 20.6 \text{ in·lbs}$

Sun gear operating pitch diameter = 1.60

Bearing reaction due to input torque :

$$\frac{20.6 \times 2}{3 \times 1.60} = 8.58 \text{ lbs}$$

Tangential tooth load :  $\frac{7200 \times 2}{3 \times 17.836} = 269.12 \text{ lbs}$

Radial bearing reaction :  $269.12 \times \tan 25^\circ = 125.49 \text{ lbs}$

Combined mean effective bearing load :

$$\sqrt{(102.9 + 8.58)^2 + 125.49^2} = \underline{\underline{167.85 \text{ lbs}}}$$



## DIMENSIONS AND LOAD RATINGS

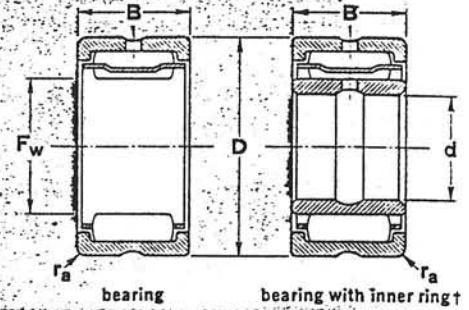
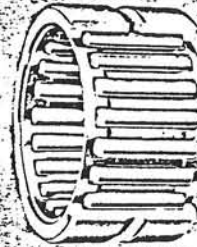
BEFORE ORDERING ANY BEARING, CHECK FOR AVAILABILITY.

Order bearings on this page from The Torrington Company, Bearings Division, Torrington, Connecticut 06790.

Bearing diameters and widths listed below are nominal. For inspection purposes, see tolerance tables on page 88-89.

Metric-inch conversions given are for the convenience of the user. The controlling dimensions are in millimetres for nominal metric bearings and in inches for nominal inch bearings.

Load ratings are given in pounds-force: 1 lbf = 0.454 kgf = 4.448 N



F <sub>w</sub> bore (nominal)		D o.d. (nominal)		B width (nominal)		bearing designation	military standard number	mass (appr.) lb	C <sub>r</sub> basic dynamic load rating ISO R 281 lbf	C <sub>0</sub> basic static load rating lbf	limiting speed rpm	r <sub>a</sub> housing fillet (max)		used with inner ring designation	
mm	inch	mm	inch	mm	inch							mm	inch		
15	.5906	26	1.0236	18	.709	FHJ-152618	—	.09	2770	2980	2410	31700	0,6	.025	FIR-101518
15	.5906	26	1.0236	21	.827	FHJ-152621	—	.10	3300	3560	3020	31700	0,6	.025	FIR-101521
15	.5906	26	1.0236	25	.984	FHJ-152625	—	.12	3720	4000	3510	31700	0,6	.025	FIR-101525
15,875	.6250	28,575	1.1250	19,05	.750	HJ-101812	MS 51961-1	.11	2980	3220	2520	30200	0,6	.025	IR-061012
17	.6693	28	1.1024	18	.709	FHJ-172818	—	.09	2940	3170	2610	27500	0,6	.025	FIR-121718
17	.6693	28	1.1024	21	.827	FHJ-172821	—	.11	3500	3780	3270	27500	0,6	.025	FIR-121721
17	.6693	28	1.1024	25	.984	FHJ-172825	—	.13	4210	4530	4140	27500	0,6	.025	FIR-121725
19,050	.7500	31,750	1.2500	19,05	.750	HJ-122012	MS 51961-2	.12	3180	3420	2540	24600	1,0	.04	IR-081212
19,050	.7500	31,750	1.2500	25,40	1.000	HJ-122016	MS 51961-3	.16	4350	4700	4120	24600	1,0	.04	IR-081216
20	.7874	32	1.2598	18	.709	FHJ-203218	—	.12	3580	3860	3210	23300	0,6	.025	FIR-152018
20	.7874	32	1.2598	21	.827	FHJ-203221	—	.13	4270	4600	4030	23300	0,6	.025	FIR-152021
20	.7874	32	1.2598	25	.984	FHJ-203225	—	.16	4850	5230	4740	23300	0,6	.025	FIR-152025
22,225	.8750	34,925	1.3750	19,05	.750	HJ-142212	MS 51961-5	.14	3540	3820	3210	20700	1,0	.04	IR-101412 IR-111412
22,225	.8750	34,925	1.3750	25,40	1.000	HJ-142216	MS 51961-6	.18	4860	5240	4810	20700	1,0	.04	IR-101416
25	.9843	37	1.4567	18	.709	FHJ-253718	—	.14	4100	4410	3900	18200	0,6	.025	FIR-172518 FIR-202518
25	.9843	37	1.4567	21	.827	FHJ-253721	—	.16	4880	5260	4890	18200	0,6	.025	FIR-172521 FIR-202521
25	.9843	37	1.4567	25	.984	FHJ-253725	—	.19	5600	6040	5830	18200	0,6	.025	FIR-172525 FIR-202525
25,400	1.0000	38,100	1.5000	19,05	.750	HJ-162412	MS 51961-8	.15	3830	4140	3670	19200	1,0	.04	IR-121612
25,400	1.0000	38,100	1.5000	25,40	1.000	HJ-162416	MS 51961-9	.20	5250	5670	5500	19200	1,0	.04	IR-121616 IR-131616
28,575	1.1250	41,275	1.6250	25,40	1.000	HJ-182616	MS 51961-11	.22	5680	6140	6190	15700	1,0	.04	IR-141816 IR-151816
28,575	1.1250	41,275	1.6250	31,75	1.250	HJ-182620	MS 51961-12	.29	7120	7690	8270	15700	1,0	.04	IR-141820 IR-151820
30	1.1811	45	1.7717	21	.827	FHJ-304521	—	.24	5870	6330	5580	15300	1,0	.04	FIR-253021
30	1.1811	45	1.7717	25	.984	FHJ-304525	—	.29	7140	7690	7170	15300	1,0	.04	FIR-253025
30	1.1811	45	1.7717	29	1.142	FHJ-304529	—	.33	8360	9010	8790	15300	1,0	.04	FIR-253029
31,750	1.2500	44,450	1.7500	25,40	1.000	HJ-202816	MS 51961-14	.24	5870	6340	6530	14000	1,0	.04	IR-162016
31,750	1.2500	44,450	1.7500	31,75	1.250	HJ-202820	MS 51961-15	.31	7360	7960	8730	14000	1,0	.04	IR-162020
34,925	1.3750	47,625	1.8750	25,40	1.000	HJ-223016	MS 51961-18	.26	6260	6750	7220	12600	1,0	.04	IR-182216
34,925	1.3750	47,625	1.8750	31,75	1.250	HJ-223020	MS 51961-19	.34	7840	8480	9650	12600	1,0	.04	IR-182220
35	1.3780	50	1.9685	21	.827	FHJ-355021	—	.26	6270	6760	6280	12900	1,0	.04	FIR-303521
35	1.3780	50	1.9685	25	.984	FHJ-355025	—	.32	7620	8210	8070	12900	1,0	.04	FIR-303525
35	1.3780	50	1.9685	29	1.142	FHJ-355029	—	.37	8930	9620	9890	12900	1,0	.04	FIR-303529

All Torrington bearings are made to the highest standards of precision and quality. For more information, contact your Torrington distributor or Torrington Company, Bearings Division, Torrington, Connecticut 06790.



Required Basic Dynamic Load Rating (C<sub>r</sub>) = Applied Load • SF • LF • HF (see page 14).  
 †See pages 96-103 for inner rings. Order inner rings separately.

BY W. Heller DATE 12-7-79 SUBJECT Ford Aerospace  
CHKD. BY \_\_\_\_\_ DATE \_\_\_\_\_ Planet Bearings

SHEET NO. 30 OF 37  
JOB NO. \_\_\_\_\_

Required bearing basic dynamic capacity :

$$\sqrt[10/3]{6.886} \times 167.85 = \underline{\underline{299 \text{ lbs}}}$$

Required bearing static capacity :

$$\frac{167.85 \times 7900}{600} = \underline{\underline{2212 \text{ lbs}}}$$

Selected :

Torrington FHJ-152618

Basic load rating "C" of an angular contact ball bearing is :

$$C = f_c (i \cdot \cos \alpha)^{.7} \cdot Z^{2/3} \cdot D^{1.8}$$

D = ball diameter = .50"

Z = number of balls = 66

i = number of rows = 1

$\alpha$  = contact angle = 45°

$$\frac{D \cdot \cos 45^\circ}{21.1} = .01676 \quad || \quad f_c/f = .1595$$

$$f = 7450$$

$$C = .1595 \cdot 7450 \cdot (\cos 45^\circ)^{.7} \cdot 66^{2/3} \cdot .5^{1.8} = \underline{\underline{4372 \text{ lbs radial}}}$$

Thrust capacity is :

$$C_a = f_c (\cos \alpha)^{.7} \cdot \tan \alpha \cdot Z^{2/3} \cdot D^{1.8}$$

$$f_c/f = .4952$$

$$C_a = .4952 \cdot 7450 \cdot (\cos 45^\circ)^{.7} \cdot \tan 45^\circ \cdot 66^{2/3} \cdot .5^{1.8} = \underline{\underline{13575 \text{ lbs axial}}}$$

These capacities can be obtained by constructing bearing balls and the two bearing races of bearing quality steel hardened to a minimum hardness of Rockwell "C" 58. For the proposed angular thrust bearing the bearing balls will be made of type 52100 steel through hardened, while inner and outer race are made of 4150 steel nitrided to a surface hardness of 50-55 Rockwell "C" with a core hardness of Rockwell "C" 28 minimum.

The hardness correction factor is :

$$f_H = \left( \frac{\text{Rockwell "C"}}{58} \right)^{3.6} = \left( \frac{50}{58} \right)^{3.6} = \underline{\underline{.5861}}$$



## 360 ROLLING BEARING FATIGUE

Equation (13.106) has been evaluated by AFBMA [13.10] Standard Section 9 for the following case: deep-groove and angular-contact ball bearings where  $f_i \leq 0.52D$  and  $f_o \leq 0.53D$ . Table 13.2 shows  $f_c/f_m$  versus  $\gamma$  for the various ball bearing types. Here  $f_m$  equals 7450 in inch-pound units for "ball bearings of good quality, hardened ball bearing steel."

For rolling bearings the material hardness of which is less than 58 Rockwell C a reduction in basic dynamic capacity according to the following formula may be used:

$$C' = C \left( \frac{RC}{58} \right)^{3.6} \quad (13.107)$$

in which  $RC$  is the Rockwell C scale hardness.

By using the AFBMA formula (13.103) and Table 13.2 for  $f_c/f_m$ , the basic dynamic capacity of a radially loaded bearing may be calculated. The pertinent  $L_{10}$  fatigue life formula is given below:

$$L = \left( \frac{C}{F_e} \right)^3 \quad (13.108)$$

in which  $F_e$  is an equivalent radial load which will cause the same  $L_{10}$  fatigue life as the applied load.

From equation (6.66) it can be seen that

$$Q_{\max} = \frac{F_r}{Z \cos \alpha J_r} \quad (6.66)$$

in which  $F_r$  is an applied radial load and  $Q_{\max}$  is the maximum rolling element load. For a rotating ring, from equation (13.82)  $Q_{eu} = Q_{\max} J_1$ ; therefore

$$Q_{eu} = \frac{F_r}{Z \cos \alpha} \times \frac{J_1}{J_r} \quad (13.109)$$

in which  $Q_{eu}$  is the mean equivalent rolling element load in a combined loading defined by  $J_r$ . At  $\epsilon = 0.5$  [see Chapter 6 and equations (13.82) and (13.84)] loading is ideal and purely radial; therefore

$$Q_{eu} = \frac{F_{eu}}{Z \cos \alpha} \times \frac{J_1(0.5)}{J_r(0.5)} \quad (13.110)$$

in which  $F_{eu}$  is the equivalent radial load.

Similarly, for a nonrotating ring

$$Q_{ev} = \frac{F_{ev}}{Z \cos \alpha} \times \frac{J_2(0.5)}{J_r(0.5)} \quad (13.111)$$

## 13.6 Fatigue Life of a Rolling Bearing 367

In equations (13.136) and (13.137) the upper signs refer to an inner raceway and the lower signs to an outer raceway.

The basic dynamic capacity of an entire thrust bearing assembly is given by

$$C_a = 7450 \left\{ 1 + \left[ \left( \frac{1 \mp \gamma}{1 \pm \gamma} \right)^{1.72} \left( \frac{r_u}{r_v} \times \frac{2r_v - D}{2r_u - D} \right)^{0.41} \right]^{3.33} \right\}^{-0.3} \\ \times \left( \frac{2r_u}{2r_u - D} \right)^{0.41} \frac{\gamma^{0.3} (1 \mp \gamma)^{1.39}}{(1 \pm \gamma)^{0.33}} (\cos \alpha)^{0.7} \tan \alpha Z^{0.67} D^{1.8} \quad (13.138)$$

For ball bearings with inner ring rotation equation (13.139) becomes

$$C_a = 7450 \left\{ 1 + \left[ \left( \frac{1 - \gamma}{1 + \gamma} \right)^{1.72} \left( \frac{f_i}{f_o} \times \frac{2f_o - 1}{2f_i - 1} \right)^{0.41} \right]^{3.33} \right\}^{-0.3} \\ \times \left[ \frac{2f_i}{2f_i - 1} \right]^{0.41} \frac{\gamma^{0.3} (1 - \gamma)^{1.39}}{(1 + \gamma)^{0.33}} (\cos \alpha)^{0.7} \tan \alpha Z^{0.67} D^{1.8} \quad (13.139)$$

Lundberg et al. [13.8] recommended a reduction in the material constant to accommodate inaccuracies in manufacturing which cause unequal internal load distribution. Hence, equation (13.139) becomes

$$C_a = 6700^*(1 - 0.33 \sin \alpha) \\ \times \left\{ 1 + \left[ \left( \frac{1 - \gamma}{1 + \gamma} \right)^{1.72} \left[ \frac{f_i}{f_o} \times \frac{(2f_o - 1)}{(2f_i - 1)} \right]^{0.41} \right]^{3.33} \right\}^{-0.3} \\ \times \left[ \frac{2f_i}{2f_i - 1} \right]^{0.41} \frac{\gamma^{0.3} (1 - \gamma)^{1.39}}{(1 + \gamma)^{0.33}} (\cos \alpha)^{0.7} \tan \alpha Z^{0.67} D^{1.8} \quad (13.140)$$

In (13.140) as recommended by Palmgren [13.9] the term  $(1 - 0.33 \sin \alpha)$  accounts for reduction in  $C_a$  caused by added friction due to spinning (presumably).

AFBMA [13.10] recommends the following formula for basic dynamic thrust capacity:

$$C_a = f_c (\cos \alpha)^{0.7} \tan \alpha Z^{1/6} D^{1.8} \dagger \quad (13.141)$$

from which it is apparent that (approximately)

$$f_c = 6700(1 - 0.33 \sin \alpha) \left\{ 1 + \left[ \left( \frac{1 - \gamma}{1 + \gamma} \right)^{1.72} \right. \right. \\ \left. \left. \times \left( \frac{f_i}{f_o} \times \frac{2f_o - 1}{2f_i - 1} \right)^{0.41} \right]^{3.33} \right\}^{-0.3} \frac{\gamma^{0.3} (1 - \gamma)^{1.39}}{(1 + \gamma)^{0.33}} \left[ \frac{2f_i}{2f_i - 1} \right]^{0.41} \quad (13.142)$$

\* This value can be as high as 7080 for thrust-loaded, angular-contact ball bearings.

† AFBMA [13.9] recommends using  $D$  raised to the 1.4 power in lieu of 1.8 for bearings having balls of diameter greater than 1 in.

Proposed inner and outer race conformity is 55%. For other values of conformity the correction factor is:

$$f_c = \left( \frac{2f}{2f-1} \right)^{.41} / \left( \frac{2+.53}{2+.53-1} \right)^{.41} = \underline{\underline{.82345}}$$

Corrected radial basic dynamic capacity is:

$$C = 4372 \times .5861 \times .82345 = \underline{\underline{2110 \text{ lbs}}}$$

Corrected axial basic dynamic capacity is:

$$C_a = 13575 \times .5861 \times .82345 = \underline{\underline{6552 \text{ lbs}}}$$

Total number of bearing revolutions is:

$$1 \times 364 \times 30 = \underline{\underline{.01092 \times 10^6}}$$

For such low numbers of revolutions standard load-life relationships do not apply. Based on a 3000 lbs axial load and a 6552 lbs axial basic dynamic capacity the expected failure rate during 30 years life should be much less than 1%.

414 ROLLING BEARING FATIGUE

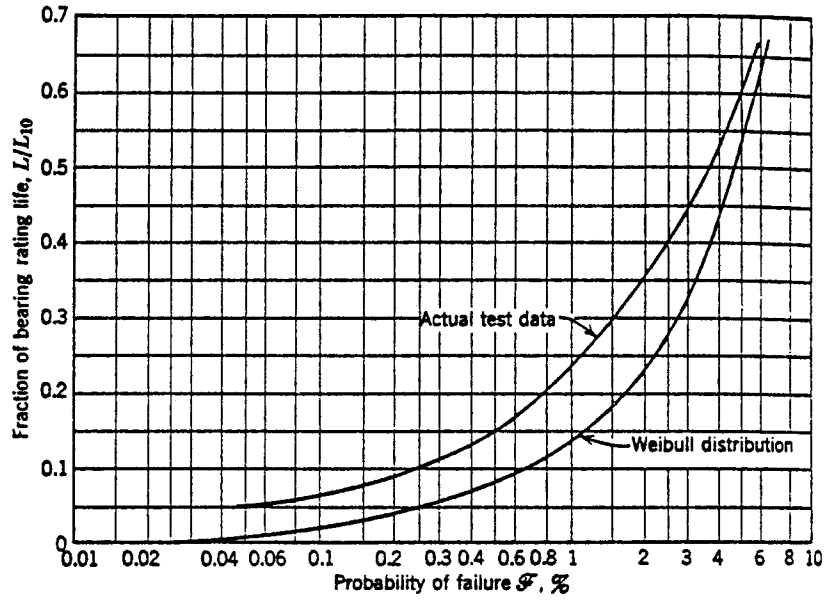


Fig. 13.41 Fraction of  $L_{10}$  life versus probability of failure.

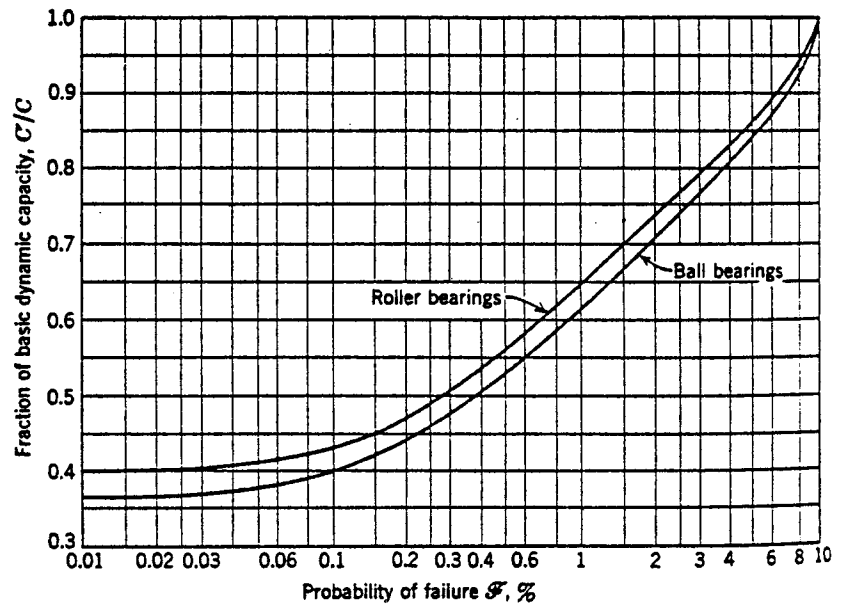
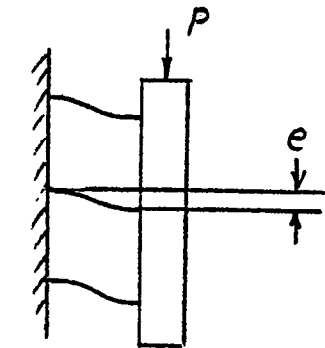


Fig. 13.42 Reduction in basic dynamic capacity required for increased reliability.

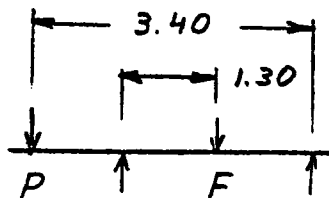
$$\text{Moment of inertia} = \frac{b \times h^3}{12} = .530697 \text{ in}^4$$

$$b = .10 \text{ ''}$$



$$e = \frac{P \cdot l^3}{3 \cdot E \cdot I \cdot 12}$$

$$\rightarrow l \leftarrow 2.687$$

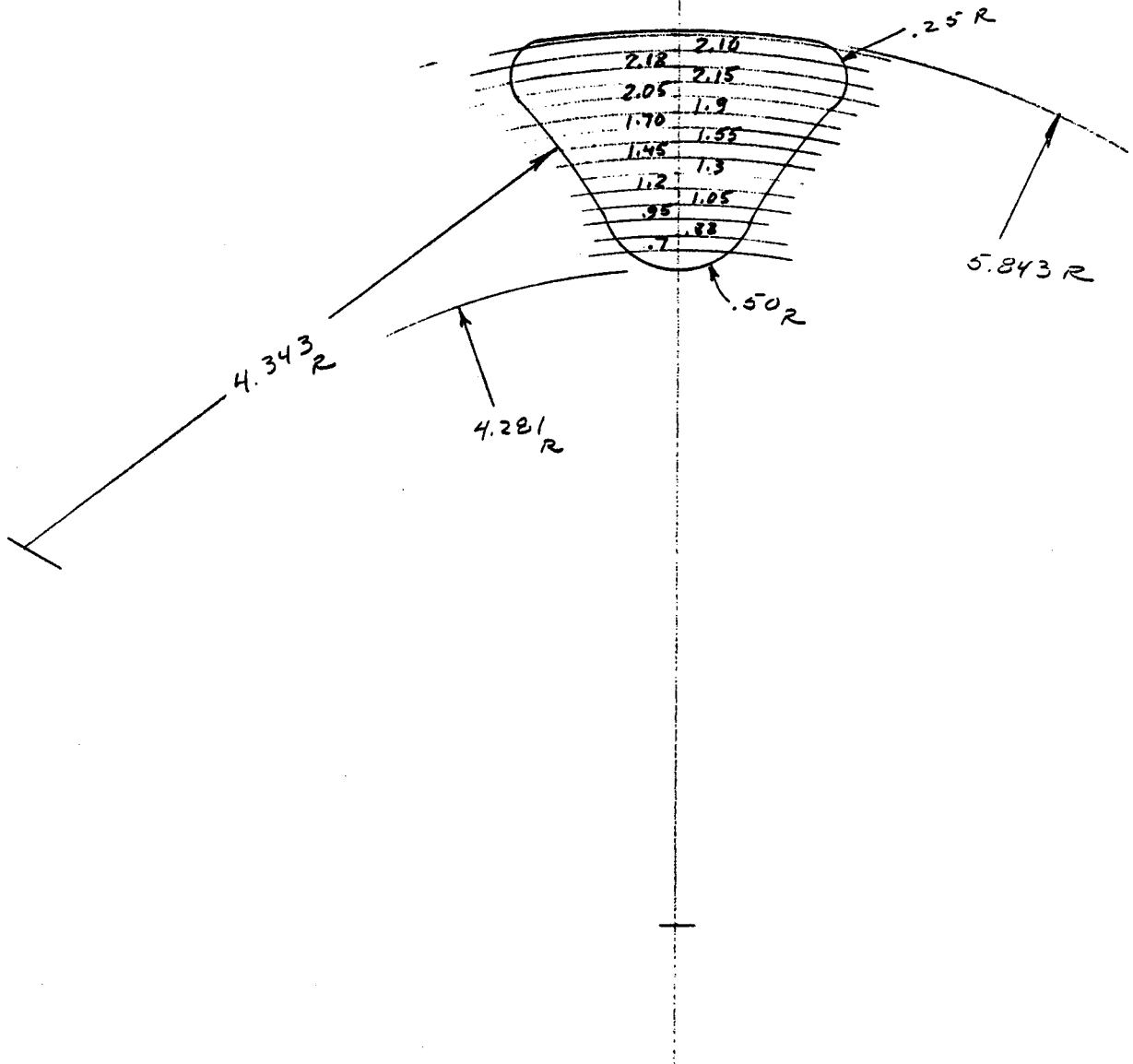


$$\text{Maximum output torque} = 7800 \text{ lbs} \cdot \text{ft}$$

$$\text{Total tangential tooth load} = \frac{7800 \cdot 12 \cdot 2}{17.836} = 10495 \text{ lbs}$$

$$P = \frac{10495 \times 1.30}{3.40} = 4013 \text{ lbs}$$

$$e = \frac{4013 \cdot 2.687^3}{3 \cdot 29 \cdot 10^6 \cdot .530697 \cdot 12} = \underline{\underline{.0001405 \text{ ''}}}$$





REPORT E-2

ELEVATION DRIVE TRADE STUDIES

FOR

GIMBAL/ACTUATOR DRIVE ASSEMBLY

FOR

BOEING SECOND GENERATION HELIOSTAT

JUNE 27, 1980

Reference: FACC TM06



TABLE OF CONTENTS

SECTION

1.0 INTRODUCTION

2.1 SUMMARY

2.2 CONCLUSIONS AND RECOMMENDATIONS

• DRIVE CONFIGURATIONS:

FIG. 1A & 1B - ROTARY DRIVE - FIXED OPEN GEAR

FIG. 2A & 2B - ROTARY DRIVE - ROTATING OPEN GEAR

FIG. 3 - ROTARY DRIVE - ENCLOSED GEARING

FIG. 4 - LINEAR ACTUATOR DRIVE

3.0 CALCULATIONS

• TABLE I - COST COMPARISON, FIG'S. 1, 2, 3, & 4

• TABLE II - DESIGN COMPARISON, FIG'S. 1, 2, 3, & 4

• TABLE III - TYPICAL ANTENNA DRIVE COSTS

## 1.0 INTRODUCTION

The purpose of this Tech Memo is to investigate various types of rotary drive systems for rotating the mirror array about the elevation axis and to compare these to a machine screw type linear actuator. The comparison is for cost as well as design characteristics with the costs intended to convey an approximate comparison among the various designs.

The linear actuator used for this comparison study is the type selected in Report Appendix E-3 and is shown in Figure 4. The following rotary type drive systems were sized based on brief load analyses:

- o Figure 1 Fixed open gear
- o Figure 2 Rotating Open Gear
- o Figure 3 Enclosed Gearing

## 2.1 SUMMARY

The items included in the cost comparison, Table I, are all those whose configuration is influenced by the various drive designs. Costs are relative and at this stage do not represent large production process evaluation. It can be seen from the cost and design comparisons, Table I and II respectively, that the linear actuator offers distinct advantages over rotary type drives. The principle advantages of the rotary type drive that cannot be matched by the linear actuator type selected are overall efficiency and uniform ratio over the entire travel range. As a result of the lower efficiency, the linear actuator drive requires a 1/3 HP motor compared to 1/4 HP for the rotary drive.

Table III summarizes the cost history of several rotary and linear type antenna drives. It is included herein to provide a frame of reference for the cost estimates in Table I.

## 2.2 CONCLUSIONS AND RECOMMENDATIONS

Based on this investigation, it is concluded that the machine screw type linear actuator drive recommended in Report Appendix E-3, and depicted in Figure 4, be utilized to drive the mirror array about the elevation axis.

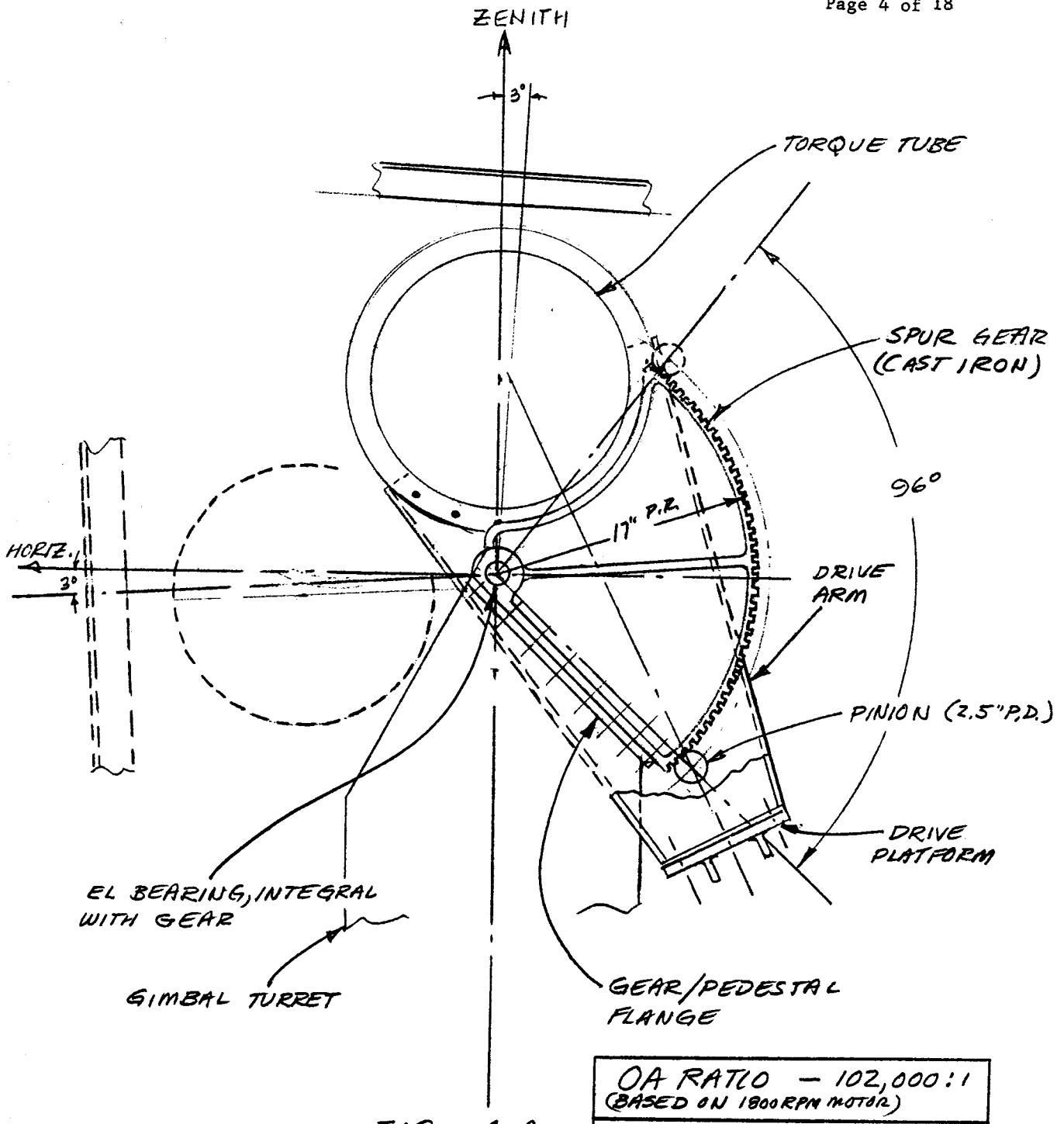


FIG 1 A

ROTARY DRIVE (FIXED OPEN GEAR)

(SIDE ELEVATION)

EM 12/5/79

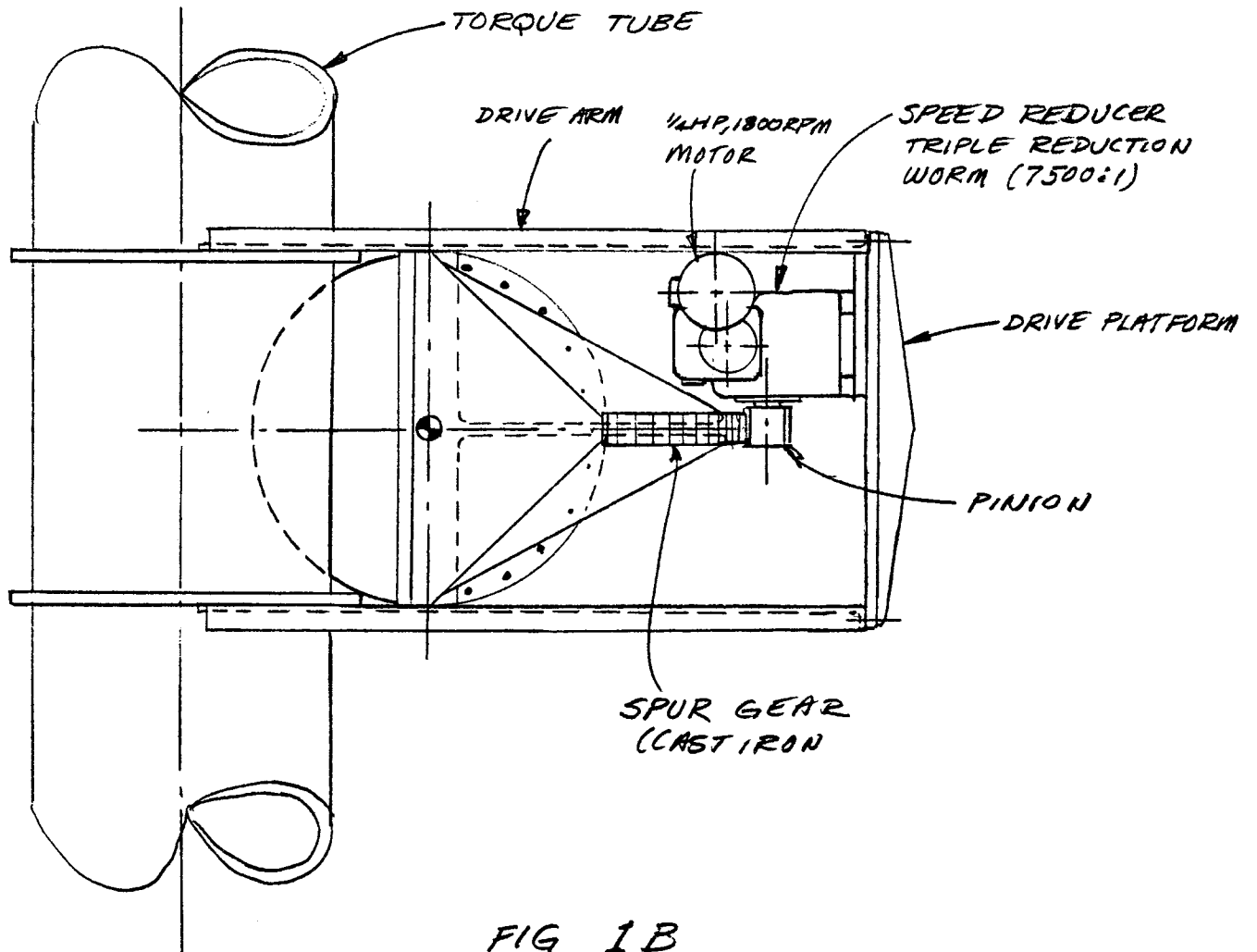


FIG 1B  
ROTARY DRIVE (FIXED OPEN GEAR)  
(PLAN VIEW)

EM 12/5/79

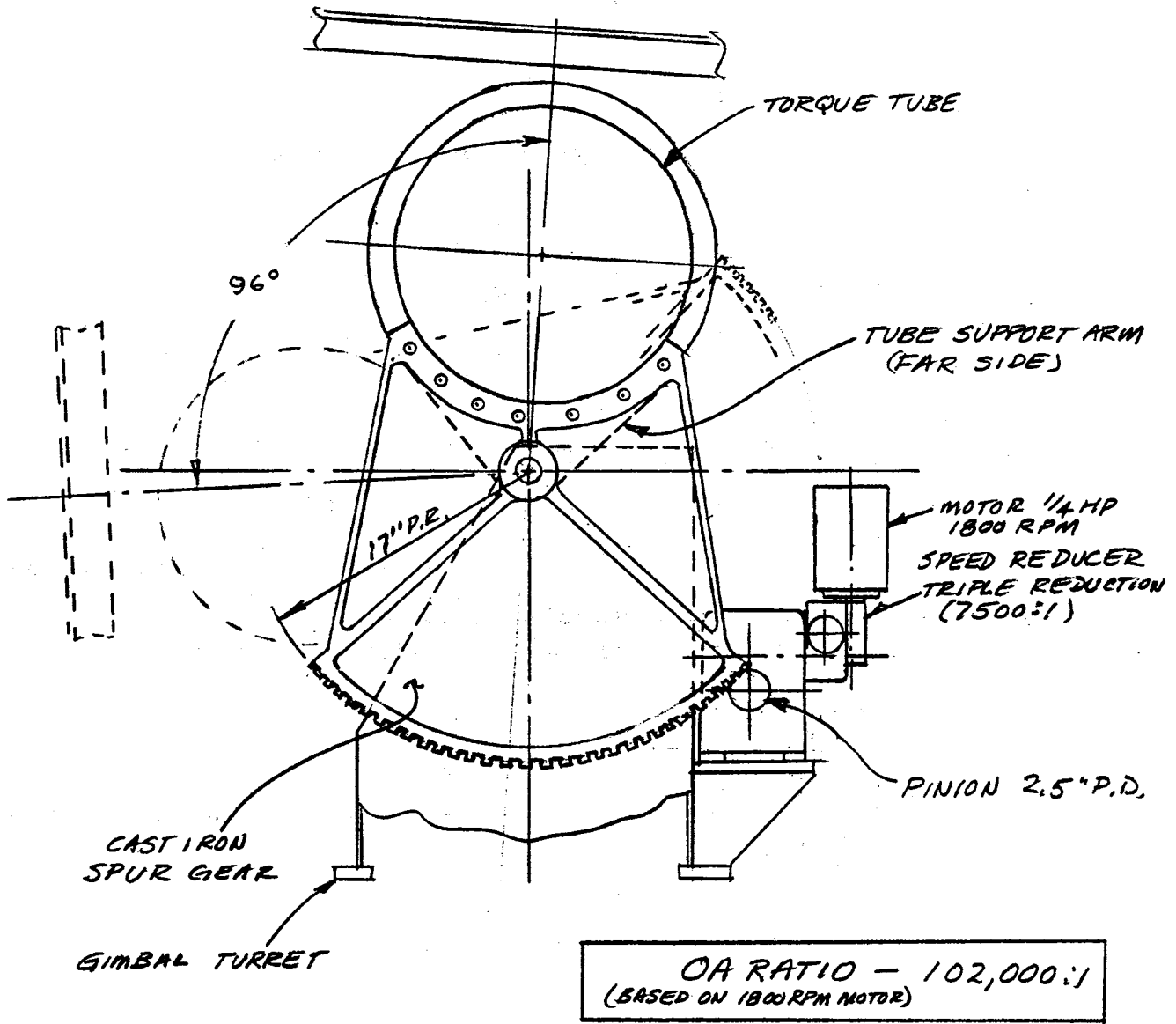


FIG. 2A  
ROTARY DRIVE (ROTATING OPEN GEAR)  
(SIDE ELEVATION)

EM 12/5/79

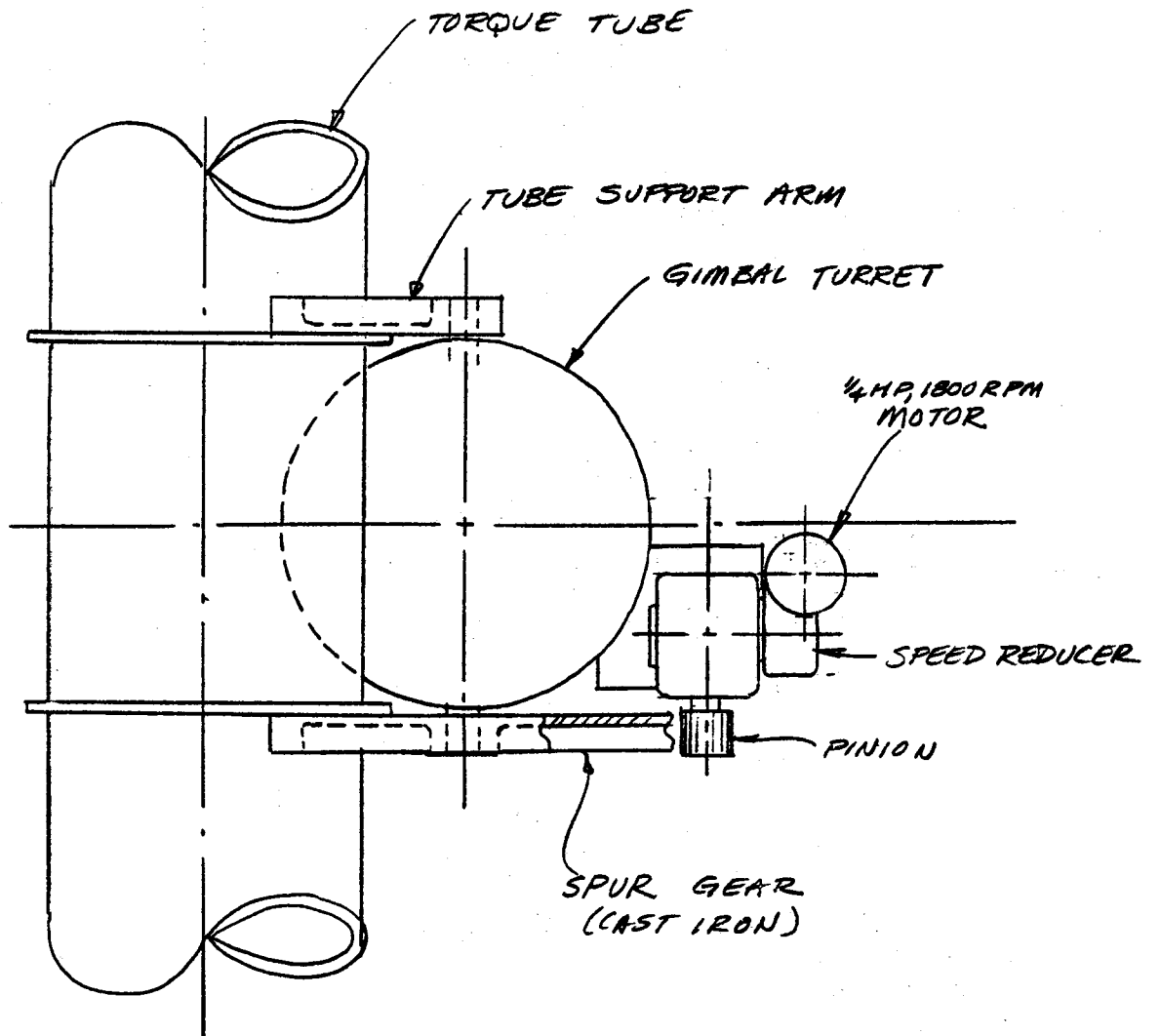


FIG. 2B  
ROTARY DRIVE (ROTATING OPEN GEAR)  
(PLAN VIEW)

EM 12/5/79

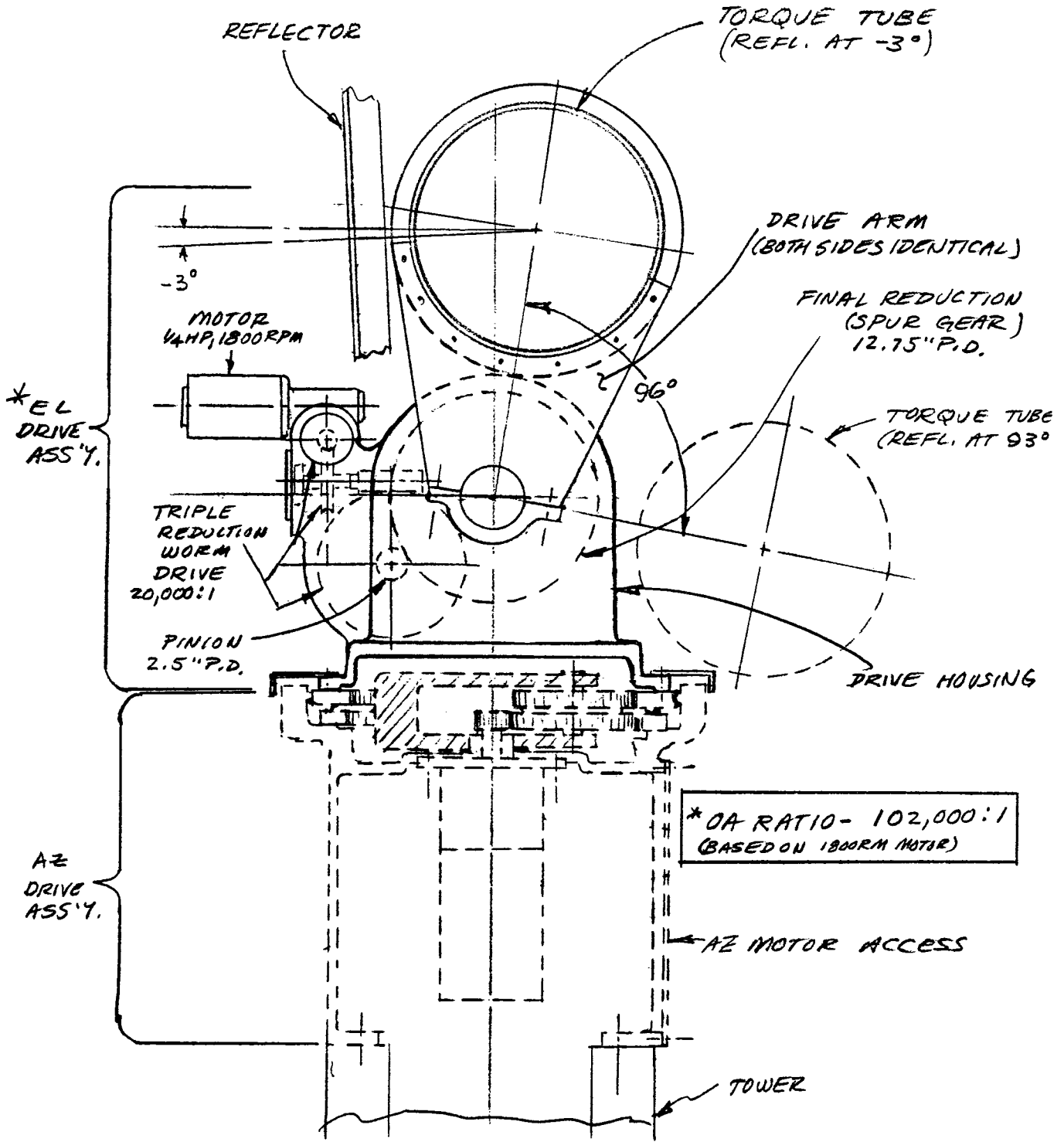


FIG 3

ROTARY DRIVE (ENCLOSED GEARING)  
(SIDE ELEVATION)

EM 12/6/79

SECT. A-A

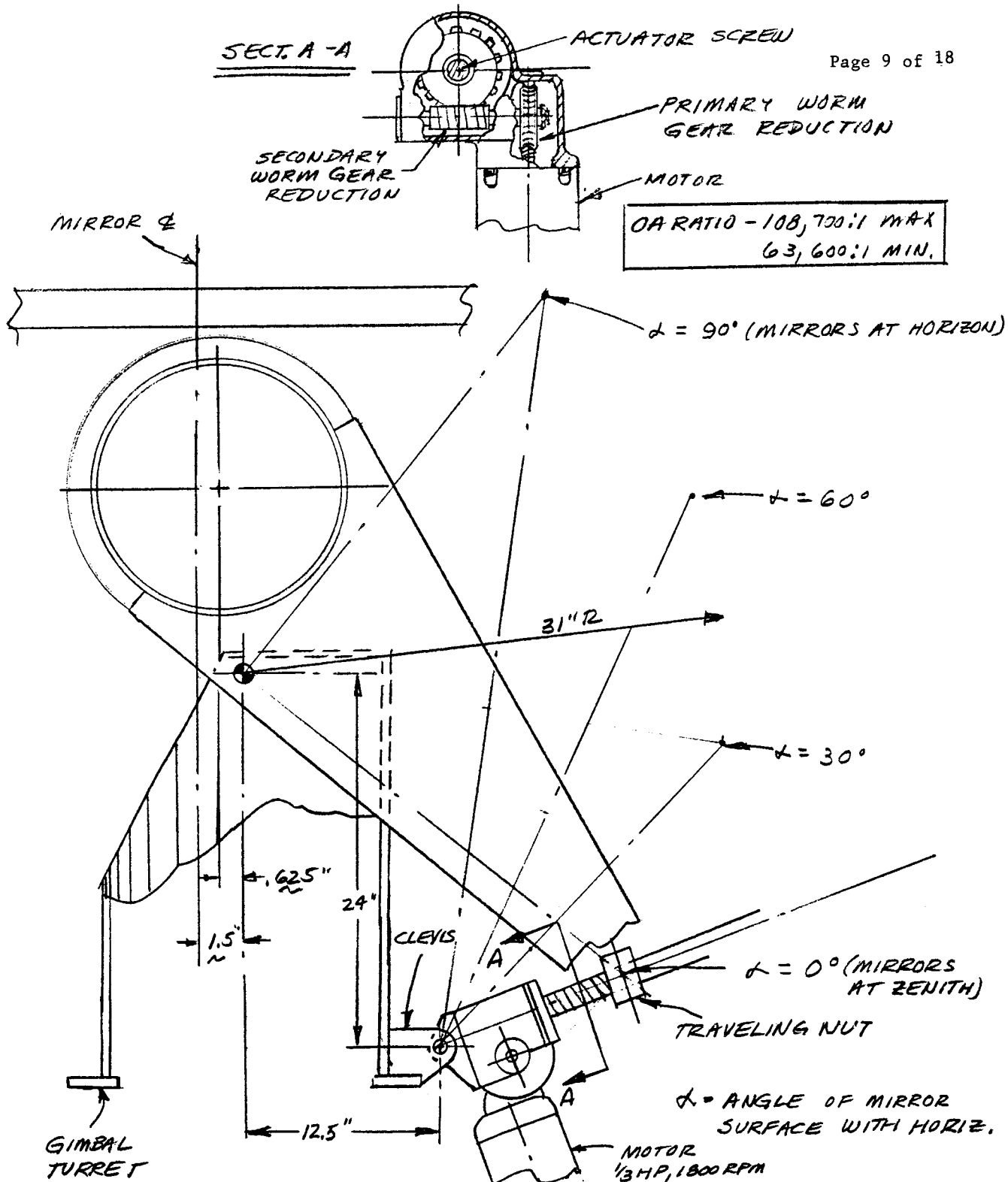


FIG 4  
LINEAR ACTUATOR DRIVE

SIDE ELEVATION  
SCALE - 1/8

EM 12/10/79



### 3.0 CALCULATIONS

#### FIGURES 1 AND 2

BULL GEAR PITCH RADIUS = 17" (34" P.D.)

PINION PITCH DIA. = 2.5"

$$\text{RATIO, FINAL REDUCTION} = \frac{34}{2.5} = 13.6 : 1$$

$$\begin{aligned} \text{REQ'D AXIS RATE} & \frac{93 \text{ DEG}}{15 \text{ MIN}} = 6.2 \text{ DEG/MIN} \\ & = .017 \text{ RPM} \end{aligned}$$

$$\text{SPEED REDUCER OUTPUT SPEED} = .017 \times 13.6 = .23 \text{ RPM}$$

$$\begin{aligned} \text{O.A. SPEED REDUCER RATIO} & = \frac{1750}{.23} = 7570 : 1 \\ \text{(ASSUMING 1750 RPM MOTOR)} & \end{aligned}$$

BASED ON FIG. 3.2.1-1 OF APPENDIX 1, BOEING SPEC., REQ'D.

$$\text{OUTPUT TORQUE OF SPEED REDUCER} = \frac{72,000 \text{ IN-LB}}{13.6} = 5295 \text{ IN-LB}$$

NEAREST AVAILABLE COMMERCIAL GEARBOX WITH  
REQ'D RATIO - WINSMITH TRIPLE REDUCTION  
SERIES MCTTW, 7500 : 1 O.A. RATIO, SIZE 7  
OT RATING - 6664 IN-LB (@ 1800 RPM INPUT)  
INPUT HP - .25  
OUTPUT TORQUE - 6414 IN-LB

$$\begin{aligned} \therefore \text{O.A. EFFICIENCY OF GEARBOX} & = \frac{6414 \times 1800}{63,000 \times .25 \times 7500} \\ & = .097 \text{ OR } 9.7\% \end{aligned}$$

$$\therefore \text{REQ'D HP} = \frac{5295 \times .23}{63,000 \times .097} = .199 \text{ HP}$$

$\therefore$  1/4 HP O.K.

### 3.0 CALCULATIONS (CONT'D.)

#### FIGS. 1 & 2 CONT'D. BULL GEAR/PINION DESIGN

ASSUME BULL GEAR IS MADE OF CAST IRON  
AGMA GRADE 40 (200 BHN MIN.)

THEN  $S_{at} = 13,000 \text{ PSI}$  (PHILY GEAR CAT. G-76 P 63)

$$\text{STR. HP RATING } P_{at} = \frac{n_p d K_v}{12600} \times \frac{F}{K_m} \times S_{at} \times \frac{J}{P_d} \times \frac{K_L}{K_S}$$

ASSUME  $6 P_d \neq 3''$  FACE WIDTH,  $20^\circ \text{ PA}$ , FULL FILLET

$$n_p = \text{PINION SPEED} = .23 \text{ RPM}$$

$$d = \text{PINION P.D.} = 2.5 \text{ IN.}$$

$$K_v = C_v = \frac{50}{50 + \sqrt{V}} = \frac{50}{50 + \sqrt{1.262 \times .23 \times 2.5}} = .99$$

$F = \text{ACTIVE FACE WIDTH, ASSUME} - 3''$

$K_m = \text{LOAD DIST. FACTOR} = 1.3$

$$S_{at} = 13,000 \text{ PSI}$$

$J = \text{GEOM. FACTOR} - .44$  (FOR GEAR)  
(15 TEETH IN PINION, 20 TEETH IN GEAR)

$$P_d = \frac{1.5}{2.5} = 6$$

$$K_L = \text{LIFE FACTOR} = 1.0$$

$$K_S = \text{SIZE FACTOR} = 1.0$$

$$P_{at} = \frac{(.23)(2.5)(.99)}{12600} \times \frac{3}{1.3} \times 13,000 \times \frac{.44}{6} \times 1.0$$

$$= .099 \text{ HP (STRENGTH RATING)}$$

$$\text{REQ'D HP AT PINION} = \frac{5295 \times .23}{63,000} = .019 \text{ HP}$$

IF FACE WIDTH IS REDUCED TO 2"

$$\text{THEN } P_{at} = .099 \left(\frac{2}{3}\right) = .066 \text{ HP} - \text{STILL OK}$$

FIGURE 3

$$\left. \begin{array}{l} \text{FINAL GEAR PD} = 12.75 \text{ IN} \\ \text{PINION P.D} = 2.5 \text{ IN} \end{array} \right\} 6 \text{ Pd}$$

$$\text{FINAL REDUCTION RATIO} = 5.1:1$$

$$\text{REQ'D AXIS RATE} = .017 \text{ RPM}$$

$$\text{PINION SPEED} = .017 \times 5.1 = .0867 \text{ RPM}$$

$$\text{O.A. RATIO, TRIPLE REDUCTION WORM} = \frac{1750}{.0867} = 20,000:1$$

BASED ON FIG. 3.2.1-1 OF APPENDIX 1 OF BOEING SPEC.  
REQ'D PINION TORQUE IS:

$$T_P = \frac{72,000}{5.1} = 14,120 \text{ IN-LB}$$

FROM WINSMITH CATALOGUE USING WORM  
GEARINGS FROM A 10MCTTW TRIPLE REDUCTION  
WORM REDUCER, OUTPUT TORQUE RATING  
FOR 20,000:1 O.A. RATIO IS 23,851 IN-LBS FOR  
1800 RPM INPUT. (THIS UNIT UTILIZES 2" C.D.,  
3" C.D. AND 6" C.D. WORM GEAR SETS FOR THE  
PRIMARY, INTERMEDIATE AND FINAL REDUCTIONS  
RESPECTIVELY)

$$\text{OUTPUT TORQUE FOR THIS UNIT IS} = 23337 \text{ IN-LB} \\ \text{FOR } \frac{1}{3} \text{ HP INPUT @ 1800 RPM}$$

$$\therefore \text{O.A. EFFICIENCY OF WORM GEARING} = \frac{23337 \times 1800}{63,000 \times .333 \times 20,000} \\ = .100 \text{ OR } 10\%$$

$$\therefore \text{REQ'D MOTOR HP} = \frac{14,120 \times .0867}{63,000 \times 0.10} = .194 \text{ HP}$$

$\therefore \frac{1}{4} \text{ HP O.K.}$

### 3.0 CALCULATIONS (CONT'D.)

#### FIG. 3 (CONT'D.)

#### BULL GEAR/PINION DESIGN

ASSUME BULL GEAR IS MADE OF THRU HARDENED STEEL W/335BHN. AND PINION IS ALSO THRU HARDENED W/375BHN.

THEN  $S_{at} = 50,000$  PSI

$$n_p = 0.0867 \text{ RPM}$$

$$d = 2.5 \text{ IN}$$

$$K_v = C_v = \frac{50}{50 + \sqrt{1.262 \times 0.0867 \times 2.5}} = .995$$

$$F = 3" \text{ (FACE WIDTH)}$$

$$K_m = 1.3$$

$$S_{at} = 50,000 \text{ PSI}$$

$$J = .434 \text{ (FOR } 20^\circ \text{ P.A. GEAR)}$$

$$P_d = 6$$

$$K_L = 1.0$$

$$K_s = 1.0$$

$$P_{at} \text{ (STRENGTH)} = \frac{P_{at} \text{ (HP RATING)}}{12600} = \frac{(0.0867)(2.5)(.995)}{12600} \times \frac{3}{1.3} \times 50,000 \times \frac{.434}{6} \times 1.0$$

$$P_{at} = .143 \text{ HP}$$

$$\text{REQ'D HP. @ PINION} = \frac{14,120 \times 0.0867}{63,000} = .019$$

THEREFOR ABOVE BULL GEAR IS O.K.

IF FACE WIDTH REDUCED TO 2"

$$\text{THEN } P_{at} = .143 \left(\frac{2}{3}\right) = .096 \text{ HP. STILL O.K.}$$

∴ MAKE GEAR 2" WIDE

### 3.0 CALCULATIONS (CONT'D.)

#### FIG. 4

EL TRAVEL  $93^\circ$  IN 15 MINUTES

FROM FIG. 4 STROKE =  $49.5 - 10.3 = 39.2$

$$\text{REQ'D LINEAR SPEED} = \frac{39.2}{15} = 2.6 \text{ IN/MIN.}$$

ST'D RATIO FOR DUFF-NORTON 1805 ACTUATOR  
IS 16 TURNS OF INPUT SHAFT FOR 1 INCH RAISE

$$\therefore \text{WORM SPEED} = 16 \times 2.6 = 42 \text{ RPM}$$

THEN SPEED REDUCER RATIO FOR 1750 RPM MOTOR

$$\text{IS} = \frac{1750}{42} = 41.7:1$$

FROM FIG 4 & FIG 3.2.1-1 →

MAX. ACTUATOR LOAD  $L_A$  FOR 27 MPH  
WIND + GRAVITY = 4110 Lb

PER DUFF-NORTON CATALOGUE

$$\text{INPUT TORQUE} = \frac{4110 \times 230}{5000}$$

$$= 189 \text{ IN-LB}$$

THIS IS ALSO MIN. REQ'D RATED O.T. FOR  
SPEED REDUCER.

WINSMITH IMCT 40:1 RATED 214 IN-LB O.T.  
AT 1800 RPM INPUT. AND 0.36 INPUT HP

$$\text{REQ'D MOTOR SIZE} = \frac{189 \times 0.36}{214} = .32 \text{ HP}$$

USE  $\frac{1}{3}$  HP, 1800 RPM MOTOR

27 MPH WIND + GRAV.			
$\alpha$	R (INCH)	MA (IN-LB)	LA (LB)
0	26.9	22,000	820
30	25.6	60,000	2350
60	21.5	72,000	3350
90	15.8	65,000	4110

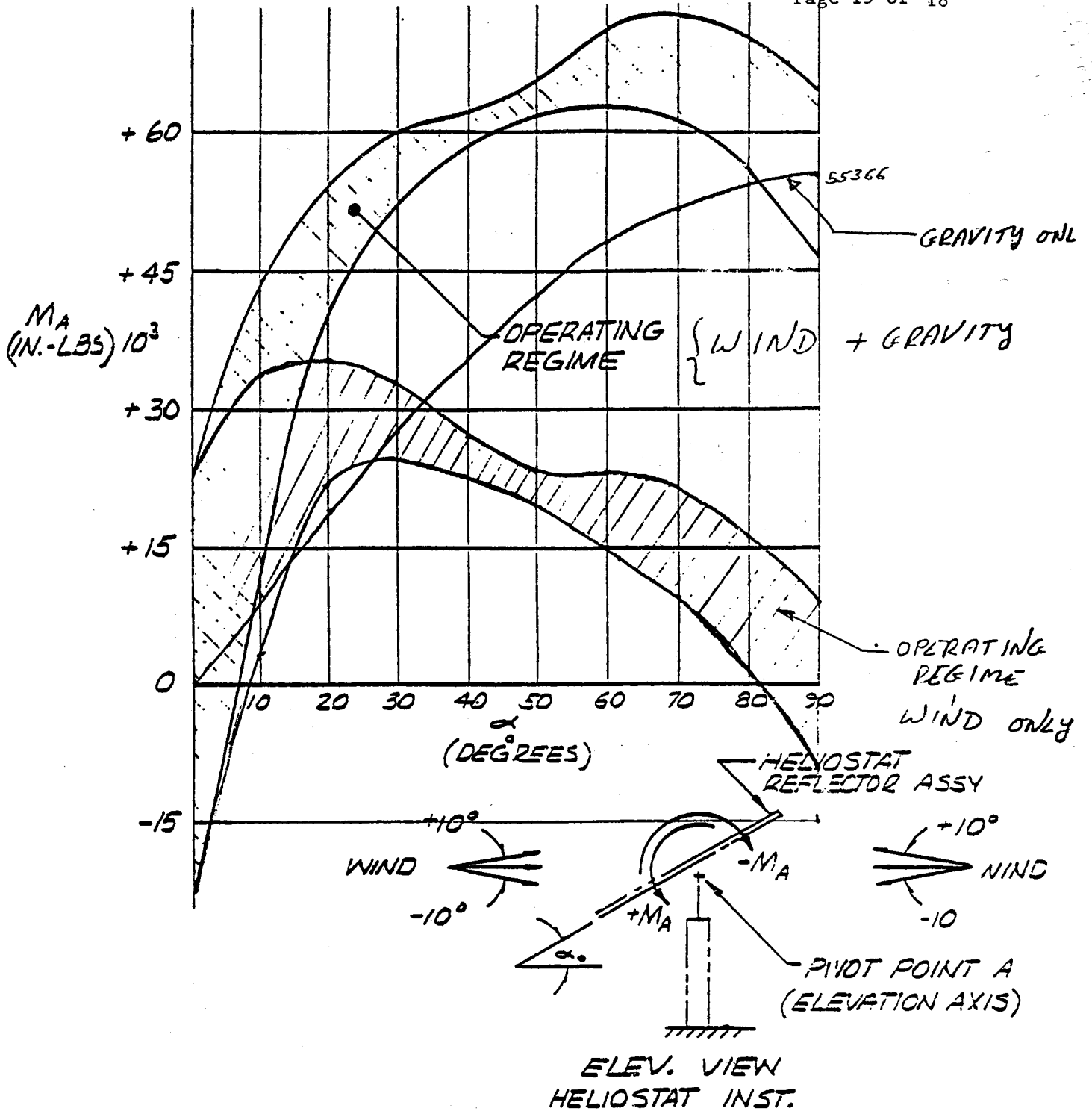


FIGURE 3.2.1-1  
 NORMAL OPERATING CONDITIONS  
 ELEVATION AXIS TORQUE LOADS  
 $M_A = \Sigma (27 \text{ MPH WINDS}) + (\text{GRAVITY})$

FROM APPENDIX I  
 BOEING SPECS.

TABLE I - COST COMPARISON

	CONCEPT								
	FIG. 1		FIG. 2		FIG. 3		FIG. 4		
	QTY. 1	QTY. 50K	QTY. 1	QTY. 50K	QTY. 1	QTY. 50K	QTY. 1	QTY. 50K	
SPUR GEAR	WT.(Lb)	180		90		55		X	
	\$/Lb	10	3	10	3	12	4		
	\$	1800	540	900	270	660	220		
SPEED REDUCER.	WT.(Lb)	135		135		220		X	
	\$/Lb	11	4	11	4	12	4.5		
	\$	1485	540	1485	540	2640	990		
PINION	WT.(Lb)	4		4		4		X	
	\$/Lb	35	10	35	10	35	10		
	\$	140	40	140	40	140	40		
DRIVE HOUSING OR GIMBAL TURRET	WT.(Lb)	110		125		200		140	
	\$/Lb	7	2	7	2	5	2.5	6.5	2
	\$	770	220	875	250	1000	500	910	280
ACTUATOR ASSEMBLY (INCLUDING NUT)	WT.(Lb)	X		X		X		75	
	\$/Lb							7.0	3.0
	\$							525	225
NUT HOUSING (TRUNION)	WT.(Lb)	X		X		X		15	
	\$/Lb							10	3
	\$							150	45
CLEVIS PIN	WT.(Lb)	X		X		X		5	
	\$/Lb							8	3
	\$							40	15
DRIVE ARMS	WT.(Lb)	45		X		20		40	
	\$/Lb	6	2			7	2	6.5	2
	\$	270	90			140	40	260	80
TUBE SUPPORT ARM	WT.(Lb)	X		17		X		X	
	\$/Lb			9.5	2.5				
	\$			160	43				
DRIVE PLATFORM	WT.(Lb)	10		X		X		X	
	\$/Lb	5	2.5						
	\$	50	25						
MOTOR	\$	80	35	80	35	80	35	90	40
TOTAL UNIT COST - \$		4595	1490	3640	1178	4660	1825	1975	685

TABLE II  
DESIGN COMPARISON

CONCEPT	ADVANTAGES	DISADVANTAGES
FIG. 1	<ol style="list-style-type: none"> <li>1. KINEMATIC ACCURACY MACHINED INTO SINGLE CASTING</li> <li>2. OA RATIO CONSTANT THROUGHOUT TRAVEL RANGE</li> </ol>	<ol style="list-style-type: none"> <li>1. GREATER ERECTION TIME: <ul style="list-style-type: none"> <li>• SET BACKLASH</li> <li>• ALIGN GEAR/PINION MESH</li> </ul> </li> <li>2. INCREASED COST</li> <li>3. REDUCER DESIGNED FOR STIFFNESS NOT TORQUE</li> <li>4. EXPOSED GEAR</li> <li>5. TRAVELING REDUCER</li> </ol>
FIG. 2	<ol style="list-style-type: none"> <li>1. DITTO ABOVE</li> <li>2. STATIONARY REDUCER</li> </ol>	<ol style="list-style-type: none"> <li>1. DITTO 1-4 ABOVE</li> <li>2. ASYMMETRICAL TORQUE ON TUBE</li> </ol>
FIG. 3	<ol style="list-style-type: none"> <li>1. ALL GEARING ENCLOSED</li> <li>2. OA RATIO CONSTANT THROUGHOUT TRAVEL RANGE</li> <li>3. AZ <math>\frac{1}{2}</math> EL DRIVES FACTORY ASSEMBLED: <ul style="list-style-type: none"> <li>• REDUCED ERECTION TIME</li> <li>• BUILT-IN BACKLASH AND GEAR MESH ACCURACY</li> </ul> </li> </ol>	<ol style="list-style-type: none"> <li>1. INCREASED COST (BOTH AZ <math>\frac{1}{2}</math> EL)</li> <li>2. REDUCER DESIGNED FOR STIFFNESS NOT TORQUE</li> <li>3. REQUIRES GAP IN MIRRORS TO CLEAR TOWER</li> <li>4. COMPLICATES AZ DRIVE: <ul style="list-style-type: none"> <li>• AZ MOTOR ACCESS</li> <li>• OIL RETENTION</li> </ul> </li> </ol>
FIG. 4	<ol style="list-style-type: none"> <li>1. LOWER COST</li> <li>2. SIZED FOR LOAD NOT STIFFNESS</li> <li>3. REDUCED ERECTION TIME: <ul style="list-style-type: none"> <li>• PROPER BACKLASH AUTOMATIC</li> <li>• NO GEAR MESHES TO ALIGN</li> <li>• TWO-PIN CONNECTION</li> </ul> </li> <li>4. STATIONARY (NON-TRANSLATING) REDUCER</li> <li>5. QUICK CHANGEOUT IF NEEDED</li> </ol>	<ol style="list-style-type: none"> <li>1. LARGER MOTOR</li> <li>2. KINEMATIC ACCURACY DERIVED FROM TWO MATING PIECES.</li> <li>3. OA RATIO VARIES OVER TRAVEL RANGE</li> </ol>



**TABLE III**  
**TYPICAL ANTENNA DRIVE COSTS**

PROGRAM	QTY	ITEM	YEAR	WT.(LB)	\$/LB	\$/K	REMARKS
USASCA 60' HT	2	AZ GEARBOX	1979	3000	8.7	26.0	CUSTOM BUILT TO FACC SPECS
30 M TELESPAZIO	4	EL GEARBOX	1978	1100	3.6	4.0	MODIFIED STANDARD (SUMITOMO)
	4	AZ GEARBOX		5400	2.25	12.0	
SCT-8	21	EL ACTUATOR	1978	20	12.5	0.25	2 TON, 18" RAISE TRANS. MACH. SCREW WITH ANTI-B.L. NUT & BOOT. (DUFF-NORTON)
NATO III	9	AZ ACTUATOR	1979	300	6.3	1.9	25 TON, 31" RAISE TRANS. BALL SCREW (DUFF-NORTON)
	9	EL ACTUATOR		600	4.6	2.8	25 TON, 14" RAISE TRANS. BALL SCREW (DUFF-NORTON)
BOEING	2	NUT TEST RIG	1979	20	12.8	0.26	2 TON, 10" RAISE TRANS. NUT (BRONZE) (DUFF-NORTON)
10 M INDONESIA ANTENNA	15	HA ACTUATOR	1975	300	3.0	0.9	25 TON, 37" RAISE TRANS. MACH. SCREW, ANTI-B.L. NUT, LIMIT SWITH PKG. (DUFF-NORTON)

NOTE: MOTOR, BRAKE AND COUPLINGS  
NOT INCLUDED IN ABOVE COSTS



REPORT E-3

ELEVATION ACTUATOR TRADE STUDIES

FOR

GIMBAL/ACTUATOR DRIVE ASSEMBLY

FOR

BOEING SECOND GENERATION HELIOSTAT

JUNE 27, 1980

Reference: FACC TM03



**Ford Aerospace &  
Communications Corporation**

TABLE OF CONTENTS

Section

1.0 Introduction

2.0 Summary

3.0 Conclusions and Recommendations

Appendix A Comparison of Various Actuator Designs

Appendix B Comparison of Ball Screw & Machine Screw

## 1.0 INTRODUCTION

The purpose of this technical memo is two fold.

1. To investigate various actuator designs and to compare them for advantages and disadvantages when used as an elevation actuator for a heliostat.
2. To compare machine screw vs ball screw for the actuator in this application.

## 2.0 SUMMARY

### Actuator Concepts:

Various actuator designs are compared in Appendix A and their advantages and disadvantages are tabulated on page 18. The four designs that were investigated are as follows:

1. Baseline proposal design using a non-rotating screw and a rotating nut with a boot cover.
2. Design using a rotating screw and a non-rotating, translating metal nut with a boot cover.
3. Design using a rotating screw and a non-rotating translating polymeric nut without a boot cover.
4. Baseline design with an extended housing to keep the threaded portion of the screw inside the housing (no boot).

From the summary on page 18, it is seen that concept number 3 does not need any boot nor any lubrication at the nut to screw interface. Therefore, if exposure of this interface to open environment does not cause any problem, this option is very attractive. It is recommended to proceed with this concept and conduct operational tests on the units.

### Machine Screw Vs Ball Screw:

Machine screw and ball screw are compared in Appendix B. It is seen that the ball screw is about 3 times more efficient and consequently the elevation drive motor would be one third as big, however, the ball screw for the same size is about 30% more expensive, will need lubrication and a boot cover, and will have much higher lead error resulting in larger pointing error. It is recommended to use the machine screw.

3.0 CONCLUSIONS AND RECOMMENDATIONS

From this investigation, it is recommended that the heliostat elevation drive utilize a rotating machine screw with a traveling nut without a boot. Different materials for the nut will be tested for this application and an appropriate material will be selected at the conclusion of the tests.

**APPENDIX A**  
**COMPARISON OF ACTUATOR DESIGNS**

COMPARISON OF VARIOUS ACTUATOR DESIGNS

PURPOSE: The object of this analysis is to investigate various actuator designs and to compare them for advantages and disadvantages. Any of the discussed designs can use either machine screw or ball screw.

ANALYSIS

DESIGN OPTION #1:

Concept using proposal design with fixed screw and rotating nut & translating housing at the upper end with boot between upper end and lower end - See Figures 1a and 1b.

ADVANTAGES:

1. Short load path - from one hinge point to other hinge point resulting in high stiffness.
2. Conventional design
3. Only one lubrication point at the housing.
4. Can incorporate anti-backlash feature at minimal added cost.

DISADVANTAGES:

1. Need to use a boot cover to protect the screw.
2. Difficult to retain lubricant in the housing as housing moves up and down on threaded part of the screw. Gravity helps lubricant to leak out.

ALTERNATE:

A similar concept with a fixed screw and a rotating nut could be utilized in an inverted position concept.

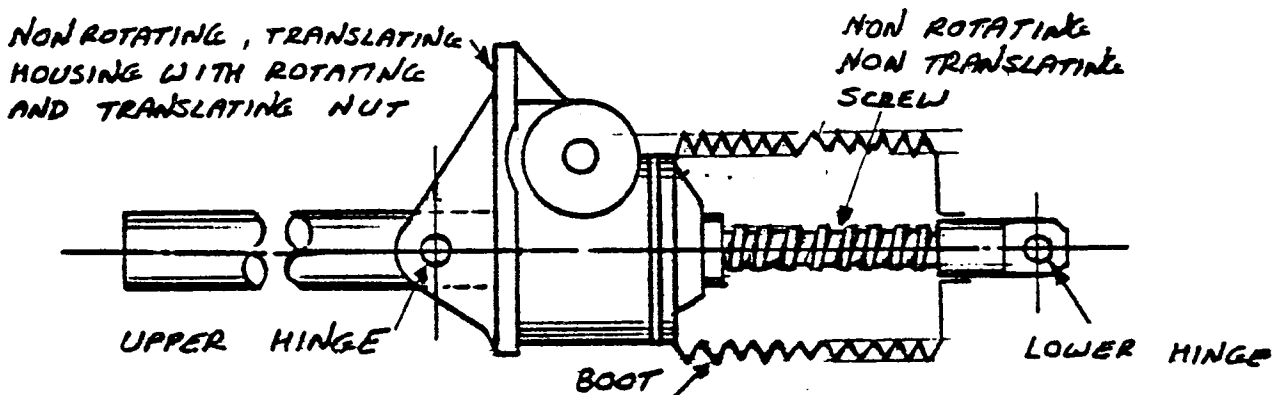
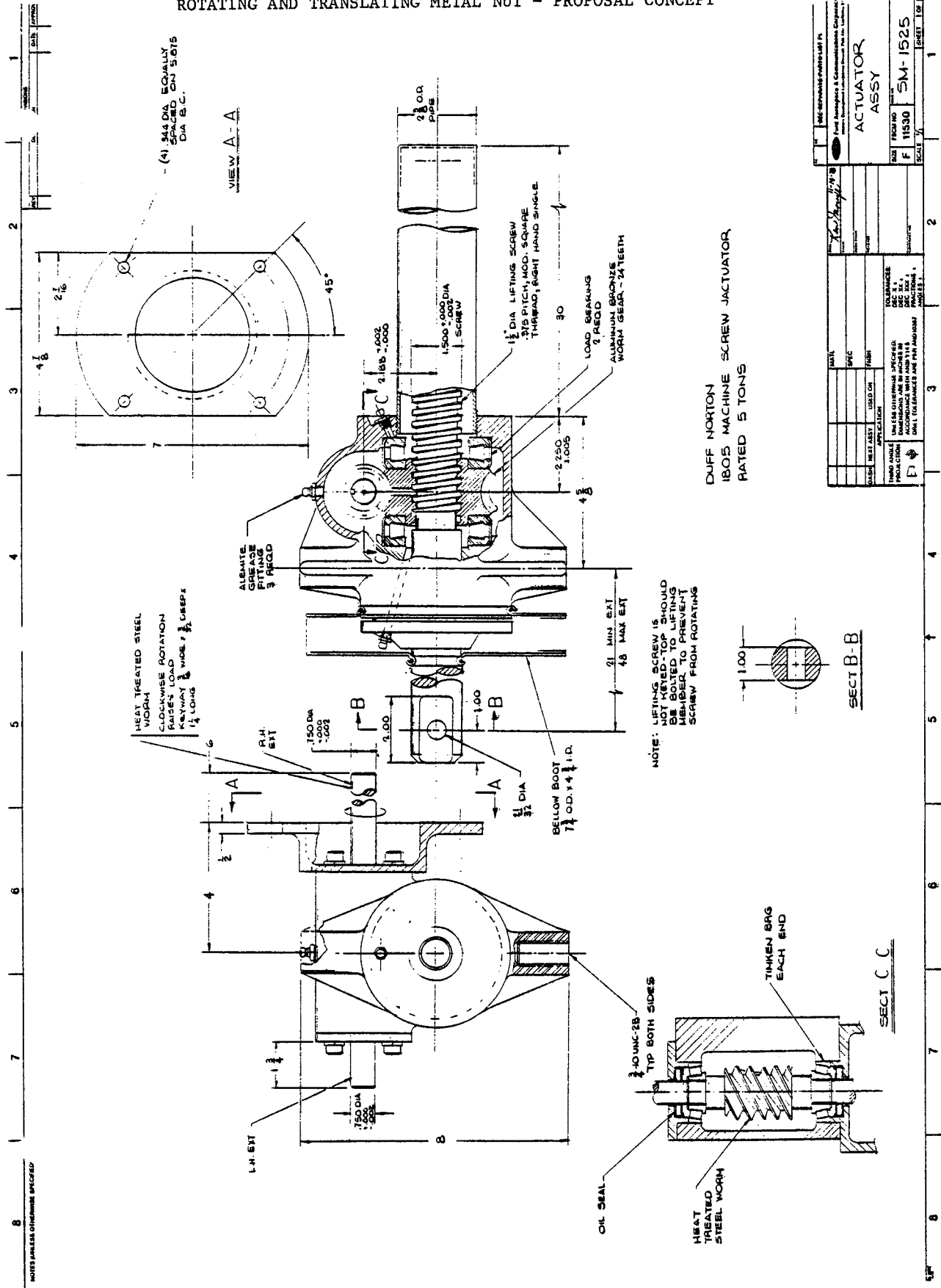


Figure 1a



Figure 1b  
 ROTATING AND TRANSLATING METAL NUT - PROPOSAL CONCEPT



DUFF NORTON  
 1805 MACHINE SCREW JACTUATOR  
 RATED 5 TONS

DATE	DRAWN	CHECKED	APPROVED	APPLICATION
TOLERANCES UNLESS OTHERWISE SPECIFIED: DIMENSIONS ARE IN INCHES UNLESS OTHERWISE INDICATED. FINISHES:				
SIZE	FROM NO	DATE	SCALE	SHEET NO
F 1530	5M-1525			1

SECTION B-B

SECTION C-C

NOTES: DIMENSIONS UNLESS OTHERWISE SPECIFIED

DESIGN OPTION #2:

Concept using translating non-rotating nut at the upper end, rotating and non-translating screw and non-translating housing at the lower end with a boot cover between the nut and housing - see Figure 2.

ADVANTAGES:

1. Short load path - from one hinge point to other hinge point resulting in high stiffness.
2. Conventional design
3. Portion of the screw going into the housing is cylindrical resulting in easy sealing between screw and housing.
4. Simplified wiring harness to motor since housing does not translate.

DISADVANTAGES:

1. Two lubrication points, one at nut and one at housing.
2. Need to use a boot cover to protect the screw.
3. Difficult to retain lubricant in the nut as the nut moves up and down on threaded part of the screw. Gravity helps lubricant to leak out.
4. No standard design for anti-backlash arrangement.

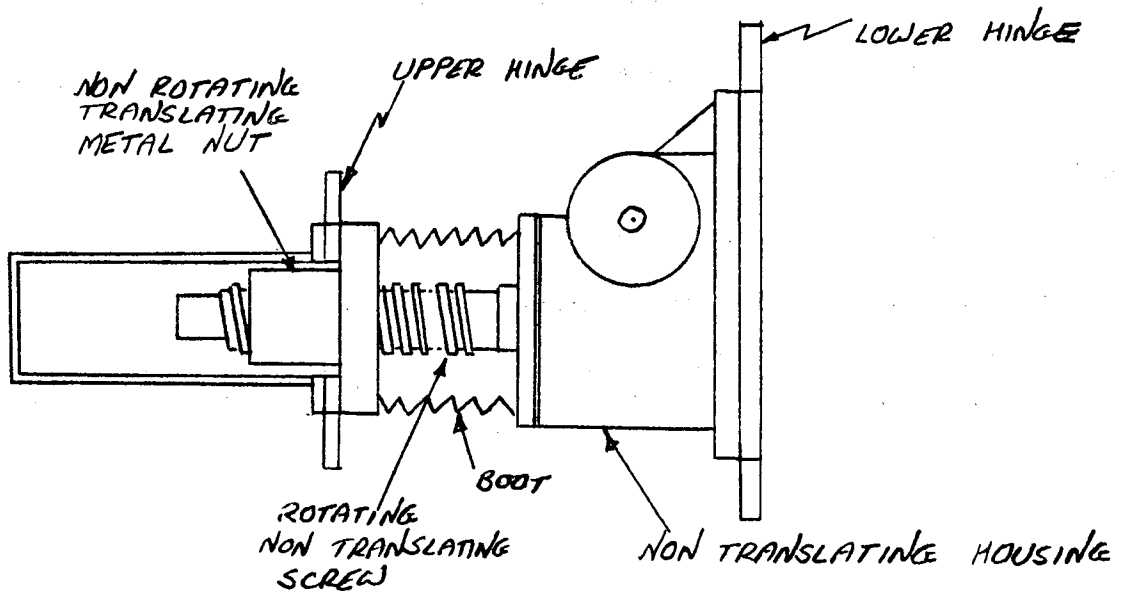


FIGURE 2

NON ROTATING METAL NUT

DESIGN OPTION #3

Same as concept #2 except for use on polymeric nut without a boot cover - see Figure 3.

ADVANTAGES:

1. No boot and no steel cover required.
2. No lubrication required between plastic nut and metal screw as there is no metal-to-metal contact.
3. Portion of the screw going into the housing is cylindrical, resulting in easy sealing between screw and housing.
4. Short load path - from one hinge point to other hinge point resulting in high stiffness.
5. Simplified wiring harness to motor since housing does not translate.

DISADVANTAGES:

1. Requires plating or stainless steel screw to prevent corrosion, resulting in increased costs.
2. Requires testing to determine if sand and debris in the threads cause unacceptable wear or performance.
3. Coefficient of thermal expansion for the proposed polymeric nut material is greater than that of steel. This will require additional backlash to avoid jamming at extreme ambient temperatures.
4. No standard design available for antibacklash feature.

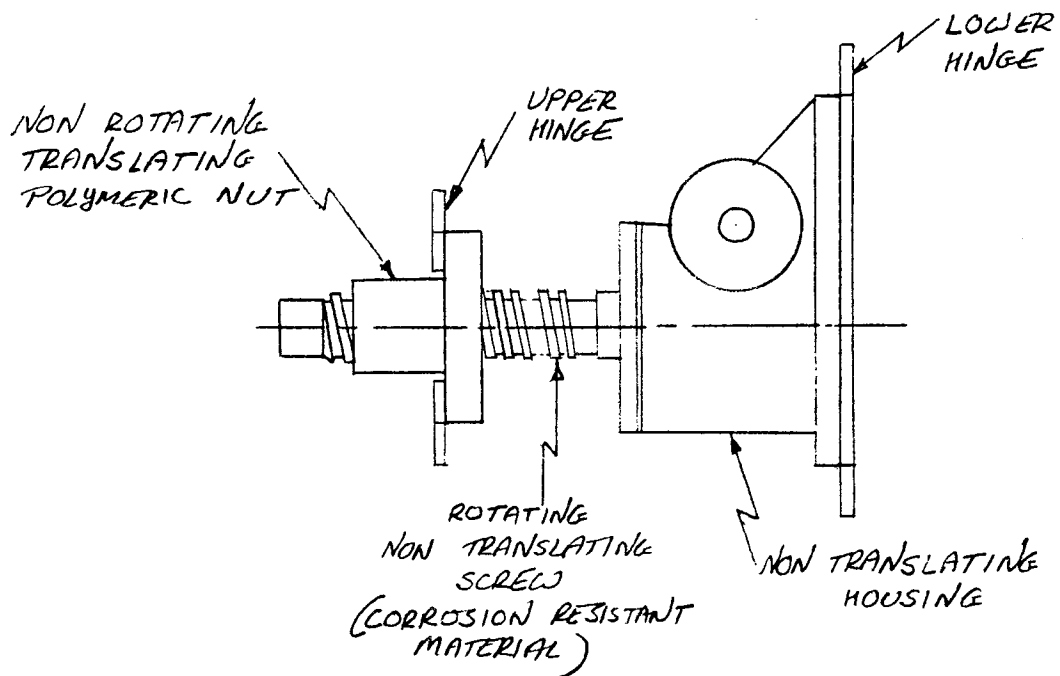


FIGURE 3

USE OF POLYMERIC NUT

DESIGN OPTION #4

Concept similar to option 1 with actuator housing and screw length extended such that the portion of the screw protruding out of actuator housing is cylindrical (without thread). Threaded portion stays inside the housing - see Figure 4.

ADVANTAGES:

1. No boot required.
2. Easy to retain lubrication in actuator housing because the portion of the screw protruding out of actuator housing is cylindrical and threaded portion stays inside the housing.

DISADVANTAGES:

1. Cost of screw increases because of
  - a. Increased length. Increase in length compared to other options = stroke.
  - b. Portion of the screw protruding out of actuator housing has to be plated for corrosion resistance.
2. Cost of actuator housing increases because of added length.
3. Compliance of actuator increases because of added screw length and added housing length. Loaded portion is the screw from lower hinge to nut and the housing from nut to upper hinge.
4. Overall length is overall length of other options plus stroke. (For present design extended length = 10 ft vs 7 ft).
5. Screw is subjected to added gravity moment because of added housing weight. This also causes added loads on the hinges.
6. Complicates wiring harness to motor since housing translates.

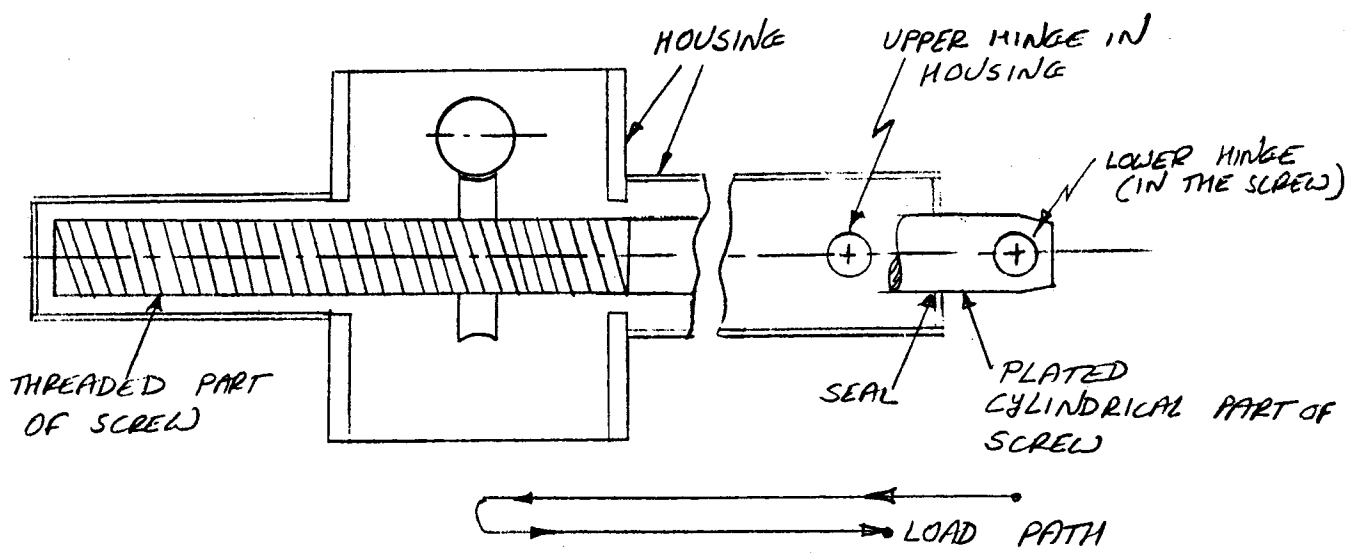


FIGURE 4

USE OF LONG SCREW WITH CYLINDRICAL PORTION

DESIGN CALCULATIONS FOR OPTION #4  
ESTIMATE OF ADDED COMPLIANCE:

ASSUME THE FOLLOWING:

1. 30 INCH ADDED LENGTH OF 1.5 INCH ROD - STEEL
2. 30 INCH LENGTH OF STEEL TUBE BETWEEN UPPER HINGE & WORM - 2 1/2" SCH. 80 PIPE - 2.875" O.D. x 2.323 I.D.
3. MOMENT ARM = 12 INCH

ADDED AXIAL COMPLIANCE

$$C_A = \left(\frac{L}{AE}\right)_{\text{SCREW}} + \left(\frac{L}{AE}\right)_{\text{PIPE}}$$

$$A_{\text{PIPE}} = \frac{\pi}{4} (2.875^2 - 2.323^2)$$

$$= 2.25 \text{ SQ INCH}$$

$$A_{\text{SCREW}} = \frac{\pi}{4} (1.5)^2$$

$$= 1.77 \text{ SQ INCH}$$

$$C_A = 30 \left[ \frac{1}{1.77 \times 30 \times 10^6} + \frac{1}{2.25 \times 30 \times 10^6} \right]$$

$$= 30 \left[ 1.88 \times 10^{-8} + 1.48 \times 10^{-8} \right]$$

$$= 1.0 \times 10^{-6} \text{ INCH/LB}$$

AXIS ROTARY COMPLIANCE

$$= \frac{C_A}{(\text{MOMENT ARM})^2} = \frac{1 \times 10^{-6}}{(12)^2} = 0.7 \times 10^{-8} \text{ RAD/IN LBS}$$

27 MPH WIND TORQUE = 33360 IN LBS MAX.

THEREFORE, MAXIMUM ADDED POINTING ERROR

$$= 1.4 \times 10^{-8} \times 33360 = 2.3 \times 10^{-4} \text{ RADIANS}$$

$$= 0.23 \text{ MR}$$



ESTIMATE OF ADDED WEIGHT :

WITH THE ASSUMPTIONS ON PREVIOUS PAGE

ADDED STEEL WEIGHT =  $30 \times 1.77 \times 0.283 = 15 \text{ LBS} - \text{SCREW}$

ADDED STEEL WEIGHT =  $30 \times 2.25 \times 0.1 = 19 \text{ LBS} - \text{PIPE}$

STEEL STUFFING BOX -  $5'' \times 4'' \times 2''$ , W =  $5 \times 4 \times 2 \times 0.283 = 11 \text{ LBS}$

ESTIMATE OF TOTAL WEIGHT :

FOR 6 INCH RAISE,

WEIGHT OF DUFF NORTON 5 TON JACK = 35 LBS

WEIGHT FOR EACH ADDITIONAL 1 INCH RAISE = 0.85 LBS

THEREFORE FOR 30" RAISE

WEIGHT FOR DUFF NORTON 5 TON JACK

=  $35 + (30 - 6) \times 0.85$

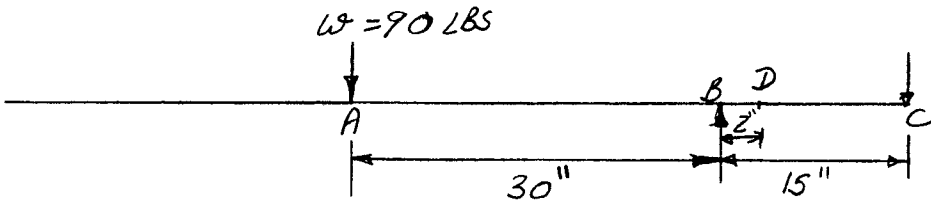
= 55 LBS

INCLUDING THE ADDITIONAL WEIGHT CALCULATED ABOVE

TOTAL ESTIMATED WEIGHT =  $55 + 15 + 19 + 11$

= 100 LBS

ESTIMATE OF MOMENT ON THE SCREW :



B & C ARE THE ACTUATOR HINGE POINTS & THEY ARE APPROXIMATELY 15 INCH APART WHEN ACTUATOR IS IN HORIZONTAL ORIENTATION. D IS THE POINT WHERE SCREW EXITS FROM THE HOUSING.

OUT OF TOTAL 100 LBS. ASSUMED OVERHUNG WEIGHT = 90 LBS

MOMENT AT D,  $M = 90 \times \frac{30}{15} (15-2)$   
 $= 2340 \text{ IN LBS}$

BENDING STRESS

$$\sigma = \frac{M}{Z}$$

WHERE  $Z =$  SCREW SECTION MODULUS

$$= \frac{\pi}{32} (1.5)^3$$
$$= 0.33 \text{ IN}^3$$

STRESS  $\sigma = \frac{2340}{0.33}$   
 $= 7100 \text{ PSI.} \quad \text{--- LOW} \quad \underline{\text{O.K.}}$

ESTIMATE OF ADDED COST — PRODUCTION UNITS

ADDED PIPE — ASSUME @ \$1.00/LB = \$19.0

ADDED SCREW WEIGHT

— ALLOY STEEL

— PLATED

ASSUME @ \$2.00/LB = \$30

STUFFING BOX: ASSUME \$11 ADDITIONAL OVER BASELINE

PROPOSAL CONCEPT

REDUCTION DUE TO BOOT — ASSUME \$15

THUS, ADDED COST =  $19 + 30 + 11 - 15$   
 $= \$45$

SUMMARY FOR OPTION #4:

- a. Added weight = 45 lbs.
- b. Added cost = \$45
- c. Added bending stress in screw = 7100 PSI
- d. Added pointing error in worst orientation 27 MPH wind = 0.23 mr

SUMMARY

OPTION FEATURE	#1 PROPOSAL BASELINE DESIGN	#2, NONROTATING TRANSLATING METAL NUT	#3, NON ROTATING TRANSLATING POLYMERK NUT	#4, BASELINE DESIGN WITH EXTENDED HOUSING
SCREW	NON ROTATING NON TRANSLATING	ROTATING NON TRANSLATING	ROTATING NON TRANSLATING	NON ROTATING NON TRANSLATING
NUT	ROTATING TRANSLATING	NON ROTATING TRANSLATING	NON ROTATING TRANSLATING	ROTATING TRANSLATING
HOUSING	TRANSLATING	NONTRANSLATING	NON TRANSLATING	TRANSLATING
BOOT (MAY NEED PERIODIC REPLACEMENT)	BETWEEN HOUSING & END OF SCREW	BETWEEN NUT AND HOUSING	NONE	NONE
DESIGN	CATALOG ITEM	CATALOG ITEM	NON CATALOG ITEM	NON CATALOG ITEM
LUBRICATION POINTS	AT HOUSING	AT HOUSING & AT NUT	AT HOUSING	AT HOUSING
ANTIBACKLASH FEATURE *	CATALOG ITEM	NON CATALOG ITEM	NON CATALOG ITEM	CATALOG ITEM
LUBRICANT RETENTION	DIFFICULT TO RETAIN IN HOUSING BECAUSE THREADED PART OF SCREW MOVES IN & OUT OF HOUSING.	FOR THE SAME REASON EASY TO RETAIN IN HOUSING BUT DIFFKULT TO RETAIN IN NUT	EASY TO RETAIN IN HOUSING, NO LUBKATION AT NUT	EASY TO RETAIN IN HOUSING BECAUSE CYLINDRICAL PART OF SCREW MOVES IN & OUT OF HOUSING
LOAD PATH-COMPLIANCE	SHORT LOAD PATH & LOW COMPLIANCE	SAME AS BASELINE	SAME AS BASELINE	LONG LOAD PATH, HIGH COMPLIANCE ADDED ERROR OF 0.23 MR IN 27 MPH WORST CASE WIND
BACKLASH	LOW	SAME AS BASELINE	HIGH BECAUSE OF HIGH EXPANSION COEFFKIENT OF NUT	SAME AS BASELINE
ENVIRONMENT PROTECTION OF NUT TO SCREW INTERFACE	GOOD	GOOD	SAND PARTICLES CAN JAM THE NUT	GOOD
PRODUCTION COST - INITIAL	—	SAME AS BASELINE	SAME - NO BOOT & CAN BUT PLATED SCREW	\$ 45 MORE THAN BASELINE

\* OPTIONAL, MAY NOT BE NECESSARY

APPENDIX B

COMPARISON OF MACHINE SCREW AND BALL SCREW

PURPOSE: TO COMPARE MACHINE SCREW AND BALL SCREW FOR ELEVATION ACTUATOR.

COMPARISION:

	BALL SCREW	MACHINE SCREW
1. ANTIBACKLASH FEATURE	NO STANDARD DESIGN AVAILABLE.	STANDARD DESIGN WITH VARIOUS ACTUATOR MANUFACTURERS.
2. BACKLASH (PER DUFF NORTON CATALOG)	0.005 TO 0.010 INCH	0.008 TO 0.013 NORMAL, 0.003 TO 0.004 WITH ANTIBACKLASH DESIGN
3. EFFICIENCY & MOTOR SIZE (PER DUFF NORTON CATALOG)	39 % AT FULL LOAD, NON SELF LOCKING	12.1 % AT FULL LOAD, MOTOR WILL BE APPROX 3 TIMES LARGER, SELF LOCKING WITH OPTION RATIO WORM GEARING
4. PRODUCTION COST	PER DUFF NORTON BALL SCREWS WILL BE APPROX. 30 % MORE EXPENSIVE, \$400 VS \$300 FOR 5 TON ACTUATOR	
5. LEAD ERROR (PER DUFF NORTON CATALOG)	0.045 INCH MAX. FOR 30 INCH STROKE	0.010 INCH MAXIMUM FOR 30 INCH STROKE
6. SIDE LOADING	BALL SCREW MORE SUSCEPTIBLE TO DAMAGE FROM SIDE LOADING THAN MACHINE SCREW	
7. LUBRICATION	BECAUSE OF POINT LOADING BETWEEN BALLS & SCREW, LUBRICATION BETWEEN BALL NUT & SCREW IS ESSENTIAL WHICH WILL ALSO REQUIRE USE OF BOOT.	WITH TRAVELLING PLASTIC NUT ARRANGEMENT, IT MAY NOT REQUIRE LUBRICATION AT NUT TO SCREW INTERFACE. THIS WILL ELIMINATE REQUIREMENT FOR BOOT



REPORT E-4

COST TRADE - PLASTIC VS BRONZE NUT FOR ELEVATION ACTUATOR

FOR

GIMBAL/ACTUATOR DRIVE ASSEMBLY

FOR

BOEING SECOND GENERATION HELIOSTAT

JUNE 27, 1980

Reference: FACC TM13



Ford Aerospace &  
Communications Corporation



TABLE OF CONTENTS

Section

1.0 Introduction

2.0 Summary

3.0 Conclusions and Recommendations

Table I Initial Cost Per Unit

Table II Maintenance Cost Per Unit

Figure 1 Alternate Designs

Figure 2 Protective Boot

Figure 3 Nut Detail, Concept B

Figure 4 Nut Detail, Concept A

## 1.0 INTRODUCTION

The purpose of this Appendix is to investigate the relative life-cycle costs of two different screw/nut material combinations for the elevation drive actuator.

## 2.0 SUMMARY

Concept A

Concept A consists of a non-lubricated machine screw, utilizing a stainless steel screw and a plastic nut specially compounded for non-lubricated operation. This screw would operate fully exposed to the elements. The type of actuator is the one recommended in Appendix E-3.

Concept B

Concept B consists of a lubricated machine screw utilizing conventional carbon steel screw and a bronze nut. Since this screw must be constantly lubricated, it would operate fully protected from the elements by means of a protective flexible boot and a steel cover.

Final determination of the type of nut material for the non-lubricated Concept (A) will be based on accelerated life tests using various candidate materials. However, the Cost Study in this Appendix assumes the use of a proprietary plastic (Turcite 'A') with an established record of successful applications involving non-lubricated machine screws.

Based on the information in Tables I (initial cost) and II (maintenance cost) the total life cycle cost is:

Concept A = \$276 each

Concept B = \$350 each

The above costs include initial hardware cost plus parts and labor costs over a 30 year period expressed in 1980 dollars.

3.0

CONCLUSIONS AND RECOMMENDATIONS

Based on this investigation, it is concluded that due to its lower cost, Concept (A) with a non-lubricated plastic nut should be the design employed. Questions regarding the viability of this concept will be resolved analytically as well as empirically to the satisfaction of FACC and Boeing.

HELIOSTAT ELEVATION DRIVE

TABLE I INITIAL COST PER UNIT ①

ITEM	CONCEPT			
	-A-		-B-	
	QTY 1 (#)	QTY, 50K (#)	QTY 1 (#)	QTY, 50K (#)
PROTECTIVE STEEL COVER	—	—	100	20
PROTECTIVE BOOT (WITH CLAMPS)	—	—	150	35
ACTUATOR (WITH SCREW)	400	205	365	180
NUT	125	20	235	40
NUT PIVOT BRKTS (2)	150	40	175	40
TOTAL	\$675	\$265	\$1025	\$315

TABLE II MAINTENANCE COST PER UNIT ①

PROCEDURE	CONCEPT															
	-A-								-B-							
	FRE- QUENCY (YRS)	M-HRS EACH OCCUR.	COST (\$)						FRE- QUENCY (YRS)	M-HRS EACH OCCUR.	COST (\$)					
			EACH OCCUR.		LIFE CYCLE		RESULT. PER YEAR				EACH OCCUR.		LIFE CYCLE		RESULT. PER YEAR	
		LAB.	MAT.	LAB.	MAT.	LAB.	MAT.			LAB.	MAT.	LAB.	MAT.	LAB.	MAT.	
REPLACE NUT	10	1	20	20	40	40	1.3	1.3	10	1.1	22	40	44	80	1.5	2.7
REPLACE BOOT	—	—	—	—	—	—	—	—	10	0.4	8	35	16	70	.53	2.3
LUBRICATE NUT	—	—	—	—	—	—	—	—	2	0.12	2.4	.20	36	3	1.2	0.1
TOTAL	—		80				2.6		—		249				8.33	

SUMMARY CONCEPT -A-

① TOTAL MAINT. COST = \$80  
 PRESENT VALUE OF \$80  
 OVER 30 YR PERIOD = \$11.4  
 INITIAL COST = \$265.0  
 ① GRAND TOTAL = \$276.4

SUMMARY CONCEPT -B-

① TOTAL MAINT. COST = \$249  
 PRESENT VALUE OF \$249  
 OVER 30 YEAR PERIOD = \$35.6  
 INITIAL COST = \$315.0  
 ① GRAND TOTAL = \$350.6

① 1980 DOLLARS.

E. MONTESANTO 1/29/80





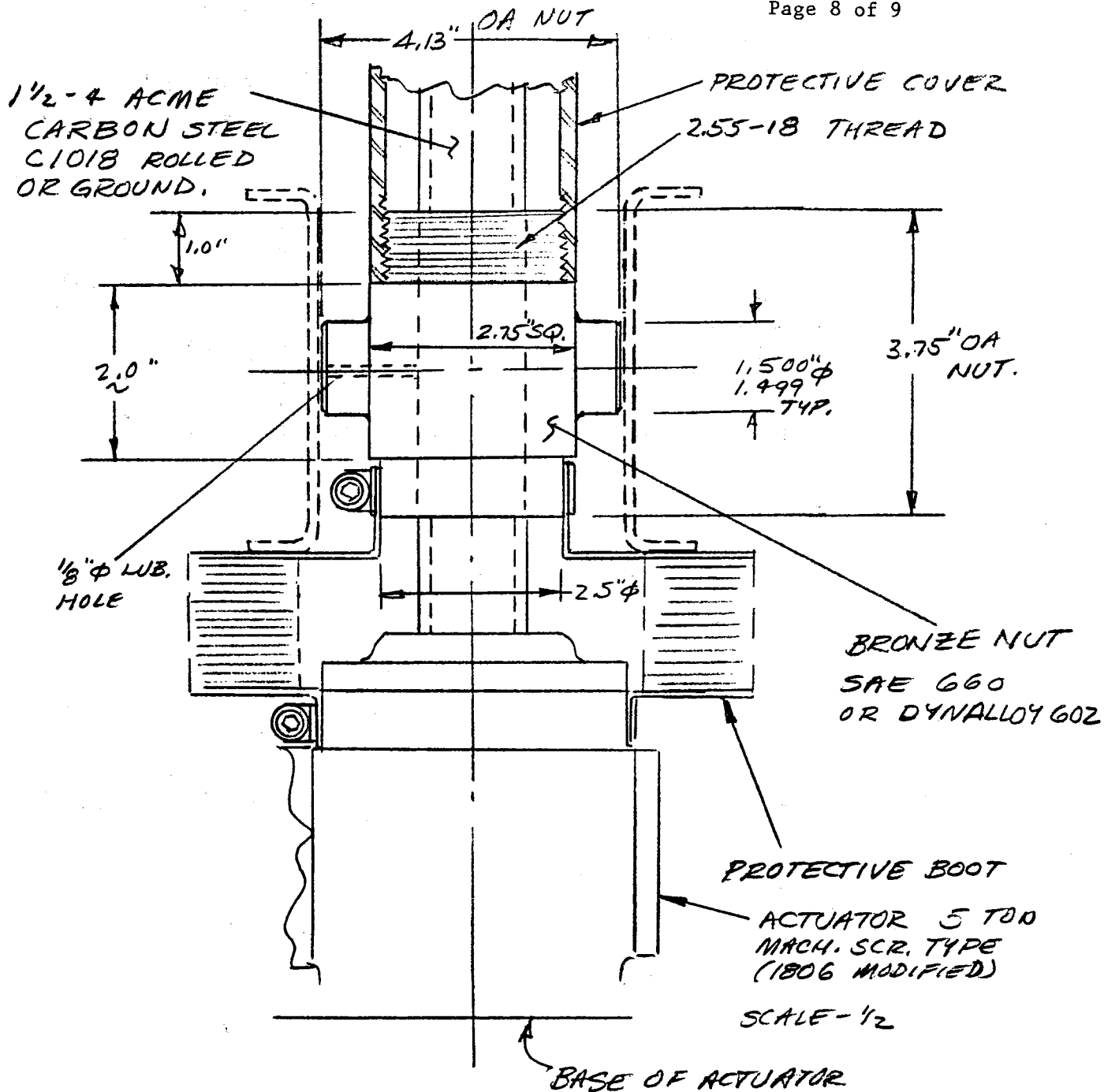


FIG 3  
NUT DETAIL  
CONCEPT-B-

E. MONTESANTO  
1/23/82

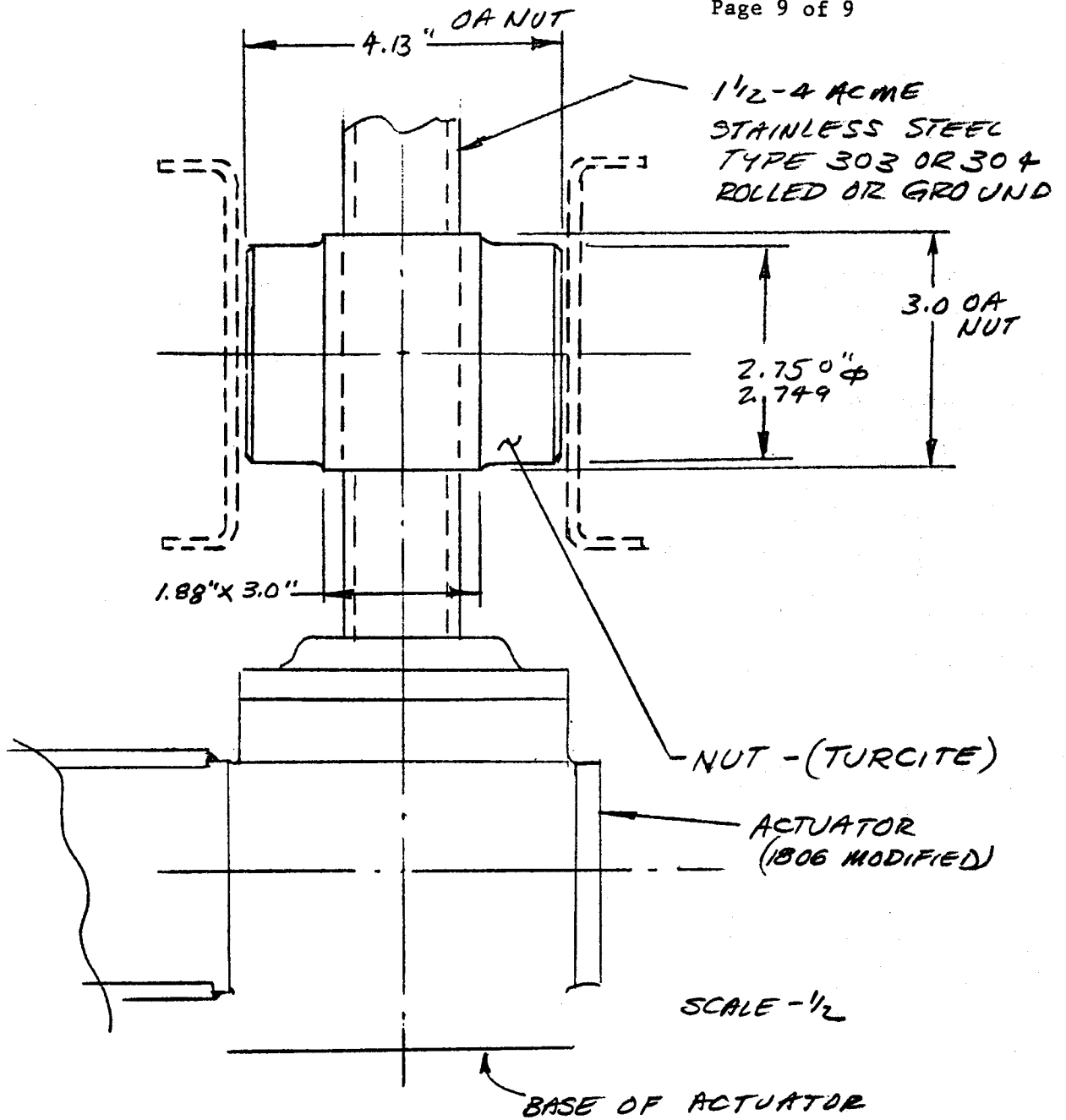


FIG. 4  
NUT DETAIL  
CONCEPT - A -

E. MONTESANTO  
1/23/80





REPORT E-5

GIMBAL HOUSING AND TORQUE TUBE/ARMS ASSEMBLY STRUCTURAL ANALYSIS

FOR

GIMBAL/ACTUATOR DRIVE ASSEMBLY

FOR

BOEING SECOND GENERATION HELIOSTAT

JUNE 27, 1980

Reference: FACC TM17

## CONTENTS

		<u>PAGES</u>
1.0	PURPOSE	3
2.0	SUMMARY OF STRESS ANALYSIS	3
3.0	SUMMARY OF COMPLIANCE ANALYSIS	3
4.0	GEOMETRY	7
5.0	ACTUATOR ARM STRESS ANALYSIS	12
6.0	GIMBAL HOUSING STRESS ANALYSIS	23
7.0	TORQUE TUBE STRESS ANALYSIS	28
8.0	ACTUATOR ARM COMPLIANCE	30
9.0	GIMBAL HOUSING COMPLIANCE	32
10.0	TORQUE TUBE COMPLIANCE	44

## 1.0 PURPOSE

The purpose of this analysis is to determine the material stress levels and the deflection compliance constants for the structural components of the gimbal/actuator drive assembly.

Note: The gimbal housing was revised to a low mount casting after this analysis was completed. Since the casting process requires a minimum thickness of 0.19 inches and the load path geometry reduced the gimbal loads, the stress levels will be lower than the analyzed gimbal.

## 2.0 SUMMARY OF STRESS ANALYSIS

The maximum stresses were determined as follows:

Torque Tube	10.6 ksi
Actuator Arm	38.6 ksi *
Pedestal Support	8.8 ksi

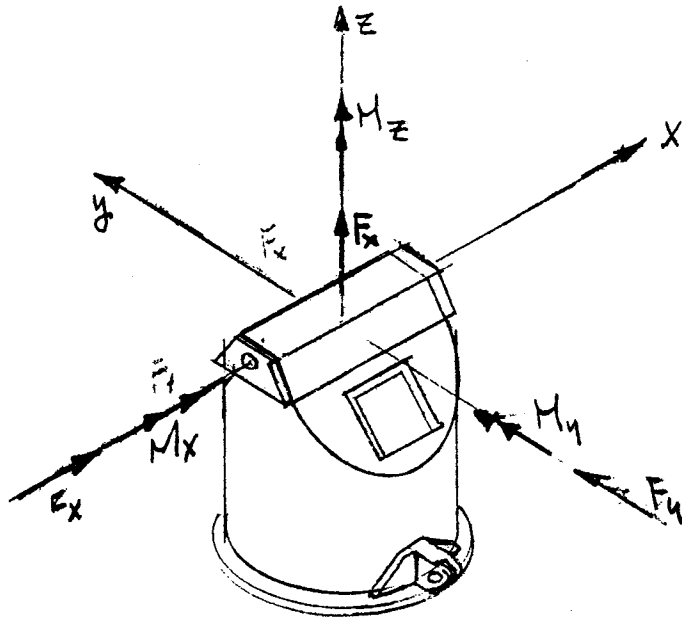
\* Note: The arms design was revised after this analysis to prevent torsional warping by restraining the arm rotation with an additional member at the end of the arm.

Expected stress levels will be much lower than indicated.

## 3.0 SUMMARY OF COMPLIANCE ANALYSIS

The deflections due to unit loads and moments are shown on Tables 3.1, 3.2 and 3.3.

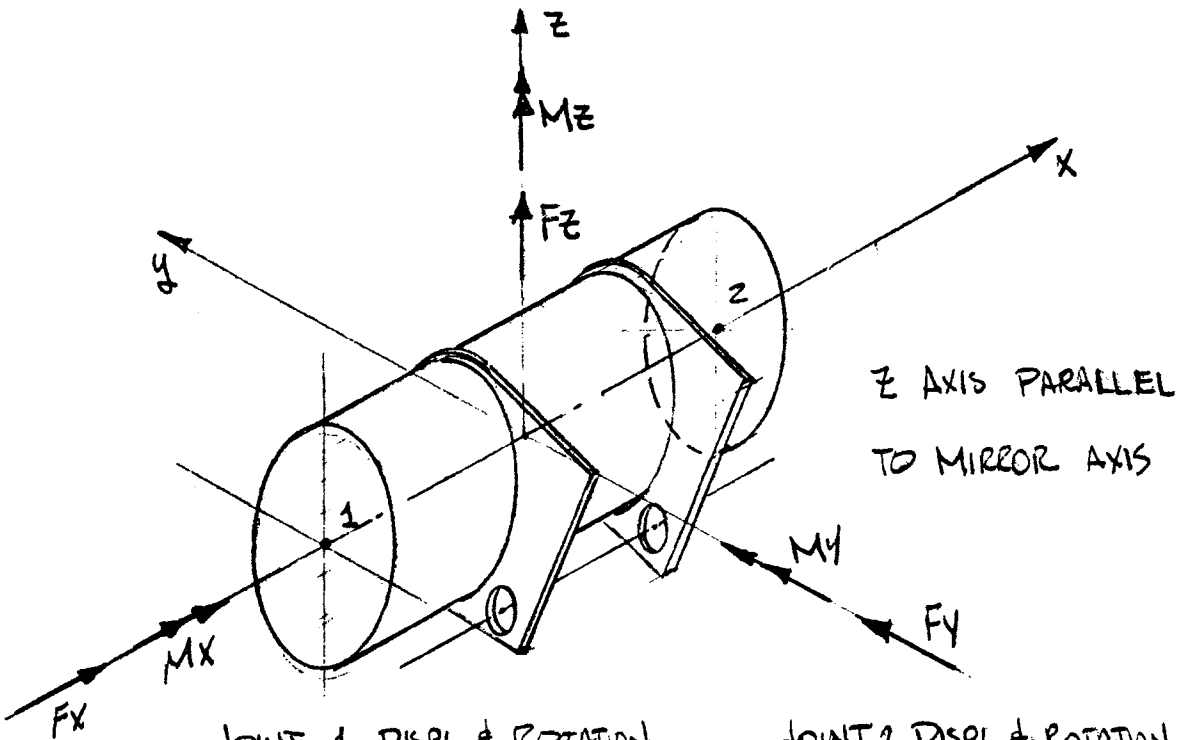
PEDESTAL UNIT LOAD COMPLIANCE SUMMARY



UNIT LOAD	$\Delta x$	$\Delta y$	$\Delta z$	$\Theta_x$	$\Theta_y$	$\Theta_z$
lbs & n	in $\times 10^{-8}$	in $\times 10^{-8}$	in $\times 10^{-8}$	rad $\times 10^{-10}$	rad $\times 10^{-10}$	rad $\times 10^{-10}$
Fx	217	-	-	-	523	-15
Fy	-	197	-	-646	-	-
Fz	-	-	22	-	-	-
Mx*	-	-6.46	-	31.4	-	-
My	5.23	-	-	-	45.7	-
Mz	-0.15	-	-	-	-	72

\* VARIES WITH MIRROR ELEVATION, VALUE SHOWN IS MAXIMUM WITH MIRROR AT ZENITH POSITION.

TORQUE TUBE UNIT LOAD COMPLIANCE

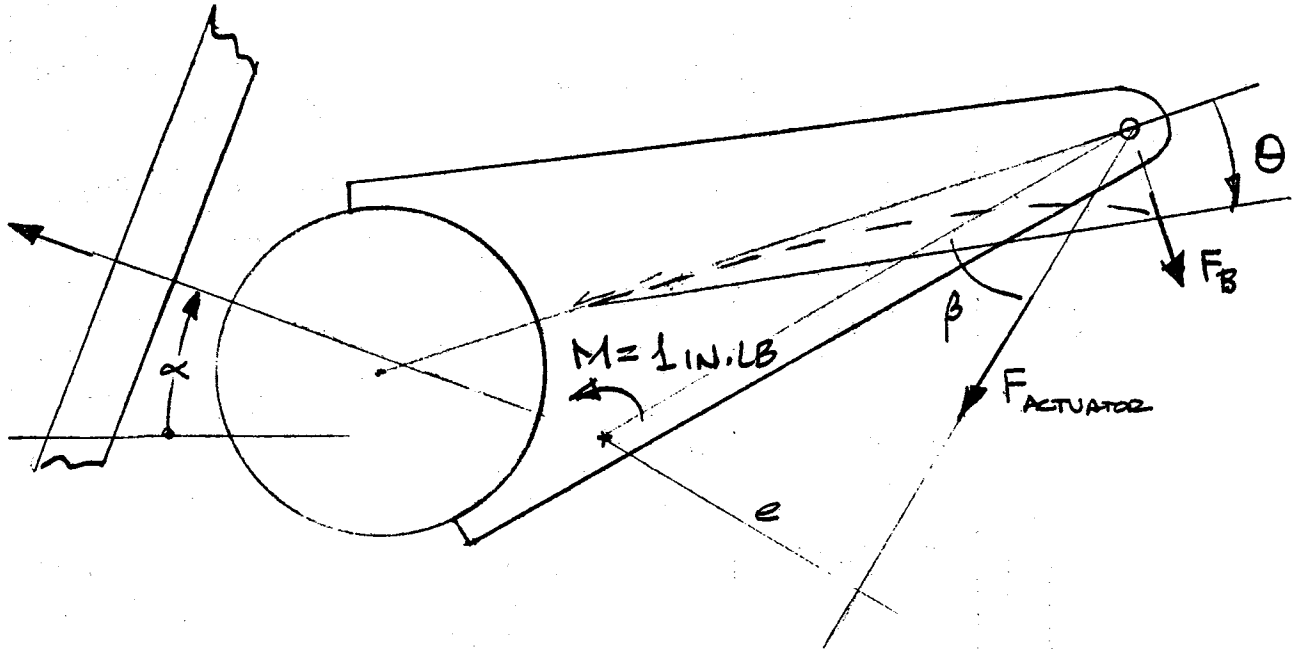


JOINT 1 DISPL & ROTATION

JOINT 2 DISPL & ROTATION

JOINT LOAD	$\Delta_{x1}$	$\Delta_{y1}$	$\Delta_{z1}$	$\Theta_{x1}$	$\Theta_{y1}$	$\Theta_{z1}$	$\Delta_{xz}$	$\Delta_{yz}$	$\Delta_{zz}$	$\Theta_{xz}$	$\Theta_{yz}$	$\Theta_{zz}$
LBS & IN-LB	IN·10 <sup>-8</sup>	IN·10 <sup>-8</sup>	IN·10 <sup>-8</sup>	RAD·10 <sup>-10</sup>	RAD·10 <sup>-10</sup>	RAD·10 <sup>-10</sup>	IN·10 <sup>-8</sup>	IN·10 <sup>-8</sup>	IN·10 <sup>-8</sup>	RAD·10 <sup>-10</sup>	RAD·10 <sup>-10</sup>	RAD·10 <sup>-10</sup>
$F_{1x} = 1$	2940	-9	64	4	293	-29	2930	-9	-64	-4	293	29
$F_{1y} = 1$	-9	2930	-46	-3730	-97	+1970	-9	-12	1010	-3110	-97	-1230
$F_{1z} = 1$	64	-46	273	182	1090	97	64	11	-78	152	348	97
$M_{1x} = 1$	.04	-3730	1.82	441	0	10	0.04	-31.10	1.52	370	0	10
$M_{1y} = 1$	293	-0.97	10.09	0	72	3	293	0.97	-348	0	15	3
$M_{1z} = 1$	0.29	-19.70	0.97	-10	3	102	0.29	12.30	-0.97	-10	3	45
$F_{1x} = F_{2x} = 0.5$	2930	-9	64	4	293	29	2930	9	-64	-4	293	29
$F_{1y} = F_{2y} = 0.5$	0	423	-18	-3420	0	-373	0	423	-18	0	-3420	373
$F_{1z} = F_{2z} = 0.5$	0	-18	97	167	372	0	0	-18	97	167	-372	0
$M_{1x} = M_{2x} = 0.5$	0	-34.2	1.67	406	0	0	0	-34.2	1.67	406	0	0

ACTUATOR ARM UNIT LOAD COMPLIANCE SUMMARY

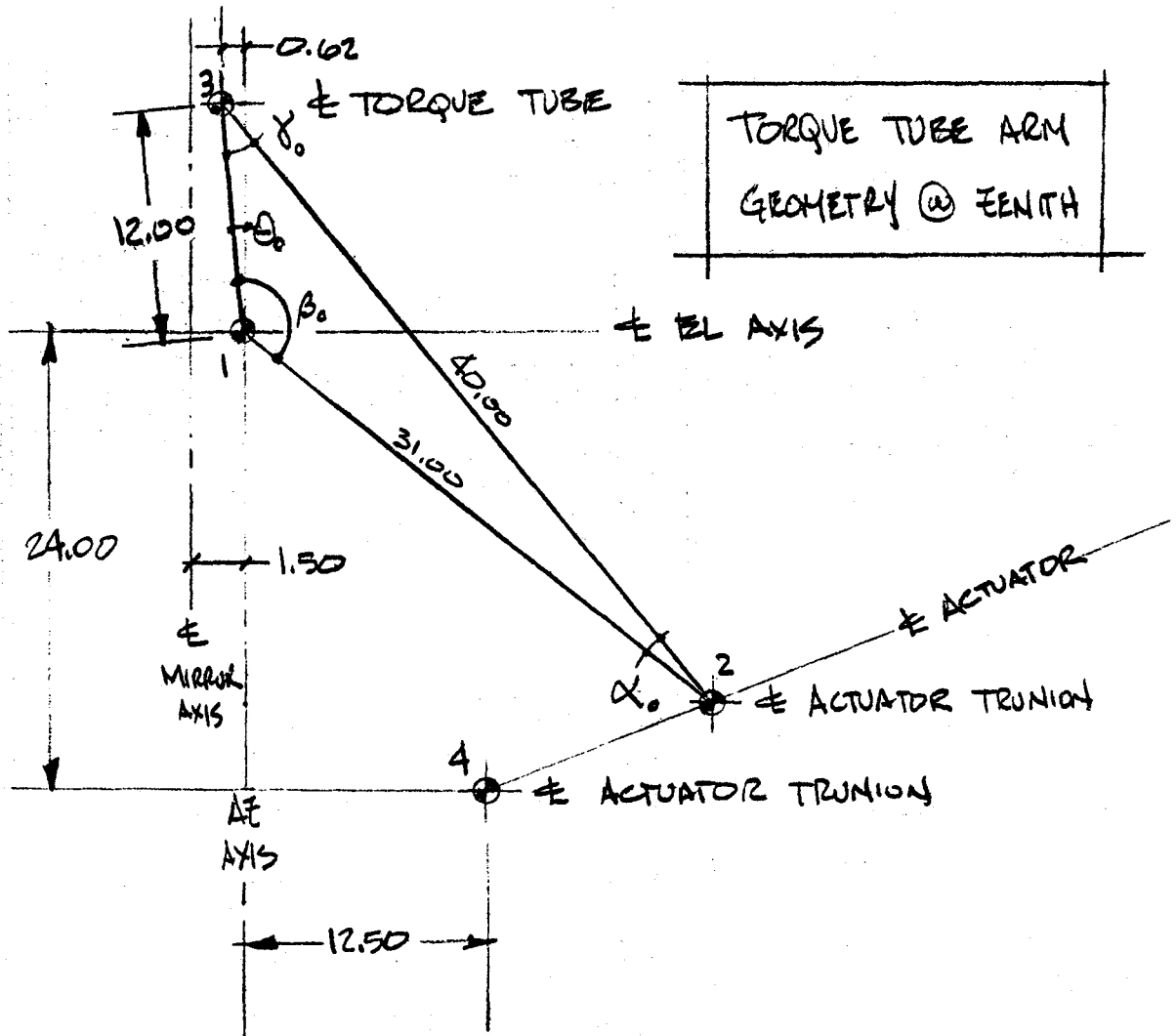


$\alpha$	$e$	$\beta$	$\theta$ ( $10^{-10}$ RAD)
0	15.8	43.54°	83.7
20	19.2	52.43°	79.3
70	26.4	71.47°	69.0
90	26.9	73.18°	68.3

$$\theta_{MAX} = 83.7 \times 10^{-10} \text{ RAD / IN·LB}$$

4.0 GEOMETRY

REFERENCE FIGURES 1 &amp; 2



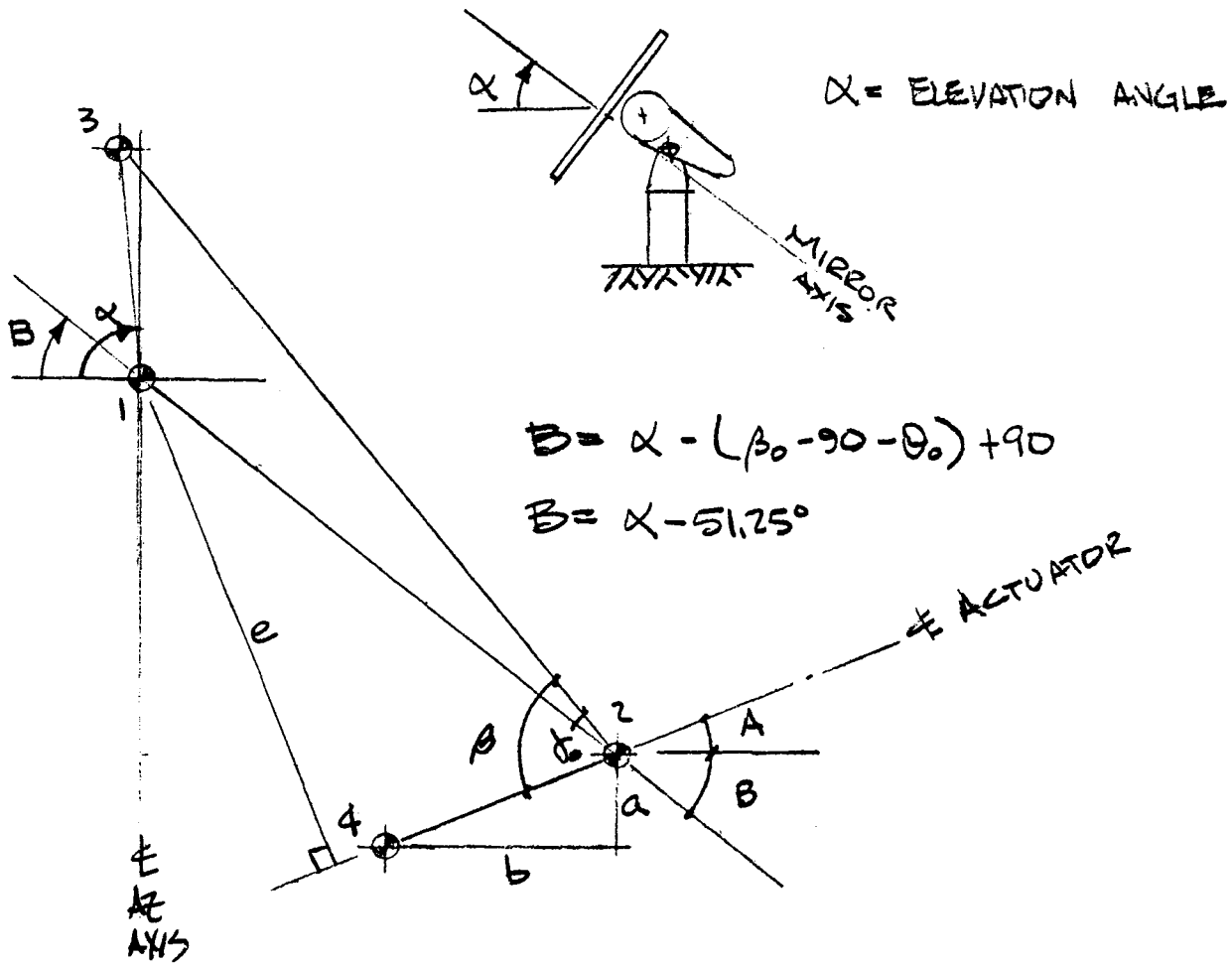
$$\theta_0 = \tan^{-1} [(0.62) / (12.00)] = 2.957652^\circ$$

$$\alpha_0 = \cos^{-1} [(40)^2 + (31)^2 - (12)^2] / (2)(40)(31) = 12.94212979^\circ$$

$$\beta_0 = \cos^{-1} [(12)^2 + (31)^2 - (40)^2] / (2)(12)(31) = 131.7070777^\circ$$

$$\gamma_0 = 180 - \alpha_0 - \beta_0 = 35.35079250^\circ$$



4.10 GEOMETRY

$$a = 24 - 31 \sin B$$

$$e = 31 \sin(\beta - 80)$$

$$b = 31 \cos B - 12.5$$

$$A = \tan^{-1} \frac{a}{b}$$

$\alpha$	$B$	$a$	$b$	$A$	$\beta$	$e$
0	$-51.25^\circ$	48.18	6.90	$81.85^\circ$	$43.54^\circ$	15.8
20	$-31.25^\circ$	40.08	14.00	$70.74^\circ$	$52.43^\circ$	19.2
70	$18.75^\circ$	14.04	16.85	$39.78^\circ$	$71.47^\circ$	26.4
90	$38.75^\circ$	4.60	11.68	$21.49^\circ$	$73.18^\circ$	26.9

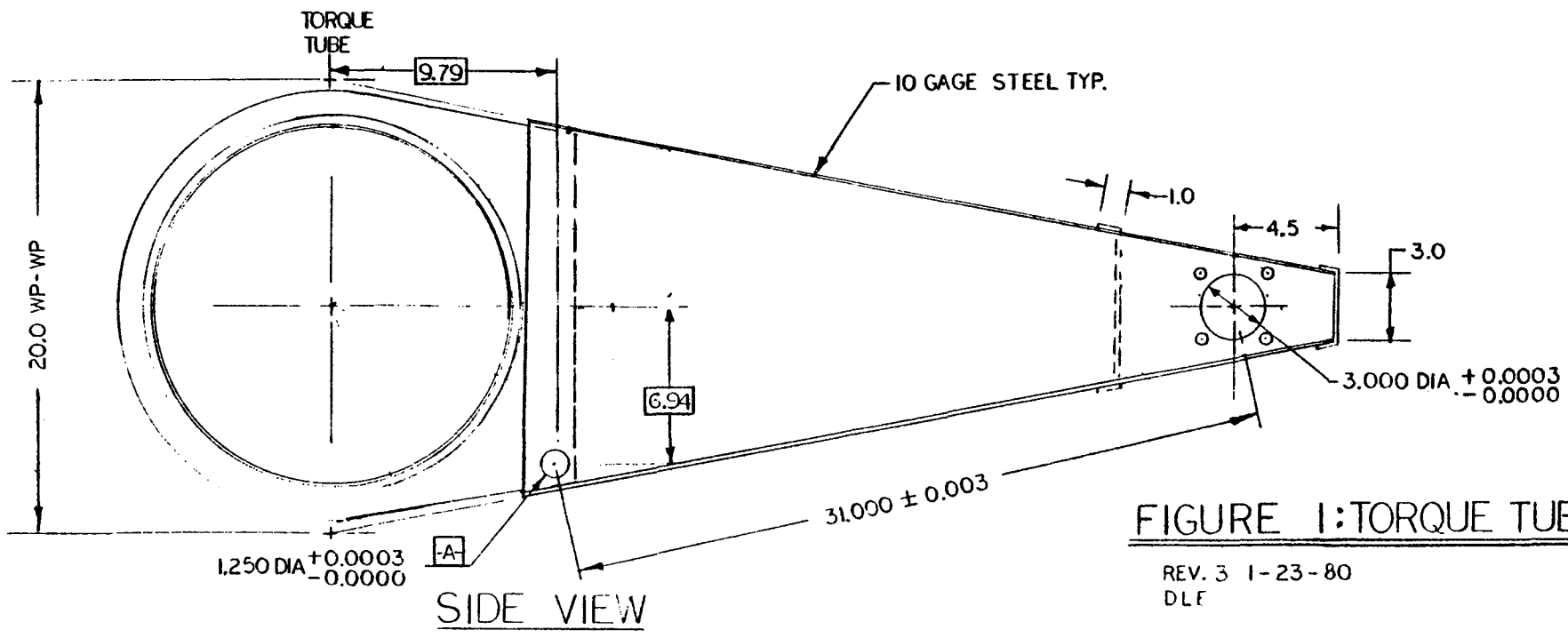
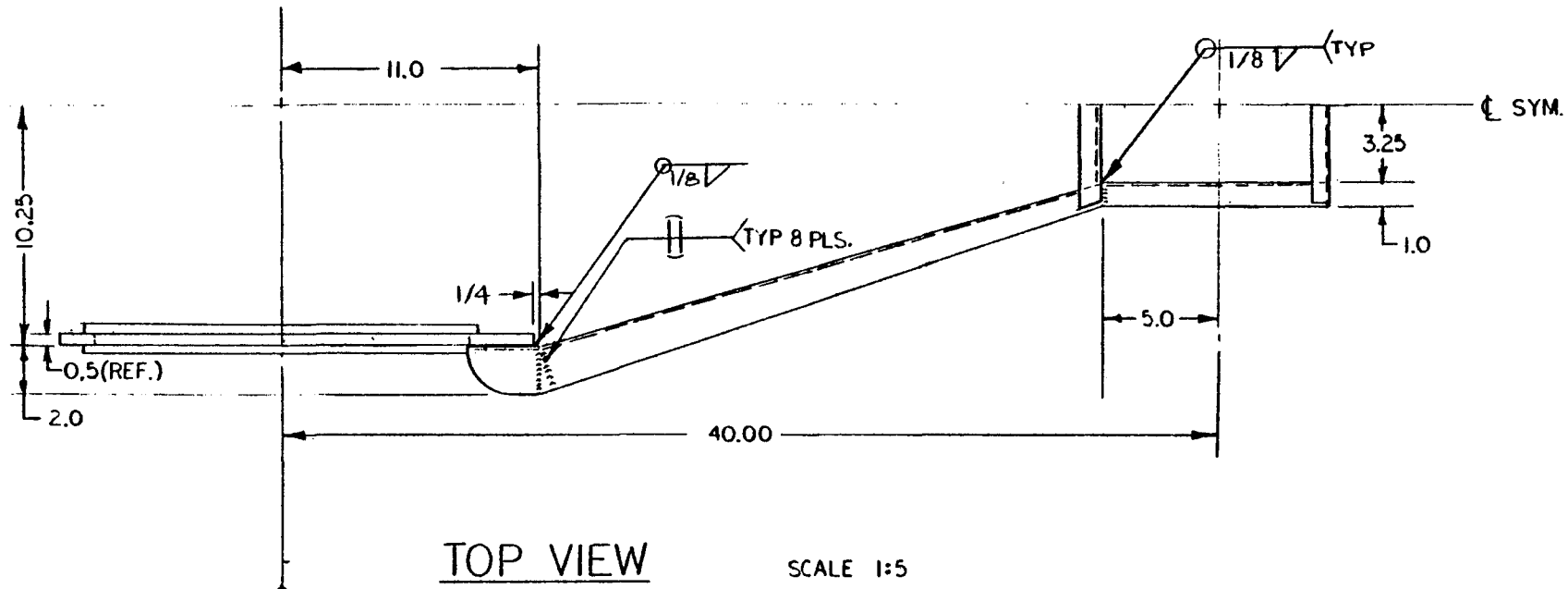


**FIGURE 1: TORQUE TUBE ARM**  
 REV. 3 1-23-80  
 DLF



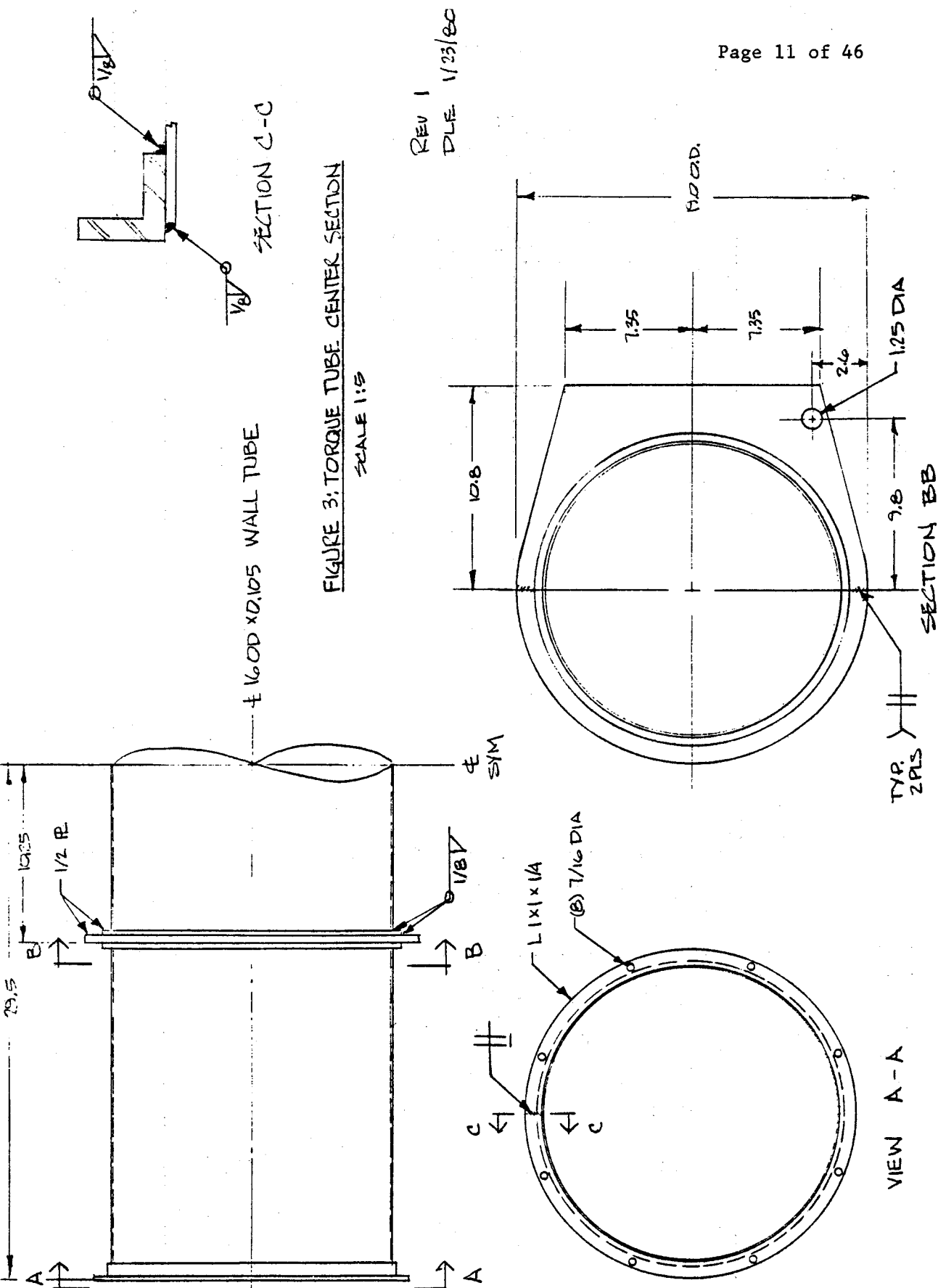


FIGURE 3; TORQUE TUBE CENTER SECTION  
SCALE 1:5

REV 1  
DLE 1/23/80

VIEW A-A

SECTION BB

± 16.00 x 0.105 WALL TUBE

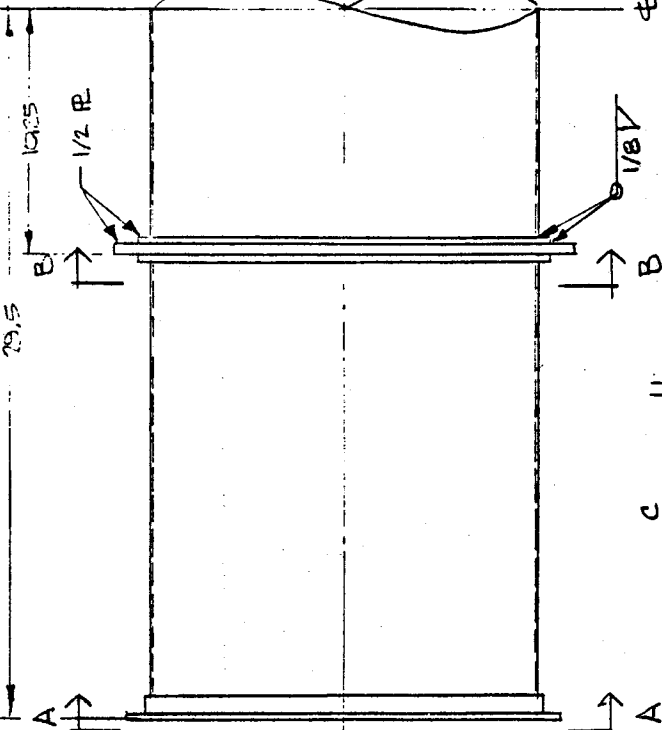
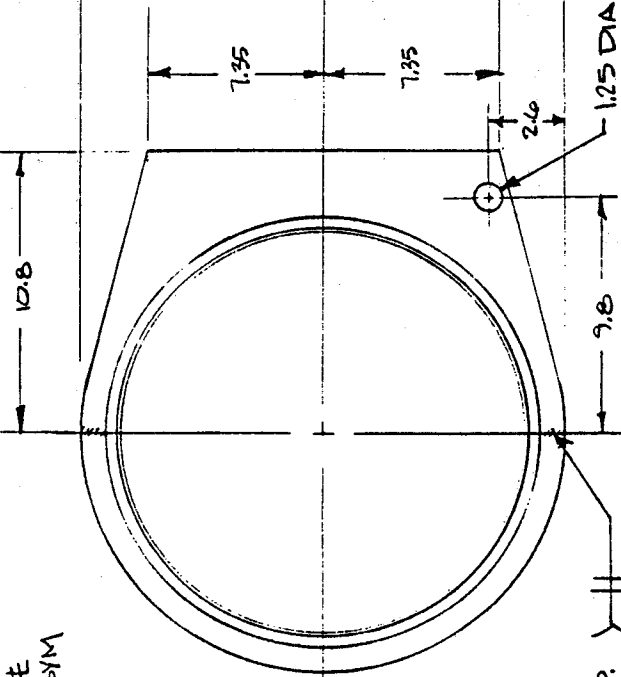
SECTION C-C

TYP. 2PLS

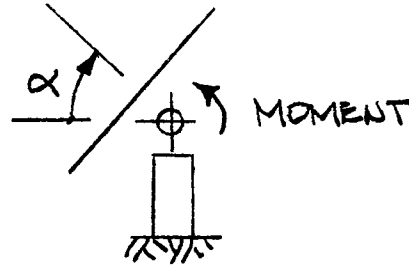
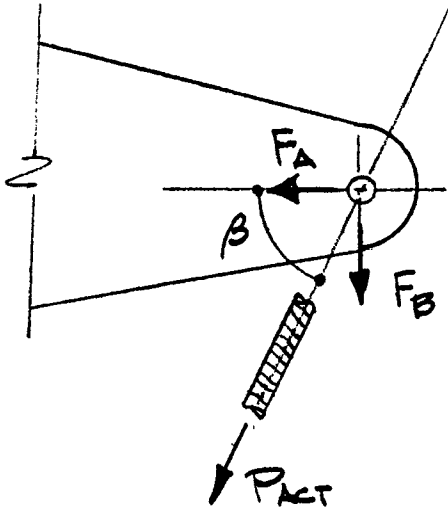
HEAD.

ε SYM

L 1 x 1/4  
(B) 7/16 DIA



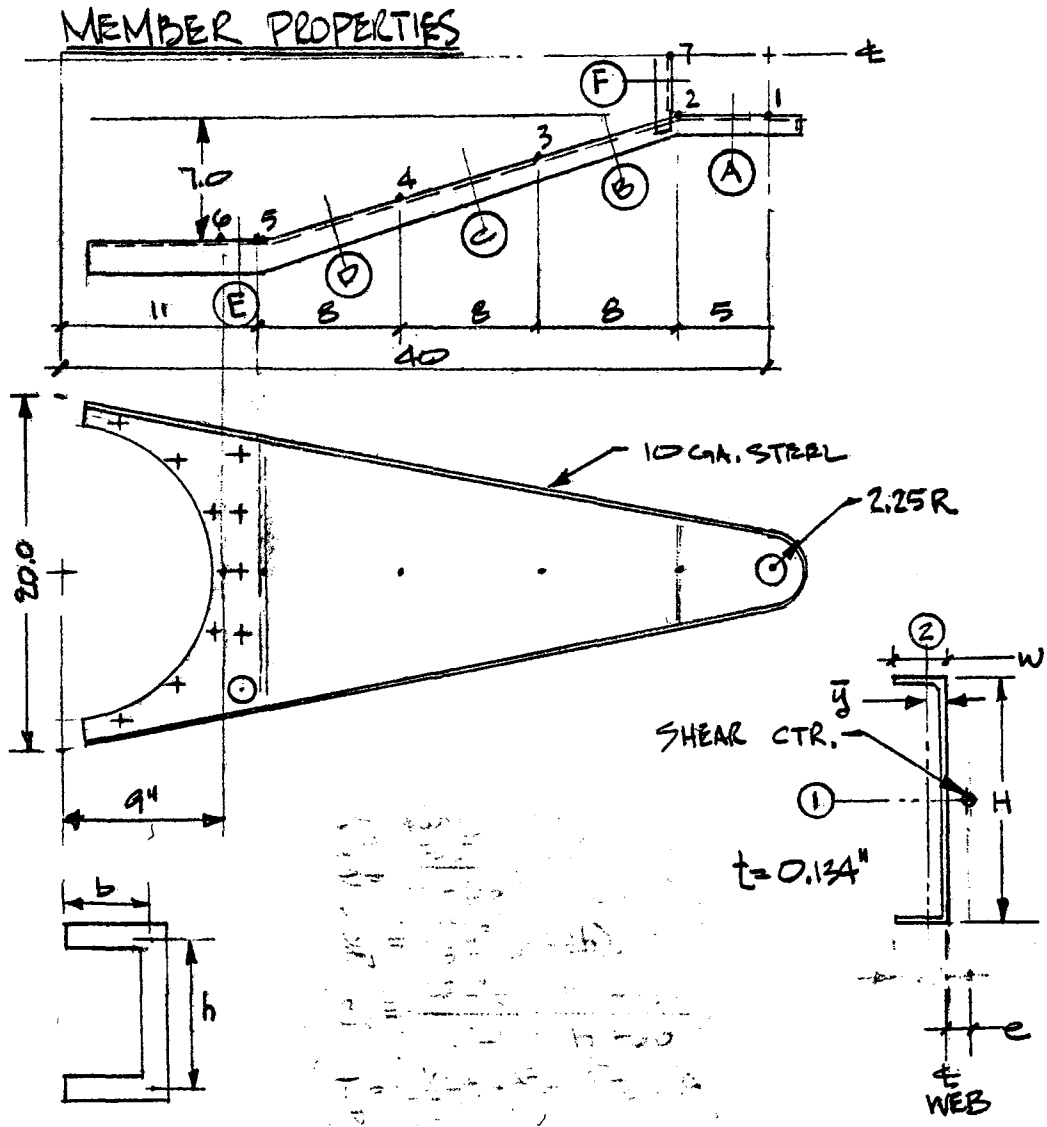
50 ACTUATOR ARM ANALYSIS  
SURVIVAL LOADS



ELEVATION ANGLE

ELEVATION ANGLE	MAX MOMENT (KIP-IN)	PACT (KIPS)	FA (KIPS)	FB (KIPS)
0	+ 252	+16	+11.6	+ 11.0
20	+ 278	+14.5	+ 8.8	+ 11.5
70	+ 164	+6.2	+ 2.0	+ 5.9
90	± 241	± 9	± 2.6	± 8.6

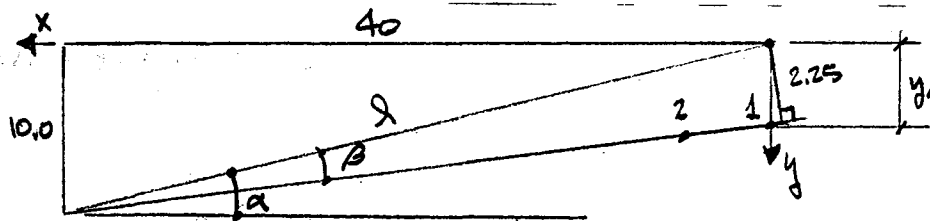
MAX MOMENT FROM: APPENOX 1, EXTERNAL LOADS  
 REQUIREMENTS FOR GIMBAL/ACTUATOR DRIVE ASSEMBLY,  
 REC'D WDL 11/13/79 FROM BOEING CORP.



PT	W (INCHES)	H (INCHES)	A (IN <sup>2</sup> )	I <sub>x</sub> (IN <sup>4</sup> )	I <sub>y</sub> (IN <sup>4</sup> )	K <sub>y</sub> (IN <sup>3</sup> )	C <sub>w</sub> (IN <sup>6</sup> )	$\bar{y}_c$ (INCHES)	e (INCHES)
1	1.00	4.58	0.846	2.22	0.0575	0.00506	0.209	0.2096	0.243
2	1.00	6.51	1.10	5.44	0.0616	0.00610	0.479	0.1732	0.204
3	1.33	9.59	1.61	17.0	0.154	0.00961	2.68	0.2005	0.355
4	1.67	12.68	2.11	39.0	0.315	0.0126	9.77	0.2034	0.558
5	2.00	15.76	2.61	74.2	0.553	0.0156	26.8	0.2589	0.796
6	2.00	16.53	2.72	84.1	0.556	0.0163	29.9	0.2516	0.774
7	1.00	6.20	1.12	5.64	0.0613	0.00668	0.494	0.1720	0.202

## MEMBER PROPERTIES

SOLVE FOR DIMENSION H (DEPTH OF CHANNEL)



$$2 = (40^2 + 10^2)^{1/2}$$

$$y_0 = 10 - 40 \tan(\alpha - \beta) = 2.2914$$

$$\beta = \sin^{-1}(2.25/2)$$

$$y = y_0 + (10 - y_0)(x/40)$$

$$\alpha = \tan^{-1}(10/40)$$

$$H = 2y$$

SEE MEMBER PROP. TABLE FOR RESULTS

## MEMBER PROPERTY EQUATIONS

$$A = t(H + 2W - 2t) \quad \text{EQ (1)}$$

$$I_1 = [t(H - 2t)^3 + Wt^3/12] + 2Wt(h/2)^2 \quad \text{EQ (2)}$$

$$\bar{y} = [(1/2)(H - 2t)^3 - t^3 + W^2t]/A \quad \text{EQ (3)}$$

$$I_2 = (2tW^3 + (H - 2t)t^3)/12 + 2Wt(W/2 - \bar{y})^2 + (H - 2t)t(\bar{y} - t/2)^2 \quad \text{EQ (4)}$$

$$K_y = t^3(h + 2b)/3 \quad \text{EQ (5)}$$

$$C_w = h^2b^3t(2h + 3b)/(12)(h + 6b) \quad \text{EQ (6)}$$

$$e = 3b^3/(h + 6b) \quad \text{EQ (7)}$$

REF. ROARK \*  
TABLE 21, CASE 1

\* REFERENCE 1:

FORMULAS FOR STRESS AND STRAIN, 5TH ED, ROARK & YOUNG

MCGRAW-HILL, 1975

STRESS ANALYSIS

MAXIMUM BENDING AND AXIAL FORCES OCCUR AT HORIZON UNDER GRAVITY, ICE & SNOW LOADS.

$$F_A = 11.6 \text{ KIPS} \ \& \ F_B = 11.0 \text{ KIPS} \ (\text{REF. SURVIVAL LOADS})$$

MEMBER (A)

BEARING STRESS AT TRUNION HOLE

$$f_p = \frac{1}{2} (16 \text{ K}) / (0.134)(1.5) = \underline{39.8 \text{ KSI}}$$

SHEAR STRESS ADJ. TO TRUNION HOLE, USE PT. 1 PROP

$$f_v = 1.5 V / A_w = (1.5)(5.5) / (4.58)(1.34) = \underline{13.4 \text{ KSI}}$$

AXIAL STRESS

$$f_a = (5.8) / (0.846) = \underline{6.9 \text{ KSI}}$$

BENDING STRESS AT PT. 2

$$f_b = (0.2)(11.0)(5) (1/2)(6.51) / (5.44) = \underline{16.5 \text{ KSI}}$$

STRESSES DUE TO TORSION. REF. 1, TABLE 21, CASE 1 AND TABLE 22, CASE 1b. USE AVERAGE MEMBER PROP. FOR PT 1 & 2

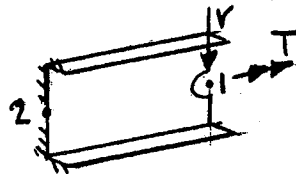
$$k_{t1} = (1/2)(575 + 610)(10^{-9}) = 0.00593$$

$$C_w = (1/2)(0.209 + 0.479) = 0.344$$

$$e = (1/2)(0.243 + 0.204) = 0.224$$

$$\beta = (k_t G / C_w E)^{1/2} = (0.00593)^{1/2} (1(5 \cdot 10^6) / (0.344)(30 \cdot 10^6)) = 0.0066$$

$$T = V e = (1/2)(11)(0.244) = 1.34 \text{ KIP-IN}$$



FREE TO WRAP & TWIST @ PT 1

FIXED @ PT 2



## STRESS ANALYSIS

$$\underline{\Theta_{\text{MAX}} @ X=0 \text{ (PT 1)}}$$

$$\Theta_{\text{MAX}} = \frac{T}{C_w E \beta^2} (\beta L - \text{Tanh } \beta L)$$

$$\Theta_{\text{MAX}} = [(1340) / (0.344)(30 \cdot 10^6)(0.0066)^2] [(0.0066)(5) - \text{Tanh}\{(0.0066)(5)\}]$$

$$\Theta_{\text{MAX}} = 3.6 \cdot 10^{-5} \text{ RAD } (\sim 0.0001'' \text{ AT TOP \& BOTTOM OF CHANNEL})$$

$$\Theta'_{\text{MAX}} = \frac{-T}{C_w E \beta^2} \left(1 - \frac{1}{\cosh \beta L}\right) @ X=0$$

$$\Theta'_{\text{MAX}} = [(-1340) / (0.344)(30 \cdot 10^6)(0.0066)^2] \left[1 - \frac{1}{\cosh(0.0066)(5)}\right]$$

$$\Theta'_{\text{MAX}} = -1.62 \cdot 10^{-5} \text{ RAD/IN}$$

$$\tau_1 = t G \Theta' = (0.134)(11.5 \cdot 10^6)(1.62 \cdot 10^{-5}) = 25 \text{ PSI}$$

$$\Theta''_{\text{MAX}} = \frac{T}{C_w E \beta} \text{Tanh } \beta L \text{ at } x=L$$

$$\Theta''_{\text{MAX}} = [(1340) / (0.344)(30 \cdot 10^6)(0.0066)] \cdot \text{Tanh}(0.0066)(5)$$

$$\Theta''_{\text{MAX}} = 6.5 \cdot 10^{-4} \text{ RAD/IN}^2$$

$$\sigma_x = \frac{hb}{2} \cdot \frac{h+3b}{h+6b} E \cdot \Theta'' = \text{MAX. AT PT 2 (X=L)}$$

$$\text{WHERE } h = 16.51 - 0.134 = 6.38 ; b = 1.10 - 0.067 = 1.03$$

$$\sigma_x = \left(\frac{1}{2}\right)(6.38)(1.03) \frac{(6.38+3)(1.03)}{(6.38+6)(1.03)} (30 \cdot 10^6)(6.5 \cdot 10^{-4}) / (6.38+6)(1.03)$$

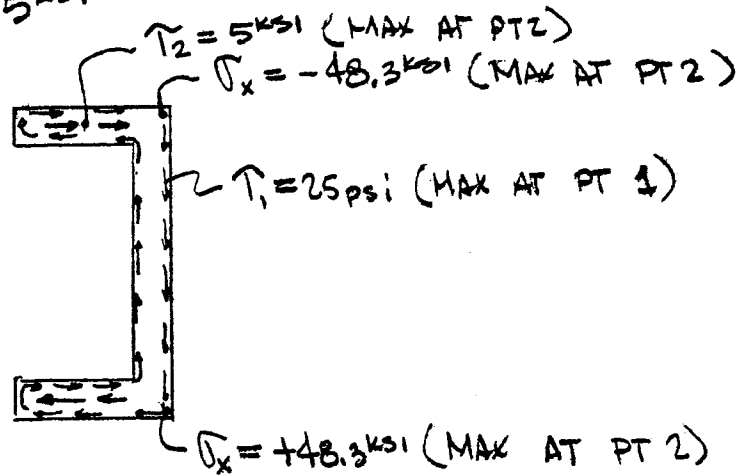
$$\sigma_x = \pm 48.3 \text{ KSI}$$

## STRESS ANALYSIS

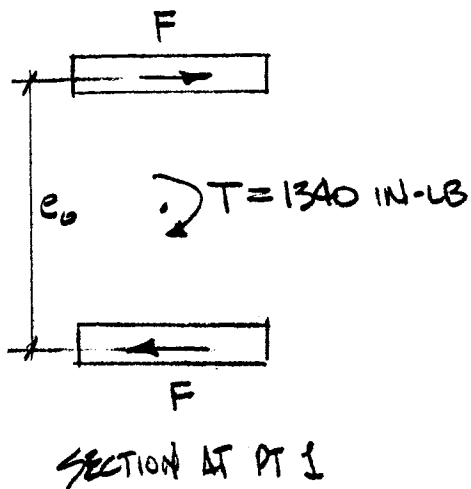
$$\Theta_{\text{MAX}}^{\text{III}} = \frac{T}{C_w E} \quad \neq \quad \tau_2 = \frac{hb^2}{4} \left[ \frac{h+2b}{h+6b} \right] E \Theta^{\text{III}} \quad \text{@ PT 2 (X=L)}$$

$$\tau_2 = (1340)(6.38)(1.03)^2 (6.38 + (2)1.03) / (0.344)(4)(6.38 + (6)1.03)$$

$$\tau_2 = 5 \text{ ksi}$$



CHECK SOLUTION BY APPROX. ANAL. - CONSIDER ONLY CHANNEL FLANGES RESIST TORSION.



$$e_0 = H - t = 4.58 - .134 = 4.45$$

$$F = T/e_0 = 301 \text{ LBS}$$

$$S_{\text{FLANG}} = \frac{tW^2}{6} = (1/6)(0.134)(1)^2 = 0.0223$$

$$f_b = \frac{M}{S} = (300)(5) / 0.0223 = 67.5 \text{ ksi}$$

$$f_v = (1.5)(300) / (0.134)(1) = 3.4 \text{ ksi}$$

## STRESS ANALYSIS

ESTABLISH LOWER BOUND STRESS LEVEL - ASSUME NON-WARPING SECTION - CASE 1d

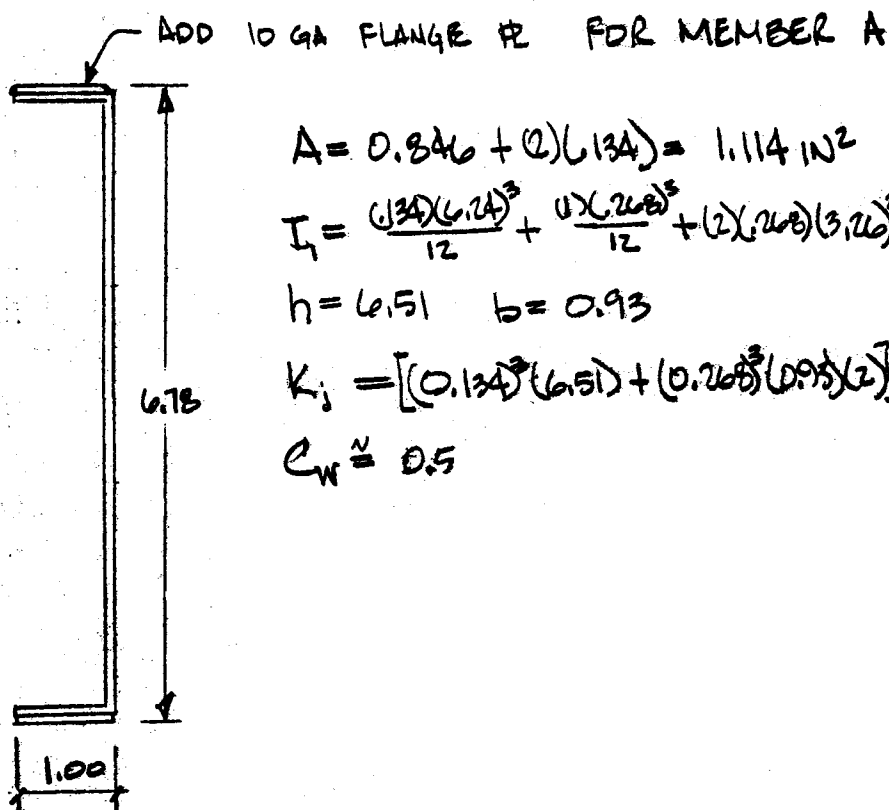
$$\theta'' = \frac{\pm T}{C_w E \beta} \tanh \frac{\beta s}{2} \quad \& \quad \sigma_x = \theta'' \cdot E \cdot \frac{hb}{2} \frac{h+3b}{h+6b} \quad (x=0 \leq x \leq s)$$

$$\sigma_x = [(1.34 \text{ k-in}) (0.38) (1.03) (6.38+3) (1.03) / (0.344) (0.0006) (6.38+6) (1.03) (2)] \cdot [\tanh (0.0006) (5) / 2]$$

$$\sigma_x = 24 \text{ ksi}$$

STRESS LEVEL TOO HIGH.  $\sigma_x + f_b + f_a = 24 + 6 + 7 = 47 \text{ ksi}$  (LOWER BOUND)

THE CHANNEL FLANGES WILL BUCKLE BEFORE THIS LEVEL OF STRESS IS REACHED. REVISE SECTION AT PT 2 BY ADDING COVER PLATES TO FLANGES.



$$A = 0.846 + (2)(6.134) = 1.114 \text{ IN}^2$$

$$I_x = \frac{(1.34)(6.74)^3}{12} + \frac{(1)(2.68)^3}{12} + (2)(2.68)(3.26)^2 = 8.41 \text{ IN}^4$$

$$h = 6.51 \quad b = 0.93$$

$$K_i = [(0.134)^3 (6.51) + (0.268)^3 (0.93)(2)] (1/3) = 0.0172$$

$$C_w \approx 0.5$$

STRESS ANALYSISBENDING, AXIAL & SHEAR STRESSES

$$f_b = (1/2)(11)(5) \cdot (1/2)(6.73) / (8.41) = 11.1 \text{ ksi}$$

$$f_a = (5.8^k) / (1.117) = 5.2 \text{ ksi}$$

$$f_v \approx 13.4 \text{ ksi (SAME AS BEFORE)}$$

TORSIONAL STRESSES (NON-WARPING SECTION)

$$C_w = (1/2)(0.5 + 0.209) = 0.35$$

$$K_1 = (1/2)(0.0172 + 0.00506) = 0.0111$$

$$\beta = (KG / C_w E)^{1/2} = [(0.0111)(11.5 \cdot 10^6) / (0.35)(30 \cdot 10^6)]^{1/2} = 0.012$$

$$\tau_x = \frac{\pm 1.34 \text{ ksi}}{(0.35)(0.012)} \cdot \frac{(6.51)(0.93)}{2} \cdot \frac{(6.51 + 3)(0.93)}{(6.51 + 6)(0.93)} \tanh(0.012)(5)(1/2)$$

0.769

$$\tau_x = 22.3 \text{ ksi}$$

$$\tau_2 = \frac{hb^3}{4} \left[ \frac{h+3b}{h+6b} \right]^2 \cdot \frac{T}{C_w} = \frac{(6.51)(0.93)^3}{4} (0.769)^2 \cdot \frac{1.34}{0.35} = 3.0 \text{ ksi}$$

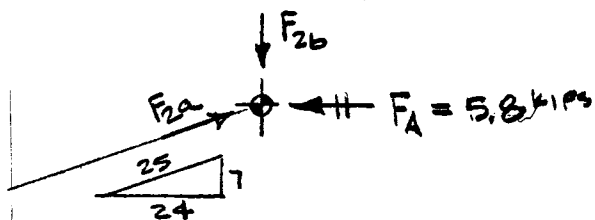
$$\text{MAX FIBER STRESS} = \tau_x + f_b + f_a = 22.3 + 11.1 + 5.2 = \underline{\underline{38.6 \text{ ksi}}} \quad *$$

$$\text{MAX SHEAR STRESS} = f_v + \tau_1 \approx \underline{\underline{13.5 \text{ ksi}}}$$

\* Note: Design was revised after this analysis to prevent torsional warping by restraining the arm rotation with an additional member at the end of the arm. Expected stress levels will be much lower than indicated.

## STRESS ANALYSIS

RESOLVE AXIAL LOAD AT JT. 2 INTO TIE BEAM AND ACTUATOR ARM AXIAL LOADS



$$F_{2a} = (25/24)(5.8) = 6.0 \text{ KIPS}$$

$$F_{2b} = (7/24)(5.8) = 1.7 \text{ KIPS}$$

$$f_a = F_{AXIAL} / A$$

$$f_b = M_B \cdot (H/2) / I$$

$$f_v = 1.5V / A_w = 1.5V / t \cdot H$$

BENDING, AXIAL & SHEAR STRESSES

PT	$F_{AXIAL}$ (KIPS)	$M_B$ (KIP-IN)	$V$ (KIPS)	$A$ (IN <sup>2</sup> )	$H$ (IN)	$I$ (IN <sup>4</sup> )	$f_a$ (KSI)	$f_b$ (KSI)	$f_v$ (KSI)
2	6.0	28.6	5.5	1.10	6.57	5.44	5.5	17.1	9.5
3	↓	73.3	↓	1.61	9.59	17.0	3.7	20.7	6.4
4	↓	119	↓	2.11	12.68	39.0	2.8	19.3	4.9
5	6.0	165	5.5	2.61	15.76	74.2	2.3	17.5	3.9
7	1.7	8.0	0	1.12	6.60	5.64	1.5	4.7	0



## STRESS ANALYSIS

### TORSIONAL STRESS BETWEEN PTS 2 & 5

SINCE THE SECTION RESISTS TORSIONAL TWIST PRIMARILY BY BENDING OF THE TOP & BOTTOM FLANGES THE WARPING AND TORSIONAL STIFFNESS PROPERTIES AND THE TORSIONAL LOAD WILL BE APPROXIMATED BY USING THE AVERAGE PROPERTIES BETWEEN PTS. 3 & 4 (REF MEMBER PROPERTY TABLE).

$$K_j = (1/2)(961 + 1260)(10^{-5}) = 0.0111 \text{ IN}^4$$

$$C_w = (1/2)(2.68 + 9.77) = 6.23$$

$$e = (1/2)(0.355 + 0.558) = 0.457$$

$$t_o = V_e / Q = (1/2)(11 \text{ KIPS})(0.457) / 25 = 0.10 \text{ KIPS/IN}$$

$$\beta = (K_j / C_w E)^{1/2} = [(0.0111)(11.5 \cdot 10^6) / (6.23)(29 \cdot 10^6)]^{1/2} = 0.0266$$

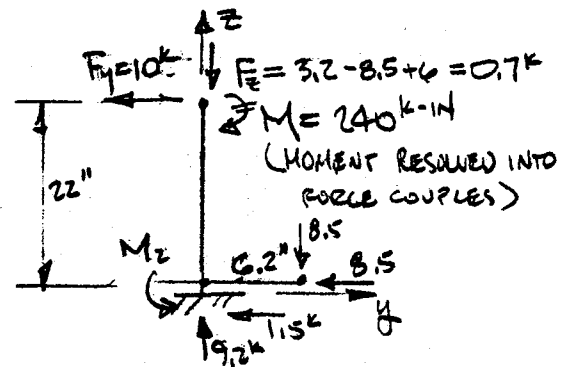
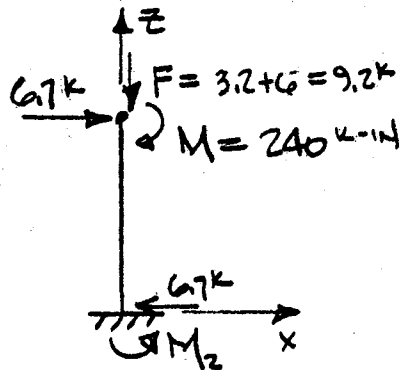
EVALUATE  $\theta'$  @  $x = L/2$  (REF EQ (8))

$$\theta' = \left[ (0.10)(25) / (2)(6.23)(30 \cdot 10^3)(0.0266)^2 \right] \left[ (0.0266)(25) / (4) + (\cosh(0) - \cosh\{(0.0266)(25) / (2)\}) / \sinh\{(0.0266)(25) / (2)\} \right]$$

(ANALYSIS STOPPED AT THIS POINT AS ARM DESIGN WAS CHANGED)

## 6.0 SURVIVAL ANALYSIS (90 MPH, ZENITH STOW)

REFERENCE LOAD ANALYSIS FOR TORQUE TUBE BRACKET ACTUATOR ARM.



① D.L. + W.L. ALONG EL AXIS

$$M_2 = (6.7)(22) + 240 = 387 \text{ k-in}$$

② D.L. + W.L. ALONG X-EL AXIS

$$F_y^{\text{WIND}} = (2' \times 25') (1.2) (20.7) = 1.2 \text{ k}$$

(WIND LOAD ON TORQUE TUBE)

$$F_y = 1.2 + 8.5 = 9.7 \text{ SAY } 10 \text{ k}$$

240 k-in      220 k-in

$$M_2 = 8.5(6.2 + 22) + (10)(22)$$

$$M_2 = 460 \text{ KIP-IN}$$

### STRESSES AT EL. AXIS SECTION

①

$$f_b = M/S_y = 240/34.7 = 6.9 \text{ ksi} < F_b \approx 22 \text{ ksi}$$

$$f_{vx} = 1.5V/A_{vx} = (1.5)(6.7)/(4.6) = 2.1 \text{ ksi} < F_v \approx 18 \text{ ksi}$$

②

$$f_b = 0$$

$$f_v = (1.5)(10 \text{ k}) / (1.7) = 8.8 \text{ ksi} < F_v = 18 \text{ ksi}$$

Note: MAX.  $F_z = 3.2 + 8.5 + 6.0 = 17.7 \text{ k}$  (OPPOSITE WIND)

$$f_a = 17.7 \text{ k} / 6.56 \text{ in}^2 = 2.7 \text{ ksi} < F_a \approx 20 \text{ ksi}$$



SURVIVAL ANALYSISSTRESSES AT BASE SECTION

$$\textcircled{1} \quad f_b = M/S_y = 240/325 = 0.8 \text{ ksi} < F_b \approx 22 \text{ ksi}$$

$$f_v = 1.5V/A_b = (1.5)(6.7)/3.3 = 3.0 \text{ ksi} < F_v = 18 \text{ ksi}$$

$$\textcircled{2} \quad f_b = 460/325 = 1.4 \text{ ksi} < F_b$$

$$f_v = (10)(1.5)/3.3 = 4.5 \text{ ksi} < F_v$$

<p>STRESS LEVELS OKAY FOR D.L. + 90 MPH WIND LOAD AT ZENITH STOW POSITION</p>
---

NOTE: MAY BE POSSIBLE TO REDUCE MATERIAL THICKNESS TO 0.05 INCH FOR THIS PIECE. P.E. ANALYSIS FOR 27 MPH WIND MAY GOVERN DESIGN THICKNESS. ALSO NEED TO CHECK 50 MPH DRIVE TO STOW CONDITION ( $F_{50} = (\frac{50}{90})^2 F_{90} = 0.31 F_{90}$ ). FURTHER ANALYSIS REQUIRED.

SURVIVAL ANALYSIS

INERTIA LOADS:

$$\text{ASSUME } \ddot{\theta} = 1^\circ/s^2 = (1/60) \text{ rad}/s^2$$

FROM BOEING LOAD ANALYSIS

$$\frac{M_y}{\ddot{\theta}} = 50 \text{ KIP} \cdot \text{FT} \cdot \text{S}^2$$

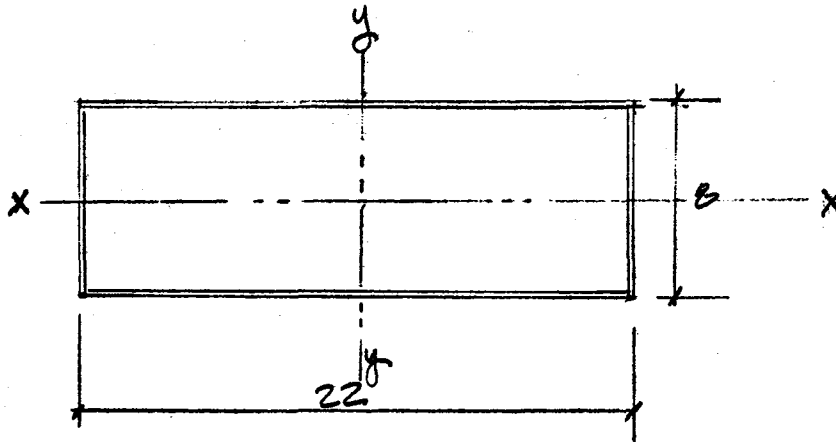
$$M_y = (50) (1/60) \times 12 \text{ IN}/\text{FT} = 10 \text{ K} \cdot \text{IN}$$

$$\frac{M_z}{\ddot{\theta}} = 75 \text{ KIP} \cdot \text{FT} \cdot \text{S}^2$$

$$M_z = (75) (1/60) (12) = 15 \text{ K} \cdot \text{IN}$$

INERTIA LOADS VERY SMALL AS COMPARED TO WIND LOADS. DESIGN FOR WIND LOAD CONDITION.

## EL AXIS SECTION



$$P = (22 + 8) \times 2 = 60'' \times 62.9 \text{ okay}$$

$$I_x = \frac{(22)(8)^3}{12} - \frac{(21.79)(7.79)^3}{12} = 80.3 \text{ IN}^4$$

$$I_y = (1/12)[(8)(22)^3 - (7.79)(21.79)^3] = 382 \text{ IN}^4$$

$$A = 6.56 \text{ IN}^2$$

$$S_x = \frac{I_x}{c} = 80.3/4 = 20.1 \text{ IN}^3$$

$$S_y = \frac{I_y}{c} = 382/11 = 34.7 \text{ IN}^3$$

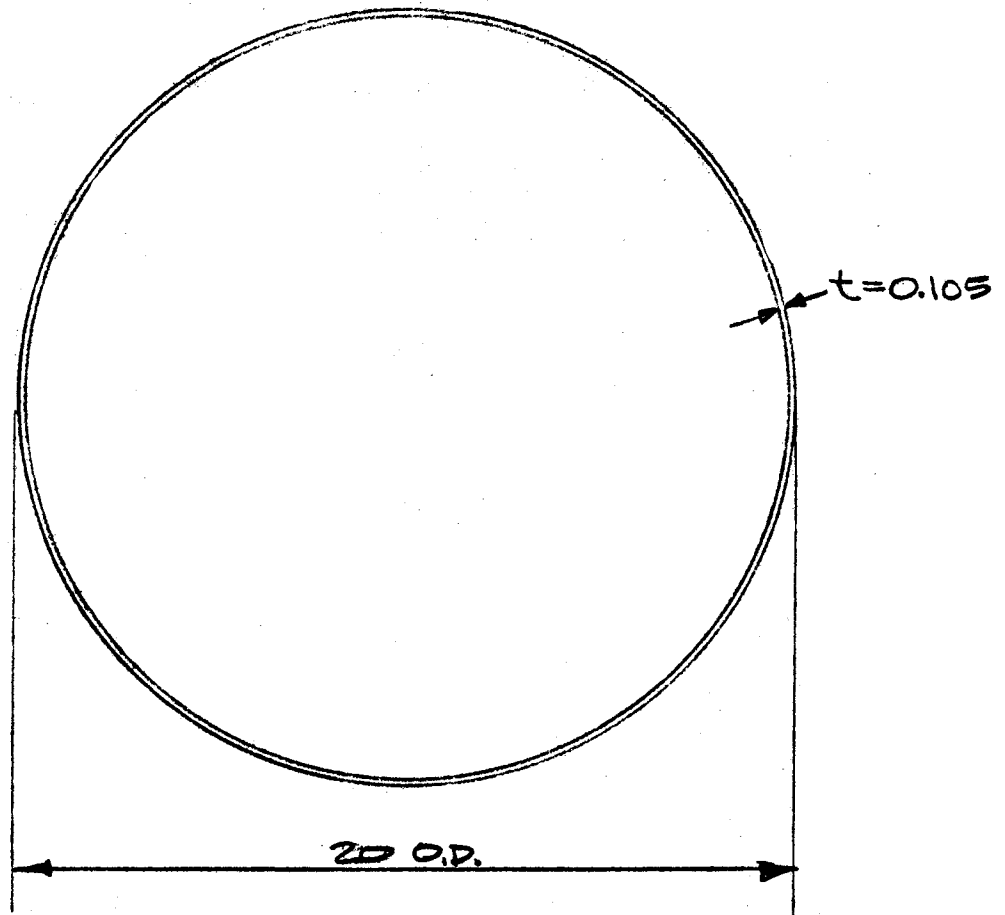
$$A_{sx} = (0.105)(44) = 4.6 \text{ IN}^2$$

$$A_{sy} = (0.105)(16) = 1.7 \text{ IN}^2$$

$$J = 2t(a-t)^2(b-t)^2/a+b = (2)(0.105)(22-0.105)^2(8-0.105)^2/30$$

$$J = 209 \text{ IN}^4 \quad (\text{Roark, Table IX, Case II, 4th Ed})$$

## BASE SECTION



$$P = \pi D = 62.83$$

$$I = \frac{\pi}{64} (d^4 - d_i^4) = \frac{\pi}{64} (20^4 - 19.79^4) = 324.7 \text{ in}^4$$

$$A = \frac{1}{2} \pi t (d + d_i) = 6.56 \text{ in}^2$$

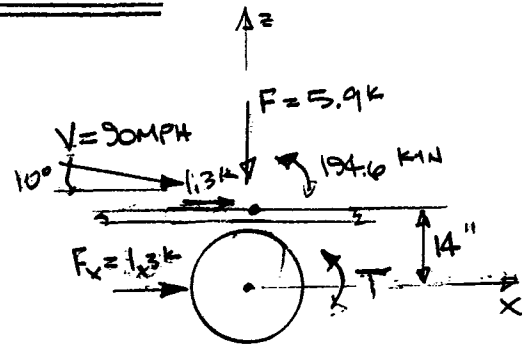
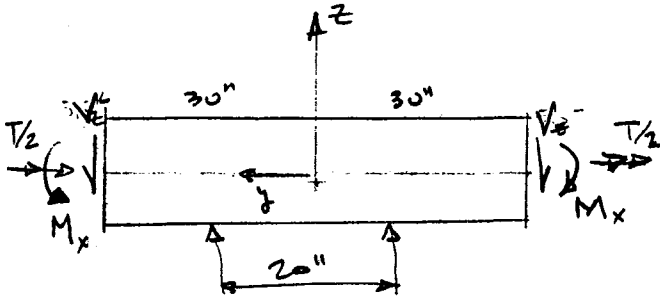
$$S = \frac{\pi}{32d} (d^4 - d_i^4) = \frac{\pi}{(20)(32)} (20^4 - 19.79^4) = 32.15 \text{ in}^3$$

$$A_s = \frac{1}{2} A = 3.3 \text{ in}^2$$

$$J = I_x + I_y = 2I = 649 \text{ in}^4$$

## 7.0 TORQUE TUBE SURVIVAL STRESSES

MAX. LOAD CASE:  $V=90\text{MPH}$ ,  $\alpha=90^\circ$



$$V_z = (1/2)(5.9) = 2.85\text{ k}$$

$$M_x = (2.85) \cdot 60 = 171\text{ k-in}$$

$$T = 194.6 - 1.3(14) = 176.4\text{ k-in}$$

$$T/2 = 88.2\text{ k-in}$$

$$V_x = 1/2(1.3) = 0.65\text{ k}$$

$$M_y = (0.65)(60) = 39\text{ k-in}$$

$$f_{bx} = \frac{M_x}{S} = \frac{171 + (2.85)(20)}{172/8} = 10.6\text{ ksi}$$

$$f_{by} = \frac{M_y}{S} = \frac{39 + (0.65)(20)}{172/8} = 2.5\text{ ksi}$$

$$f_b = (f_{bx}^2 + f_{by}^2)^{1/2} = 10.9\text{ ksi}$$

$$f_v = (2.85 + 0.65) / (1/2)(5.44) = 1.3\text{ ksi}$$

$$\tau = \frac{T}{rA} = \frac{176.4}{(8)(5.44)} = 4.1\text{ ksi}$$

## TORQUE TUBE STRESSES

CHECK FOR BUCKLING

FOR BENDING ONLY (REF TABLE 35, CASE 16 (1))

$$M_{cr} = \frac{30 \cdot 10^3 \text{ ksi}}{1 - 0.3^2} (8)(0.109)^2 = 3135 \text{ K-IN}$$

FOR TORSIONAL SHEAR STRESS (TABLE 35, CASE 17b)

$$T_{cr} = \frac{A E T}{(1 - \nu^2)} \left( \frac{t}{r} \right) \left( -2.39 + [9.69 + 0.605 H^{1.5}]^{1/2} \right)$$

$$H = (1 - \nu^2)^{1/2} \left( \frac{r^2}{\nu r} \right) = \quad r = 20", t = 0.109$$

$$H = (1 - 0.3^2)^{1/2} \left( \frac{20^2}{(0.3)(8)} \right) = 159$$

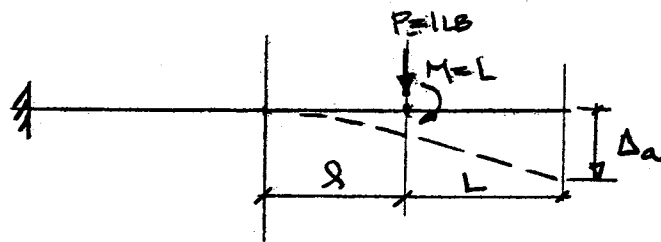
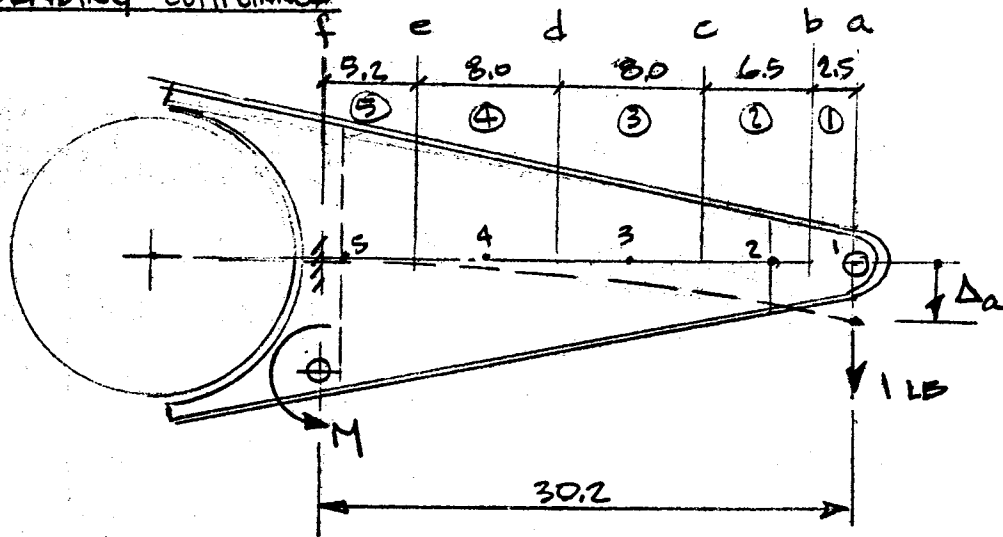
$$T_{cr} = 264,307 \text{ KIPS}$$

GENERAL BUCKLING OF TUBE WILL NOT OCCURE,  
 (LOCAL BUCKLING MAY GOVERN DESIGN - MAX DESIGN  
 LOADS WILL BE APPLIED DURING LOAD TEST TO  
 DEMONSTRATE ADEQUATE DESIGN.)

(1) FORMULAS FOR STRESS & STRAIN, R. ROARK ET AL, 5TH ED., MCGRAW HILL

## 8.0 COMPLIANCE

### BENDING COMPLIANCE



$$\Delta_a = \Delta_p + \Delta_m + \theta_p \cdot L + \theta_m \cdot L + \Delta_v$$

$$\Delta_a = \frac{PL^3}{3EI} + \frac{ML^2}{2EI} + \frac{PL^2}{2EI} \cdot L + \frac{ML}{EI} \cdot L + \frac{1.2L}{A_wG}$$

$$\Delta_a = \frac{L^3}{3EI} + \frac{L^2L}{2EI} + \frac{L^2L}{2EI} + \frac{L^2L}{EI} + \frac{1.2L}{A_wG}$$

$$\Delta_a = \frac{L^3}{3EI} + \frac{L^2L}{EI} + \frac{L^2L}{EI} + \frac{1.2L}{A_wG}$$

$$E = 30 \cdot 10^6 \text{ PSI}$$

$$G = 12 \cdot 10^6 \text{ PSI}$$

NOTE: 1 LB BENDING LOAD APPLIED TO BOTH CHANNEL SECTIONS.

COMPLIANCE

## BENDING DEFLECTION OF ARM

SPAN	Q	L	I *	A <sub>w</sub> *	$\frac{Q^3}{3EI}$	$\frac{Q^2L}{EI}$	$\frac{QL^3}{EI}$	$\frac{1.2Q}{A_w G}$	$\Delta_a$
	IN	IN	IN <sup>4</sup>	IN <sup>2</sup>	IN <sup>3</sup> × 10 <sup>8</sup>	IN <sup>2</sup> × 10 <sup>8</sup>	IN × 10 <sup>8</sup>	IN × 10 <sup>8</sup>	IN × 10 <sup>8</sup>
a-b	2.5	0	4.44	1.23	3.9	-		20.3	24.2
b-c	6.5	2.5	10.88	1.74	28.0	32.4	12.4	37.4	110.2
c-d	8.0	9.0	34.0	2.57	16.7	56.5	63.5	31.1	167.8
d-e	8.0	17.0	78.0	3.40	7.3	46.5	98.8	23.5	176.1
e-f	5.2	25.0	148.4	4.22	1.1	15.2	73.0	12.3	101.6
									579.6

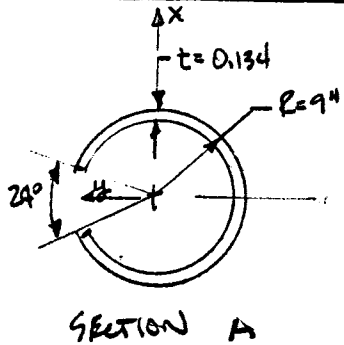
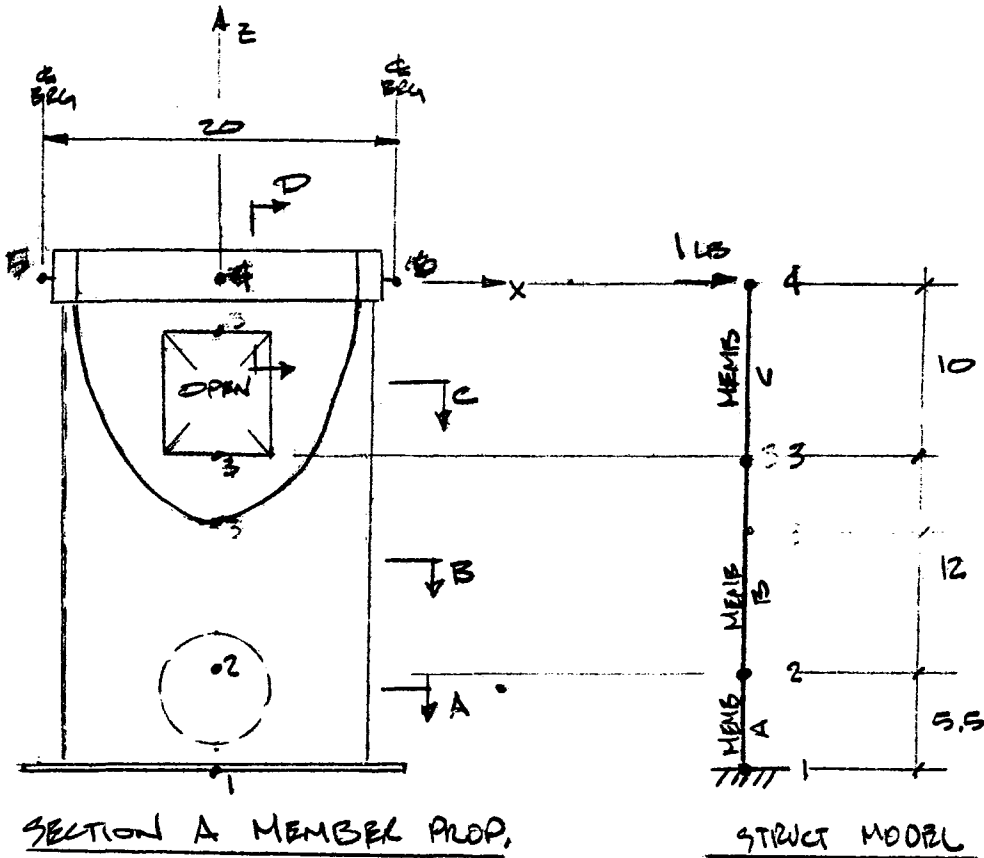
\* REF MEMBER PROP. TABLE

$$\Delta_a = 579.6 \times 10^{-8} \text{ IN/LB}$$

$$\Theta = \Delta_a / Q = 579.6 \times 10^{-8} / 30.2 = \underline{\underline{19.2 \times 10^{-8} \text{ RAD/LB}}}$$



# 9.0 GIMBAL MOUNT COMPLIANCE ANALYSIS



SECTION A MEMBER PROP.

STRUCT MODEL

$$A_n = \pi (18 - 0.134) \left( \frac{336}{360} \right) (0.134) = 7.0 \text{ IN}^2$$

$$I_{y_n} = (9)^3 (0.134) \left[ 1 - \frac{(3)(0.134)}{(2)(9)} + \frac{(0.134)^2}{(9)^2} - \frac{(0.134)^3}{(4)(9)^3} \right] (2.93 - \sin 12^\circ \cos 12^\circ)$$

$$I_{y_n} = 260 \text{ IN}^4$$

$$I_{y_a} = (9)^3 (0.134) \left[ \left( 1 - \frac{(3)(0.134)}{(2)(9)} + \frac{(0.134)^2}{(9)^2} - \frac{(0.134)^3}{(4)(9)^3} \right) (2.93 + 8 \sin 12^\circ \cos 12^\circ) - \frac{(2)(\sin^2 12^\circ)}{2.93} \right] + \left( \frac{(0.134)^2}{(3)(9)^2 (2.93)} (2 - \frac{0.134}{9}) \right) \left( 1 - \frac{0.134}{9} + \frac{(0.134)^2}{(9)^2} \right)$$

$$I_{y_a} = 297 \text{ IN}^4$$

SHEAR AREA  $\frac{2}{3} A_{\text{THIN}} = 2.3 \text{ IN}^2$  (FOR  $F_x$  LOADS)  
 $A = \frac{1}{2} A_T = 3.5 \text{ IN}^2$  (FOR  $F_y$  LOADS)

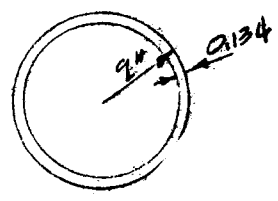
SECTION A PROP. (CONT)

SINCE WARPING IS VERY SMALL OVER SHORT LENGTH ASSUME K (TORSIONAL STIFF. CONST) IS 1/2 OF K FOR FULL SECTION

$$K = \frac{1}{2} \cdot \left(\frac{1}{2}\right) (\pi) (9^4 - 8.866^4) = 300 \text{ IN}^4$$

ASSUME SHEAR CENTER 1" OFF C TUBE

SECTION B MEMBER PROP



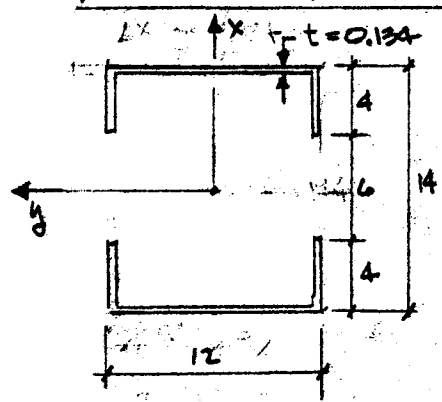
$$A = \pi (18 - 0.134) (0.134) = 7.52 \text{ IN}^2$$

$$I_{xx} = I_{yy} = \left(\frac{\pi}{4}\right) (\pi) (9^4 - 8.866^4) = 300$$

$$K = 2I = 600 \text{ IN}^4$$

$$A_s = \frac{1}{2} A = 3.8 \text{ IN}^2$$

SECTION C MEMBER PROP.



$$A = (40) (0.134) = 5.4 \text{ IN}^2$$

$$I_{xx} = \frac{(8)(0.134)^3}{12} (2) + \frac{(0.134)(12)^3}{12} (2)$$

$$+ (8)(0.134)(2)(6)^2 = 116 \text{ IN}^4$$

$$I_{yy} = \frac{(0.134)(4)^3}{12} (4) + \frac{(12)(0.134)^3}{12} (2)$$

$$+ (4)(0.134)(4)(5)^2 + (12)(0.134)(2)(6.93)^2$$

$$I_{yy} = 211 \text{ IN}^4$$

$$k = \frac{2a^2b^3}{(4tb)^2 - 2t^2} = 294 \text{ IN}^4$$

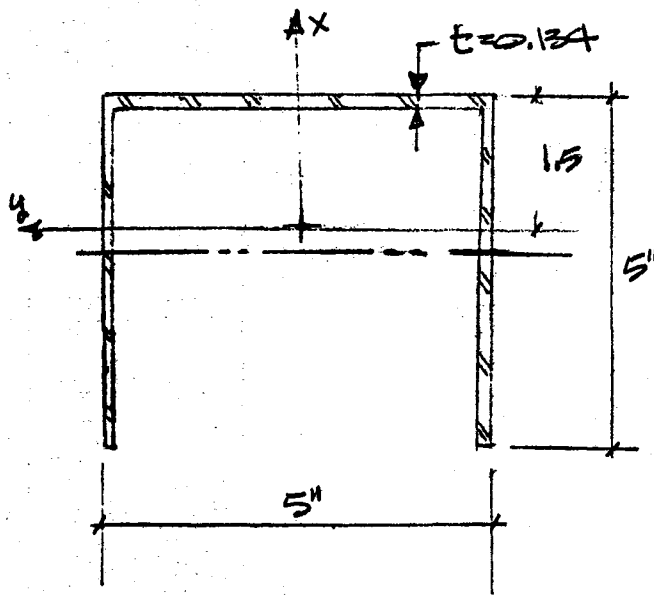
$$A_{F_{ox}} = (16) (0.134) = 2.1 \text{ IN}^2 \quad (\text{FOR } F_x \text{ LOADS})$$

$$A_{C_{sy}} = (24) (0.134) = 3.2 \text{ IN}^2 \quad (\text{FOR } F_y \text{ LOADS})$$

$$k = \dots = 125 \text{ IN}^4$$

9-3

## SECTION D MEMBER PROPERTIES



$$\bar{X} = \frac{(5)(0.134)(1.366) + (5)(0.134)(2)(-1.0)}{(5)(0.134)}$$

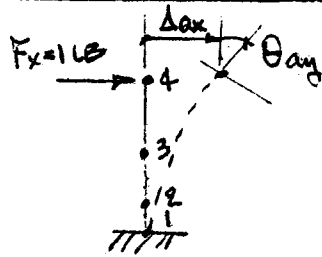
$$\bar{X} = -0.21''$$

$$I_{dx} = \frac{(0.134)(5)^3}{12} + \frac{(2)(5)(0.134)^3}{12} + (2)(5)(2.43)^2 = 60 \text{ IN}^4$$

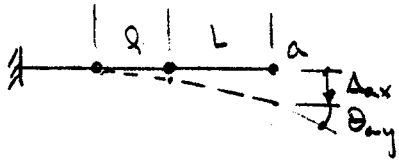
$$I_{dy} = \frac{(5)(0.134)^3}{12} + \frac{(2)(0.134)(5)^3}{12} + (2)(5)(0.134)(0.79)^2 + (5)(0.134)(0.79)^2$$

$$I_{dy} = 5.16 \text{ IN}^4$$

LOAD CASE 1:  $F_x = 1 \text{ LB}$



APPLY UNIT LOAD AT JT 4  
IN X DIRECTION



$$\Delta_{ax} = \Delta_p + \Delta_m + \Theta_p \cdot L + \Theta_n \cdot L + \Delta_r$$

$$\Delta_{ax} = \frac{PQ^3}{3EI} + \frac{MQ^2}{2EI} + \frac{PQ^2}{2EI} \cdot L + \frac{ML}{EI} \cdot L + \frac{12Q}{A_s G}$$

$$\Delta_{ax} = \frac{Q^3}{3EI} + \frac{Q^2 L}{EI} + \frac{QL^2}{EI} + \frac{12Q}{A_s G}$$

$$\Theta_{ay} = \Theta_p + \Theta_n = \frac{PQ^2}{2EI} + \frac{MQ}{EI} = \frac{Q^2}{2EI} + \frac{QL}{EI}$$

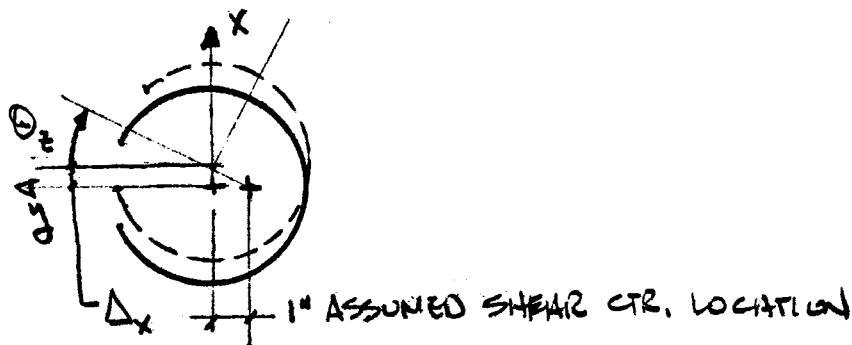
FX: GIBBAL BENDING & SHEAR DISPLACEMENTS & ROTATIONS

SPAN	Q	L	I	A <sub>sx</sub>	$\frac{Q^3}{3EI}$	$\frac{Q^2 L}{EI}$	$\frac{QL^2}{EI}$	$\frac{12Q}{A_s G}$	$\frac{Q^2}{2EI}$	$\frac{QL}{EI}$	$\Delta_{ax}$	$\Theta_{ay}$
	IN	IN	IN <sup>4</sup>	IN <sup>2</sup>	IN × 10 <sup>-8</sup>	IN × 10 <sup>-8</sup>	IN × 10 <sup>-8</sup>	IN × 10 <sup>-8</sup>	RAD × 10 <sup>10</sup>	RAD × 10 <sup>10</sup>	IN × 10 <sup>-8</sup>	RAD × 10 <sup>-10</sup>
1-2	5.5	22	297	2.3	0.6	7.5	29.9	23.9	111	136	67.9	155
2-3	12	10	300	3.8	6.4	16.0	13.3	31.6	80	133	67.3	213
3-4	14	0	211	2.1	14.4	0	0	66.7	155	0	88.1	195
TOTALS											217	523

9-5

LOAD CASE 1;  $F_x = 1 \text{ LB}$  (CON'T)

SECTION A TORSION DUE TO OFFSET SHEAR CENTER  
CAUSES DISPLACEMENT IN X-DIRECTION AND ROTATION  
ABOUT Z AXIS AS FOLLOWS;



$$\theta_z = \frac{Tl}{Kt} = \frac{(1)(1)(5.5)}{(300)(12.10^6)} = 15. \times 10^{-10} \text{ RAD/LB}$$

$$\Delta_x = \theta_z \cdot e = (15. \times 10^{-10})(6) = 0.2 \times 10^{-8} \text{ IN/LB}$$

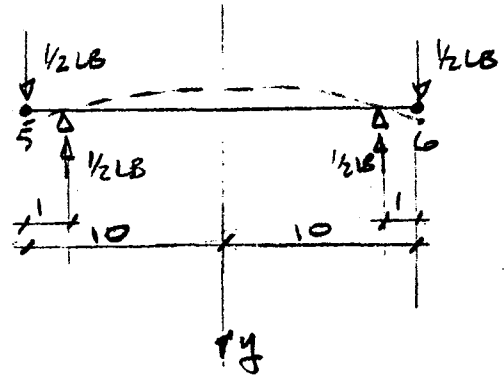
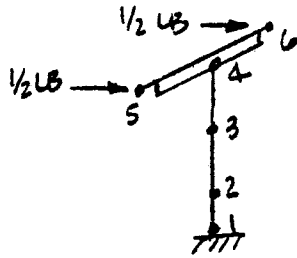
COMBINED BENDING, SHEAR & TORSIONAL DISPLACEMENTS

$$\Delta_{F_x}^x = 217 \times 10^{-8} \text{ IN/LB}$$

$$\theta_{F_x}^y = 523 \times 10^{-10} \text{ RAD/LB}$$

$$\theta_{F_x}^z = 15 \times 10^{-10} \text{ RAD/LB}$$

### LOAD CASE 2: $F_4 = 1 \text{ LB}$



$$\Delta_{5y} = \Delta_{6y} = \theta \cdot l + \frac{Pl^3}{3EI} = \frac{1/2 L \theta}{EI_{dx}} + \frac{Pl^3}{3EI}$$

$$\Delta_{5y} = \frac{(1/2)(10)(1)}{(30 \cdot 10^6)(60)} + \frac{(1)(1)^3}{3(30 \cdot 10^6)(60)} = 0.5 \times 10^{-8} \text{ IN}$$

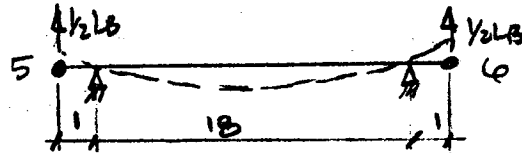
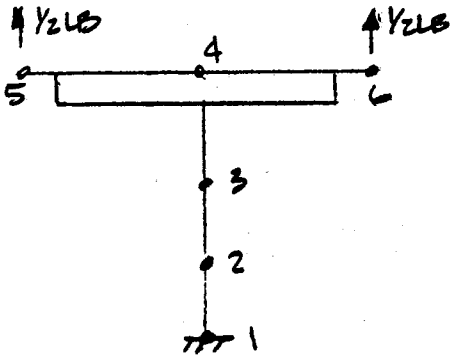
SPAN	$l$	$L$	$\bullet I$	$A_{5x}$	$\frac{l^3}{3EI}$	$\frac{l^2 \cdot L}{EI}$	$\frac{l L^2}{EI}$	$\frac{1.2 l}{A_{5G}}$	$\Delta_{4y}$
	IN	IN	IN <sup>4</sup>	IN <sup>2</sup>	IN <sup>3</sup> × 10 <sup>-8</sup>	IN <sup>2</sup> × 10 <sup>-8</sup>	IN × 10 <sup>-8</sup>	IN × 10 <sup>-8</sup>	IN × 10 <sup>-8</sup>
1-2	5.5	22	260	3.5	0.7	8.5	34.1	15.7	59.0
2-3	12	10	300	3.8	6.4	16.0	13.3	31.6	67.3
3-4	14	0	116	3.2	26.2	0	0	43.8	70.0
									196.3

$$\Delta_{F4}^y = 197 \times 10^{-8} \text{ IN/LB}$$

$$\theta_{F4}^x = \sin^{-1} \frac{\Delta_{F4}^y \sin \delta}{L_{57} - \Delta_{F4}^y \cos \delta} = 646 \times 10^{-10} \text{ RAD/LB}$$

(REF. LOAD CASE 4 FOR  $\theta_{F4}^x$  EQUATION)

9-7

LOAD CASE 3:  $F_z = 1 \text{ LB}$ 

$$\Delta_{5z} = \Delta_{6z} = 0.2 + \frac{PQ^3}{3EC} = \frac{(1/2)(18)(1)}{(30.10^6)(5.6)} + \frac{(1)(18)^3}{(30.10^6)(3)(5.6)}$$

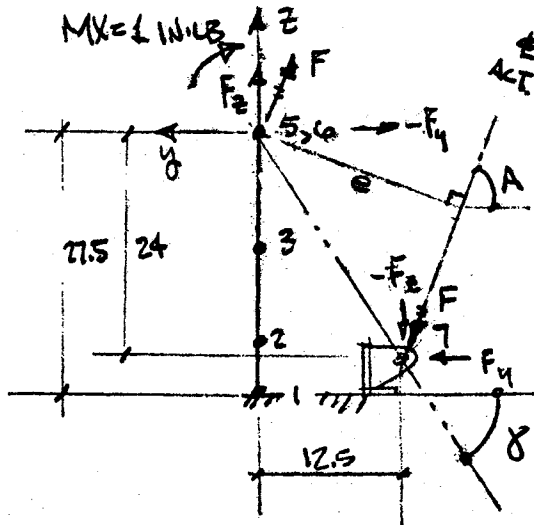
$$\Delta_{5z} = 5.6 \times 10^{-8} \text{ IN}$$

$$\Delta_{4z} = \frac{PQ}{AE} = \frac{(5.5)}{(1)(30.10^6)} + \frac{(12)}{(1.52)(30.10^6)} + \frac{(14)}{(5.4)(30.10^6)} = 16.6 \times 10^{-8} \text{ IN}$$

$$\Delta_{Fz}^z = (16.6 + 5.6) \times 10^{-8} = 22.2 \times 10^{-8} \text{ IN/LB}$$

9.8

LOAD CASE 4:  $M_X = 1 \text{ W} \cdot \text{LB}$

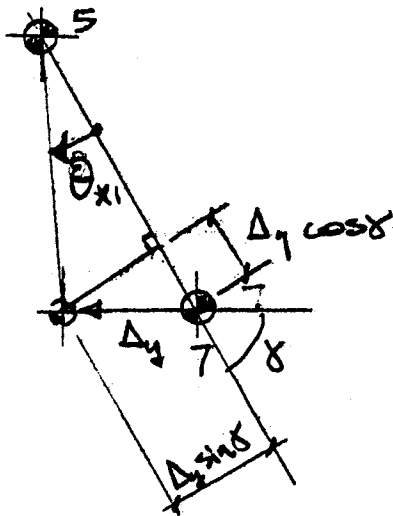


REF GEOMETRY CAL'S FOR DISTANCE  $e$  & ANGLE  $A$

$$F = M/e$$

$$F_y = F \cos A$$

$$F_z = F \sin A$$

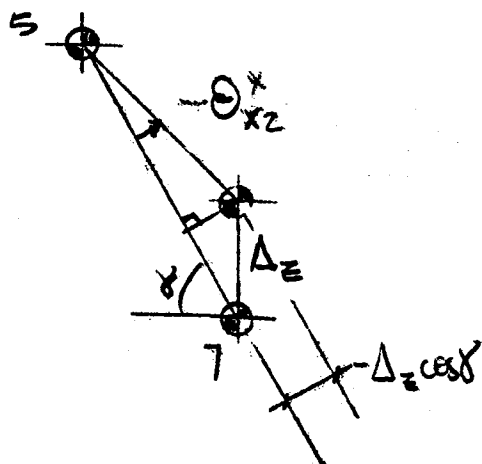


$$\delta = \tan^{-1} \frac{24}{12.5} = 62.5^\circ$$

$$\Delta_y = \Delta_{7y} - \Delta_{5y}$$

$$\theta_{x1} = \sin^{-1} \frac{\Delta_y \sin \delta}{L_{57} - \Delta_y \cos \delta}$$

$$L_{57} = (24^2 + 12.5^2)^{1/2}$$



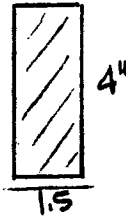
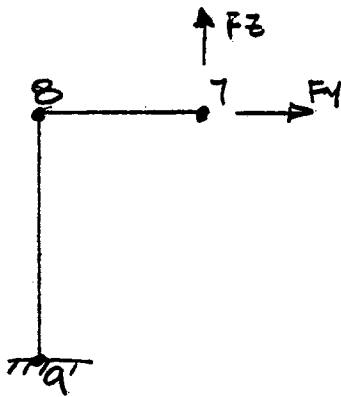
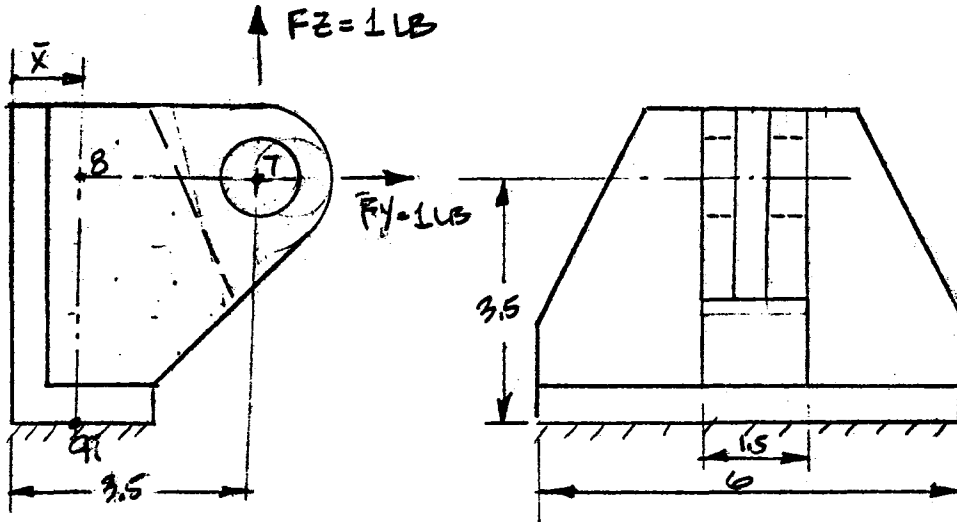
$$\Delta_z = \Delta_{7z} - \Delta_{5z}$$

$$\theta_{x2} = \sin^{-1} \frac{\Delta_z \cos \delta}{L_{57} - \Delta_z \sin \delta}$$

$$\theta_{MX}^x = \theta_{x1} - \theta_{x2}$$



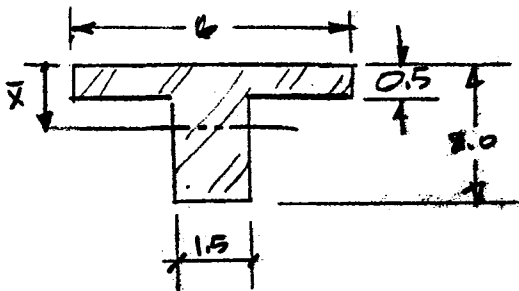
ACTUATOR BRACKET COMPLIANCE (LOAD CASE 4 CONT)



CONSIDER SHEAR DEFL. ONLY  
 $A_x = 6 \text{ IN}^2$

SECTION 7-8

STRUCTURAL MODEL



$$x = \frac{(6)(0.5)(2.5) + (1.5)(1.5)(1.25)}{(1.5)^2 + (3)}$$

$$\bar{x} = 0.68$$

$$A = 5.25 \text{ IN}^2 ; A_y = (1.5)(2) = 3 \text{ IN}^2$$

$$I_x = \frac{(1.5)(1.5)^3}{12} + \frac{(6)(0.5)^3}{12} + (3)(0.43)^2 + (1.5)^2(1.07)^2 = 1.05 \text{ IN}^4$$

$$\Delta_{Ez} = \frac{(1)(2.82)}{(6)(12,100)} + \frac{(2.82)(3.5)}{(30,100)(1.05)} + \frac{(1)(3.5)}{(5,25)(30,100)} = 9.2 \times 10^{-8} \text{ IN/LB}$$

$$\Delta_{Ey} = \frac{(1)(3.5)^3}{(3)(30,100)(1.05)} + \frac{(3.5)}{(3)(12,100)} = 5.5 \times 10^{-8} \text{ IN/LB}$$

9-10

LOAD CASE 4;  $M_X = 1$  IN·LB (CON'T)

$$\Delta_{SY} = F_Y \cdot \Delta_{FYS}^Y = F_Y (197 \times 10^{-8} \text{ IN/LB})$$

$$\Delta_{SZ} = F_Z \cdot \Delta_{FZS}^Z = F_Z (22 \cdot 10^{-8} \text{ IN/LB})$$

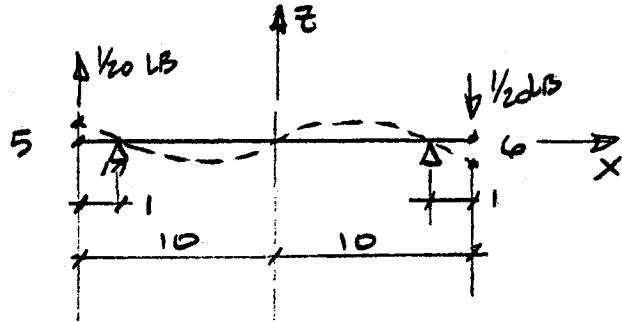
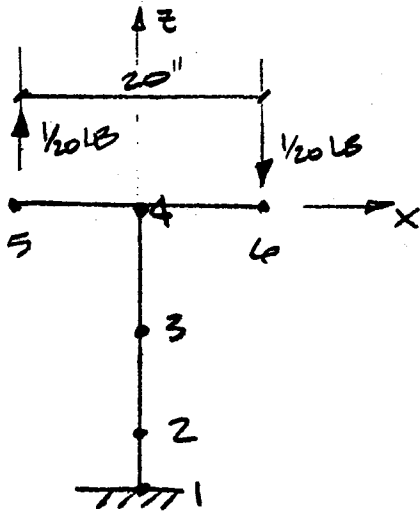
$$\Delta_{TY} = F_Y \cdot \Delta_{FYT}^Y = F_Y (55 \times 10^{-8} \text{ IN/LB})$$

$$\Delta_{TZ} = F_Z \cdot \Delta_{FZT}^Z = F_Z (99 \times 10^{-8} \text{ IN/LB})$$

$\alpha$	$F_Y$	$F_Z$	$\Delta_{SY}$	$\Delta_{SZ}$	$\Delta_{TY}$	$\Delta_{TZ}$	$\Theta_{X1}$	$\Theta_{XZ}$	$\Theta_{MX}^X$
DEG	LB $\times 10^{-3}$	LB $\times 10^{-3}$	IN $\cdot 10^{-8}$	IN $\cdot 10^{-8}$	IN $\cdot 10^{-8}$	IN $\cdot 10^{-8}$	RAD $\times 10^{-10}$	RAD $\times 10^{-10}$	RAD $\times 10^{-10}$
0	9.0	62.7	-1.77	+1.38	+0.50	-6.21	7.4	-13.0	20.4
20	17.2	49.2	-3.39	+1.08	+0.95	-4.87	14.2	-10.2	24.2
70	29.1	24.2	-5.73	+0.53	+1.60	-2.40	24.0	-5.0	29.0
90	34.6	13.6	-6.82	+0.30	+1.90	-1.35	28.6	-2.8	31.4

$$\Theta_{MX}^X = 31.4 \times 10^{-10} \text{ RAD/IN·LB (MAX @ } \alpha = 90^\circ)$$

9-11

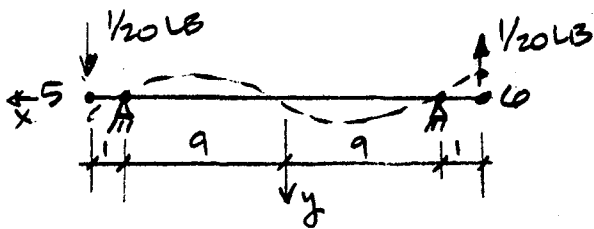
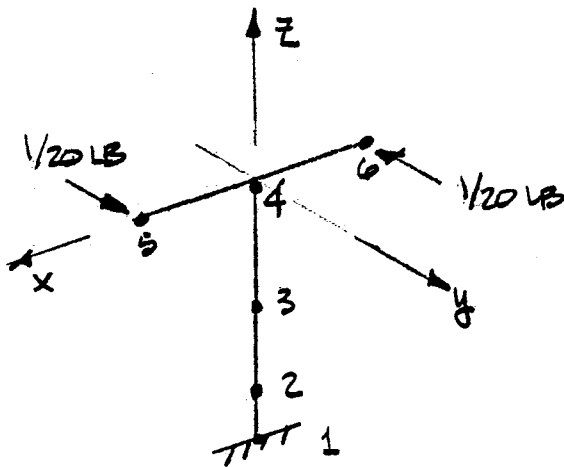
LOAD CASE 5:  $M_4 = 1 \text{ IN} \cdot \text{LB}$ 

$$\Delta_{5z} = \theta_{4y} \cdot l + \frac{Pl^3}{3EI} = \frac{(1/20)(1)(9)}{(30 \cdot 10^6)(5.6)} + \frac{(1)(1)^3}{(3)(30 \cdot 10^6)(5.6)} = 40.6 \cdot 10^{-10} \text{ IN}$$

$$\theta_{4y} = \frac{Ml}{EI} = \left[ \frac{(5.5)}{(297)} + \frac{(12)}{(300)} + \frac{(14)}{(211)} \right] \cdot \left( \frac{1}{30 \cdot 10^6} \right) = 41.6 \cdot 10^{-10} \text{ RAD}$$

$$\theta_{4y}^{M_4} = \theta_{4y} + (\Delta_{5z}/10) = 45.7 \cdot 10^{-10} \text{ RAD / IN} \cdot \text{LB}$$

9-12

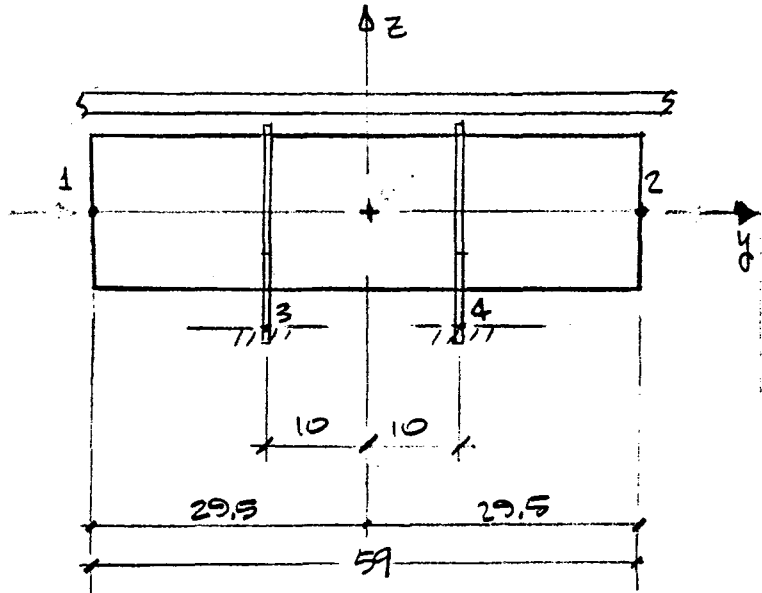
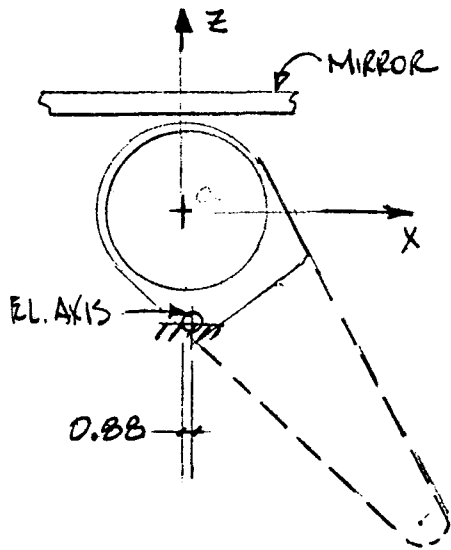
LOAD CASE 6:  $M_E = 1 \text{ IN}\cdot\text{LB}$ 

$$\Delta_{5y} = \theta_{11} \cdot 1 + \frac{P y^3}{3EI} = \frac{(1/20)(1)(9)}{(30 \cdot 10^6)(60)} + \frac{(1)(1)^3}{(3)(30 \cdot 10^6)(60)} = 4.35 \cdot 10^{-10} \text{ IN}$$

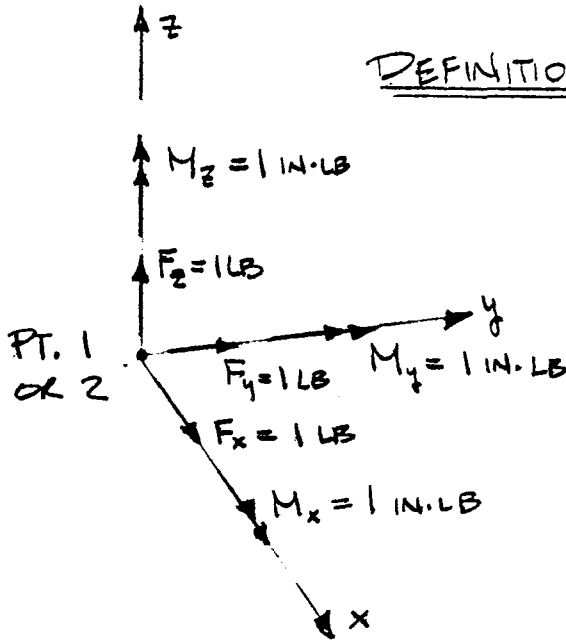
$$\theta_4^z = \frac{T D}{J G} = \left[ \frac{5.5}{300} + \frac{12}{600} + \frac{14}{294} \right] \cdot \left( \frac{1}{12 \cdot 10^6} \right) = 72 \cdot 10^{-10} \text{ RAD}$$

$$\theta_{ME}^z = \theta_4^z + (\Delta_{5y} / .10) = 72 \times 10^{-10} \text{ RAD} / \text{IN}\cdot\text{LB}$$

TORQUE TUBE COMPLIANCE



DEFINITION OF UNIT LOADS



UNIT LOADS ARE APPLIED AT POINT 1 IN THE X, Y & Z DIRECTIONS AND THE RESULTING DEFLECTIONS AND ROTATIONS ARE DETERMINED FOR POINTS 1 & 2.

USED LARGE FRAME COMPUTER PROGRAM WITH STRUCT. MODEL & UNIT LOADS SHOWN TO ESTABLISH COMPLIANCE.

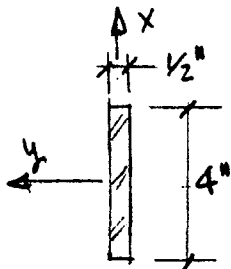
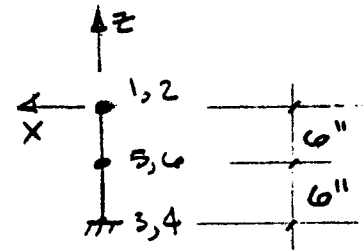
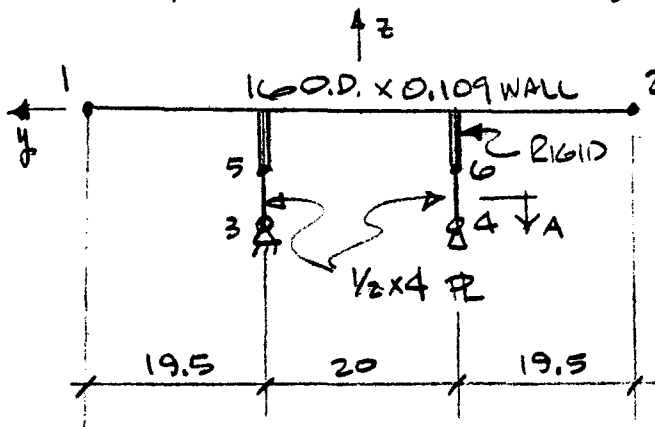
$M_x = 1 \text{ in} \cdot \text{lb}$

$F_z = 1 \text{ lb}$

10-2

# TORQUE TUBE

APPROXIMATE STRUCTURAL MODEL FOR TORQUE TUBE COMPLIANCE CALCULATIONS;



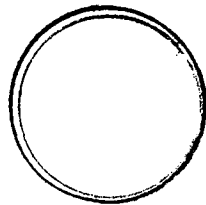
SECTION A

$$A_a = 2.1 \text{ in}^2$$

$$I_{ax} = (4) \left(\frac{1}{2}\right)^3 / 12 = 0.042 \text{ in}^4$$

$$I_{ay} = \left(\frac{1}{2}\right) (4)^3 / 12 = 2.67 \text{ in}^4$$

REF. MEMBER PROPERTY CALS



SECTION B

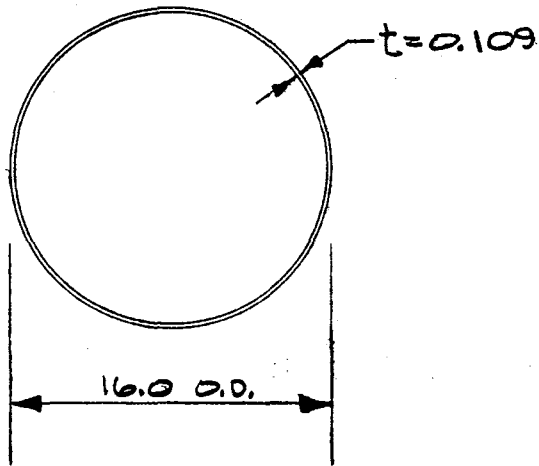
$$A_b = 5.44 \text{ in}^2$$

$$I = 172 \text{ in}^4$$

$$J = 344 \text{ in}^4$$

$$A_s = \frac{1}{2} A_b$$

TORQUE TUBE SECTION PROP.



$$A = (16 - 0.109)\pi(0.109) = 5.44 \text{ IN}^2$$

$$W = (5.44)(12)(490)/(1728) = 18.51 \text{ LBS/FT} \quad (1.54 \text{ LBS/IN})$$

$$I = (\pi/4)[8.0^4 - (7.891)^4] = 172 \text{ IN}^4$$

$$J = 2I = 344 \text{ IN}^4$$





REPORT E-6

ELEVATION DRIVE DESIGN ANALYSIS

FOR

GIMBAL/ACTUATOR DRIVE ASSEMBLY

FOR

BOEING SECOND GENERATION HELIOSTAT

JUNE 27, 1980

Reference: FACC TM16

TABLE OF CONTENTS

Section

- 1.0 Introduction
- 2.0 Basis of Analysis
- 3.0 Analysis Summary
- 4.0 Elevation Drive Analysis

## 1.0 INTRODUCTION

The purpose of this appendix is to analyze the various components of elevation drive and to verify that they are adequate for the heliostat application.

## 2.0 BASIS OF ANALYSIS

Load data from Appendix I of Boeing Specification is used to estimate loads for elevation drive.

## 3.0 ANALYSIS SUMMARY:

The first part of the analysis determines the elevation drive kinematics and estimates the loads on the elevation actuator (Pages 4 through 8).

The second part of the analysis reviews the nut design and determines that selected nut has an adequate factor of safety. (Pages 9 through 10).

The third part of the design estimates the elevation drive compliance (Pages 11 through 14). The elevation actuator compliance near horizon is  $2.2 \times 10^{-6}$  in/lb and near zenith is  $0.9 \times 10^{-6}$  in/lb.

The fourth part of the analysis contains design data on various nut materials and information on different companies that fabricate nuts and screws. (Pages 15 through 18).

The fifth part of the analysis involves motor sizing (Pages 19 through 22). It shows that 1/3 H.P. motor has more than adequate capacity to drive against 50 mph wind.

The sixth part of the analysis verifies the design of the actuator emergency stops (Pages 23 through 28). It shows that the stop design is adequate. The actuator screw has  $1\frac{1}{2}$ " - 4 acme thread. The actuator moment arm varies from 10.865 inch minimum to 19.277 inch maximum. This ratio plus gear-box gear ratio of 240 results in an overall ratio of 65536 to 116276. The actuator arrangement is such that  $93^\circ$  axis rotation will take 15 minutes.

## 4.0 ELEVATION DRIVE ANALYSIS

ELEVATION DRIVE KINEMATICS - REF FIG. 1

- FOR REFLECTOR AT ZENITH:

$$\theta_0 = \tan^{-1} \left( \frac{1.5}{11.97} \right) = 7.14269$$

$$\begin{aligned} \alpha_0 &= \cos^{-1} \left[ \frac{(32.856)^2 + (29.0)^2 - (12.06)^2}{2(32.856)(29.0)} \right] \\ &= 21.34125 \end{aligned}$$

$$\begin{aligned} \beta_0 &= \cos^{-1} \left[ \frac{(12.06)^2 + (29)^2 - (32.856)^2}{2(12.06)(29)} \right] \\ &= 97.63596^\circ \end{aligned}$$

$$\gamma_0 = 180 - \alpha_0 - \beta_0 = 61.02229$$

- FOR THE GENERAL CASE:

LET  $\alpha$  = ELEVATION ANGLE

$$\text{THEN } B = \alpha - (\beta_0 - 90 - \theta_0) + 90$$

$$= \alpha - 89.5061$$

$$r = 29 \sin(\beta - \alpha_0)$$

$$a = 10 - 29 \sin B$$

$$b = 29 \cos B - 16.5$$

$$A = \tan^{-1} \frac{a}{b}$$

$$A + B = \beta - \alpha_0$$

$$r = 29 \sin(A + B)$$

$$c = \sqrt{a^2 + b^2}$$

SEE TABLE I FOR CALCULATED VALUES OF THE ABOVE PARAMETERS

TABLE I (REF FIG 1)

$\alpha$	B	a	b	A	a	c
-3	-92.5061	38.972	-17.768	-65.491	10.86	42.831
0	-89.5061	38.999	-16.250	-67.380	11.38	42.248
15	-74.5061	37.946	-8.753	-77.01	13.83	38.942
30	-59.5061	34.989	-1.784	-87.081	15.97	35.03
45	-44.5061	30.328	4.182	-82.148	17.71	30.61
60	-29.5061	24.283	8.737	70.207	18.91	25.81
75	-14.5061	17.264	11.575	56.139	19.27	20.78
90	+0.4939	9.750	12.499	37.954	18.03	15.852
93	+3.4939	8.233	12.446	33.485	17.44	14.92

TABLE II EL DRIVE LOADS

$\alpha$	A		B		C		D		E		F		G	
	GRAV. ONLY		GRAV. + 27 MPH		GRAV. + 35 MPH		GRAV. + ICE + SNOW + 50 MPH		GRAV. + 90 MPH		GRAV. + 50 MPH		27 MPH WIND ONLY	
	MA (KIP-IN)	PACT (KIPS)	MA (KIP-IN)	PACT (KIPS)	MA (KIP-IN)	PACT (KIPS)	MA (KIP-IN)	PACT (KIPS)	MA (KIP-IN)	PACT (KIPS)	MA (KIP-IN)	PACT (KIPS)	MA (KIP-IN)	PACT (KIPS)
0	55.4	4.8	64.1	5.6	70	6.1	252	21.9			25.6	2.2	-8.7	-7.6
											85	7.4	8.7	7.6
10	54.5	4.1	69.4	5.2	79.5	6.0	269	20.3			106	8.0	14.9	1.1
20	52	3.5	72.8	5.0	87	5.96	279	19.1			123	8.4	20.8	1.4
30	47.9	3.0	72	4.5	83.4	5.2	273	17.0			131	8.1	24.1	1.5
40	42.4	2.5	66.3	3.8	82.4	4.8	250	14.5			124	7.2	23.8	1.4
50	35.6	2.0	63.1	3.5	81.8	4.5	235	12.9			130	7.1	27.5	1.5
60	27.7	1.5	61	3.2	83.1	4.4	222	11.7			141	7.4	33	1.7
70	18.9	1.0	51	2.7	72.8	3.8	183	9.5			129	6.7	32.1	1.7
80	9.6	0.5	40.8	2.1	62	3.3	143	7.5			116	6.1	31.2	1.6
90	0	0	22.2	1.2	37.3	2.1	-74.5	-4.2	247	13.8	76	4.2	22.2	1.2

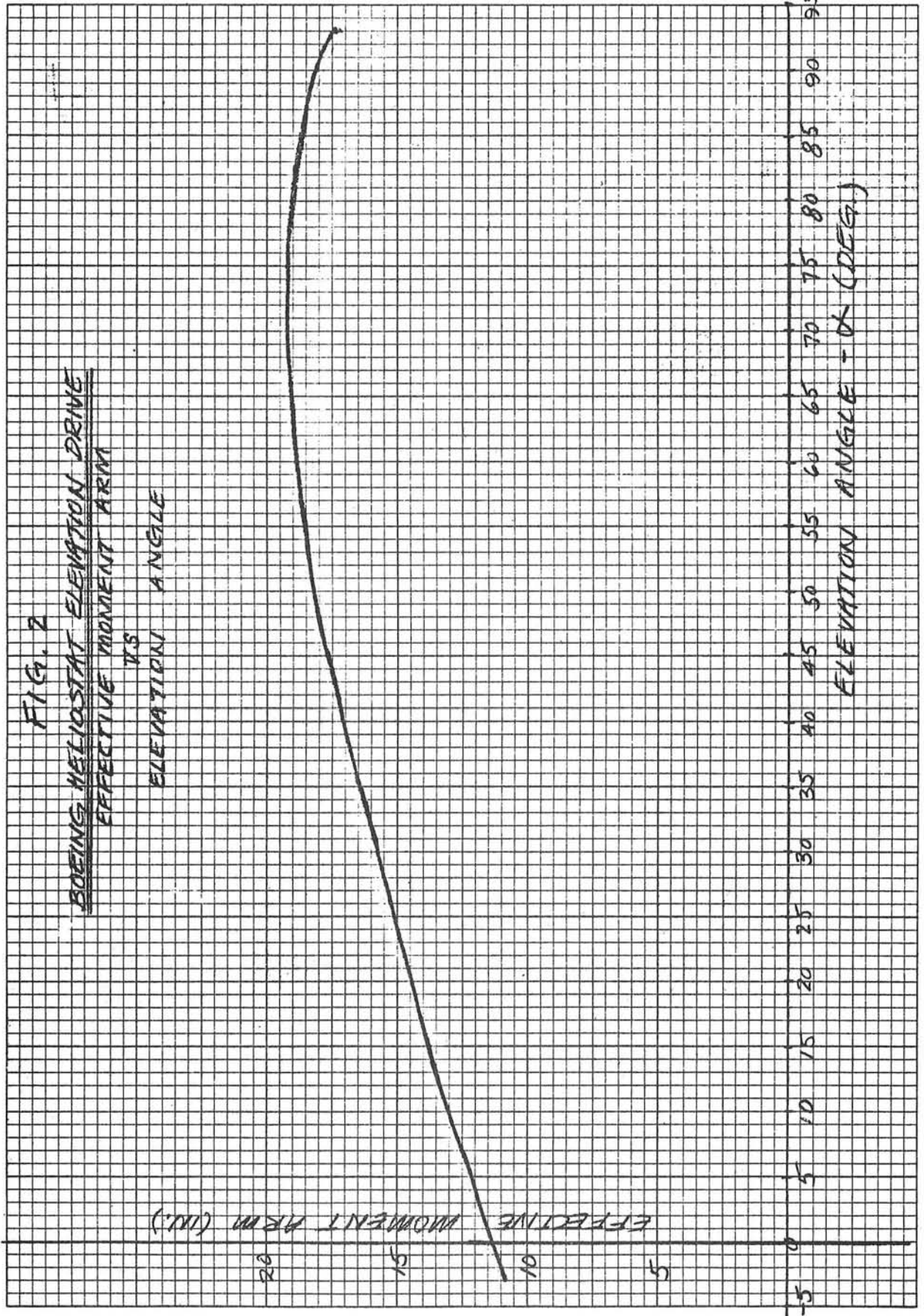
MA - EL AXIS TORQUE (BOEING APPENDIX I)

PACT - ACTUATOR LOAD (MINUS SIGN DENOTES SCREW IN COMPRESSION)

$\alpha$  = ELEVATION ANGLE

NOTE: FOR -90 MPH WIND, MIRROR IS STOWED AND ONLY  $\alpha = 90^\circ$  CASE IS PERTINENT.





DRIVE LOADS

REF: TABLE II AND FIG'S 2, 3, &amp; 4

A. MAX. STATIC LOAD (CASE 'D') = +22 KIPS (TENSION)B. MAX. OPERATING LOADS:

(1) 50 MPH WIND DRIVE TO STOW (CASE F)

MAXIMUM DRIVE LOAD = 8.4 K (TENSION)

(2) 'ADVERSE TRACKING' - 27 MPH WIND (CASE 'B')

MAX. DRIVE LOAD = +5.6 KIPS(3) 'NO WIND' - +4.8 KIPS

C. MAXIMUM COMPRESSION LOAD ON SCREW:

MAXIMUM COMPRESSION LOAD IS STATIC AND OCCURS DURING LOAD CASE 'D' WITH REFLECTOR AT  $\alpha = 90^\circ$  AND PRESENTS NO BUCKLING PROBLEM SINCE NUT IS ALMOST FULLY RETRACTED

MAX. COMP. LOAD = -4.2 KIPS



NUT DESIGN

NUT MATERIAL - TURCITE (TFE FILLED DELRIN, USED TO MAKE "SUPER NUT" & DURONUT)

PROPERTIES OF MATERIAL:  
(RE: SHAMBAH "DURONUT CAT.")

$$E = 133 \times 10^6 \text{ PSI}$$

$$\text{COEF. THERM. EXPAN.} = 55 \times 10^{-6} \text{ IN/IN/}^\circ\text{F}$$

COEF. FRICTION DRY  
(ON STEEL) - 0.08

$$S_t = 5,500 \text{ PSI (AT } 77^\circ\text{F)}$$

$$S_s = 5,700 \text{ PSI (AT } 77^\circ\text{F)}$$

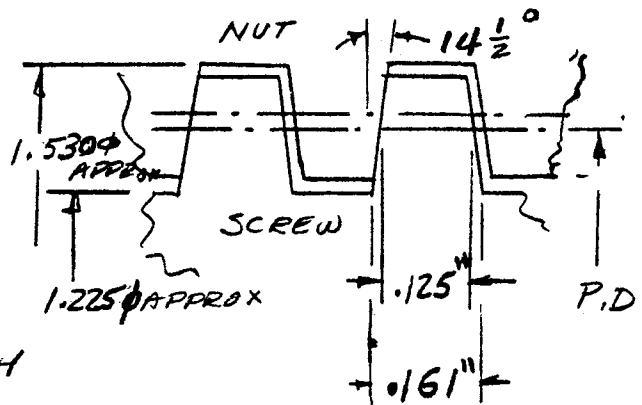
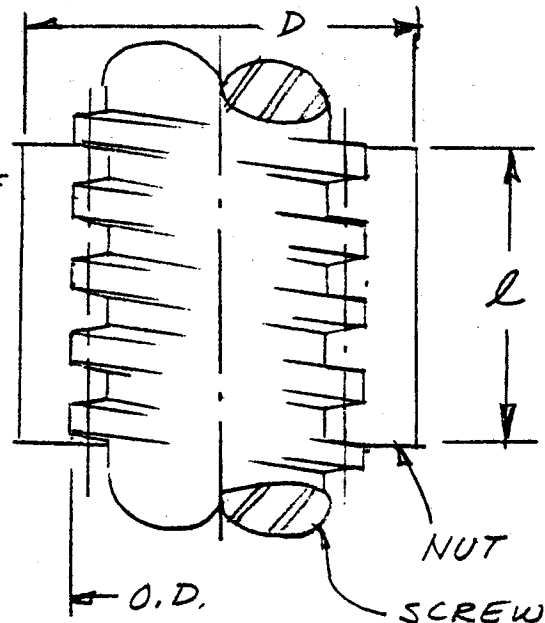
SCREW THREADS:

PITCH - 0.25 IN

P.D. - 1.370 / 1.363 DIA

O.D. - 1.5 IN

TYPE -  $1\frac{1}{2}$  - 4 ACME THREAD



CALCULATE NUT LENGTH  $L$   
AND COMPARE VALUE WITH  
DATE FOR MAX. LOAD ON  
STANDARD ACME TH'D "DURONUT"  
OF SIMILAR PROPORTIONS.

ASSUME S.F. = 2 AGAINST SHEAR FAILURE  
SHEAR  
THREAD TOOTH, AREA PER INCH OF NUT LENGTH

$$A = \frac{(.1617)(1.53)}{0.250} = 3.10 \text{ IN}^2$$

BASED ON THIS AND S.F. OF 1 THE MAX. LOAD PER  
INCH OF NUT IS:

$$P = 5700 \times 3.1 = 17,700 \text{ LB}$$

NUT DESIGN (CONT'D.)

FROM BOEING AXIS MOMENT DATA AND EL DRIVE  
KINEMATICS MAX. ACTUATOR LOAD = 22 KIPS  
(EL ANGLE = 0°)

$$\text{THEN } l = \frac{2 \times 22,000}{17,700} = 2.5 \text{ IN (FOR S.F. = 2)}$$

CHECK THIS USING DATA FROM "DURONUT" CATALOGUE  
FOR 1<sup>3</sup>/<sub>4</sub>-4 DURONUT MAX LOAD PER INCH OF  
LENGTH = 14,000 LB, BUT THIS IS FOR AN  
ACME THREAD, S.F. UNKNOWN

$$R_N = .422P - .259 \times \text{OD ALLOW.}$$

$$\text{OD ALLOW.} = .0125"$$

$$R_N = .422(.25) - .259(.0125)$$

$$= .102"$$

$$R_T = P - .102 = .25 - .102 = .148"$$

THREAD TOOTH <sup>SHEAR</sup> AREA PER INCH OF NUT LENGTH

$$A = \frac{(.148 \pi)(1.756)}{.25} = 3.26 \text{ IN}^2$$

ASSUMING S.F. = 1 &  $S_s = 5700 \text{ PSI}$

$$\text{THEN LOAD/IN OF NUT LENGTH} = 5700 \times 3.26$$

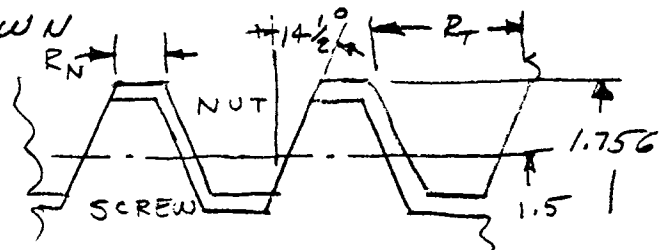
$$\text{TO CAUSE FAILURE (S.F. = 1)} = 18,600 \text{ LB}$$

GREATER

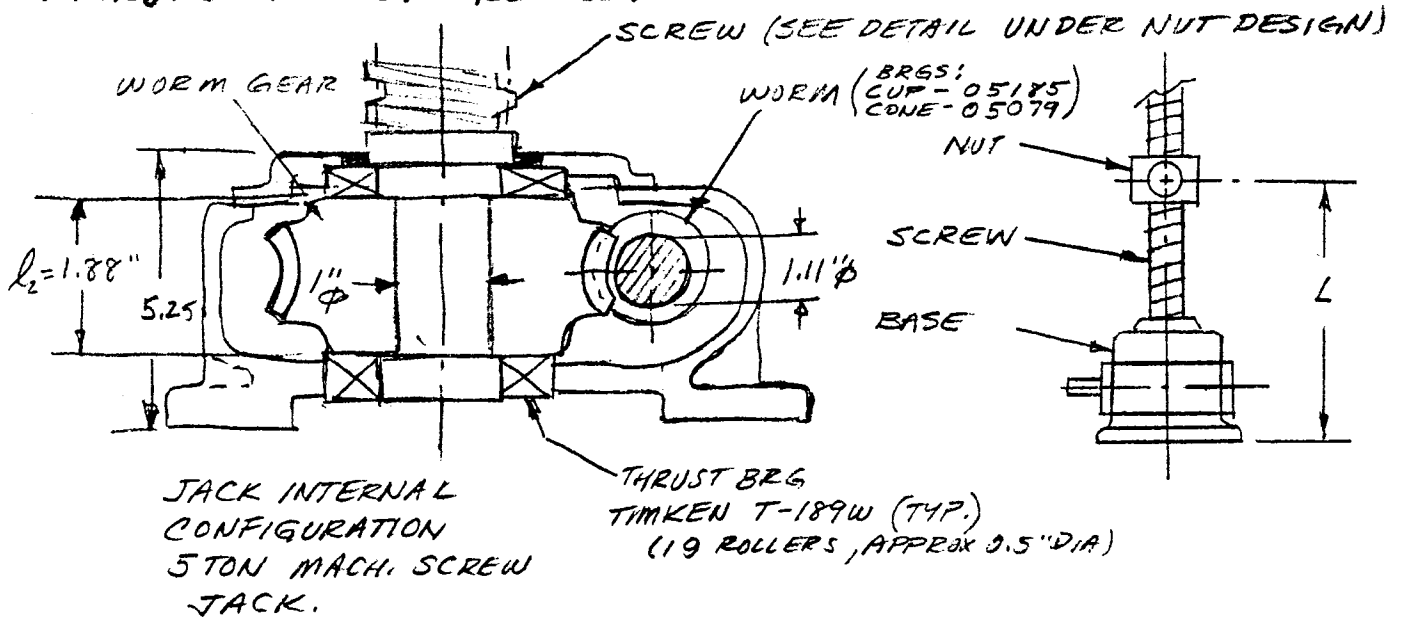
BASED ON ALLOWABLE LOAD OF 14,000 LB PER  
"DURONUT" CAT. THE APPARENT S.F. AGAINST  
SHEAR FAILURE =  $\frac{18600}{14,000} = 1.33$

USE MIN. S.F. = 2, AS INDICATED ABOVE  
AND MAKE NUT MINIMUM 2.25" LONG.

ACTUAL THREAD LENGTH = 3.50"



COMPLIANCE: THIS ANALYSIS WAS DONE ON ORIGINAL DESIGN AND LATEST DESIGN IS DIFFERENT BUT COMPLIANCE NUMBERS WILL BE ABOUT SAME AND THEREFORE ANALYSIS IS NOT REVISED.



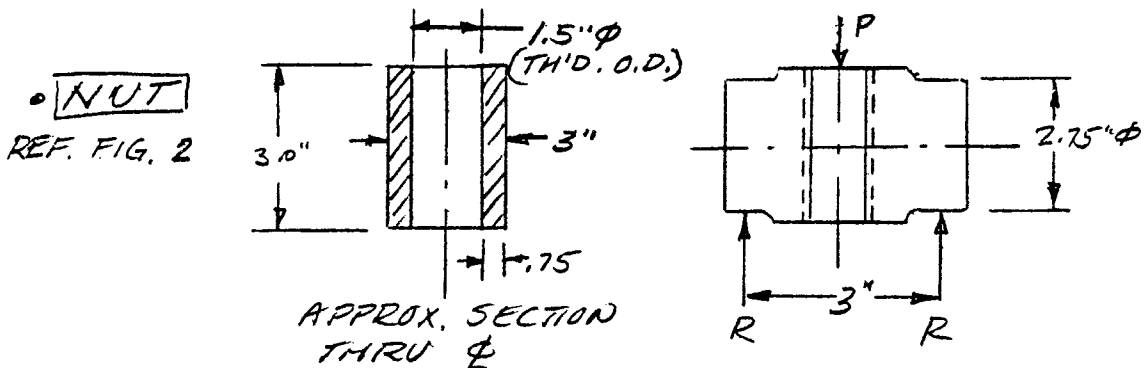
$L = 7.4 \text{ IN MIN (AT } \theta = 93^\circ) ; 47.2 \text{ IN MAX. (AT } \theta = -3^\circ)$

COMPLIANCE OF ELEMENTS ALONG SCREW AXIS :

• **SCREW**:  $A_1 = (1.12)^2 \pi \times .25 = .985 \text{ IN}^2 \text{ (ROOT AREA)}$   
 $E = 30 \times 10^6$   
 $\delta = \frac{l_1}{A_1 E} + \frac{l_2}{A_2 E}$   
 $l_1 = (L - 5.25) = 8.4 - 5.25 = 3.2 \text{ MIN}$   
 $\phantom{l_1} = 47.2 - 5.25 = 42 \text{ MAX}$   
 $A_2 = \frac{\pi}{4} = .78 \text{ IN}^2 \text{ (SHANK AREA)}$   
 $l_2 = 1.88 \text{ IN}$

$\delta_{\text{MIN}} = \frac{1}{30 \times 10^6} \left( \frac{3.2}{.985} + \frac{1.88}{.78} \right) = \underline{\underline{.19 \times 10^{-6} \text{ IN/LB}}}$

$\delta_{\text{MAX}} = \frac{1}{30 \times 10^6} \left( \frac{42}{.985} + \frac{1.88}{.78} \right) = \underline{\underline{1.5 \times 10^{-6} \text{ IN/LB}}}$



COMPLIANCE (CONT'D.)• NUT CONT'D.

CONSIDER BENDING DEFLECTION AS A SIMPLE BEAM  
 THEN AT  $\ell$ ,  $I = \frac{2(.75)(3)^3}{12} = 3.37 \text{ IN}^4$  ASSUME NUT  
 HAS THIS SECTION  
 MODULUS ACROSS  
 ENTIRE WIDTH

$$E = .33 \times 10^6 \text{ PSI (TURCITE)}$$

$$\delta = \frac{P\ell^3}{48EI} = \frac{(1)(3)^3}{48(.33 \times 10^6)(3.37)} = \underline{\underline{.5 \times 10^{-6} \text{ IN/LB}}}$$

CONSIDER SHEAR DEFLECTION OF NUT TEETH

ASSUME LOAD IS CONCENTRATED  
 AT CENTER OF TOOTH, FURTHER,  
 ASSUME TOOTH WIDTH IS  
 UNIFORMLY THAT AT THE PITCH  
 LINE.

NO PRINTED INFO FOUND  
 ON SHEAR MODULUS (G) OF  
 ACETAL, MUCH LESS 'TURCITE'.

HOWEVER THE FOLLOWING RELATIONSHIP  
 HOLDS :

$$E = 2(1 + \mu)(G)$$

WHERE:  $\mu = \text{POISSON'S RATIO} \approx .4$

$$E = .33 \times 10^6 \text{ PSI (TURCITE)}$$

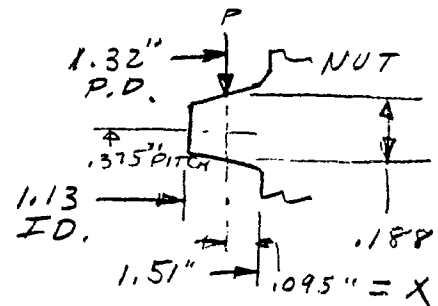
$$\text{THEN } G = \frac{E}{2(1 + \mu)} = \frac{.33 \times 10^6}{2(1.4)} = .12 \times 10^6 \text{ PSI}$$

LENGTH OF THREAD FOR 3" LG. NUT

$$\ell = \frac{1.32 \pi \times 3}{.375} = 33 \quad A = .188 \times 33 = 6.2 \text{ IN}^2$$

THEN SHEAR DEFLECTION PER UNIT NUT LOAD  
 IS :

$$\delta = \frac{X}{AG} = \frac{.095}{(6.2)(.12 \times 10^6)} = \underline{\underline{.13 \times 10^{-6} \text{ IN/LB}}}$$



COMPLIANCE (CONT'D)BEARING

FOR AXIAL DEFLECTION OF TAPERED ROLLER BEARINGS:

$$\delta_c = \frac{0.0000009}{\sin \alpha} \times \frac{Q^{0.9}}{l_w^{0.8}}$$

$$Q = \text{LOAD ON ROLLER} = \frac{P}{19}$$

$$l_w = \text{ROLLER LENGTH} = 0.5 \text{ IN}$$

$$\alpha \approx 85^\circ \text{ (CONTACT ANGLE)}$$

TO FIND AXIAL DEFLECTION PER UNIT LOAD (COMPLIANCE) FIND  $\delta_c$  WITH BRG LOAD BETWEEN 500 LB AND 501 LB.

FOR  $P = 501 \text{ LB}$

$$\delta_c = \frac{0.0000009}{\sin 85} \times \frac{(26.31578947)^{0.9}}{0.5^{0.8}} = .0000298481 \text{ IN}$$

FOR  $P = 500 \text{ LB}$

$$\delta_c = \frac{0.0000009}{\sin 85} \times \frac{(26.36842105)^{0.9}}{0.5^{0.8}} = .0000299018 \text{ IN}$$

$$\text{COMPLIANCE} = .054 \times 10^{-6} \text{ IN/LB.}$$

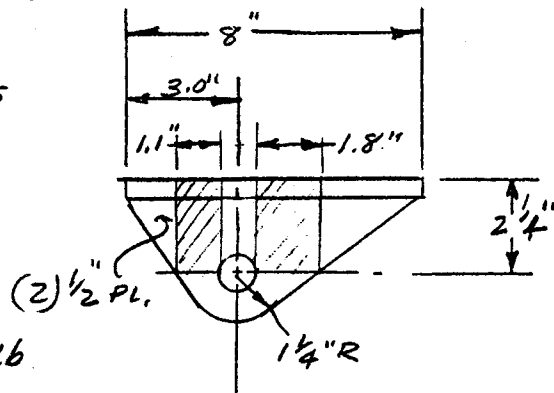
TRUNNION REF. FIG. 1

FOR COMPLIANCE MODEL AS SHOWN IN SHADED AREAS

$$\delta = \frac{l}{AE}$$

$$A = (1.8 + 1.1)(2)(.5) = 2.9 \text{ IN}^2$$

$$\delta = \frac{2.25}{2.9 \times 30 \times 10^6} = .026 \times 10^{-6} \text{ IN/LB.}$$



COMPLIANCE (CONT'D.)

NEGLECTING COMPLIANCE OF ACTUATOR HOUSING AND CLEVIS PIN (BOTH SHOULD BE VERY SMALL COMPARED TO ELEMENTS COVERED) TOTAL COMPLIANCE MEASURED ALONG SCREW AXIS IS

$$\delta_{\text{MAX}} = (1.5 + .5 + .13 + .054 + .026) \times 10^{-6} \text{ IN/LB}$$

$$\left( \begin{array}{l} \text{AT } \alpha = 93^\circ \\ \text{EL} = -3^\circ \end{array} \right) = 2.2 \times 10^{-6} \text{ IN/LB}$$

$$\delta_{\text{MIN}} = (.19 + .5 + .13 + .054 + .026) \times 10^{-6} \text{ IN/LB}$$

$$\left( \begin{array}{l} \text{AT } \alpha = -3^\circ \\ \text{EL} = 93^\circ \end{array} \right) = 0.9 \times 10^{-6} \text{ IN/LB}$$

NOTE:

COMPLIANCE AT  $\alpha = 0^\circ$  &  $\alpha = 90^\circ$  VERY CLOSE TO THE ABOVE NUMBERS.

O.A RATIO

ACME SCREW TH'D 1 1/2" - 4 (1/4" PITCH)  
 EL TRAVEL - 93° IN 15 MINUTES

FROM TABLE I STROKE =  $42.249 - 14.923 = 27.326$  IN

REQ'D NUT LINEAR SPEED =  $\frac{27.326}{15} = 1.822$  IN/MIN.

∴ REQ'D GEARING RATIO =  $\frac{1750}{1.822 \times 4} = 240 : 1$

(ACTUAL RATIO IS 24:1 PRIMARY  
 & 10:1 SECONDARY  
 TOTAL 240:1 )

INFORMATION GATHERED ON DIFFERENT NUT MATERIALS  
 & DIFFERENT COMPANIES THAT MAKE SCREWS AND NUTS  
 IS INCLUDED IN THE FOLLOWING 3 PAGES FOR  
 REFERENCE. SELECTED NUT MATERIAL IS TURCITE A.

BOEING HELIOSTAT ACTUATOR

CANDIDATE NUT MATERIALS

NO	MATERIAL	MODULUS OF ELASTICITY X 10 <sup>6</sup>	COEFFICIENT OF THERMAL EXPANSION (IN/IN/°F X 10 <sup>-6</sup> )	COEFF. OF FRICTION (ON STEEL)	TENSILE STRENGTH (KSI)
1	BRONZE	15.5	9.0	0.15 (LUBED)	95
2	TURCITE <i>A</i>	.33	55	0.08	5.5 (AT 77°F)
3	MACOR	9.3	5.2	0.12	_____
4	RYNITE 545	2.1(AT 73°F)	13	0.2	28 (AT 73°F)
5	RULON - J	≈1.0(AT 75°F)	49-52	0.12 - 0.20	1.2
6	NYLATRON GS	0.45 - 0.6 (AT 73°F)	35	0.15 - 0.35	12 (AT 73°F)
7	TEFLON	.05 - .09	55-75	0.04 - 0.10	2.0 (AT 73°F)
8	DELTRIN AF-313	.42	58	0.05 - 0.10	7.0 (AT 73°F)

- (1) TYPE WCF-150 CENTRIFUGALLY CAST - USED BY DUFF-NORTON ON TRANSLATING NUT MACHINE SCREW JACKS.
- (2) TFE FILLED DELTRIN - USED IN "SUPERNUT" AND "DURONUT".
- (3) MACHINABLE CERAMIC - CORNING GLASS WORKS
- (4) GLASS FIBER REINFORCED POLYESTER - DUPONT PLASTICS
- (5) PROPRIETARY REINFORCED TEFLON (TFE) FORMULATED TO RUN AGAINST STAINLESS STEEL - DIXON PLASTICS
- (6) 2½% MOS<sub>2</sub> FILLED NYLON 6/6
- (7) TFE, UNREINFORCED
- (8) 20% TFE FILLED DELTRIN MATERIAL - DUPONT PLASTICS

EM 12/19/79



NOOK IND. POWER LEAD SCREWS

SCREWS - ROLLER BURNISHED (1 1/2-4 ACME)  
4140-HT STEEL, ROCKWELL 'C' 24-34

NUTS - BRONZE - "BRONZ/AC", S<sub>4P</sub> - 50 KSI  
S<sub>TEN</sub> - 65 KSI, R<sub>B</sub> - 75 HARDNESS

PLASTIC - 'PLASTAC', MATERIAL  
SUPPLIED BY SHAMBAN INC. ('TURCITE')

SHAMBAN INC. - MANUFACTURERS OF 'DURONUT' AND SUPPLIERS OF PLASTICS TO OTHERS

NUTS - SUPPLY 'TURCITE' FROM WHICH PLASTIC  
NUTS ARE MADE BY VARIOUS  
MANUFACTURER'S. ALSO SUPPLY 'DURONUT';  
'TURCITE' IS TFE FILLED DELRIN  
(ACETAL) RESIN. (1 1/2-5 ACME)

SCREWS - TESTS SHOW MATING SCREW SHOULD  
HAVE 16-32 RMS FINISH. CHROME  
PLATING NOT ADVISED - POOR RESULTS  
CARBON STEEL O.K. STAINLESS STEEL  
CONSIDERED LESS THAN IDEAL IF  
SURFACE IS PASSIVATED (CAN IN-  
CREASE ABRASION)

BALL SCREWS & ACTUATORS - CUSTOM ACTUATORS AND LEAD SCREW KITS

SCREWS - ROLLED THREAD, 1018 STEEL (1 1/2-4 ACME)  
ALSO AVAILABLE IN STAINLESS STEEL

NUTS - BRONZE - SAE-660  
PLASTIC - 'SUPER NUT' MADE OF 'TURCITE'

DUFF-NORTON MANUFACTURERS OF BALL AND  
MACHINE SCREW JACKS.

SCREWS (MACHINE) - MACHINED OR ROLLED, CARBON STEEL  
1/2", 3/8" PITCH, MODIFIED SQ. TH'D.

TESTS INDICATE ROLLED THREADS  
CAUSE FAR LESS WEAR ON NUTS  
THAN MACHINED THREADS, FOR  
NON-LUBRICATED APPLICATIONS.

DRY FILM LUB. (TFE OR MOLY) ON  
SCREW NOT SUCCESSFUL.

NUTS

- USE WCF150 & WCF175 (CAST)  
BRONZE,  $S_{TEN} = 95-100$  KSI  
ALSO USE DYNALLOY 602 (BAR)  
WHICH IS SUPERIOR WEARING.

HAVE TESTED "OILON" PV80  
AND "ZYTEL" ON NON-LUB'D.  
APPLICATION, HAVE NOT TESTED  
'TURCITE'.

MOTOR SIZING :SCREW :

TORQUE REQUIRED TO RAISE THE LOAD

$$T_{UP} = \frac{F d_m}{2} \left( \frac{l + \pi \mu d_m}{\pi d_m - \mu l} \right)$$

TORQUE REQUIRED TO LOWER THE LOAD,

$$T_{DOWN} = \frac{F d_m}{2} \left( \frac{\pi \mu d_m - l}{\pi d_m + \mu l} \right)$$

 $\mu$  = FRICTION COEFF. = 0.08 FOR TURCITE A $d_m$  = MEAN DIAMETER, INCHES = 1.375 FOR SCREW

$$l = \text{PITCH} = \frac{1}{\text{THREADS PER INCH}} = 0.25$$

$$F = 10000 \text{ LBS}$$

$$T_{UP} = \frac{10000 \times 1.375}{2} \left( \frac{0.25 + \pi \times 0.08 \times 1.375}{\pi \times 1.375 - 0.08 \times 0.25} \right)$$

$$= 952 \text{ IN LBS}$$

NOTE : FOR  $\mu = 0$ ,  $T_{UP} = 398 \text{ IN LBS}$ , &  $\eta_{NUT} = \frac{398}{952} = 0.418$ 

$$T_{DOWN} = \frac{10000 \times 1.375}{2} \left( \frac{\pi \times 0.08 \times 1.375 - 0.25}{\pi \times 1.375 + 0.08 \times 0.25} \right)$$

$$= 153 \text{ IN LBS}$$

THUS IT REQUIRES, 952 IN LBS TO RAISE 10000 LBS LOAD

&amp; 153 IN LBS TO LOWER 10000 LBS LOAD

THUS SCREW IS SELF LOCKING

WINSMITH GEAR BOX EFFICIENCY = 40.1 % (PER WINSMITH)

$$\& \text{ OVERALL EFFICIENCY} = 0.418 \times 0.401$$

$$= 0.168 \text{ OR } 16.8 \%$$

FOR 1/3 H.P. 1750 RPM MOTOR

MOTOR TORQUE = 1 FT LBS OR 12 IN LBS

FOR 240:1 RATIO & 40.1% EFFICIENT GEAR BOX,  
 GEAR BOX OUTPUT TORQUE = 240 x 12 x 0.401  
 = 1154.88 IN LBS

FROM PREVIOUS PAGE

952 IN LBS GEAR BOX OUTPUT TORQUE IS REQUIRED TO RAISE 10000 LBS LOAD

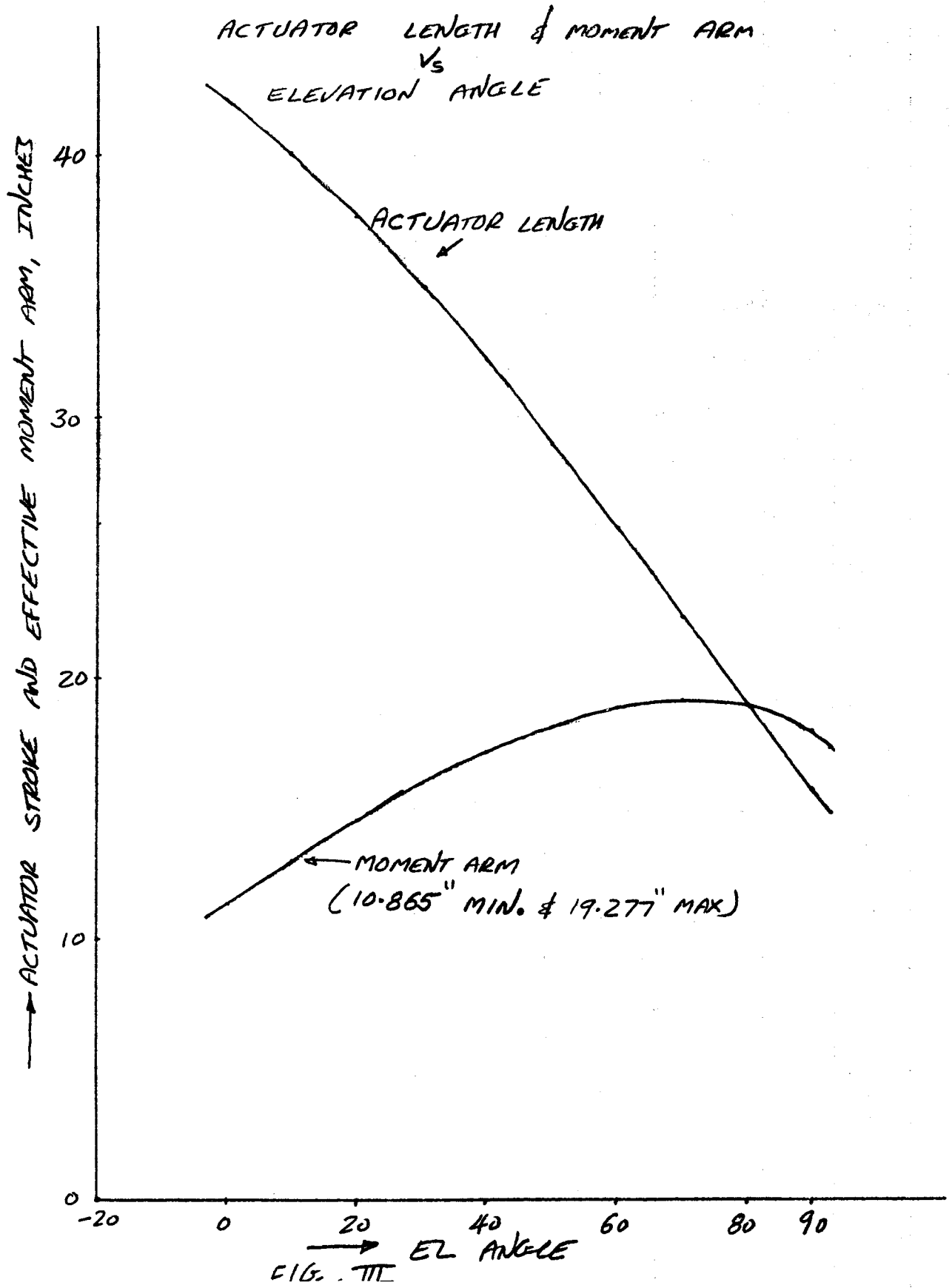
THEREFORE, AT RATED MOTOR TORQUE,

RATED ACTUATOR LOAD  
 =  $\frac{1154.88 \times 10000}{952}$   
 = 12130 LBS

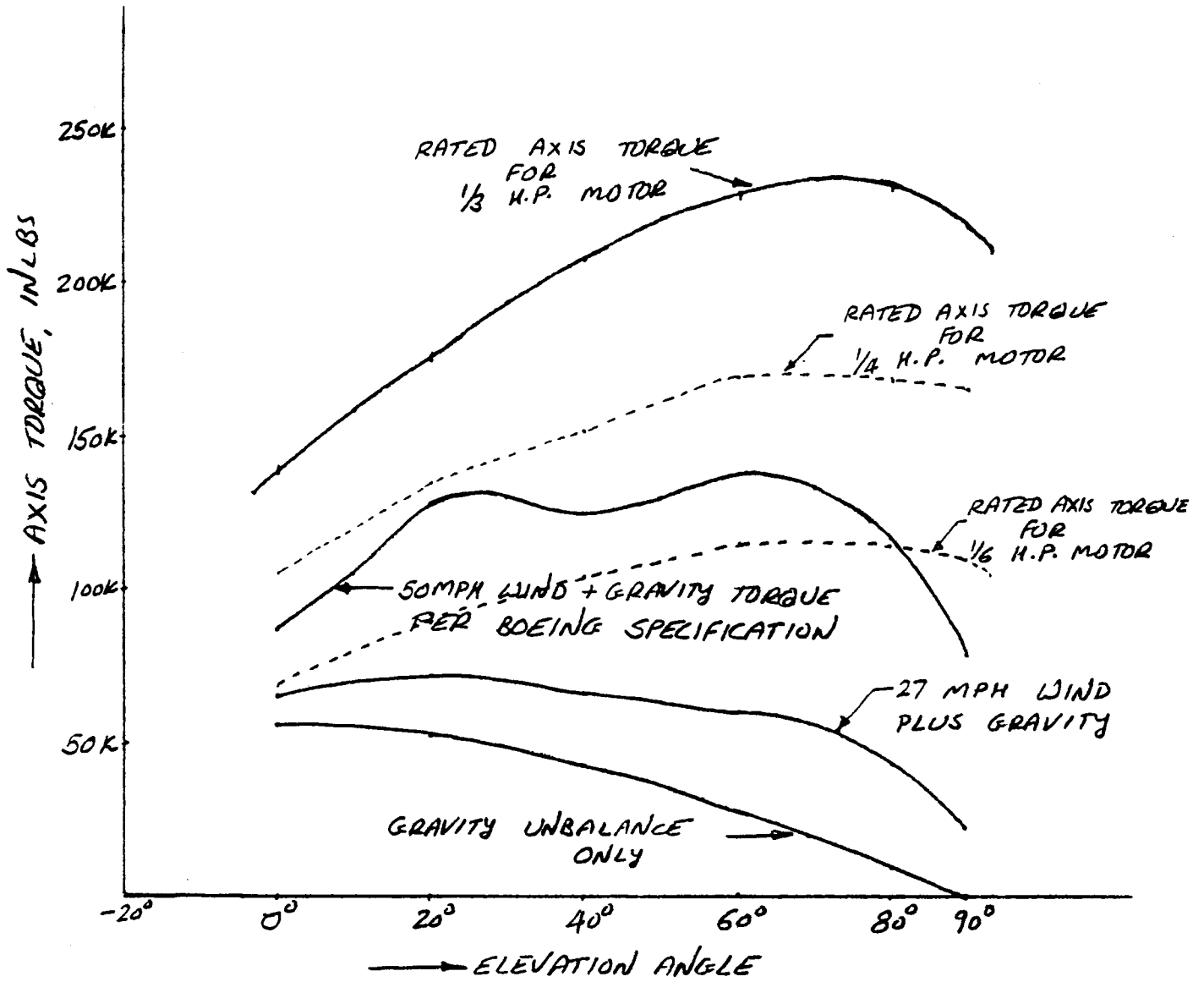
RATED AXIS TORQUE = 12130 X EFFECTIVE MOMENT ARM

ACTUATOR LENGTH & MOMENT ARM ARE PLOTTED ON THE NEXT PAGE. (FIG. 3)

FIG. IV IS FOR REQUIRED EL AXIS TORQUE & AVAILABLE AXIS TORQUE VS. ELEVATION ANGLES FOR DIFFERENT MOTOR SIZES. IT SHOWS THAT SELECTED 1/3 H.P. MOTOR HAS MORE THAN ADEQUATE AVAILABLE TORQUE.



ELEVATION AXIS TORQUE  
 √  
 ELEVATION ANGLE



NOTE: NO ICE OR SNOW

FIG. IV

ACTUATOR EMERGENCY STOPS:

TO VERIFY THE DESIGN AS PROPOSED IN ATTACHED SKETCHES FOR ELEVATION ACTUATOR EMERGENCY STOPS (FIG. V & VI)

1. ZENITH (INNER) STOP:

SURVIVAL LOAD:  $\frac{1}{3}$  H.P. 1750 RPM MOTOR, DESIGNED

RATED TORQUE = 12 IN LBS

MOTOR CAN DELIVER 250% TORQUE BEFORE STALLING.

THEREFORE MAX TORQUE = 30 IN LB

SPEED REDUCER RATIO = 240:1 & EFFICIENCY = 40.2%

THEREFORE SPEED REDUCER OUTPUT TORQUE

$$= 240 \times 30 \times 0.402$$

$$= 2894 \text{ IN LBS.}$$

PER PBN ANALYSIS,

952 IN LB TORQUE RESULTS IN 10000 LBS ACTUATOR LOAD

THEREFORE ACTUATOR LOAD AT MOTOR STALL

$$= \frac{2894 \times 10000}{952}$$

$$= 30400 \text{ LBS.}$$

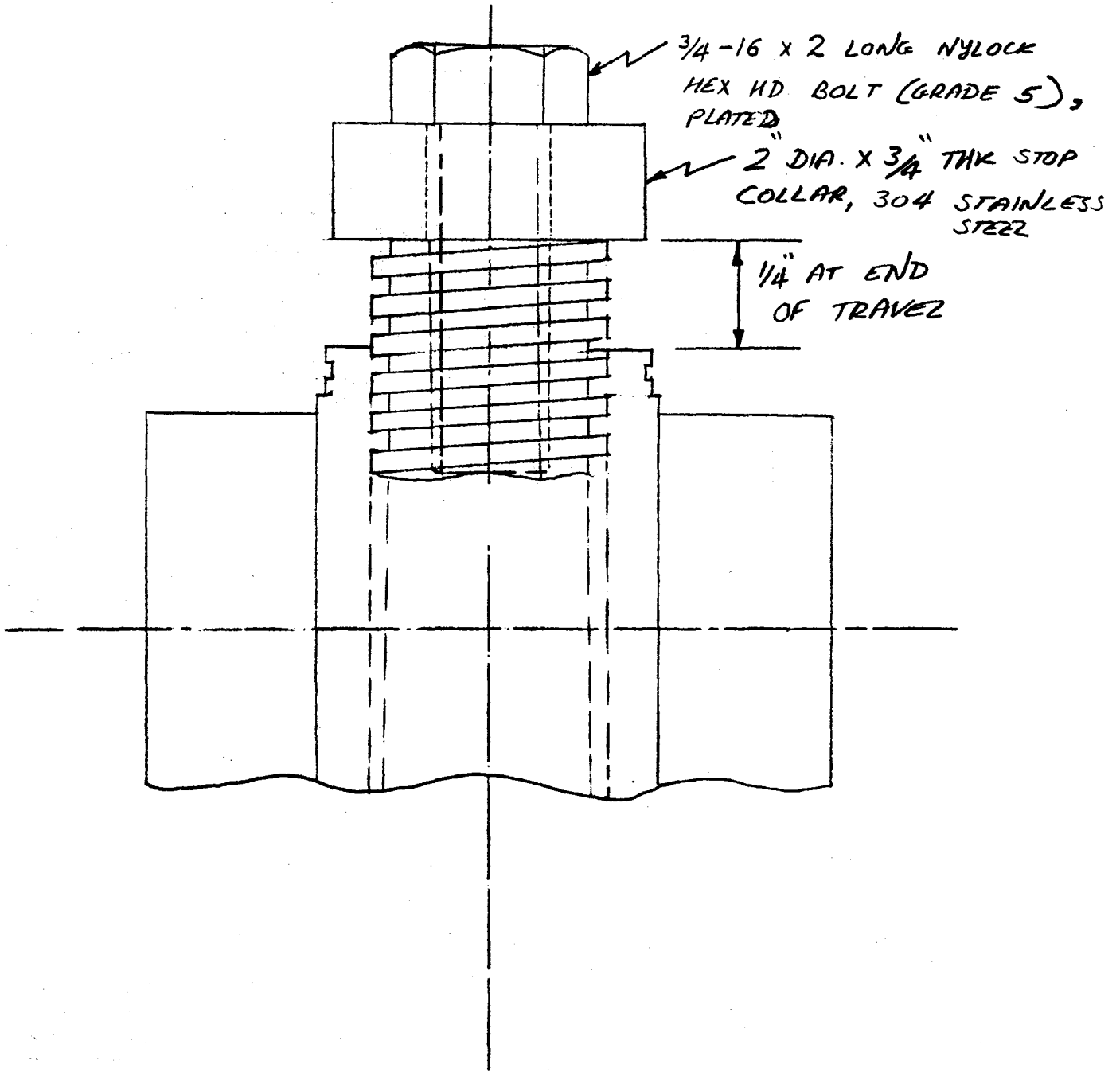
BEARING STRESS BETWEEN STOP & SCREW SHOULDER:

$$\text{BEARING AREA} = \frac{\pi}{4} (1.5^2 - 1.25^2)$$

$$= 0.54 \text{ SQ INCH}$$

$$\text{THEREFORE BEARING STRESS} = \frac{30400}{0.54} = 56300 \text{ PSI}$$

AS THIS HAPPENS IN CASE OF CONTROL FAILURE ONLY, THIS IS ACCEPTABLE STRESS LEVEL.



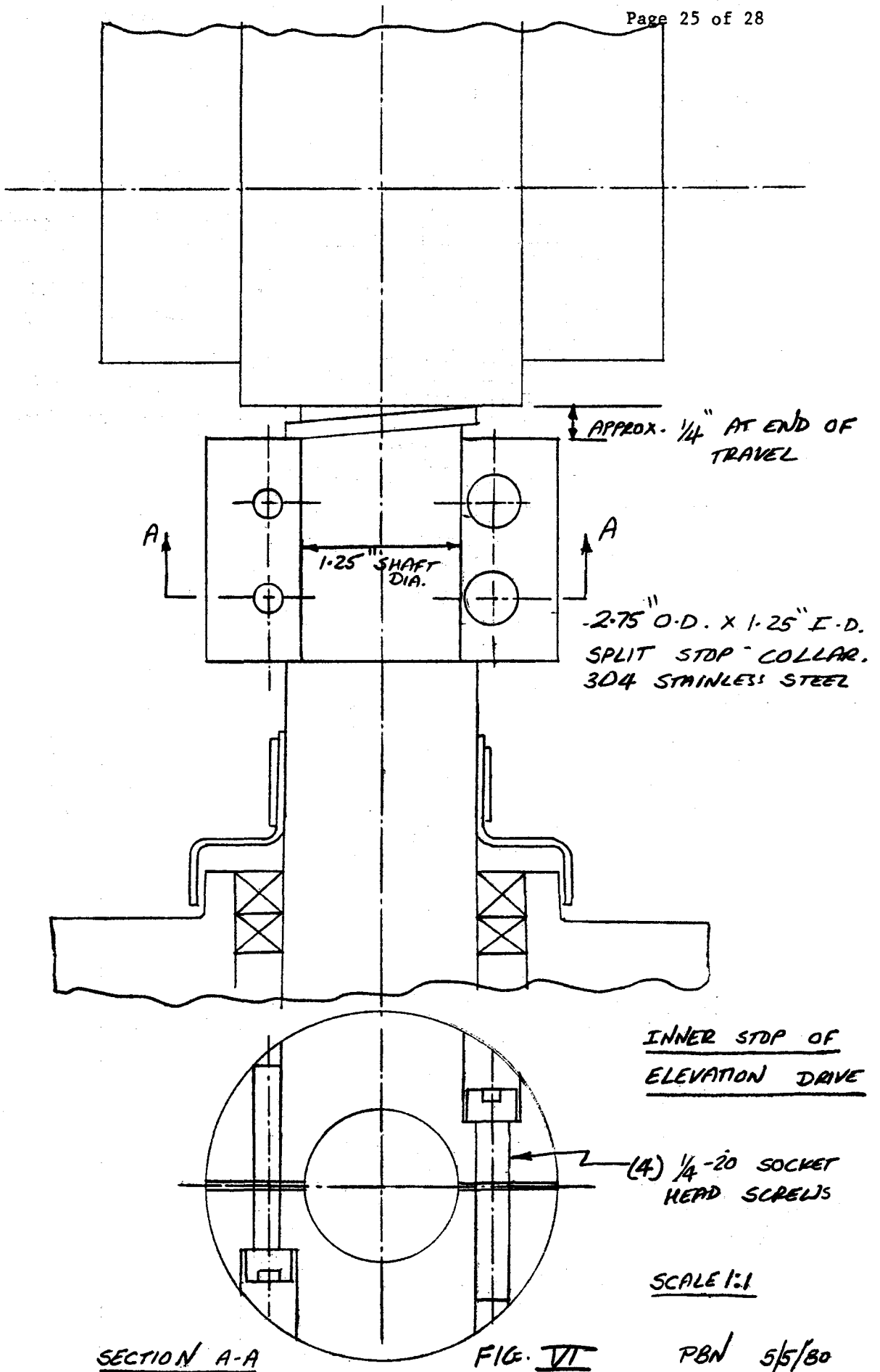
SCALE 1:1

PBN 5/5/80

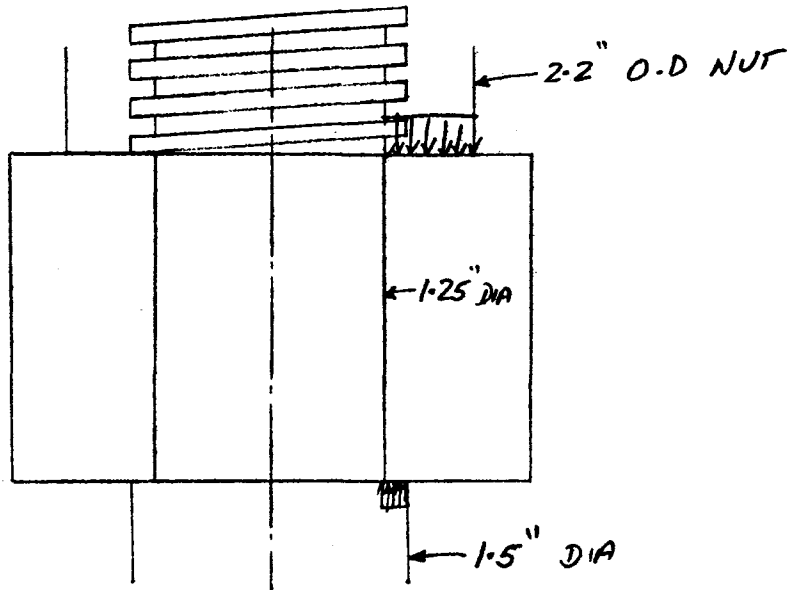
OUTER STOP OF ELEVATION DRIVE

FIG. II





LOAD IN THE 1/4-20 BOLTS :



LOAD IS ON A SEMICIRCLE ON EACH HALF.

AT THE NUT IT IS ON  $\frac{2.2+1.25}{2 \times 2} = 0.8625$  INCH MEAN RADIUS

AT THE SCREW SHOULDER  $\frac{1.5+1.25}{2 \times 2} = 0.6875$  INCH MEAN RADIUS

LOAD CENTER AT NUT =  $\frac{2 \times 0.8625}{\pi} = 0.549$  INCH

& AT SHOULDER =  $\frac{2 \times 0.6875}{\pi} = 0.438$  INCH

LOAD ON EACH HALF =  $\frac{30400}{2} = 15200$  LBS

& PRYING MOMENT ON THE CLAMP =  $15200 \times (0.549 - 0.438)$   
 = 1687 IN LBS

IGNORING THE BOLTS CLOSER TO THE SHOULDER,

BOLT LOAD =  $\frac{1687}{2 \times 1.25} = 675$  LBS

FOR SAE GRADE 5 1/4-20 BOLTS

CLAMP LOAD = 2020 LBS  $\gg$  675 LBS O.K.

2. HORIZON (OUTER) STOP :

OUTER STOP IS 3/4 INCH THICK WASHER HELD BY 3/4-16 SAE GRADE 5 BOLT  
BOLT PROOF LOAD = 31700 LBS > 30400 LBS ← O.K

COMPRESSIVE STRESS ON THE PLASTIC NUT :

$$\text{O.D. OF THE AREA} = 2.0''$$

$$\text{I.D. OF THE AREA} = 1.38$$

$$\text{AREA} = \frac{\pi}{4} (2^2 - 1.38^2)$$

$$= 1.65 \text{ SQ INCH}$$

$$\text{THEREFORE, COMPRESSIVE STRESS} = \underline{30,400}$$

$$= 18,500 \text{ PSI}$$

PER MANUFACTURER'S LITERATURE, COMPRESSIVE STRENGTH AT 25% STRAIN = 13,500 PSI.

THUS ACTUAL STRESS IS HIGH. BUT AS THIS OCCURS VERY RARELY, STRESS LEVEL IS O.K.

EFFECT OF MOTOR KINETIC ENERGY :

MOTOR RPM = 1750

MOTOR SPEED =  $\frac{1750 \times 2\pi}{60} = 183 \text{ RAD/SEC} = \omega$

MOTOR INERTIA = 0.92 LB IN<sup>2</sup>

$J = \frac{0.92 \text{ LB IN}^2}{32.2 \text{ FT/SEC}^2 \times 12 \text{ INCH/FT}}$

$J = 2.38 \times 10^{-3} \text{ LB IN SEC}^2$

THEREFORE KINETIC ENERGY

$= \frac{1}{2} J \omega^2$

$= 40 \text{ IN LBS}$

OVERALL EFFICIENCY = 16.8 %

THEREFORE, ENERGY TO BE ABSORBED BY STOP

$= 40 \times 0.168$

$\approx 7 \text{ IN LBS}$

IF THE STOP IS WITHIN 0.1 INCH.

$\text{LOAD} = \frac{7 \times 2}{0.1}$

$= 140 \text{ LBS.}$

THUS LOAD DUE TO INERTIA IS VERY SMALL COMPARED TO LOAD DUE TO MOTOR TORQUE. THUS, STOPS ARE ADEQUATE.



REPORT E-7

ELEVATION BEARING DESIGN ANALYSIS

FOR

GIMBAL/ACTUATOR DRIVE ASSEMBLY

FOR

BOEING SECOND GENERATION HELIOSTAT

JUNE 27, 1980

Reference: FACC TM07



**Ford Aerospace &  
Communications Corporation**

TABLE OF CONTENTS

Section

1.0 Introduction and Summary

2.0 Basis of Analysis

3.0 Analysis

## 1.0 INTRODUCTION AND SUMMARY

The purpose of this appendix is to estimate survival loads for the elevation bearings and to design the components of the elevation bearings.

Loads on the elevation bearing system are tabulated in Table I. Two wind conditions are considered.

- a. 50 mph wind with ice and snow, any orientation.
- b. 90 mph wind, no ice and snow, zenith stow. Loads on individual bearings are tabulated in Table II. Maximum elevation bearing loads are 17,900 lbs radial and 1,800 lbs axial. Based on these loads, elevation bearing components are designed and resulting design is shown in Figure I.

An examination of Figure I shows that the pointing error contribution due to the elevation bearings will be negligible.

The elevation bearing pin is designed for double shear loading, instead of the single shear of the original design.

## 2.0 BASIS OF ANALYSIS

Load data from Appendix I of Boeing Specification is used to estimate loads on elevation bearings.

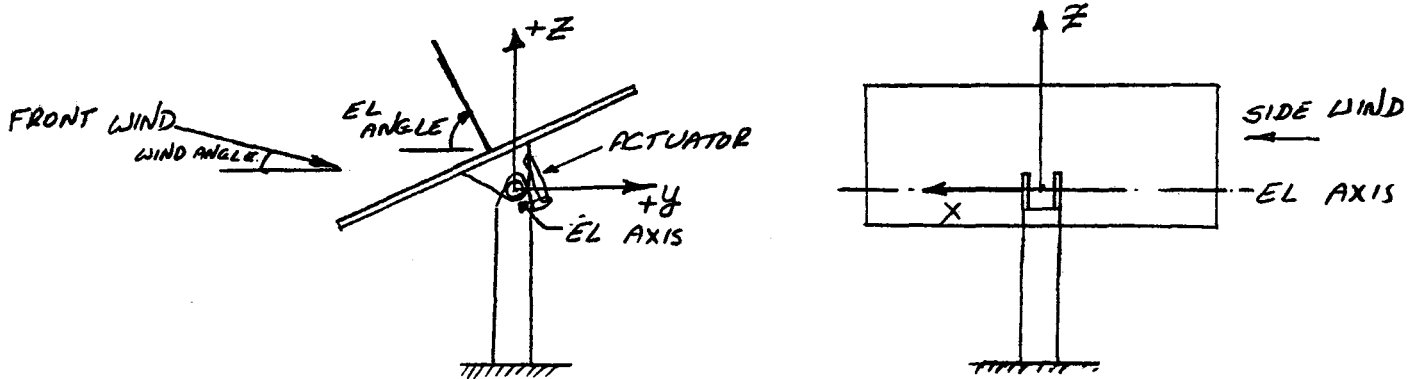


PURPOSE: TO ESTIMATE SURVIVAL LOADS ON ELEVATION BEARING SYSTEM. (REF. APPENDIX I OF BOEING SPECIFICATION.)

SURVIVAL CONDITIONS CONSIDERED ARE AS FOLLOWS:

- a. 50 MPH WIND, REFLECTOR ANY ORIENTATION, SNOW, ICE & GRAVITY.
- b. 90 MPH WIND, REFLECTOR AT ZENITH, WIND AT  $\pm 10^\circ$  TO HORIZONTAL - NO SNOW & ICE

LOAD CONVENTION:



$P_x$  = LOAD AT EL AXIS IN X DIRECTION (+VE WHEN IN +X DIR.)

$M_x$  = MOMENT ABOUT X AXIS (EL AXIS) (+VE WHEN GOING FROM +Y TO +Z DIRECTION - RIGHT HAND RULE)

LOADS ARE TABULATED ON THE NEXT PAGE FOR DIFFERENT CONDITIONS. SUMMARY NUMBERS REFERRED IN THE TABLE ARE PER APPENDIX I OF BOEING SPECIFICATION.

ELEVATION BEARING SYSTEM LOADS

	$P_x$ KIPS	$P_y$ KIPS	$P_z$ KIPS	$M_x$ KIP.IN	$M_y$ KIP.IN	$M_z$ KIP.IN
<u>50 MPH WIND, ANY ORIENTATION,</u> SNOW ICE PLUS GRAVITY, WIND NORMAL TO EL AXIS. (SUMMARY 11)						
0° EL ANGLE	0	+3.3	-9.7	+251.5	0	0
20° EL ANGLE	0	+3.1	-8.6	+278.8	0	0
70° EL ANGLE	0	+1.0	-12.5	+164.1	0	0
<u>50 MPH WIND, REFL. AT HORIZON,</u> SNOW, ICE PLUS GRAVITY, WIND DIRECTION CREATES MAX. AZIMUTH TORQUE (SUMMARY 12)	0.1	+2.4	-9.7	+222.2	+1.6	93.4
<u>90 MPH WIND AT ±10° TO</u> HORIZONTAL, NORMAL TO EL AXIS, REFLECTOR AT ZENITH (SUMMARY 3)	0	0	-5.9	±240.6	0	0
<u>90 MPH UPWARD WIND AT +10° TO</u> HORIZONTAL, PARALLEL TO EL AXIS, REFLECTOR AT ZENITH. (SUMMARY 15)	+3.5	0	+0.5	0	+230.6	0
<u>90 MPH DOWNWARD WIND AT -10° TO</u> HORIZONTAL, PARALLEL TO EL AXIS, REFLECTOR AT ZENITH (SUMMARY 16)	+1.3	0	-5.9	0	-176.1	0
<u>90 MPH HORIZONTAL WIND, PARALLEL</u> TO EL AXIS, REFLECTOR AT ZENITH, (SUMMARY 17)	+1.5	0	-2.7	0	+21	0

TABLE I

EFFECT ON INDIVIDUAL BEARING OF LOADS ON THE BEARING SYSTEM.

LET  $L$  = DISTANCE BETWEEN TWO BEARINGS = 14.5 INCH

$R$  = ACTUATOR MOMENT ARM

$\Theta$  = ACTUATOR ANGLE TO HORIZONTAL.

$P_V$  = VERTICAL RADIAL LOAD ON EL BEARING

$P_H$  = HORIZONTAL RADIAL LOAD ON EL BEARING

$P_A$  = AXIAL LOAD ON EL BEARING.

$\underline{P_x}$  -  $P_V = P_H = 0$ ,

$P_A = \frac{P_x}{2}$

$\underline{P_y}$  -  $P_A = P_V = 0$

$P_H = \frac{P_y}{2}$

$\underline{P_z}$  -  $P_A = P_H = 0$

$P_V = \frac{P_z}{2}$

$\underline{M_x}$  -  $P_A = 0$

$P_V = -\frac{M_x}{2R} \sin \Theta$

$P_H = -\frac{M_x}{2R} \cos \Theta$

EL ANGLE	R	$\Theta$
0	11.53"	111.75°
20	14.5"	98.37°
70	18.2"	57.53°
90	16.13"	32.12°

FROM E. MONTESANTO ANALYSIS

$\underline{M_y}$  -  $P_A = P_H = 0$

$P_V = \pm \frac{M_y}{L}$

$\underline{M_z}$  -  $P_A = P_V = 0$

$P_H = \pm \frac{M_z}{L}$

THUS,

$$P_A = \frac{P_x}{2}$$

$$P_V = \frac{P_z}{2} - \frac{M_x}{2R} \sin \theta + \frac{M_y}{R}$$

$$P_H = \frac{P_y}{2} - \frac{M_x}{2R} \cos \theta + \frac{M_z}{R}$$

ELEVATION BEARING LOADS

	AXIAL LOAD $P_A$ KIPS	VERTICAL RADIAL LOAD $P_V$ KIPS	HORIZONTAL RADIAL LOAD $P_H$ KIPS	RESULTANT RADIAL LOAD $P_R$ KIPS $P_R = \sqrt{P_H^2 + P_V^2}$
50 MPH WIND NORMAL TO EL AXIS, WIND PLUS ICE + SNOW + GRAVITY EL ANGLE = $0^\circ$	0	-15.0	5.7	16.0
$20^\circ$	0	-13.8	2.9	14.1
$70^\circ$	0	-10.1	-1.9	10.3
50 MPH WIND, REFLECTOR AT HORIZON, SNOW + ICE + GRAVITY, WIND RESULTS IN MAX. AZIMUTH TORQUE	0	-13.9	11.2, -1.7	17.9
90 MPH WIND, REFLECTOR AT ZENITH, $\pm 10^\circ$ WIND NORMAL TO EL AXIS	0	-1.0, -6.9	$\pm 6.3$	9.4
90 MPH WIND PARALLEL TO EL AXIS REFLECTOR AT ZENITH				
- UPWARD WIND, $+10^\circ$ TO HORIZONTAL	1.8	16.2	0	16.2
- DOWNWARD WIND, $-10^\circ$ TO HORIZONTAL	0.7	15.1	0	15.1
- HORIZONTAL WIND	0.8	2.8	0	2.8

TABLE II

SUMMARY: MAXIMUM ELEVATION BEARING LOADS ARE AS FOLLOWS:

16.2 KIPS RADIAL & 1.8 KIPS AXIAL LOAD

OR

17.9 KIPS RADIAL LOAD

PURPOSE : TO SIZE ELEVATION BEARING COMPONENTS FOR SURVIVAL  
 LOADS OF 16200 LBS RADIAL & 1800 LBS AXIAL LOAD  
 OR 17900 LBS RADIAL LOAD.

ANALYSIS :

a. SHEAR STRESS IN THE PIN:

ASSUMING STAINLESS STEEL PIN,

ASSUME ALLOWABLE SHEAR STRESS = 15,000 PSI. (PER DESIGN DATA

THEN, REQUIRED SHEAR AREA

$$= \frac{17900}{15,000}$$

$$= 1.193 \text{ SQ INCH}$$

$$\text{AREA} = \frac{\pi}{4} (D^2) \times 2 \quad \text{FOR DOUBLE SHEAR}$$

THEREFORE,

$$\text{DIAMETER } D = \frac{2 \times 1.193}{\pi}$$

$$= 0.76 \text{ INCH.}$$

IF 1 INCH PIN IS USED,

$$\text{SHEAR STRESS} = \frac{17900}{\frac{\pi}{4} (1)^2 \times 2}$$

$$= 11400 \text{ PSI}$$

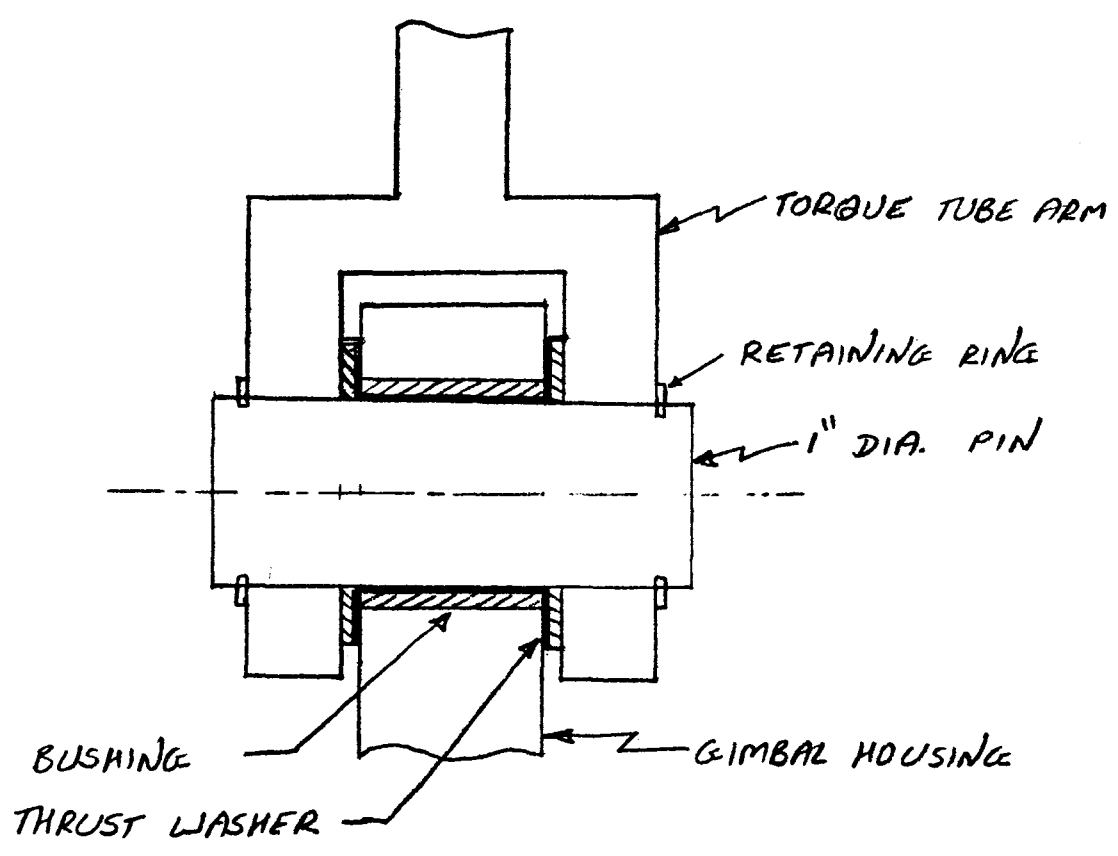
SAFETY FACTOR AGAINST ULTIMATE SHEAR STRENGTH (SEE ABOVE REFERENCE)

$$= \frac{45,000}{11400}$$

$$= 3.95$$

O.K.

THEREFORE USE 1 INCH PIN.



ELEVATION BEARING ARRANGEMENT

FIGURE I

b. BEARING STRESS BETWEEN PIN & BUSHING

WIDTH OF BEARING AREA = 1"

PIN DIAMETER AT BEARING AREA = 1.0 INCH.

$$\begin{aligned} \text{THEREFORE BEARING AREA} &= 1.0 \times 1.0 \\ &= 1.0 \text{ SQ INCH} \end{aligned}$$

THEREFORE,

$$\begin{aligned} \text{SURVIVAL BEARING STRESS} &= \frac{17,900}{1.0} \\ &= 17,900 \text{ PSI} \end{aligned}$$

CALCULATE BEARING STRESS UNDER GRAVITY LOAD ONLY:

CONSIDER REFLECTOR AT HORIZON. THIS CASE IS SIMILAR TO FIRST CASE IN "ELEVATION BEARING SYSTEM LOADS" TABLE.

HERE  $P_x = P_y = M_y = M_z = 0$

$$P_z = -3000 \text{ LBS}$$

$$M_x = +55366 \text{ IN LBS}$$

$$R = 11.53 \text{ INCH}$$

$$\theta = 111.75^\circ$$

$$\begin{aligned} P_V &= \frac{P_z}{2} - \frac{M_x}{2R} \sin \theta \\ &= -\frac{3000}{2} - \frac{55366}{2 \times 11.53} \sin(111.75) \end{aligned}$$

$$= -1500 - 2230$$

$$= -3730 \text{ LBS}$$

$$P_H = -\frac{M_x}{2R} \cos \theta$$

$$= -\frac{55366}{2 \times 11.53} \cos(111.75)$$

$$= 890 \text{ LBS}$$



RESULTANT RADIAL LOAD

$$P_R = \sqrt{P_V^2 + P_H^2}$$
$$= 3835 \text{ LBS.}$$

$$\& \text{ BEARING STRESS} = \frac{3835}{1.0}$$
$$= \underline{3835 \text{ PSI}}$$

PITCH LINE VELOCITY FOR AVERAGE SLEW VELOCITY:

$$\text{AVERAGE SLEW VELOCITY} = \frac{93^\circ}{15 \text{ MIN}}$$
$$= 6.2^\circ/\text{MIN.}$$

$$\text{PIN RADIUS AT BEARING} = 0.5 \text{ INCH}$$

$$\text{RUBBING VELOCITY} = 6.2^\circ/\text{MIN} \times 0.01745 \frac{\text{RAD}}{\text{DEG}} \times 0.5 \text{ INCH}$$
$$= \underline{0.054 \text{ INCH/MIN.}}$$

TOTAL TRAVEL IN 30 YEARS:

ASSUME  $0^\circ$  TO  $90^\circ$  &  $90^\circ$  TO  $0^\circ$  OR TOTAL OF  $180^\circ$  TRAVEL PER DAY.

# OF REVOLUTIONS FOR 30 YEARS

$$= 30 \times 365 \times \frac{180}{360}$$
$$= 5475 \text{ REVS.}$$

PIN CIRCUMFERENCE AT BEARING

$$= \pi \times 1.0 = 3.14 \text{ INCH}$$

$$30 \text{ YEAR TRAVEL} = \underline{17205 \text{ INCH}}$$

THUS, SUMMARIZING.

{ AVERAGE SLEW VELOCITY = 0.054 INCH/MIN.  
TOTAL TRAVEL = 17200 INCH  
BEARING STRESS = 3835 PSI UNDER GRAVITY UNBALANCE ONLY  
                  & 17900 PSI SURVIVAL

GAR-FIL BEARINGS BY GARLOCK HAVE DYNAMIC CAPACITY OF 25,000 PSI & STATIC CAPACITY OF 50,000 PSI. O.K.  
THEREFORE USE GAR-FIL BEARING.

ALSO USE GARLOCK DU BEARING AS THRUST WASHER



REPORT E-8

POINTING ERROR ANALYSIS

FOR

GIMBAL/ACTUATOR DRIVE ASSEMBLY

FOR

BOEING SECOND GENERATION HELIOSTAT

JUNE 27, 1980

Reference: FACC TM18



Ford Aerospace &  
Communications Corporation

TABLE OF CONTENTS

SECTION

1.0 Introduction

2.0 Summary

3.0 Analysis

Appendix A

Appendix B

Appendix C

## 1.0 INTRODUCTION

The purpose of this appendix is to present the pointing error analyses for the gimbal/actuator drive assembly portion for the second generation heliostat. Both the calm weather (no-wind) and the 27 mph wind conditions are described.

## 2.0 SUMMARY

The specification for calm weather (no-wind) requires that the pointing error shall not exceed 0.50 mrad standard deviation ( $1\sigma$ ) after control system corrections during a daily track with normal operating conditions for either the elevation or cross-elevation axis. Table I shows the contributing factors with the summation of 0.26 mrad for the elevation axis and 0.46 mrad for the cross-elevation axis. The largest contribution to the elevation axis error is manufacturing tolerances of the elevation drive arrangement which include elevation actuator lead error and inaccuracies of actuator pivot point locations from one heliostat to another heliostat. The largest contributor to the cross-elevation axis error is azimuth drive backlash. As indicated in the analysis, measurable/predictable errors will be removed by calibration.

The specification requirement for pointing error due to a 27 mph wind velocity is not to exceed 3.0 mrad peak ( $3\sigma$ ) for either axis under the worst conditions of wind direction and heliostat orientation. Table II shows that the peak elevation axis pointing error is 2.18 mrad which occurs at zenith look (reflector horizontal); the peak azimuth axis pointing error is 1.8 mrad which occurs at horizon look (reflector vertical) and decreases significantly as the heliostat points to higher elevation angles. The largest contributors to azimuth wind pointing error are azimuth drive backlash and azimuth drive compliance. The largest contributor to elevation wind pointing error is torque tube compliance. The elevation error is maximum at zenith because the assembly goes through backlash. Below approximately  $85^\circ$  elevation angle, the elevation drive is always loaded in one direction due to unbalance torque and as a result, there is no backlash effect.

CALM WEATHER POINTING ERRORS (MRAD)

<u>ERROR SOURCE</u>	<u>RMS 1 <math>\sigma</math></u>	
	<u>ELEVATION</u>	<u>CROSS-ELEVATION</u>
BACKLASH	0*	0.42
MANUFACTURING TOLERANCES	0.23	0.12
ZERO REFERENCE REPEATABILITY	0.12	0.12
INCREMENTAL SENSORS	0.02	0.03
MOTOR STOPPING REPEATABILITY	0.02	0.03
ELEVATION AXIS ORTHOGONALITY	0	0.06
GRAVITY CALIBRATION RESIDUALS	0.03	0
SLIGHT WIND (4.5 MI/H)	0.03	0.03
**	_____	_____
RSS TOTALS	<u>0.26 MRAD</u>	<u>0.46 MRAD</u> ***

2-AXIS VECTOR SUM = 0.53 MRAD

TABLE I

- \* No backlash under 85° elevation angle.  
 \*\* Other error sources considered (temperature and mechanical wear) are negligible.  
 \*\*\* Cross-elevation assumes uniform elevation angle distribution; otherwise error = 0.17 mrad @ 75° elev., 0.46 mrad @ 45° and 0.63 mrad @ 15°.

POINTING ERROR ANALYSIS = (27 MPH WIND)A. ELEVATION - MIRROR AT ZENITH - 22,500 IN LBS MOMENT

1.	TORQUE TUBE COMPLIANCE ( $406 \times 10^{-10}$ RAD/IN LBS)	=	0.91 MRAD
2.	ELEVATION DRIVE COMPLIANCE ( $15 \times 10^{-10}$ RAD/IN LBS)	=	0.03
3.	ELEVATION DRIVE BACKLASH (ASSUME <u>+0.6 MR</u> )	=	0.60
4.	ELEVATION BEARING COMPLIANCE ( $0.3 \times 10^{-10}$ RAD/IN LBS)	=	0.00
5.	GIMBAL HOUSING COMPLIANCE ( $31.4 \times 10^{-10}$ RAD/IN LBS)	=	0.07
6.	AZIMUTH DRIVE COMPLIANCE (SPEC - $150 \times 10^{-10}$ RAD/IN LBS)	=	0.34
7.	ARM COMPLIANCE ( $100 \times 10^{-10}$ RAD/IN LBS)	=	0.23
			<hr/>
			2.18 MRAD PEAK

B. AZIMUTH - MIRROR AT HORIZON - 28,000 IN LBS TORQUE

1.	AZIMUTH DRIVE BACKLASH ( <u>+0.61 MR</u> )	=	0.61 MRAD
2.	DRIVE COMPLIANCE (SPECIFICATION - $300 \times 10^{-10}$ RAD/IN LBS)	=	0.84
3.	GIMBAL HOUSING COMPLIANCE ( $72 \times 10^{-10}$ RAD/IN LBS)	=	0.20
4.	TORQUE TUBE COMPLIANCE ( $10 \times 10^{-10}$ RAD/IN LBS)	=	0.03
5.	ELEVATION BEARING CLEARANCE (ASSUME <u>+0.001"</u> )	=	0.11
6.	ELEVATION BEARING COMPLIANCE ( $< 3 \times 10^{-10}$ RAD/IN LBS)	=	0.01
			<hr/>
			1.80 MRAD PEAK

TABLE II



3.0 ANALYSIS

The analysis of the gimbal/actuator drive assembly are presented in the following appendices:

Appendix A - Calm Weather Pointing Error Analysis

Appendix B - Back-up Calculations for the Calm Weather Pointing Error Analysis

Appendix C - 27 MPH Wind Pointing Error Analysis

APPENDIX - A

CALM WEATHER POINTING ERROR ANALYSIS

# GIMBAL POINTING ERROR

## (CALM WEATHER)

### ERROR SOURCES

BACKLASH  
 MANUFACTURING TOLERANCES  
 ANGLE SENSOR RESOLUTION/REPEATABILITY  
 MOTOR STOPPING DISTANCE  
 EL AXIS ORTHOGONALITY  
 GRAVITY ERROR CALIBRATION  
 "SMALL" WIND DEFLECTIONS

### ANALYSIS ASSUMPTIONS

- BEST ESTIMATES OF COMPONENT TOLERANCES
- ALL PREDICTABLE/MEASURABLE ERRORS REMOVED BY CALIBRATION
- ENCODING SYSTEM SET TO READ TRUE AT 30° ELEVATION (TYPICAL)
- 4.5 mi/h MINIMAL WIND
- ALL ERROR COMPONENTS RMS'ED
  - OVER TRAVEL RANGES (UNIFORM AZ & EL DISTRIBUTIONS)
  - OVER TOLERANCE RANGES
- ERROR COMPONENTS UNCORRELATED
- MOTOR STOPPING DISTANCE =  $\pm 1$  REVOLUTION

## BACKLASH EFFECTS

### ELEVATION

NEGLIGIBLE BECAUSE OF UNBALANCE

### AZIMUTH

- 1.2 mrad MAX
- AZ PROGRAMMED TO STOP  
0.6 mrad BEFORE PREDICT POINT -  
THEREFORE MAX ERROR =  $\pm 0.6$  mrad
- ASSUME ERROR IS 50/50 +0.6, -0.6 mrad

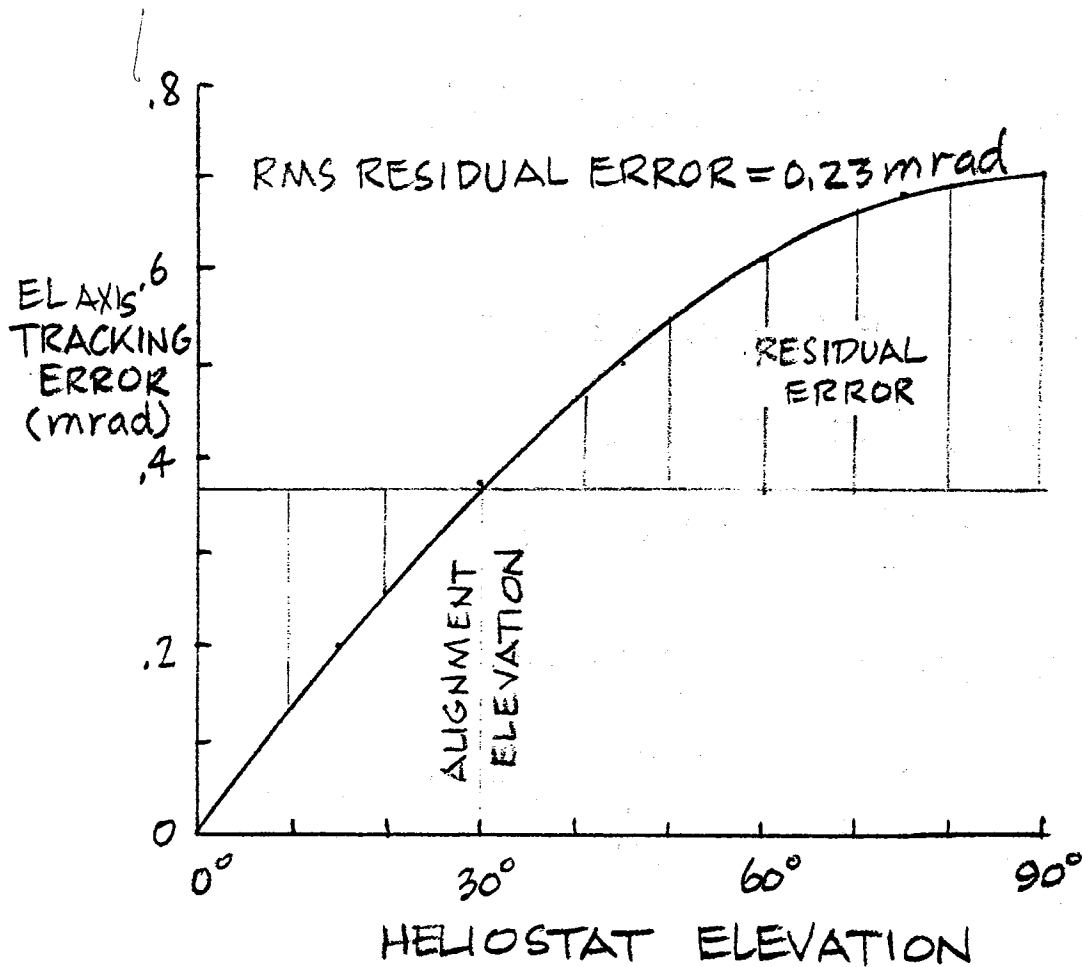
THEN

$$\sigma_{AZ} = 0.6 \text{ mrad}$$

- ASSUME UNIFORM EL DISTRIBUTION

THEN

$$\sigma_{X-EL} = \frac{\sigma_{AZ}}{\sqrt{2}} = .42 \text{ mrad}$$



INCLUDES:

- ACTUATOR LEAD ERROR  $\pm 0.004$  INCH/FT
- ACTUATOR PIVOT LOCATION  
RELATIVE TO EL AXIS  $\pm 0.002$  IN

EFFECTS OF GIMBAL & EL DRIVE  
MANUFACTURING TOLERANCES

## AZ DRIVE TOLERANCES

- QUALITY 8 GEARING
- INCLUDES ALL MESHES
- RMS AZ ERROR

$$\sigma_{AZ} = 0.17 \text{ mrad}$$

- RMS X-EL ERROR

$$\sigma_{X-EL} = \frac{0.17}{\sqrt{2}} = 0.12 \text{ mrad}$$

# ENCODING SENSOR REPEATABILITY

## ON-AXIS "ZERO" REFERENCE

### FACTORS

SENSOR ASSEMBLY TOLERANCES	.001 in
SENSOR THERMAL EFFECTS	.001 in
AZ BEARING RADIAL PLAY	.002 in
TOTAL	<u>.004 in</u>

### RMS ERROR AT 10 in RADIUS\*

$$\sigma_z = \frac{.004}{10\sqrt{2}} = .115 \text{ mrad}$$

## INCREMENTAL SENSOR

### RESOLUTION / ROUNDOFF

- 1 PULSE / REV
- .06 mrad - EL
- .12 mrad - AZ

### RMS ROUNDOFF ERROR\*

$$\sigma_I = \left\{ \begin{array}{l} \frac{.06}{\sqrt{2}} = .02 \text{ mrad EL} \\ \frac{.12}{\sqrt{2}\sqrt{2}} = .03 \text{ mrad X-EL} \end{array} \right\}$$

\* ASSUMES UNIFORM ERROR DISTRIBUTION

## EL AXIS NON-ORTHOGONALITY

- MANUFACTURED TO  $0.25^\circ$  (4.4 mrad)
- MEASURED WITH  $0.01^\circ$  (0.17 mrad) ACCURACY
- COMPUTER CORRECTED TO MEASURED VALUE
- RESIDUAL CALIBRATION ERRORS

$$\epsilon_{EL} \cong 0$$

$$\epsilon_{X-EL} = \Delta_{NO} \sin E, \quad \Delta_{NO} = 0.17 \text{ mrad}$$

- RMS ERROR

$$\sigma_{X-EL}^2 = \frac{2}{\pi} \int_0^{\pi/2} [\Delta_{NO} \sin E - \Delta_{NO} \sin E_0]^2 dE$$

$$E_0 = \text{ALIGNMENT ELEVATION} = 30^\circ$$

$$\sigma_{X-EL} = 0.34 \Delta_{NO} = .06 \text{ mrad}$$



## GRAVITY CALIBRATION RESIDUALS

- ASSUME GRAVITY ERROR IS MEASURED FOR TOTAL SYSTEM IN FIRST ARTICLE TESTING
- THEN RESIDUAL ERROR IS ONLY DUE TO COMPLIANCE VARIATIONS FROM ARTICLE ( $\cong \pm 5\%$  MILL TOLERANCES) AND

$$\begin{aligned} \text{RESIDUAL P.E.} &= \text{ZHSD} \cdot \text{SMT} \cdot \text{RMSF} \\ &= \underline{0.03 \text{ mrad}} \end{aligned}$$

$$\begin{aligned} \text{ZHSD} &= \text{ZENITH/HORIZ. STRUCTURAL DEFL.} \\ &\cong 1.8 \text{ mrad (PRELIM. ANALYSIS)} \end{aligned}$$

$$\text{RMSF} = \text{ELEVATION RMS FACTOR} \cong 1/3$$

$$\text{SMT} = \text{STRUCTURAL MATERIAL TOLERANCE FACTOR} = 0.05$$

## WIND DEFLECTIONS

$$\bullet \text{ PEAK ERROR (EITHER AXIS)} \cong .06 \text{ mrad}$$

$$\bullet \text{ RMS ERROR} = .06 \times \text{WRMSF} = \underline{.03 \text{ mrad}}$$

$$\begin{aligned} \text{WRMSF} &= \text{RMS FACTOR FOR} \\ &\text{ALL WIND DIRECTIONS} \end{aligned}$$

$$\cong 1/2$$

APPENDIX - B  
BACK-UP CALCULATIONS  
FOR  
CALM WEATHER POINTING ERROR ANALYSIS



$$\text{LET } BC = BC'$$

$$\& AC' = AC''$$

$$\begin{aligned} \& CC'' &= \text{ERROR IN TORQUE ARM LENGTH} \\ &= AC - AC' = \Delta L_t \end{aligned}$$

$$\begin{aligned} \text{THEN } \Delta E &= \frac{C'C''}{L_t} \\ &= \frac{CC'' \tan \angle C'CC''}{L_t} \\ &= \frac{CC''}{L_t \tan \angle ACB} \\ &= \frac{\Delta L_t}{L_t \tan \angle ACB} \end{aligned}$$

$\angle ACB$  CHANGES FROM ABOUT  $27^\circ$  AT HORIZON TO  
MAXIMUM  $45^\circ$  & ABOUT  $40^\circ$  AT ZENITH

ASSUME AVERAGE ANGLE OF  $35^\circ$

$$\text{THEN } \Delta E = \frac{\Delta L_t}{L_t \tan 35^\circ} = \frac{\Delta L_t}{31 \times 0.7} = 0.046 \Delta L_t$$

$$\text{FOR } \Delta L_t = \pm 0.005''$$

$$\Delta E = 2.3 \times 10^{-4} \text{ RADIANS OR } \pm 0.23 \text{ MR}$$

(AT ZENITH,  $\Delta E = \pm 0.19 \text{ MR}$  & AT HORIZON,  $\Delta E = \pm 0.32 \text{ MR}$ )

$$\text{FOR } \Delta L_t = \pm 0.002''$$

$$\begin{aligned} \Delta E &= \pm 0.076 \text{ MR AT ZENITH} \\ &\& \pm 0.128 \text{ MR AT HORIZON} \end{aligned}$$



$$\text{FOR } E = 0, \quad \theta = 85^\circ$$

$$E = 40 \quad \theta = 60$$

$$E = 90 \quad \theta = 6$$

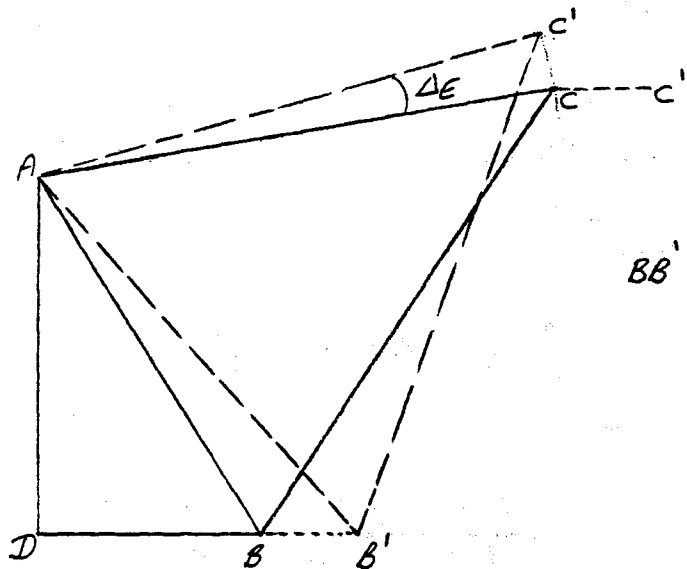
$$\begin{aligned} \text{FOR } E = 0, \quad \Delta E &= \frac{0.005}{31} \frac{\sin 95}{\sin 30} \\ &= 3.2 \times 10^{-4} \text{ RADIANS} = 0.32 \text{ MR} \end{aligned}$$

$$\begin{aligned} E = 40, \quad \Delta E &= \frac{0.005}{31} \frac{\sin 120}{\sin 45} \\ &= 2 \times 10^{-4} \text{ RADIANS} = 0.2 \text{ MR} \end{aligned}$$

$$\begin{aligned} E = 90 \quad \Delta E &= \frac{0.005}{31} \frac{\sin 174}{\sin 41} \\ &= 2.6 \times 10^{-5} \text{ RADIANS} = 0.026 \text{ MR} \end{aligned}$$

THUS, RESULTING ERROR IS FROM 0.026 TO 0.32 MR FOR  $\pm 0.005$  INCH INACCURACY. & FOR  $\pm 0.002$  INCH INACCURACY ERROR IS FROM 0.010 TO 0.128 MR.

b. INACCURACY IN HORIZONTAL DISTANCE BETWEEN A & B



$$BB' = \Delta h = \pm 0.005''$$

$$\Delta E = \frac{CC'}{AC} = \frac{CC'}{L_t}$$

$$CC' = \frac{CC'' \sin \angle CC''C'}{\sin \angle CC'C''}$$

$$CC'' = BB' = \Delta h$$

$$\angle C'CC'' = 145 - E$$

$$\begin{aligned} \angle CC'C'' &= 90^\circ - (55 - E) - (90 - \theta) \\ &= \theta + E - 55 \end{aligned}$$

$$\begin{aligned} \angle CC''C' &= 180 - (145 - E) - (\theta + E - 55) \\ &= 90 - \theta \end{aligned}$$

$$\begin{aligned} \text{THUS } \Delta E &= \frac{\Delta h}{L_t} \frac{\sin(90^\circ - \theta)}{\sin(\theta + E - 55)} \\ &= \frac{\Delta h}{L_t} \frac{\cos \theta}{\sin(\theta + E - 55)} \end{aligned}$$

$$\text{FOR } E = 0, \Delta E = \frac{0.005}{31} \frac{\cos 85}{\sin 30} = 8 \times 10^{-5} \text{ RAD} = 0.08 \text{ MR}$$

$$E = 40, \Delta E = \frac{0.005}{31} \frac{\cos 60}{\sin 45} = 1.1 \times 10^{-4} \text{ RAD} = 0.11 \text{ MR}$$

$$E = 90, \Delta E = \frac{0.005}{31} \frac{\cos 6}{\sin 41} = 2.4 \times 10^{-4} \text{ RAD} = 0.24 \text{ MR}$$

THUS, RESULTING ERROR IS FROM 0.08 TO 0.24 MR FOR  $\pm 0.005$  INCH ACCURACY & FOR  $\pm 0.002$  INCH ACCURACY ERROR IS FROM 0.032 TO 0.096 MR.

## 4. WIND POINTING ERROR:

FOR 27 MPH WIND, WORST CASE POINTING ERROR

$$= 3 \text{ MR FOR EACH AXIS.}$$

ASSUME 1 MR IS FOR BACKLASH

THEN WORST CASE WIND DEFLECTION IS 2 MR IN 27 MPH WIND.

FOR 4.5 MPH WORST ORIENTATION WIND.

$$\begin{aligned} \text{POINTING ERROR IN EACH AXIS} &= 2 \times \left(\frac{4.5}{27}\right)^2 \\ &= 0.056 \text{ MR} \end{aligned}$$

## 5. ELEVATION ACTUATOR LEAD ERROR

PER DUFF NORTON CATALOG, THERE IS 0.002 TO 0.004 INCH PER FOOT LEAD ERROR IN THEIR MACHINE SCREW THREADS. THIS LEAD ERROR IS CUMULATIVE.

APPROXIMATE NUT TRAVEL = 30 INCH.

$$\begin{aligned} \text{THEREFORE, TOTAL LEAD ERROR} &= \frac{30}{12} (0.002 \text{ TO } 0.004) \\ &= 0.005 \text{ TO } 0.010 \text{ INCH} \\ &\text{OR } 0.010 \text{ INCH MAXIMUM} \end{aligned}$$



BY..... DATE..... SUBJECT.....

SHEET NO. .... OF .....

CHKD. BY..... DATE.....

JOB NO. ....

AT ZENITH, MOMENT ARM = 22 INCH

THEREFORE 0.010 INCH LEAD ERROR

$$= \frac{0.010}{22}$$

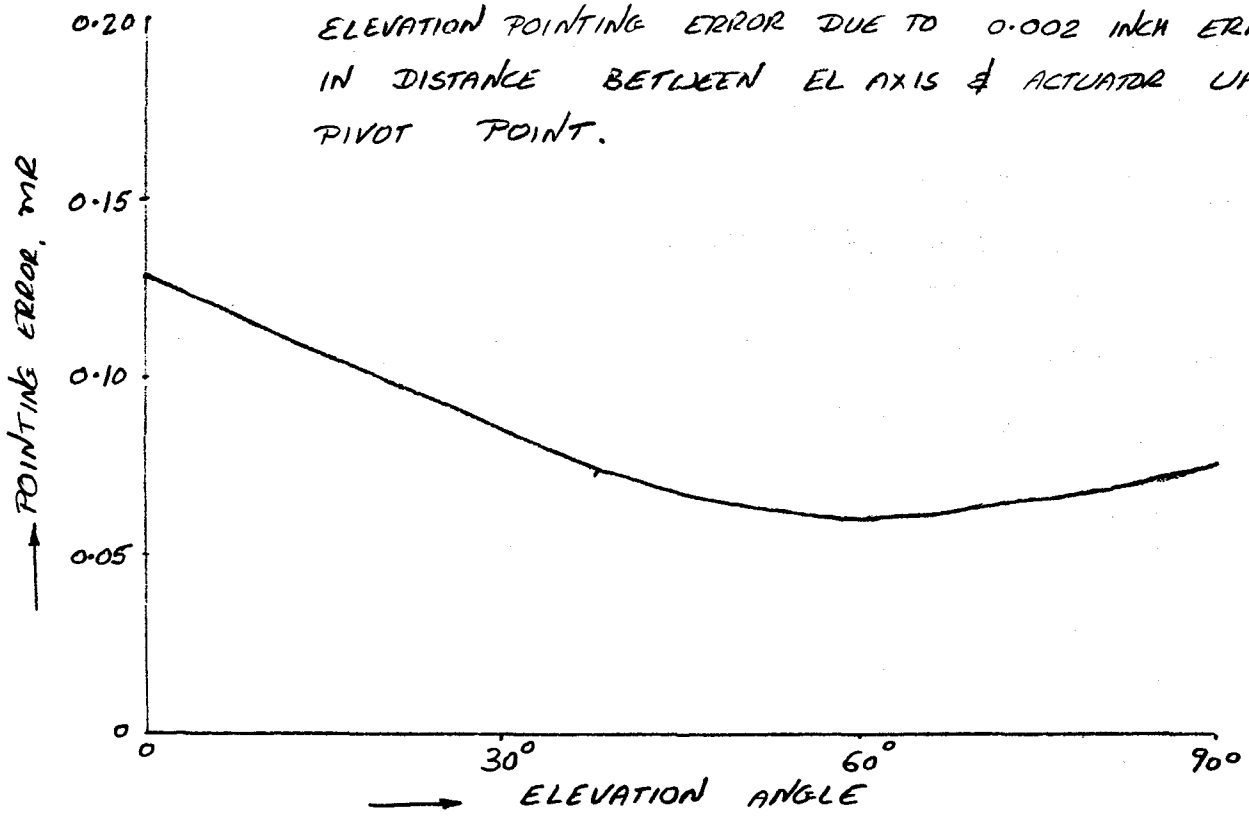
$$= 4.5 \times 10^{-4} \text{ RADIANS}$$

$$= 0.45 \text{ MR}$$

THUS, MAXIMUM POINTING ERROR DUE TO LEAD ERROR

$$= 0.45 \text{ MR}$$

ELEVATION POINTING ERROR DUE TO 0.002 INCH ERROR IN DISTANCE BETWEEN EL AXIS & ACTUATOR UPPER PIVOT POINT.



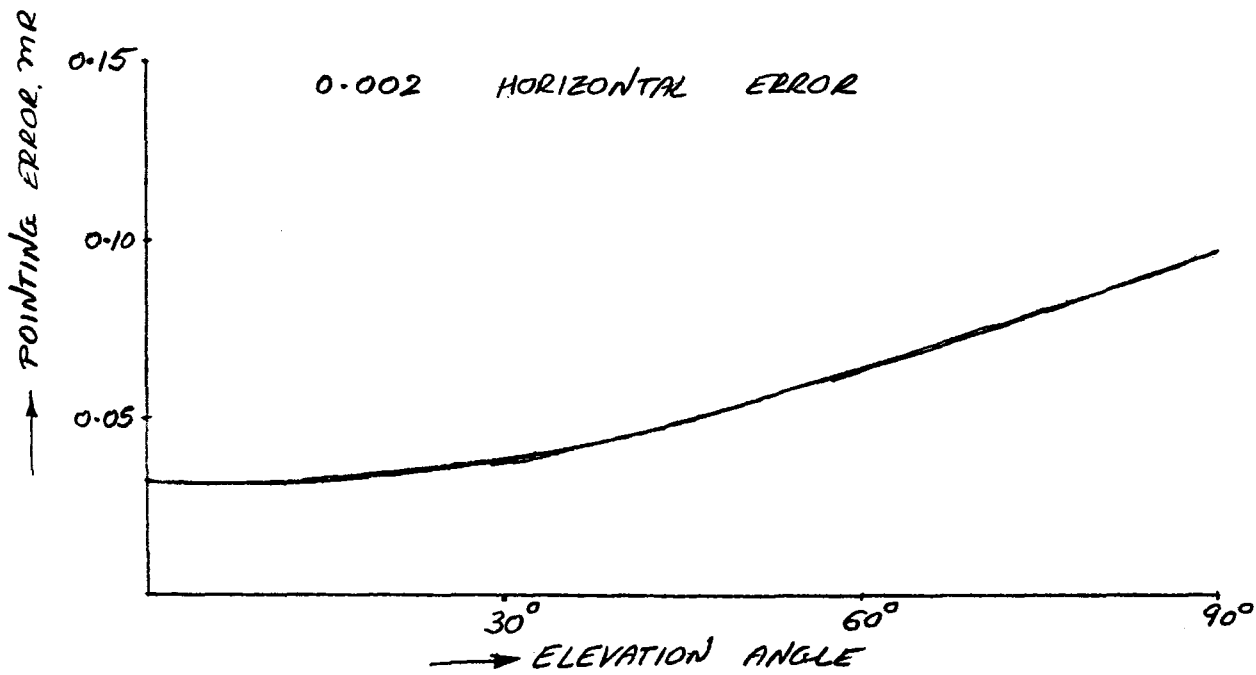
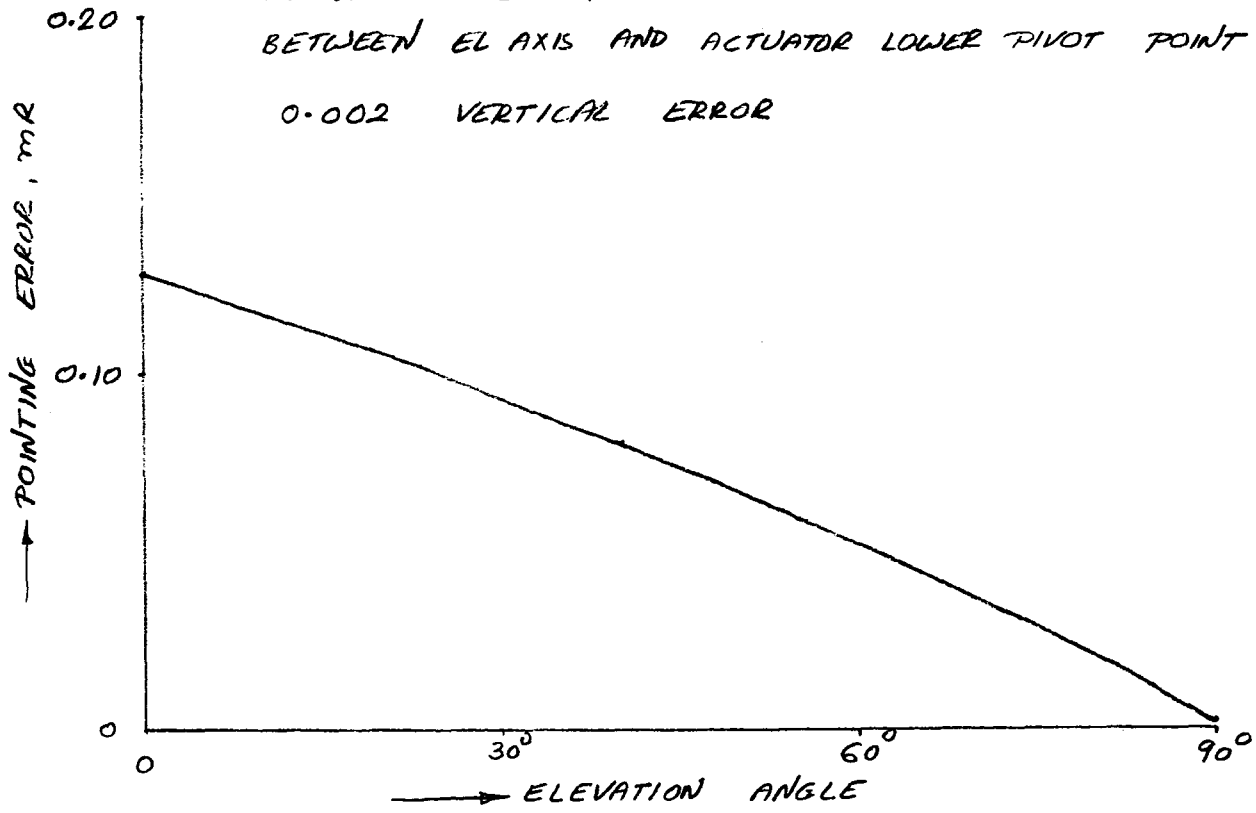
BY PBN DATE 11/29/79 SUBJECT POINTING ERROR

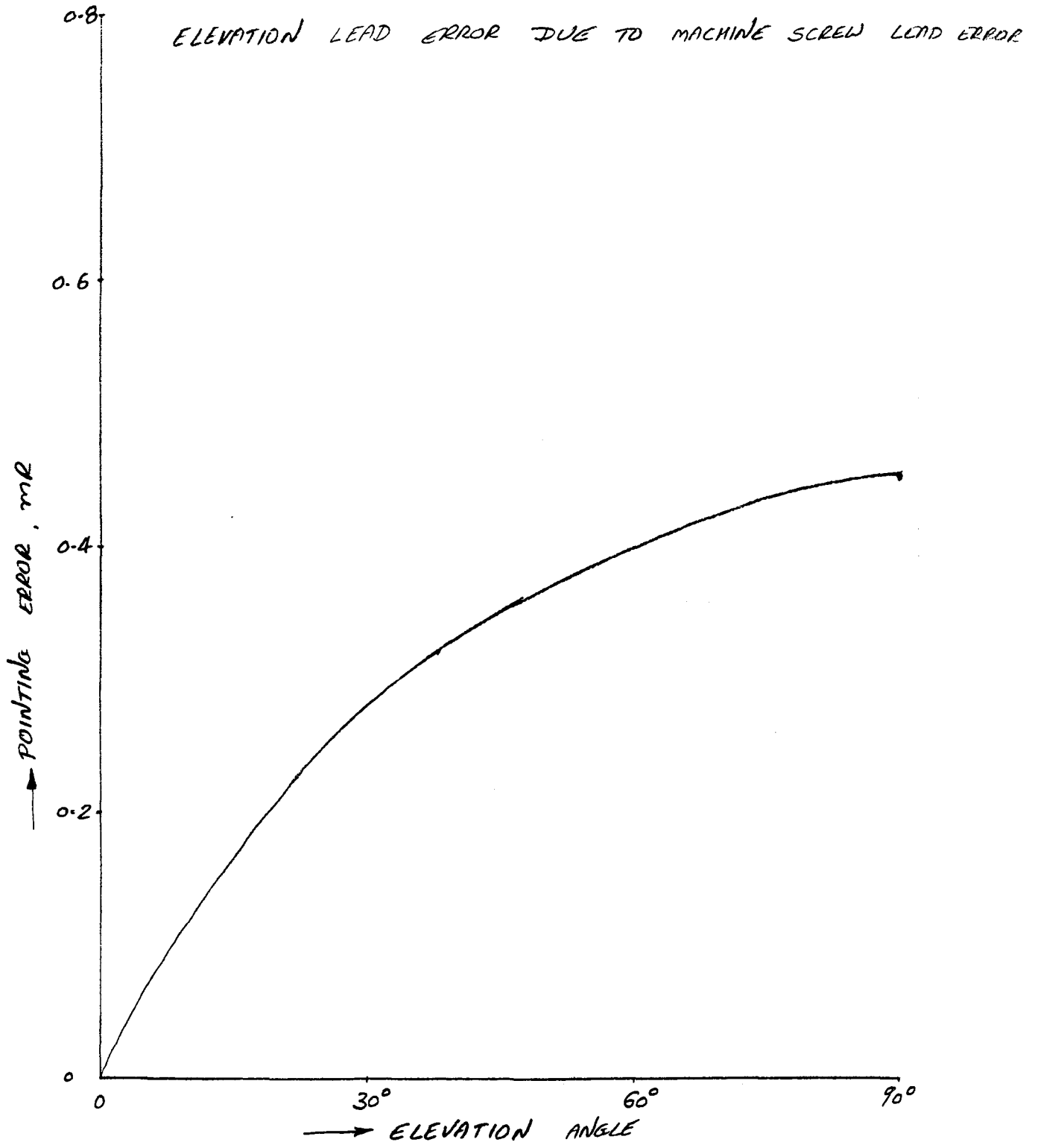
SHEET NO. 24 OF 24

JOB NO. BOEING HELIOSTAT

ELEVATION POINTING ERROR DUE TO ERROR IN DISTANCE  
BETWEEN EL AXIS AND ACTUATOR LOWER PIVOT POINT :

0.002 VERTICAL ERROR





PURPOSE : TO ESTIMATE AZIMUTH POINTING ERROR DUE TO TOOTH TO TOOTH ERROR OF AZIMUTH GEARING

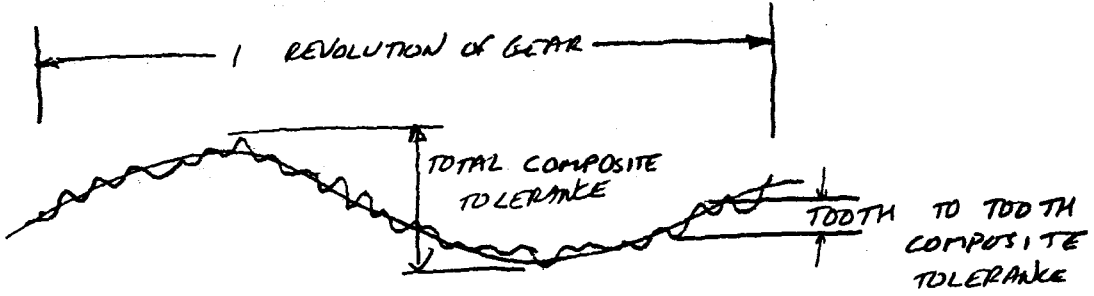
ASSUME QUALITY B GEARS, 25° PRESSURE ANGLE

a. ROTATING BULL GEAR :

PITCH DIAMETER = 19.2 INCH, 10 DP  
PER AGMA 390.03

TOTAL COMPOSITE TOLERANCE = 0.0055 INCH

TOOTH TO TOOTH COMPOSITE TOLERANCE = 0.0015 INCH



$$\text{RMS ERROR} = \left( \frac{\sqrt{A^2 + B^2}}{\text{GEAR RADIUS}} \right) \tan 25 \text{ RADIANS}$$

WHERE  $B = \frac{\text{TOOTH TO TOOTH COMPOSITE TOLERANCE}}{2} = 0.00075 \text{ INCH}$

$A = \frac{\text{TOTAL COMPOSITE} - \text{TOOTH TO TOOTH COMPOSITE}}{2} = 0.002$

$$\text{RMS ERROR} = \left( \frac{\sqrt{0.002^2 + 0.00075^2}}{9.6} \right) \tan 25$$

$$= 0.0001 \text{ RADIANS OR } 0.1 \text{ MR}$$

b. FIXED BULL GEAR :

FIXED BULL GEAR IS ABOUT SAME AS ROTATING BULL GEAR. THEREFORE RMS ERROR = 0.1 MR

c. UPPER PLANET GEAR:

PITCH DIAMETER = 8.7 INCH, 10 DP

HERE, TOTAL COMPOSITE TOLERANCE = 0.004 INCH

TOOTH TO TOOTH COMPOSITE TOLERANCE = 0.0015 INCH

HERE  $B = 0.00075$  INCH

$$\& A = \frac{0.004 - 0.0015}{2} = 0.00125 \text{ INCH}$$

$\&$  RMS ERROR ABOUT PLANET'S C/WN AXIS

$$= \left( \frac{\sqrt{(0.00125^2 + 0.00075^2)}}{4.35} \right) \tan 25$$

$$= 0.00016 \text{ RADIANS OR } 0.16 \text{ MR}$$

$\&$  RMS ERROR ABOUT GEAR AXIS

$$= 0.16 \times \frac{4.35}{9.6}$$

$$= 0.07 \text{ MR}$$

d. LOWER PLANET GEAR

THIS IS ABOUT THE SAME AS UPPER PLANET GEAR

THEREFORE RMS ERROR = 0.05 MR.

$$\begin{aligned} \text{e. OVERALL DRIVE RMS ERROR} &= \sqrt{0.1^2 + 0.1^2 + 0.07^2 + 0.07^2} \\ &= 0.17 \text{ MR} \end{aligned}$$

APPENDIX - C

27 MPH WIND POINTING ERROR ANALYSIS

LIST OF COMPLIANCES:

1. ACTUATOR : MOMENT COMPLIANCE =  $100 \times 10^{-10}$  RADIAN'S/IN LBS @ HORIZON  
 $\& 15 \times 10^{-10}$  RADIAN'S/IN LBS @ ZENITH
2. ARM COMPLIANCE - MOMENT =  $100 \times 10^{-10}$  RADIAN'S/IN LBS  
 (PER STRUCTURAL ANALYSIS TECH MEMO)
3. GIMBAL COMPLIANCE - MOMENT =  $31.4 \times 10^{-10}$  RADIAN'S/IN LBS MAX - @ ZENITH  
 $\& 20.4 \times 10^{-10}$  RADIAN'S/IN LBS @ HORIZON  
 TORSIONAL =  $72 \times 10^{-10}$  RADIAN'S/IN LBS.
4. AZIMUTH DRIVE - SPECIFICATION NUMBERS TO WINSMITH  
 - MOMENT =  $150 \times 10^{-10}$  RADIAN'S/IN LBS  
 TORSIONAL =  $300 \times 10^{-10}$  RADIAN'S/IN LBS
5. TORQUE TUBE COMPLIANCE : MOMENT =  $406 \times 10^{-10}$  RAD/IN LBS  
 TORSIONAL =  $10 \times 10^{-10}$  RAD/IN LBS
6. ELEVATION BEARING COMPLIANCE -  
 MOMENT =  $0.3 \times 10^{-10}$  RAD/IN LBS  
 TORSIONAL =  $3 \times 10^{-10}$  RAD/IN LBS



ELEVATION ACTUATOR COMPLIANCE :

PER ACTUATOR TECH MEMO LINEAR COMPLIANCE IS AS FOLLOWS :

AT HORIZON, COMPLIANCE =  $2.2 \times 10^{-6}$  IN/LB - MAXIMUM

AT ZENITH COMPLIANCE =  $0.9 \times 10^{-6}$  IN/LB - MINIMUM

MOMENT ARM AT HORIZON = 15.8 INCH

MOMENT ARM AT ZENITH = 26.9 INCH

THEREFORE,

MOMENT COMPLIANCE AT HORIZON

$$= \frac{2.2 \times 10^{-6}}{(15.8)^2} = 88 \times 10^{-10} \text{ RADIANS/IN LB}$$

MOMENT COMPLIANCE AT ZENITH =

$$= \frac{0.9 \times 10^{-6}}{(26.9)^2} = 12 \times 10^{-10} \text{ RADIANS/IN LB}$$

INCLUDING MISCELLANEOUS EFFECTS,

ASSUME MOMENT COMPLIANCE OF

$100 \times 10^{-10}$  RADIANS/IN LB AT HORIZON

&  $15 \times 10^{-10}$  RADIANS/IN LB AT ZENITH

TORQUE TUBE COMPLIANCE: (PER STRUCTURAL ANALYSIS TELH MEMO)

1. MOMENT COMPLIANCE ABOUT ELEVATION AXIS:

$$\text{MOMENT COMPLIANCE} = 406 \times 10^{-10} \text{ RADIANS/IN LB}$$

2. TORSIONAL COMPLIANCE ABOUT AZIMUTH AXIS WITH REFLECTOR AT HORIZON:

$$\begin{aligned} \text{TORSIONAL COMPLIANCE} &= \frac{(273+78) \times 10^{-8}}{(59)^2} \\ &= 10 \times 10^{-10} \text{ RAD/IN LB} \end{aligned}$$

ELEVATION BEARING :

1. MOMENT COMPLIANCE WITH REFLECTOR AT ZENITH

$$\begin{aligned} \text{MOMENT COMPLIANCE} &= \frac{7 \times 10^{-7}}{22,500} \\ &= 0.3 \times 10^{-10} \text{ RAD/IN LBS} \end{aligned}$$

2. TORSIONAL COMPLIANCE WITH REFLECTOR AT HORIZON

$$\begin{aligned} \text{TORSIONAL COMPLIANCE} &= \frac{8 \times 10^{-6}}{28,000} \\ &= 2.9 \times 10^{-10} \\ &\text{SAY } 3 \times 10^{-10} \text{ RADIANS/IN LBS} \end{aligned}$$

NOTE : CONTRIBUTION FROM ELEVATION BEARING WITH REVISED DESIGN IS EVEN SMALLER THAN SHOWN ABOVE.



REPORT E-9

COMBINED STRUCTURAL COMPLIANCES

FOR

GIMBAL/ACTUATOR DRIVE ASSEMBLY

FOR

BOEING SECOND GENERATION HELIOSTAT

JUNE 27, 1980

Reference: FACC TM19



Ford Aerospace &  
Communications Corporation

## 1.0 INTRODUCTION

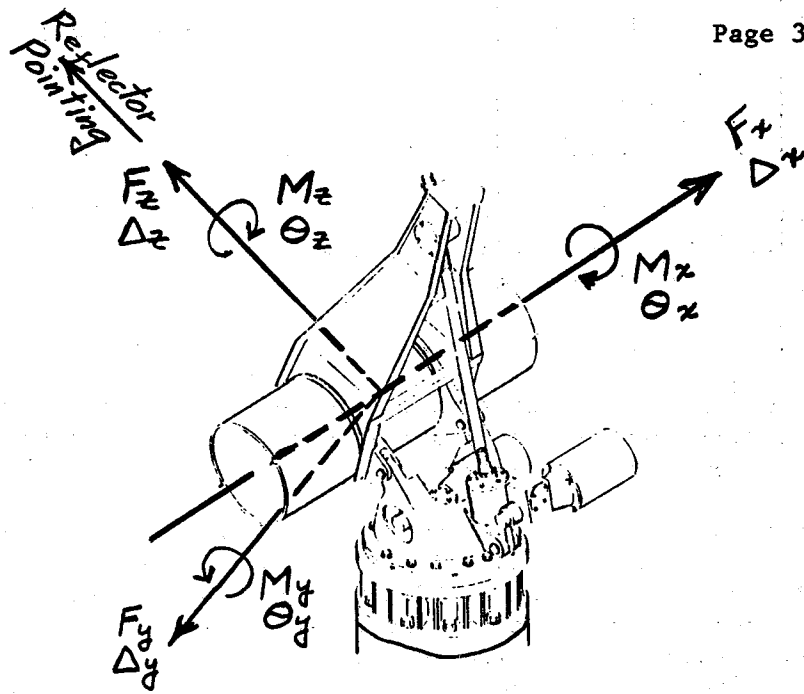
The purpose of this appendix is to present the total compliance of the gimbal/actuator drive assembly by combining the individual component compliances.

## 2.0 SUMMARY

Loads are applied at the two ends of the center portion of the torque tube, and the total compliance of the gimbal/actuator drive assembly includes all components to the top of the pedestal.

The compliances are calculated for six (6) degrees of freedom, i.e., forces and deflections are along three (3) orthogonal axes, and moments and rotations are about the same three axes. The x-axis is established through the center of the torque tube parallel to the elevation axis. The y-axis is cross-elevation, the z-axis is the reflector mirror normal, and both axes rotate in elevation with the reflector. Two sets of compliances have been calculated: (1) with the reflector at horizon look (mirror vertical) and (2) with the reflector at zenith look (mirror horizontal).

The compliance summary table is shown on page 3.



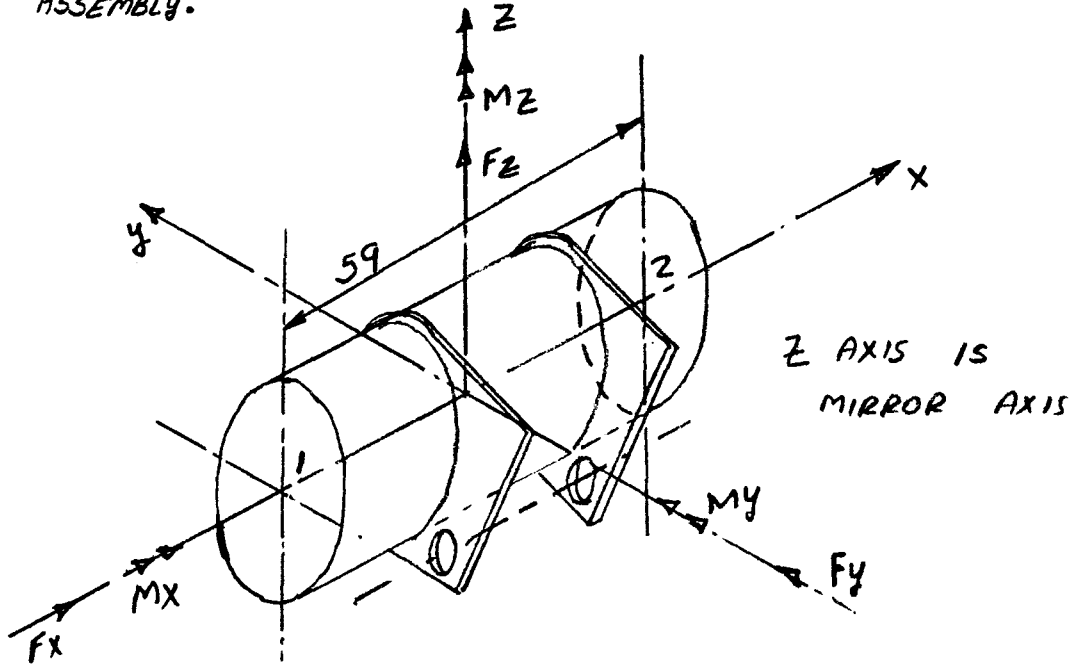
COMPLIANCE SUMMARY

REFLECTOR AT			HORIZON LOOK			LOAD	REFLECTOR AT			ZENITH LOOK		
MRAD x 10 <sup>-2</sup> θ <sub>x</sub> θ <sub>y</sub> θ <sub>z</sub>			Inches x 10 <sup>-4</sup> Δ <sub>x</sub> Δ <sub>y</sub> Δ <sub>z</sub>				MRAD x 10 <sup>-2</sup> θ <sub>x</sub> θ <sub>y</sub> θ <sub>z</sub>			Inches x 10 <sup>-4</sup> Δ <sub>x</sub> Δ <sub>y</sub> Δ <sub>z</sub>		
						Moment In.Kips						
7.8	--	--	--	-8.0	-2.2	M <sub>x</sub>	7.0	--	--	--	-9.5	--
--	3.9	--	4.5	--	--	M <sub>y</sub>	--	2.1	--	4.8	--	--
--	--	2.2	2.4	--	--	M <sub>z</sub>	--	--	4.0	--	--	--
						Force Kips						
--	48	24	400	--	--	F <sub>x</sub>	--	51	--	440	--	--
-80	--	--	--	100	25	F <sub>y</sub>	-95	--	--	--	200	--
-22	--	--	--	25	30	F <sub>z</sub>	--	--	--	--	--	14
y-axis vertical z-axis horizontal							y-axis horizontal z-axis vertical					

3.0 ANALYSIS



PURPOSE : TO COMBINE INDIVIDUAL COMPONENT COMPLIANCES TO ESTIMATE OVERALL COMPLIANCE OF GIMBAL ACTUATOR ASSEMBLY.



AXIS CONVENTION

a. MIRROR AT ZENITH (IGNORE THE 1.5" HORIZONTAL OFFSET BETWEEN TORQUE TUBE & EL AXIS)

1. EFFECT OF  $M_x$

$$M_{1x} = M_{2x} = \frac{M_x}{2} = 0.5$$

$\theta_x$	—	AZIMUTH DRIVE — SPEC. NUMBER	$150 \times 10^{-10}$	RADIANS/IN LB
		GIMBAL	$31.4 \times 10^{-10}$	RADIANS/IN LBS
		ACTUATOR	$15 \times 10^{-10}$	RADIANS/IN LBS
		ARM	$100 \times 10^{-10}$	RADIANS/IN LBS
		TORQUE TUBE	$406 \times 10^{-10}$	RADIANS/IN LBS
		TOTAL	<u><math>702.4 \times 10^{-10}</math></u>	RADIANS/IN LB
		SAY	$700 \times 10^{-10}$	RADIANS/IN LBS

BY..... DATE..... SUBJECT..... SHEET NO..... OF.....  
 CHKD. BY..... DATE..... JOB NO.....

$$\underline{\Delta y - \text{AZIMUTH DRIVE}} = -150 \times 10^{-10} (11.75 + 11.97) \\ = -3558 \times 10^{-10} \text{ IN/IN LB}$$

$$\text{GIMBAL} = -646 \times 10^{-10} - 31.4 \times 10^{-10} (11.97) \\ = -1021.9 \times 10^{-10} \text{ IN/IN LBS}$$

$$\text{ACTUATOR} = -15 \times 10^{-10} (11.97) \\ = -179.6 \times 10^{-10} \text{ IN/IN LBS}$$

$$\text{ARM} = -100 \times 10^{-10} (11.97) \\ = -1197 \times 10^{-10} \text{ IN/IN LBS}$$

$$\text{TORQUE TUBE} = -3420. \times 10^{-10} \text{ IN/IN LBS}$$

$$\underline{\text{TOTAL}} = -9376.5 \times 10^{-10} \text{ IN/IN LBS}$$

INCLUDING THE DEFLECTION AT TOP OF AZIMUTH DRIVE.

$$\text{ASSUME } \Delta y = -9500 \times 10^{-10} \text{ IN/IN LBS}$$

## 2. EFFECT OF $f_y$ (0.5 LBS AT EACH FLANGE)

$$\Theta_x - \text{BY RECIPROCITY} \\ = -9500 \times 10^{-10} \text{ RADIANS/LBS}$$

$$\Delta y - \text{AZIMUTH DRIVE} = 150 \times 10^{-10} (11.75 + 11.97)^2 \\ = 844 \times 10^{-8} \text{ INCH/LB}$$

$$\text{GIMBAL} = 197 \times 10^{-8} + 646 \times 10^{-10} \times 11.97 + 11.97 \times 6.46 \times 10^{-8} \\ + (11.97)^2 \times 31.4 \times 10^{-10} \\ = 396.6 \times 10^{-8} \text{ INCH/LB}$$

$$\text{ACTUATOR} = 15 \times 10^{-10} (11.97)^2 = 21.5 \times 10^{-8} \text{ INCH/LB}$$

$$\text{ARM} = 100 \times 10^{-10} (11.97)^2 = 143.3 \times 10^{-8} \text{ INCH/LB}$$

$$\text{TORQUE TUBE} = 423 \times 10^{-8} \text{ INCH/LB}$$

TOTAL  $\Delta_y = 1828.4 \times 10^{-8}$  INCH/LB

INCLUDING DEFLECTION AT THE TOP OF AZIMUTH DRIVE,

ASSUME,  $\Delta_y = 2000 \times 10^{-8}$  INCH/LB

3. EFFECT OF  $M_z$

$\theta_z$  - AZIMUTH DRIVE - SPEC. NUMBER =  $300 \times 10^{-10}$  RADIANS/IN LB

- GIMBAL -  $72 \times 10^{-10}$  RADIANS/IN LB

- TORQUE TUBE -  $\frac{(858+12) \times 10^{-8}}{(59)^2}$  NOTE:  $M_z$  RESULTS IN  $F_y$  AT EACH FLANGE.

=  $25 \times 10^{-10}$  RADIANS/IN LB

TOTAL =  $397 \times 10^{-10}$  RADIANS/IN LB

SAY  $400 \times 10^{-10}$  RADIANS/IN LB

4. EFFECT OF  $F_z$

$\Delta_z$  - GIMBAL -  $22 \times 10^{-8}$  INCH/LB

TORQUE TUBE -  $97 \times 10^{-8}$  INCH/LB

TOTAL =  $119 \times 10^{-8}$  INCH/LB

INCLUDING EFFECT OF AZIMUTH DRIVE

ASSUME  $140 \times 10^{-8}$  INCH/LB

5. EFFECT OF  $M_y$  - (THIS RESULTS IN EQUAL & OPPOSITE  $F_z$  FORCES AT FLANGES)

$\theta_y$  - AZIMUTH DRIVE - SPEC. NUMBER  $150 \times 10^{-10}$  RADIANS/IN LB

GIMBAL -  $45.7 \times 10^{-10}$  RADIANS/IN LB

TORQUE TUBE -  $\frac{(273+78) \times 10^{-8}}{(59)^2} = 10 \times 10^{-10}$  RADIANS/IN LB

TOTAL =  $205.7 \times 10^{-10}$  RADIANS/IN LB

SAY  $210 \times 10^{-10}$  RADIANS/IN LB

$$\Delta_x - \text{AZIMUTH DRIVE} = +150 \times 10^{-10} (11.75 + 11.97) \\ = +3558 \times 10^{-10} \text{ IN/IN LB}$$

$$\text{GIMBAL} = 523 \times 10^{-10} + 45.7 \times 10^{-10} (11.97) \\ = 1070 \times 10^{-10} \text{ IN/IN LB}$$

$$\text{TORQUE TUBE} = 0$$

---


$$\text{TOTAL} = 4628 \times 10^{-10} \text{ IN/IN LB}$$

INCLUDING DEFLECTION AT TOP OF AZIMUTH DRIVE,

$$\text{ASSUME } \Delta_x = 4800 \times 10^{-10} \text{ INCH/IN LB}$$

### 6. EFFECT OF $F_x$ -

BECAUSE OF ELEVATION BEARING CLEARANCE, ASSUME THAT ALL THIS AXIAL LOAD  $F_x$  IS TAKEN AT BEARING # 1. i.e.  $F_{1x} = 1$

$$\Theta_y - \text{AZIMUTH DRIVE} = +150 \times 10^{-10} (11.75 + 11.97) \\ = +3558 \times 10^{-10} \text{ RAD/LBS}$$

$$\text{GIMBAL} = 523 \times 10^{-10} + 45.7 \times 10^{-10} (11.97) \\ = 1070 \times 10^{-10} \text{ RAD/LBS}$$

$$\text{TORQUE TUBE} = 293 \times 10^{-10} \text{ RAD/LBS}$$

---


$$\text{TOTAL} = 4921 \times 10^{-10} \text{ RAD/LBS}$$

INCLUDING ROTATION AT THE TOP OF AZIMUTH DRIVE DUE TO  $F_x$ ,

$$\text{ASSUME, } \Theta_y = 5100 \times 10^{-10} \text{ RAD/LBS}$$

$$\Delta_x - \text{AZIMUTH DRIVE} = 150 \times 10^{-10} (11.75 + 11.97)^2 \\ = 844 \times 10^{-8} \text{ INCH/LB}$$

$$\text{GIMBAL} = 217 \times 10^{-8} + 2 \times 523 \times 10^{-8} \times 11.97 + (11.97)^2 \times 45.7 \times 10^{-10} \\ = 408 \times 10^{-8} \text{ INCH/LB}$$

$$\text{TORQUE TUBE} = 2940 \times 10^{-8} \text{ INCH/LB}$$

---


$$\text{TOTAL} = 4192 \times 10^{-8} \text{ INCH/LB}$$

INCLUDING, DEFLECTION AT THE TOP OF AZIMUTH DRIVE.

ASSUME,  $\Delta_x = 4400 \times 10^{-8}$  INCH/LBS

SUMMARIZING, WITH MIRROR AT ZENITH,

JOINT LOAD LBS & INLBS	$\Delta_x$ IN $\times 10^{-8}$	$\Delta_y$ IN $\times 10^{-8}$	$\Delta_z$ IN $\times 10^{-8}$	$\theta_x$ RAD $\times 10^{-10}$	$\theta_y$ RAD $\times 10^{-10}$	$\theta_z$ RAD $\times 10^{-10}$
$F_x$	+4400	-	-	-	+5100	-
$F_y$	-	+2000	-	-9500	-	-
$F_z$	-	-	+140	-	-	-
$M_x$	-	-95	-	+700	-	-
$M_y$	+48	-	-	-	+210	-
$M_z$	-	-	-	-	-	+400

NOTE : X AXIS IS ELEVATION AXIS (HORIZONTAL)  
 Y AXIS IS CROSS ELEVATION AXIS (HORIZONTAL)  
 Z AXIS IS MIRROR NORMAL AXIS (VERTICAL)

b. MIRROR AT HORIZON (IGNORE THE 1.5" VERTICAL OFFSET BETWEEN TORQUE TUBE & EZ AXIS)

1. EFFECT OF  $M_x$

$\theta_x$  - AZIMUTH DRIVE =  $150 \times 10^{-10}$  RAD/IN LBS  
 GIMBAL =  $20.4 \times 10^{-10}$  "  
 ACTUATOR =  $100 \times 10^{-10}$  "  
 ARM =  $100 \times 10^{-10}$  "  
 TORQUE TUBE =  $406 \times 10^{-10}$  "  


---

 TOTAL =  $776.4 \times 10^{-10}$  "  
 SAY  $780 \times 10^{-10}$  RAD/IN LBS

$\Delta_z$  - AZIMUTH DRIVE =  $-150 \times 10^{-10} (11.75) = 1763 \times 10^{-10}$  IN/IN LBS  
 GIMBAL =  $-420 \times 10^{-10}$  IN/IN LBS  


---

 TOTAL =  $-2183 \times 10^{-10}$  IN/IN LBS  
 SAY  $-2200 \times 10^{-10}$  IN/IN LBS

$\Delta_y$  - AZIMUTH DRIVE =  $-150 \times 10^{-10} \times 11.97 = -1796 \times 10^{-10}$  IN/IN LBS  
 GIMBAL =  $-20.4 \times 10^{-10} \times 11.97 = -244 \times 10^{-10}$  "  
 ACTUATOR =  $-100 \times 10^{-10} \times 11.97 = -1197 \times 10^{-10}$  "  
 ARM =  $-100 \times 10^{-10} \times 11.97 = -1197 \times 10^{-10}$  "  
 TORQUE TUBE =  $-3420 \times 10^{-10}$  IN/IN LBS  


---

 TOTAL =  $-7854 \times 10^{-10}$  IN/IN LBS  
 SAY  $-8000 \times 10^{-10}$  IN/IN LBS

2. EFFECT OF  $M_y$

$$\begin{aligned} \Theta_y - \text{AZIMUTH DRIVE} &= 300 \times 10^{-10} \text{ RAD/IN LBS} \\ \text{GIMBAL} &= 72 \times 10^{-10} \text{ RAD/IN LBS} \\ \text{TORQUE TUBE} &= \frac{(273+78) \times 10^{-8}}{(59)^2} = 10 \times 10^{-10} \text{ RAD/IN LBS} \\ \text{TOTAL} &= 382 \times 10^{-10} \text{ SAY } 390 \times 10^{-10} \text{ RAD/IN LBS} \end{aligned}$$

$$\begin{aligned} \Delta x - \text{AZIMUTH DRIVE} &= +300 \times 10^{-10} \times 11.97 = 3591 \times 10^{-10} \text{ IN/IN LBS} \\ \text{GIMBAL} &= +72 \times 10^{-10} \times 11.97 = 862 \times 10^{-10} \text{ " } \\ \text{TORQUE TUBE} &= 0 \\ \text{TOTAL} &= 4453 \times 10^{-10} \text{ IN/IN LBS} \\ &\text{SAY } 4500 \times 10^{-10} \text{ IN/IN LBS} \end{aligned}$$

3. EFFECT OF  $M_z$

$$\begin{aligned} \Theta_z - \text{AZIMUTH DRIVE} &= 150 \times 10^{-10} \text{ RAD/IN LBS} \\ \text{GIMBAL} &= 45.7 \times 10^{-10} \text{ RAD/IN LBS} \\ \text{TORQUE TUBE} &= \frac{(858+12) \times 10^{-8}}{(59)^2} \quad \text{NOTE: } M_z \text{ RESULTS IN } F_y \text{ AT EACH FLANGE.} \\ &= 25 \times 10^{-10} \text{ RAD/IN LBS.} \\ \text{TOTAL} &= 220.7 \times 10^{-10} \text{ RAD/IN LBS} \\ &\text{SAY } 220 \times 10^{-10} \text{ RAD/IN LBS} \end{aligned}$$

$$\begin{aligned} \Delta x - \text{AZIMUTH DRIVE} &= 150 \times 10^{-10} \times 11.75 = 1763 \times 10^{-10} \text{ IN/IN LBS} \\ \text{GIMBAL} &= 523 \times 10^{-10} \text{ IN/IN LBS} \\ \text{TORQUE TUBE} &= 0 \end{aligned}$$

TOTAL =  $2286 \times 10^{-10}$  IN/IN LBS  
INCLUDING DEFLECTION AT THE TOP OF AZIMUTH DRIVE. ASSUME  $2400 \times 10^{-10}$  IN/IN LBS

4. EFFECT OF  $F_x$  :

BECAUSE OF ELEVATION BEARING AXIAL CLEARANCE, ASSUME THAT ALL THIS AXIAL LOAD IS TAKEN AT BEARING # 1.

i.e.  $F_{ix} = 1$

$\Theta_z$  - AZIMUTH DRIVE =  $+150 \times 10^{-10} \times 11.75 = +1763 \times 10^{-10}$  RAD/LBS

GIMBAL =  $+523 \times 10^{-10}$  RAD/LBS

TORQUE TUBE =  $29 \times 10^{-10}$  RAD/LBS

TOTAL =  $2315 \times 10^{-10}$  RAD/LBS

INCLUDING ROTATION AT THE TOP OF AZIMUTH DRIVE DUE TO LOAD, ASSUME  $2430 \times 10^{-10}$  RAD/LBS

$\Theta_y$  - AZIMUTH DRIVE =  $+300 \times 10^{-10} \times 11.97 = 3591 \times 10^{-10}$  RAD/LBS

GIMBAL =  $72 \times 10^{-10} \times 11.97 = 862 \times 10^{-10}$  RAD/LBS

TORQUE TUBE =  $293 \times 10^{-10}$  RAD/LBS

TOTAL =  $4746 \times 10^{-10}$  RAD/LBS

SAY  $4800 \times 10^{-10}$  RAD/LBS

$\Delta_x$  - AZIMUTH DRIVE =  $150 \times 10^{-10} (11.75)^2 + 300 \times 10^{-10} (11.97)^2$

=  $637 \times 10^{-8}$  IN/LBS

GIMBAL =  $217 \times 10^{-8} + 72 \times 10^{-10} (11.97)^2$

=  $320 \times 10^{-8}$  IN/LBS

TORQUE TUBE =  $2940 \times 10^{-8}$  IN/LBS

TOTAL =  $3897 \times 10^{-8}$  IN/LBS

INCLUDING, DEFLECTION AT THE TOP OF AZIMUTH DRIVE

ASSUME  $\Delta_x = 4000 \times 10^{-8}$  IN/LBS



5. EFFECT OF  $F_y$  :

$\Theta_x$  - BY RECIPROCALITY,  $\Theta_x = -8000 \times 10^{-10}$  RAD/LBS

$\Delta_y$  - AZIMUTH DRIVE =  $150 \times 10^{-10} \times (11.97)^2 = 215 \times 10^{-8}$  IN/LBS

GIMBAL ACTUATOR =  $22 \times 10^{-8} + 20.4 \times 10^{-10} \times (11.97)^2 = 51 \times 10^{-8}$  IN/LBS

TORQUE TUBE =  $100 \times 10^{-10} \times (11.97)^2 = 143 \times 10^{-8}$  IN/LBS

ARM =  $100 \times 10^{-10} \times (11.97)^2 = 143 \times 10^{-8}$  IN/LBS

TOTAL =  $975 \times 10^{-8}$  IN/LBS

SAY  $1000 \times 10^{-8}$  IN/LBS

$\Delta_z$  - AZIMUTH DRIVE =  $150 \times 10^{-10} \times 11.75 \times 11.97 = 211 \times 10^{-8}$  IN/LBS

GIMBAL =  $4.2 \times 10^{-8} \times 11.97 = 50 \times 10^{-8}$  IN/LBS

TORQUE TUBE =  $-18 \times 10^{-8}$  IN/LBS

TOTAL =  $243 \times 10^{-8}$  IN/LBS

SAY  $250 \times 10^{-8}$  IN/LBS

6. EFFECT OF  $F_z$  :

$\Theta_x = -2200 \times 10^{-10}$  RAD/LBS BY RECIPROCALITY

$\Delta_y = 250 \times 10^{-8}$  IN/LBS BY RECIPROCALITY

$\Delta_z$  - AZIMUTH DRIVE =  $150 \times 10^{-10} \times (11.75)^2 = 207 \times 10^{-8}$  IN/LBS

GIMBAL =  $197 \times 10^{-8}$  IN/LBS

TORQUE TUBE =  $97 \times 10^{-8}$  IN/LBS

TOTAL =  $301 \times 10^{-8}$  IN/LBS

SAY  $300 \times 10^{-8}$  IN/LBS

BY \_\_\_\_\_ DATE \_\_\_\_\_ SUBJECT \_\_\_\_\_  
 CHKD. BY \_\_\_\_\_ DATE \_\_\_\_\_

SUMMARIZING, WITH MIRROR AT HORIZON (VERTICAL MIRROR)

JOINT LOAD, LBS & IN LBS	$\Delta x$ IN $\times 10^{-8}$	$\Delta y$ IN $\times 10^{-8}$	$\Delta z$ IN $\times 10^{-8}$	$\theta_x$ RAD $\times 10^{-10}$	$\theta_y$ RAD $\times 10^{-10}$	$\theta_z$ RAD $\times 10^{-10}$
$F_x$	4000	-	-	-	4800	2430
$F_y$	-	1000	250	-8000	-	-
$F_z$	-	250	300	-2200	-	-
$M_x$	-	-80	-22	780	-	-
$M_y$	45	-	-	-	390	-
$M_z$	24	-	-	-	-	220

NOTE: X AXIS IS ELEVATION AXIS (HORIZONTAL)  
 Y AXIS IS CROSS ELEVATION AXIS (VERTICAL)  
 Z AXIS IS MIRROR NORMAL AXIS (HORIZONTAL)



REPORT E-10

ACTUATOR SCREW/NUT TEST PROCEDURES

FOR

GIMBAL/ACTUATOR DRIVE ASSEMBLY

FOR

BOEING SECOND GENERATION HELIOSTAT

JUNE 27, 1980

Reference: TM15



Ford Aerospace &  
Communications Corporation

BOEING 2ND GENERATION HELIOSTAT

ACTUATOR SCREW AND NUT TEST PROCEDURE

The test procedure as stated in Revision 0 of this memo will be adhered to with exceptions as follows:

Only one actuator will be run. The nut sets to be tested are those of Delrin, Turcite "A", and Dynalloy in the non-antibacklash configuration only (sets numbered 2, 4, & 5). If it is desired, additional nut sets can be tested subsequently.

Only those measurements appropriate to the non-antibacklash configuration will be made.

TABLE OF CONTENTS

- 1.0 SCOPE OF TEST
- 2.0 TEST CONCEPT/PRE-TEST PREPARATION
- 3.0 PRE-ASSEMBLY MEASUREMENTS
  - 3.1 Torque Required/Each Nut
  - 3.2 Backlash of Each Nut
  - 3.3 Screw Thread Size
- 4.0 ASSEMBLY
  - 4.1 Torque Required/Nut Set
- 5.0 CONDITIONS DURING TEST
  - 5.1 Daily Measurements
  - 5.2 Environmental Simulation
- 6.0 POST TEST MEASUREMENTS
  - 6.1 Measurements Before Cleaning
  - 6.2 Measurements After Air Cleaning
  - 6.3 Measurements After Disassembly and Cleanup
- 7.0 RESULTS

DATA SHEETS A THROUGH E

APPENDIX A 3-WIRE SCREW PITCH MEASUREMENTS

BOEING 2ND GENERATION HELIOSTAT  
ACTUATOR SCREW AND NUT TEST PROCEDURE

## 1.0 SCOPE OF TEST

This document specifies the test procedure for determining the durability of the stainless steel screw/polymeric nut elevation drive proposed for use in the Boeing Engineering & Construction Second Generation Heliostat.

## 2.0 TEST CONCEPT/PRE-TEST PREPARATION

The test's scaling concept is shown in Table 1. The test concept is to test a variety of nut materials (see Table 2) on two stainless steel actuator screws on an accelerated basis to simulate actual service conditions. The anti-backlash sets are included to test the effectiveness of this design to exclude contaminants from the threads. It was decided not to include cleaning brushes on any of the nut test sets. \*

The test fixture (shown in Figure 1) is to be completed in accordance with the following. The test actuators are two Duff-Norton 2-ton traveling nut type each with a length of 65" X 1" diameter. These two actuators are mounted vertically, coupled together, and secured to the test fixture. (Non-vertical positions of the screw are not simulated). The actuators will be driven by an AC motor through a 5:1 speed reducer. Electrical limit switches are to be installed so as to provide redundant control at each end of the stroke. Further, the motor will be current limited so that should the mechanism jam, the locked rotor motor current will cause the fuse to blow (or circuit breaker to trip) before mechanical damage occurs. Alternatively, a torque limiting coupling is to be incorporated, if feasible. The fixture is to be tested to verify this feature prior to the operational portion of the test.

The screws and all parts that contact the screw/nut threads are to be free of oil and cutting fluids. This is to be accomplished by cleaning with a pure solvent. Because of the polymeric nuts, only ethanol, acetone, isopropanol, or methanol are acceptable.

The mating threaded pieces are all to be inspected for pits, burrs, etc and these defects corrected or noted. The nuts that have holes through their sides (allowing access to the threads by particulates) are to have these sealed off taking care so as not to get any sealant into the threaded area. Each nut is to be numbered with nuts of the different sets being labeled "1" through "6" and nuts of the same pair are to be labeled "A" and "B". The screws are to be labeled "I" and "II". These labels are to be applied so as to not affect threaded portions of the parts.

The test is to run round the clock seven days/week except for brief downtimes for measurements or moving the fixture outdoors.

\* See revision note, Page 2.

### 3.0 PRE-ASSEMBLY MEASUREMENTS

Prior to assembly of the nut sets on the screws, the following measurements are to be made:

- Torque required to rotate the nut with respect to the screw for each nut
- The backlash of each nut
- The screw thread size

This data will be recorded on data sheet A. Photograph test assembly and all components.

#### 3.1 Torque Required/Each Nut

Equipment: Measuring Tape  
 $\frac{1}{4}$ " combination wrench  
 Spring scale

- Procedure:
1. Measure distance to nearest 1/16" from center of screw to center of box end of wrench while open end of wrench is engaged on nut.
  2. Using spring balance scale, measure force (to +5%) required to turn nut with respect to the screw.

#### 3.2 Backlash of Each Nut

Equipment: Dial indicator with clamp  
 Measuring tape

- Procedure
1. Place each nut on the same portion of one of the screws where no nut will travel during the test.
  2. Note which thread the nut is on by measuring to the nearest 1/16" a constant distance from the top of the screw.
  3. Clamp on dial indicator to frame or screw.
  4. Measure backlash of each nut to the nearest .001".



### 3.3 Screw Thread Size

Refer to Appendix A and perform by the standard 3-wire method. The best wire size is .129" but .136" will be used to allow wear measurements.

Equipment: 3 steel wires each .136" dia X 1" long min  
2 piece flat barstock approximately 1" square X 1/4" thk.

Measuring tape

Procedure:

1. Measure to the nearest .001" the thickness of each piece of barstock
2. Measure to the nearest .001" size of screw thread used to measure nut backlash in section 3.2
3. Measure to the nearest .001" the screw thread which is in the center of each zone where nut sets will travel.
4. Record also the distance to the nearest 1/16" between each zone center and the top of the appropriate screw.

### 4.0 ASSEMBLY

Assemble the nut sets as specified in Table 2 and Figures 2 & 3. The nut sets are to be installed back-to-back on the shafts and spring loaded to simulate the maximum elevation gravity unbalance load which the actuators will see during operation. The six sets of nut assemblies are positioned on the actuator screws in such a way that each set will travel over one section of the screw without going over the other's travel zone. The screws' material is type 304 stainless steel with a tooth surface finish of approximately 63 RMS. The overall height of each set, the end plate-to-end plate height of each anti-backlash set and the backlash of each non-anti-backlash nut set at its zone center are to be measured and recorded on Data Sheet B. The torque required to turn each set is to be measured as stated below and likewise recorded.

#### 4.1 Torque Required/Nut Set

Equipment: (See Section 3.1)

Procedure: Use wrench on nut on side of set opposite to the the direction of translation. Measure torque by method of section 3.1.

## 5.0 CONDITIONS DURING TEST

## 5.1 Daily measurements

The test is to run continuously except for a brief period each workday in order to perform the following measurements:

- Overall height of each set to the nearest .001".
- Endplate-to-endplate height of each anti-backlash set and the backlash at the zone center of each non-anti-backlash nut set to the nearest .001".
- Screw size in center of each zone by 3-wire method (to the nearest .001", see section 3.3) during first half of test only.

Record the data on Data Sheet C.

## 5.2 Environmental Simulation

The first 1/2 of the test is to be run free of dust or rain except for that present in the ambient conditions. The second half of the test will simulate sandstorms, particulates in strong winds, and rain.

In the actual heliostat, the elevation drive screw is located at a height of more than 10 feet off the ground. At this height particulates in the air are largely dust and very little sand.<sup>1,2</sup> According to the typical meteorological year<sup>3</sup> (TMY) for Albuquerque, the wind is greater than or equal to 10 mph about 1.2% of the time. This wind causes the "ideal particle" to lift. Thus the test rig will have sand and dust delivered to it by a blower or fan once per workday during the second half of the test for a duration of (24 hours)  $\left( \frac{60 \text{ min}}{\text{hr}} \right) (1.2\%) \left( \frac{7 \text{ days}}{5 \text{ days}} \right) = 24.2 \text{ min/workday}$ .

Rain occurs in Albuquerque approximately once per week so that a heavy rain will be simulated by applying water to the fixture on the 16th and 28th day of testing and a light rain on the 22nd.

All simulated contaminants are to be applied while the test is running. Other environmental effects are not simulated.

Equipment: Several buckets of mixed fine dust and sand  
 Supply of water in can or pail (water shall be rainwater or tapwater and NOT distilled or de-ionized)  
 Spray bottle  
 Blower (capable of several hundred fpm of air)  
 Shallow pan

- Procedure:
1. At appropriate times, deliver the dust and sand onto the screws and nuts by blowing the particles from a shallow pan approximately equally over all moving threaded parts from a distance of about 2 feet. The blowing is to be manually controlled so as to lift and deliver to the fixture only a few % sand but a lot of dust.
  2. At the specified times, spray water from a spray bottle onto the fixture from a couple of feet away to simulate light rain. Do this much closer up and also sprinkle water on the fixture to simulate heavy rain. Dust and sand are to be delivered during the heavy rain simulation as per step 1. The screws and nuts shall be completely wetted each time.
  3. Record times and durations of particulate/ water applications on data sheet D.

## 6.0 POST TEST MEASUREMENTS

The following measurements are to be made as soon as possible after stopping the test. Record data on Data Sheet E. Take photographs (including magnified) as required to document changes from start of test condition.

### 6.1 Measurements Before Cleaning

This measurement is to be made without modification to the fixture after shutting down the test. The torque required to turn each set of nuts is to be measured as in section 4.1. Note the condition of all portions of the entire test fixture by a visual inspection.

### 6.2 Measurements After Air Cleaning

The fixture shall be thoroughly cleaned by blowing compressed air on it to remove any clinging particles. Water may be used for cleaning if the fixture is dried. Measure the height of each nut set and the end-plate-to-endplate height or set backlash at zone center where appropriate.

### 6.3 Measurements After Disassembly and Cleanup

The nut sets are to be removed from the screws and all parts thoroughly cleaned using air or water. Wet parts are to be dried before measurement. Again visually inspect all parts.

Repeat the measurements of section 3.

## 7.0 RESULTS

Baseline (no contaminants) wear is taken to be measured by the height of each nut set and the backlash or endplate-to-endplate height. This wear shall be considered three times the value the values after 15 days of testing. Actual wear is three times that occurring during the last half of the test. Analysis procedures will be determined based upon the data.

### References:

1. Encyclopedia Britanica "Wind Action"
2. Private conversation with Roscoe Champion of Sandia, Albuquerque.
3. Typical Meteorological Year for Albuquerque, N.M. as compiled by the National Climatic Center.
4. Machinery's Handbook, 19th edition.

TABLE 1

## SUMMARY OF ACTUAL AND TEST DATA/PARAMETERS

ITEM DESCRIPTION	ACTUAL	TEST
Minimum Life	30 years	47* days
Lubrication of Screws and Nuts	None	None
Actuator Capacity (tons)	5	2
Actuator Ratio	240:1	6:1
Actuator Input Speed (RPM)	1750	345
Actuator Screw Thread Type	ACME	ACME
Outside Diameter (inches)	1.500	1.000
Pitch Diameter (inches)	1.375	0.875
Pitch (inches/thread)	1/4	1/4
Nut Length (approximate) (inches)	3.2	1.5
(threads)	12.8	6.0
Operating Load on Screws (tons)	2.5 (gravity)	0.75 (spring)
Tooth Pressure (psi)	723	723
Total Circumferential Travel of Nut Relative to Screw at Pitch Line (inches)	10,550,000	6,745,000
Total Nut Linear Travel (inches)	613,200	613,400
Average Stroke (inches)	28	8
Number of Cycles/Day	1	1278**
Operating Time/Cycle (seconds)	36,000 (tracking) 900 (slewing)	68
Total Number of Cycles	10,950	38,340
Total Operating Time (millions of seconds)	394 (tracking) 986 (slewing)	2.592

\* Actual test will only be run 30 days.

\*\* Not counting daily down time for measurements.

Reference: Antenna Engineering Technical Memo 5, Revision 1  
Second Generation Heliostat Project  
"Heliostat Actuator Screw and Nut Test Plan"

TABLE 2

## NUT SETS DESCRIPTION

<u>MATERIAL</u>	<u>TYPE</u>	<u>NUMBER</u>
Turcite 'A' (Acetal-Teflon)	Anti-backlash	1*
Turcite 'A' (Acetal-Teflon)	Non Anti-backlash	2
Bronze (WCF 175)	Non Anti-backlash	3*
Bronze (Dynalloy)	Non Anti-backlash	4
Delrin AF (Acetal-Teflon)	Non Anti-backlash	5
Bronze (SAE-660)	Anti-Backlash	6*

\* Deleted, see revision note, page 2

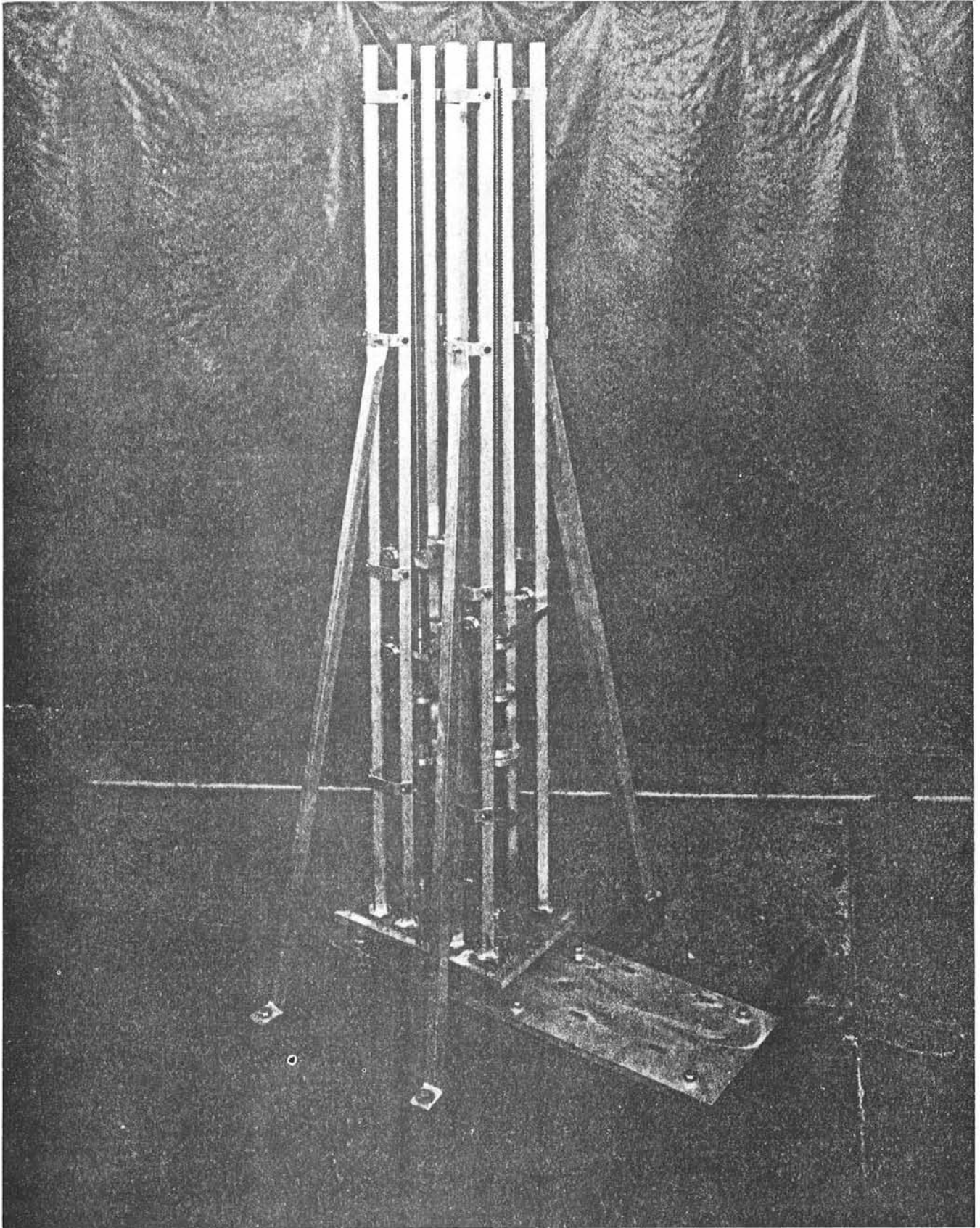


Figure 1

Figure 2  
Antibacklash Assembly

Note: All dimensions are in inches

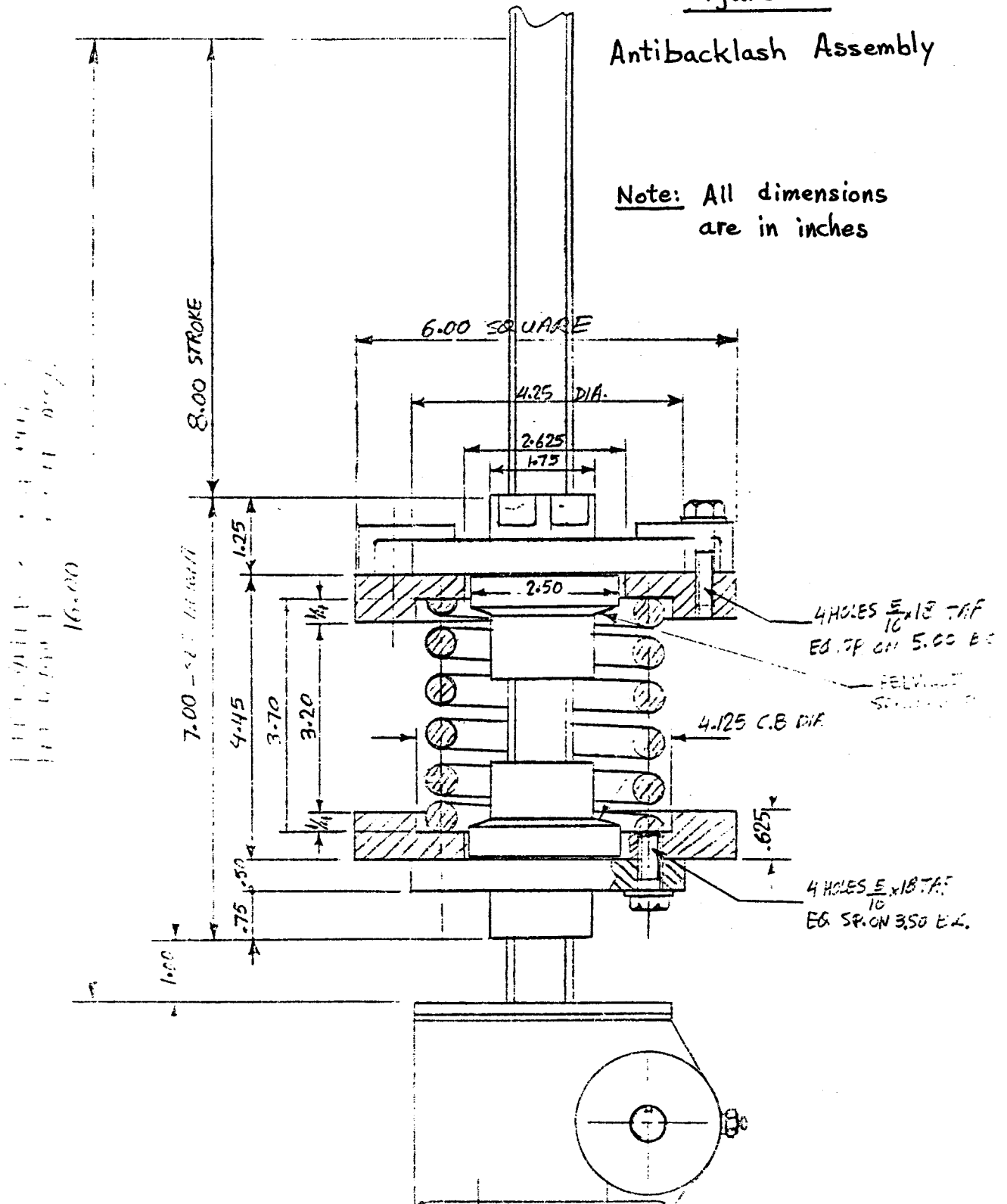
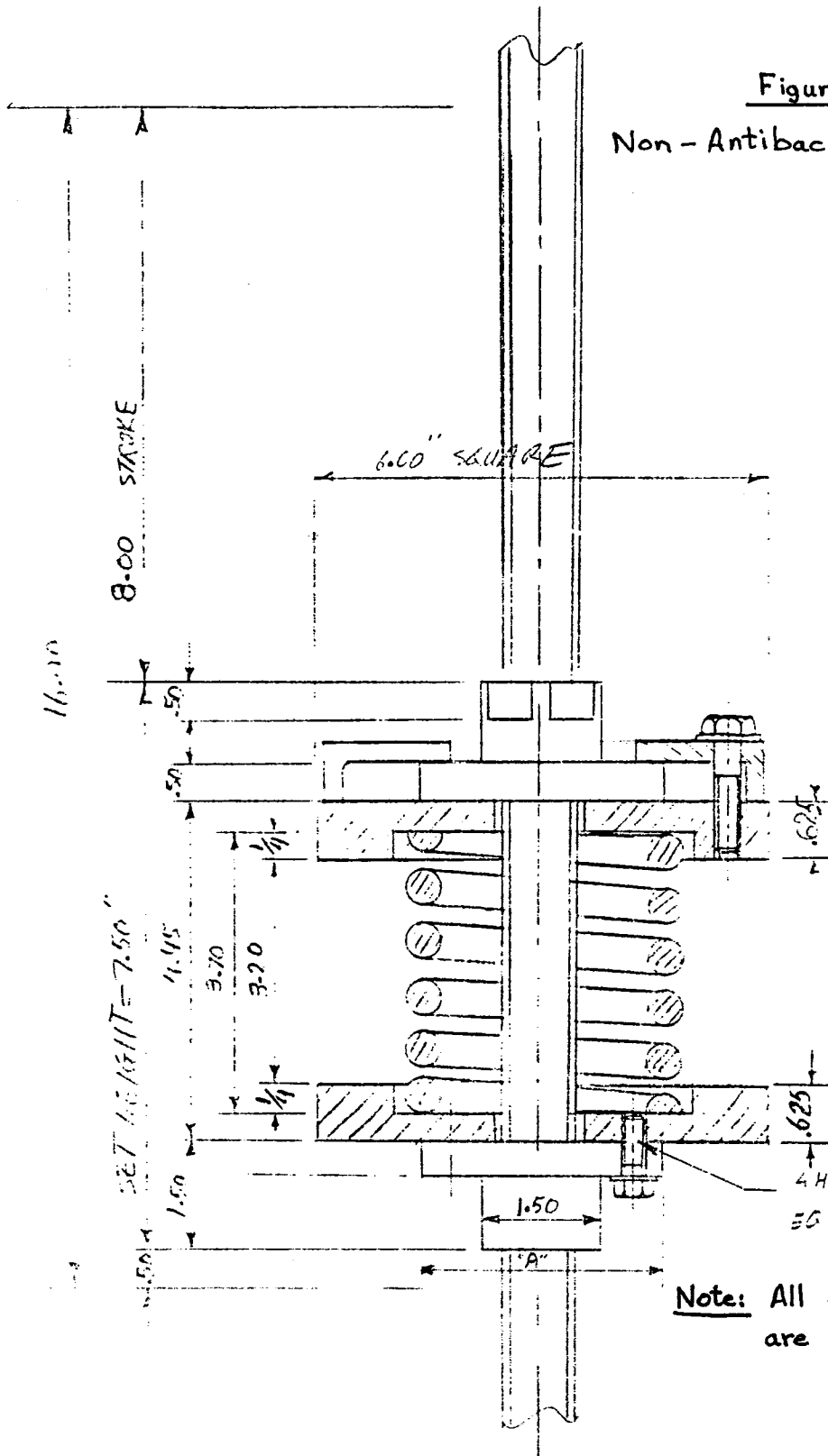




Figure 3  
Non - Ant backlash Assembly

LEFT PORTION FRONT. I A=3.25, B=2 3/4"  
RIGHT PORTION FRONT. I A=3.00, B=2 1/4"



Note: All dimensions are in inches

DATA SHEET A

Nut  $\phi$  to scale hook distance (inches) = \_\_\_\_\_

NUT #	letter	FORCE to turn (oz.)	BACKLASH (inches)		ZONE CENTER (in. from top)	SCREW size (in.)
			final	initial		
1	A					
1	B					
2	A					
2	B					
3	A					
3	B					
4	A					
4	B					
5	A					
5	B					
6	A					
6	B					
Screw # _____ Where nuts backlash measured						

Thickness of each plate in 3-wire method = \_\_\_\_\_ (inches)  
 Wire diameters \_\_\_\_\_, \_\_\_\_\_, \_\_\_\_\_; \_\_\_\_\_

Date: \_\_\_\_\_ Time: \_\_\_\_\_

Data Taken By: \_\_\_\_\_

Visual inspection comments: \_\_\_\_\_

\_\_\_\_\_

Photographs taken: \_\_\_\_\_

\_\_\_\_\_

## DATA SHEET B

SET #	OVERALL HEIGHT (inches)	ENDPLATE HEIGHT (inches) / SET * BACKLASH (inches)	FORCE /SET (lb.)
1		final - initial	
2 *			
3 *			
4 *			
5 *			
6		final - initial	

Nut  $\phi$  to scale hook distance = \_\_\_\_\_ (inches)

Date: \_\_\_\_\_ Time: \_\_\_\_\_

Data taken by: \_\_\_\_\_

Visual inspection comments: \_\_\_\_\_

\_\_\_\_\_

\_\_\_\_\_

\_\_\_\_\_

DATA SHEET C

NUT SET #	OVERALL HEIGHT (inches)	ENDPLATE / HEIGHT (inches)	SET * BACKLASH	SCREW @ Zone Center (inches)
1		final - initial		
2				
3				
4				
5				
6		final - initial		

Date: \_\_\_\_\_ Time: \_\_\_\_\_

Data taken by: \_\_\_\_\_

Visual inspection comments: \_\_\_\_\_  
 \_\_\_\_\_  
 \_\_\_\_\_  
 \_\_\_\_\_  
 \_\_\_\_\_  
 \_\_\_\_\_  
 \_\_\_\_\_

Thickness of each plate in 3-wire method = \_\_\_\_\_ (inches)  
 Wire diameters \_\_\_\_\_, \_\_\_\_\_, \_\_\_\_\_; \_\_\_\_\_



Date: \_\_\_\_\_

Time: \_\_\_\_\_

Data taken by: \_\_\_\_\_

NUT SET # letter	FORCE/set (lb.)	OVERALL HEIGHT (inches)	ENDPLATE HEIGHT / SET BACKLASH (inches)	FORCE/nut (oz.)	BACKLASH/NUT (inches) final - initial	SCREW @ Zone Center (inches)
1 A						
B						
2 A						
B						
3 A						
B						
4 A						
B						
5 A						
B						
6 A						
B						

Nut  $\phi$  to scale hook distance = \_\_\_\_\_ (inches)

Thickness of each plate in 3-wire method \_\_\_\_\_ & \_\_\_\_\_ (inches)

Wire diameters \_\_\_\_\_, \_\_\_\_\_ & \_\_\_\_\_ (inches)

(Also note photographs taken)

(Pre-Cleaning) Visual inspection comments: \_\_\_\_\_

(Post Air Cleaning) comments: \_\_\_\_\_

(Post Disassembly) comments: \_\_\_\_\_

DATA SHEET

E

APPENDIX A

3-WIRE SCREW PITCH MEASUREMENTS

MEASURING SCREW THREADS

1381

**Why Small Thread Angle Affects Accuracy of Three-wire Measurement.** — In measuring or checking Acme threads, or any others having a comparatively small thread angle *A*, it is particularly important to use a formula which compensates for the lead angle, if not entirely, for the effect of the lead angle, especially in all gage and precision work. The effect of the lead angle on the position of the wires and upon the resulting measurement *M* is much greater in the case of a 29-degree thread than in the case of a higher thread angle such, for example, as a 60-degree thread. This is because the cotangent of the thread angle increases as this angle becomes smaller; consequently, the reduction in the width of the thread groove in the normal plane due to the lead angle causes a wire of given size to rest higher in the groove of a thread having a small thread angle *A* (like a 29-degree thread) than in the groove of a thread with a larger angle (like a 60-degree American Standard).

**Acme Threads:** Three-wire measurements of high accuracy require the use of Formula 4. For most cases, however, Formula 2 or 3 gives satisfactory results. The table on page 1386 lists suitable wire sizes for use in Formulas 2 and 4.

**Dimensions Over Wires of Given Diameter for Checking Screw Threads of American National form (U. S. Standard) and the V-form**

Diam. of Screw	No. of Threads per Inch	Diam. of Wire used	Dimension over Wires, V-Thread	Dimension over Wires, U. S. Thread	Diam. of Screw	No. of Threads per Inch	Diam. of Wire used	Dimension over Wires, V-Thread	Dimension over Wires, U. S. Thread
1/4	18	0.035	0.2588	0.2708	3/8	8	0.090	0.9285	0.9556
1/4	20	0.035	0.2584	0.2792	3/8	9	0.090	0.9525	0.9766
1/4	22	0.035	0.2763	0.2861	3/8	10	0.090	0.9718	0.9935
1/4	24	0.035	0.2828	0.2919	15/16	8	0.090	0.9910	1.0181
5/16	18	0.035	0.3213	0.3333	15/16	9	0.090	1.0150	1.0391
5/16	20	0.035	0.3309	0.3417	1	8	0.090	1.0335	1.0806
5/16	22	0.035	0.3388	0.3486	1	9	0.090	1.0775	1.1016
5/16	24	0.035	0.3453	0.3544	1 1/8	7	0.090	1.1476	1.1785
3/4	16	0.040	0.3867	0.4003	1 1/8	7	0.090	1.2726	1.3035
3/4	18	0.040	0.3985	0.4108	1 1/8	6	0.150	1.5363	1.5724
3/4	20	0.040	0.4084	0.4192	1 1/8	6	0.150	1.6613	1.6974
7/8	14	0.050	0.4638	0.4793	1 1/2	5 1/2	0.150	1.7601	1.7995
7/8	16	0.050	0.4792	0.4928	1 1/2	5	0.150	1.8536	1.8969
1 1/8	12	0.050	0.5057	0.5237	1 1/2	5	0.150	1.9785	2.0219
1 1/8	13	0.050	0.5168	0.5334	2	4 1/2	0.150	2.0651	2.1132
1 1/8	14	0.050	0.5263	0.5418	2 1/4	4 1/2	0.150	2.3151	2.3632
1 1/8	12	0.050	0.5682	0.5862	2 1/4	4	0.150	2.5170	2.5711
1 1/8	14	0.050	0.5888	0.6043	2 1/4	4	0.150	2.7570	2.8211
1 1/8	10	0.070	0.6618	0.6835	3	3 1/2	0.200	3.1051	3.1670
1 1/8	11	0.070	0.6775	0.6972	3 1/4	3 1/2	0.200	3.3551	3.4170
1 1/8	12	0.070	0.6907	0.7087	3 1/2	3 1/4	0.250	3.7171	3.7837
1 1/8	10	0.070	0.7243	0.7460	3 3/4	3	0.250	3.9226	3.9948
1 1/8	11	0.070	0.7400	0.7597	4	3	0.250	4.1726	4.2448
1 1/8	10	0.070	0.7868	0.8085	4 1/4	2 3/4	0.250	4.3975	4.4729
1 1/8	11	0.070	0.8025	0.8222	4 1/2	2 3/4	0.250	4.6202	4.6989
1 1/8	12	0.070	0.8157	0.8337	4 3/4	2 3/4	0.250	4.8402	4.9227
1 1/8	9	0.070	0.8300	0.8541	5	2 1/2	0.250	5.0572	5.1438
1 1/8	10	0.070	0.8493	0.8710	.....	.....	.....	.....	.....



Table for Measuring Whitworth Standard Threads by the Three-wire Method

Diam. of Thread	No. of Threads per Inch	Diam. of Wire used	Diam. Measured over Wires	Diam. of Thread	No. of Threads per Inch	Diam. of Wire used	Diam. Measured over Wires
1/8	40	0.018	0.1420	2 1/4	4	0.150	2.3247
3/16	24	0.030	0.2158	2 3/8	4	0.150	2.4497
1/4	20	0.035	0.2808	2 1/2	4	0.150	2.5747
5/16	18	0.040	0.3502	2 3/4	4	0.150	2.6997
3/8	16	0.040	0.4015	2 3/4	3 1/2	0.200	2.9257
7/16	14	0.050	0.4815	2 3/4	3 1/2	0.200	3.0507
1/2	12	0.050	0.5249	3	3 1/2	0.200	3.1757
5/8	12	0.050	0.5874	3 1/4	3 1/2	0.200	3.3007
3/4	11	0.070	0.7011	3 1/4	3 1/2	0.200	3.3905
7/8	11	0.070	0.7636	3 3/4	3 1/2	0.200	3.5155
1 1/16	10	0.070	0.8115	3 3/4	3 1/2	0.200	3.6405
1 1/8	10	0.070	0.8740	3 3/4	3 1/2	0.200	3.7655
1 1/4	9	0.070	0.9187	3 3/4	3	0.200	3.8495
1 1/2	9	0.070	0.9812	3 3/4	3	0.200	3.9745
1 3/8	8	0.090	1.0848	4	3	0.200	4.0995
1 3/4	8	0.090	1.1473	4 1/8	3	0.200	4.2245
1 7/8	7	0.090	1.1812	4 1/4	2 3/8	0.250	4.4846
1 5/8	7	0.090	1.2437	4 3/8	2 3/8	0.250	4.6096
1 5/4	7	0.090	1.3062	4 1/2	2 3/8	0.250	4.7346
1 7/4	7	0.090	1.3687	4 5/8	2 3/8	0.250	4.8596
1 3/2	6	0.120	1.4881	4 3/4	2 3/4	0.250	4.9593
1 5/2	6	0.120	1.5506	4 3/4	2 3/4	0.250	5.0843
1 7/2	6	0.120	1.6131	5	2 3/4	0.250	5.2093
1 9/2	6	0.120	1.6756	5 1/8	2 3/4	0.250	5.3343
1 5/2	5	0.120	1.6847	5 1/4	2 3/4	0.250	5.4316
1 7/2	5	0.120	1.7472	5 3/8	2 3/4	0.250	5.5566
1 9/2	5	0.120	1.8097	5 1/2	2 3/4	0.250	5.6816
1 3/2	5	0.120	1.8722	5 3/4	2 3/4	0.250	5.8066
1 7/2	4 1/2	0.150	1.9942	5 3/4	2 1/2	0.250	5.9011
1 9/2	4 1/2	0.150	2.0567	5 7/8	2 1/2	0.250	6.0261
2	4 1/2	0.150	2.1192	6	2 1/2	0.250	6.1511
2 1/8	4 1/2	0.150	2.2442	.....	.....	.....	.....

**Buckingham Simplified Formula which Includes Effect of Lead Angle.** — The Formula 3 which follows gives very accurate results for the lower lead angles in determining measurement *M*. However, if extreme accuracy is essential, it may be advisable to use the involute helicoid formulas as explained later.

$$M = E + W (1 + \sin A_n) \text{ where } W = \frac{T \times \cos B}{\cos A_n} \quad (3 \text{ and } 3a)$$

Theoretically correct equations for determining measurement *M* are complex and cumbersome to apply. Formula 3 combines simplicity with a degree of accuracy which meets all but the most exacting requirements, particularly for lead angles below 8 or 10 degrees and the higher thread angles. However, the wire diameter used in Formula (3) must conform to that obtained by Formula (3a) to permit a direct solution or one not involving indeterminate equations and successive trials.

**Application of Buckingham Formula:** In the application of Formula (3) to screw threads or to worms, there are two general cases to be considered.

**Case 1:** The screw thread or worm is to be milled with a cutter having an included angle equal to the nominal or standard thread angle which is assumed to be the angle in the axial plane. For example, a 60 degree cutter is to be used for milling a thread. In this case, the thread angle in the plane of the axis will exceed 60 degrees by an amount increasing with the lead angle. This variation from the standard angle may be of little or no practical importance if the lead angle is small or if the mating nut (or teeth in the case of worm gearing) is formed to suit the thread as milled.

**Case 2:** The screw thread or worm is to be milled with a cutter reduced to whatever normal angle is equivalent to the standard thread angle in the axial plane. For example, a 29-degree Acme thread is to be milled with a cutter having some angle smaller than 29 degrees (the reduction increasing with the lead angle) to make the thread angle standard in the plane of the axis. Theoretically, the milling cutter angle should always be corrected to suit the normal angle; but if the lead angle is small, such correction may be unnecessary.

If the thread is cut in a lathe to the standard angle as measured in the axial plane, Case 2 applies in determining the pin size *W* and the over-all measurement *M*.

In solving all problems under Case 1, the angle *A<sub>n</sub>* used in Formulas (3) and (3a) equals one-half the included angle of the milling cutter.

When Case 2 applies, the angle *A<sub>n</sub>* for milled threads also equals one-half the included angle of the cutter, but the cutter angle is reduced and is determined as follows:

$$\tan A_n = \tan A \times \cos B$$

The included angle of the cutter or the normal included angle of the thread groove = 2 *A<sub>n</sub>*. Example: 1 and 2 which follow illustrate Cases 1 and 2.

**Example 1 (Case 1):** The example which follows illustrates the case of an Acme screw thread which is milled with a cutter having an included angle of 29 degrees; consequently, the angle of the thread is over 29 degrees in the axial section.

The outside or major diameter is 3 inches; the pitch, 1/8 inch; the lead, 1 inch; the number of threads or "starts," 2. Find pin size *W* and measurement *M*.

Pitch diameter *E* = 2.75; *T* = 0.25; *L* = 1.0; *A<sub>n</sub>* = 14.50°; tan *A<sub>n</sub>* = 0.258618; sin *A<sub>n</sub>* = 0.25038; cos *A<sub>n</sub>* = 0.968148.

$$\tan B = \frac{1.0}{3.1416 \times 2.75} = 0.115749; B = 6.6025^\circ$$

$$W = \frac{0.25 \times 0.993368}{0.968148} = 0.25651 \text{ inch}$$

$$M = 2.75 + 0.25651 \times (1 + 0.25038) = 3.0707 \text{ inches.}$$

**Note:** This value of *M* is only 0.0001 inch larger than that obtained by using the very accurate involute helicoid formula (4) referred to on the following page.

**Example 2 (Case 2):** A triple-threaded worm has a pitch diameter of 2.481 inches; pitch of 1.5 inches; lead of 4.5 inches; lead angle of 30 degrees and nominal thread angle of 60 degrees in axial plane. Milling cutter angle is to be reduced. *T* = 0.75 inch; cos *B* = 0.866025; tan *A* = 0.57735. Again use Formula (3) to see if it is applicable in this case.

Tan *A<sub>n</sub>* = tan *A* × cos *B* = 0.57735 × 0.866025 = 0.5000; hence *A<sub>n</sub>* = 26.565° making the included cutter angle 53.13°. Cos *A<sub>n</sub>* = 0.89443; sin *A<sub>n</sub>* = 0.44721.

$$W = \frac{0.75 \times 0.866025}{0.89443} = 0.72618 \text{ inch.}$$

$$M = 2.481 + 0.72618 \times (1 + 0.44721) = 3.532 \text{ inches.}$$

**Note:** If the value of measurement *M* is determined by using the following

Formula (4) it will be found that  $M = 3.5151$  inches; hence the error equals  $3.532 - 3.515 = 0.017$  inch approximately, which indicates that Formula (3) is not accurate enough in this case. The application of this simpler Formula (3) will depend upon the lead angle and thread angle (as previously explained) and also upon the class of work.

**Buckingham Exact Involute Helicoid Formula Applied to Screw Threads.** — When extreme accuracy is required in finding measurement  $M$  for obtaining a given pitch diameter, the equations which follow, although somewhat cumbersome to apply, have the merit of providing a direct and very accurate solution; consequently, they are preferable to the indeterminate equations and successive trial solutions heretofore employed when extreme precision is required. These equations are exact for involute helical gears and, consequently, give theoretically correct results when applied to a screw thread of the involute helicoidal form; they also give very close approximations for threads having intermediate profiles.

**Helical Gear Equation Applied to Screw Thread Measurement:** In applying the helical gear equations to a screw thread, use either the axial or normal thread angle and the lead angle of the helix. In order to keep the solution on a practical basis, either thread angle  $A$  or  $A_n$ , as the case may be, is assumed to equal the cutter angle of a milled thread. Actually, the profile of a milled thread will have some curvature in both axial and normal sections; hence angles  $A$  and  $A_n$  represent the angular approximations of these slightly curved profiles. The equations which follow give the values needed to solve the screw thread problem as a helical gear problem.

$$M = \frac{2 R_b}{\cos G} + W \quad (4)$$

$$\tan F = \frac{\tan A}{\tan B} = \frac{\tan A_n}{\sin B}; \quad R_b = \frac{E}{2} \cos F \quad (4a \text{ and } 4b)$$

$$T_a = \frac{T}{\tan B}; \quad \tan H_b = \cos F \tan H \quad (4c \text{ and } 4d)$$

$$\text{inv } G = \frac{T_a}{E} + \text{inv } F + \frac{W}{2 R_b \cos H_b} - \frac{\pi}{S} \quad (4e)$$

A table of involute functions is required (see Handbook pages 270 to 275 or Manual of Gear Design, Section 1, pages 100 to 129).

**Example 3:** To illustrate the application of Formula (4) and the supplementary formulas, assume that the number of starts  $S = 6$ ; pitch diameter  $E = 0.6250$ ; normal thread angle  $A_n = 20^\circ$ ; lead of thread  $L = 0.864$  inch;  $T = 0.072$ ;  $W = 0.07013$  inch.

$$\tan B = \frac{L}{\pi E} = \frac{0.864}{1.9635} = 0.44003; \quad B = 23.751^\circ$$

$$\text{Helix angle } H = 90^\circ - 23.751^\circ = 66.249^\circ$$

$$\tan F = \frac{\tan A_n}{\sin B} = \frac{0.36397}{0.40276} = 0.90369; \quad F = 42.104^\circ$$

$$R_b = \frac{E}{2} \cos F = \frac{0.6250}{2} \times 0.74193 = 0.23185$$

$$T_a = \frac{T}{\tan B} = \frac{0.072}{0.44003} = 0.16362$$

$$\tan H_b = \cos F \tan H = 0.74193 \times 2.27257 = 1.68609; \quad H_b = 59.328^\circ$$

The involute function of  $G$  is found next by Formula (4e).

$$\text{inv } G = \frac{0.16362}{0.625} + 0.16881 + \frac{0.07013}{2 \times 0.23185 \times 0.51012} - \frac{3.1416}{6} = 0.20357$$

A table of involute functions shows that  $41.350^\circ$  is the angular equivalent of 0.20357; hence  $G = 41.350^\circ$ .

$$M = \frac{2 R_b}{\cos G} + W = \frac{2 \times 0.23185}{0.71508} + 0.07013 = 0.71859 \text{ inch}$$

**Accuracy of Formulas (3) and (4) Compared.** — With the involute helicoid Formula (4) any wire size which makes contact with the flanks of the thread may be used; however, in the preceding example, the wire diameter  $W$  was obtained by Formula (3a) in order to compare Formula (4) with (3). If Example (3) is solved by Formula (3),  $M = 0.71912$ ; hence the difference between the values of  $M$  obtained with Formulas (3) and (4) equals  $0.71912 - 0.71859 = 0.00053$  inch. The included thread angle in this case is 40 degrees. If Formulas (3) and (4) are applied to a 29-degree thread, the difference in measurements  $M$  or the error resulting from the use of Formula (3) will be larger. For example, in case of an Acme thread having a lead angle of about 34 degrees, the difference in values of  $M$  obtained by the two formulas equals 0.0008 inch.

**One-Wire Method Applied to Acme Threads.** — A single wire may be used to check the size of an Acme thread. If a wire with a diameter equal to  $0.48725 \times$  the pitch is placed in the thread groove of an Acme thread, the wire will be flush with the top of the thread, provided the outside diameter and pitch diameter are of basic size.

If a General Purpose Acme thread is being checked, with allowances and tolerances as provided in the American Standard ASA B1.5, the top of the wire should be below the basic outside diameter by an amount equal to one-half the pitch diameter allowance given in Table 4 on page 1323. The top of the wire may be below this position by an additional amount up to one-half the pitch diameter tolerance given in Table 5 on page 1324.

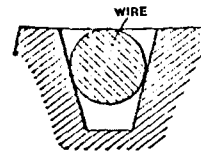
Since this method does not take the effect of lead angle into account, its use for threads of appreciable lead angle is not recommended. The effect of lead angle is to cause the wire to ride higher in the thread groove so that when the wire is flush with the thread top the thread is actually thinner than intended.

**Checking Thickness of Acme Screw Threads.** — In some instances it may be preferable to check the thread thickness instead of the pitch diameter, especially if there is a thread thickness tolerance.

A direct method, applicable to the larger pitches, is to use a vernier gear-tooth caliper for measuring the thickness in the normal plane of the thread. This measurement, for an American Standard General Purpose Acme thread, should be made at a distance below the basic outside diameter equal to  $p/4$ . The thickness at this basic pitch-line depth and in the axial plane should be  $p/2 - 0.259 \times$  the pitch diameter allowance from Table 4 on page 1323 with a tolerance of minus  $0.259 \times$  the pitch diameter tolerance from Table 5 on page 1324. The thickness in the normal plane or plane of measurement is equal to the thickness in the axial plane multiplied by the cosine of the helix angle. The helix angle may be determined from the formula:

$$\text{tangent of helix angle} = \text{lead of thread} \div 3.1416 \times \text{pitch diameter}$$

**Three-Wire Method for Checking Thickness of Acme Threads.** — The application of the 3 wire method of checking the thickness of an Acme screw thread



Wire Sizes for Three-Wire Measurement of Acme Threads

Threads per Inch	Best Size	Max.	Min.	Threads per Inch	Best Size	Max.	Min.
1	0.51645	0.65001	0.48726	5	0.10329	0.13000	0.09745
1½	0.38734	0.48751	0.36545	6	0.08608	0.10834	0.08121
2	0.34430	0.43331	0.32481	8	0.06156	0.08125	0.06091
3	0.25822	0.32501	0.24363	10	0.05164	0.06500	0.04873
4	0.20658	0.26001	0.19491	12	0.04304	0.05417	0.04061
5	0.17215	0.21667	0.16242	14	0.03689	0.04643	0.03480
6	0.12911	0.16250	0.12182	16	0.03228	0.04063	0.03045

Wire sizes are based upon zero helix angle. Best size = 0.51645 × pitch; maximum size = 0.65001 × pitch; minimum size = 0.48726 × pitch.

is included in Report of the National Screw Thread Commission. In applying the 3-wire method for checking thread thickness, the procedure is the same as in checking pitch diameter although a different formula is required. Assume that  $D$  = basic major diameter of screw;  $M$  = measurement over wires;  $W$  = diameter of wires;  $S$  = tangent of helix angle at pitch line;  $P$  = pitch;  $T$  = thread thickness at depth equal to 0.25 $P$ .

$$T = 1.12931 \times P + 0.25862 \times (M - D) - W \times (1.29152 + 0.48407 S^2)$$

This formula transposed to show the correct measurement  $M$  equivalent to a given required thread thickness is as follows:

$$M = D + \frac{W \times (1.29152 + 0.48407 \times S^2) + T - 1.12931 \times P}{0.25862}$$

*Example:* An Acme General Purpose thread, Class 2G, has a 5-inch basic major diameter, 0.5-inch pitch, and 1-inch lead (double thread). Assume the wire size is 0.258 inch. Determine measurement  $M$  for a thread thickness  $T$  at the basic pitch line of 0.2454 inch. (This is the maximum thickness at the basic pitch line and equals the basic thickness, 0.5 $P$ , - 0.259 × allowance from Table 4, page 1323.)

$$M = 5 + \frac{0.258 \times (1.29152 + 0.48407 \times 0.06701^2) + 0.2454 - 1.12931 \times 0.5}{0.25862} = 5.056 \text{ inches}$$

**Testing Angle of Thread by Three-wire Method.** — The error in the angle of a thread may be determined by using sets of wires of two diameters, the measurement over the two sets of wires being followed by calculations to determine the amount of error, assuming that the angle cannot be tested by comparison with a standard plug gage which is known to be correct. The diameter of the small wires for the American standard thread is usually about 0.6 times the pitch and the diameter of the large wires, about 0.9 times the pitch. The total difference between the measurements over the large and small sets of wires is first determined. If the thread is an American standard or any other form having an included angle of 60 degrees, the difference between the two measurements should equal three times the difference between the diameters of the wires used. Thus, if the wires are 0.116 and 0.076 inch in diameter, respectively, the difference equals 0.116 - 0.076 = 0.040 inch. Therefore the difference between the micrometer readings for a standard angle of 60 degrees equals 3 × 0.040 = 0.120 inch in this case. If the

angle is incorrect, the amount of error may be determined by the following formula, which applies to any thread regardless of angle:

$$\sin a = \frac{A}{B - A}$$

In this formula,

- $A$  = difference in diameters of the large and small wires used;
- $B$  = total difference between the measurements over the large and small wires;
- $a$  = one-half the included thread angle.

*Example:* The diameter of the large wires used for testing the angle of a thread is 0.116 inch and of the small wires 0.076 inch. The measurement over the two sets of wires shows a total difference of 0.122 inch instead of the correct difference, 0.120 inch, for a standard angle of 60 degrees when using the sizes of wires mentioned. Therefore the amount of error is determined as follows:

$$\sin a = \frac{0.040}{0.122 - 0.040} = \frac{0.040}{0.082} = 0.4878$$

By referring to a table of sines it will be seen that this value (0.4878) is the sine of 29 degrees 12 minutes, approximately. Therefore the angle of the thread is 58 degrees, 24 minutes or 1 degree 36 minutes less than the standard angle.

**Measuring Taper Screw Threads by 3-Wire Method.** — When the 3-wire method is used in measuring a taper screw thread the measurement is along a line that is not perpendicular to the axis of the screw thread, the inclination from the perpendicular equalling one-half the included angle of the taper. The formula which follows compensates for this inclination resulting from contact of the measuring instrument surfaces, with two wires on one side and one on the other. The taper thread is measured over the wires in the usual manner excepting that the single wire must be located in the thread at a point where the effective diameter is to be checked (as described more fully later). The formula shows the dimension equivalent to the correct pitch diameter at this given point. The general formula for taper screw threads follows:

$M$  = measurement over the 3 wires;  $E$  = pitch diameter;  $a$  = one-half the angle of the thread;  $N$  = number of threads per inch;  $W$  = diameter of wires;  $b$  = one-half the angle of taper

$$M = \frac{E - \frac{\cot a}{2N} + W(1 + \operatorname{cosec} a)}{\sec b}$$

This formula is not theoretically correct but it is, however, accurate for screw threads having tapers of 31 inch per foot or less. This general formula can be simplified for a given thread angle and taper. The simplified formula following (in which  $P$  = pitch) is for an American Standard Pipe Thread:

$$M = \frac{E - (0.86603 \times P) + 3 \times W}{1.00019}$$

Standard pitch diameters for pipe threads will be found in the table "American Standard Pipe Thread." The location of this pitch diameter or distance from the end of the pipe is also shown by the table. In using the formula for finding dimen-



REPORT E-11

AZIMUTH DRIVE/BEARING TEST PROCEDURES

FOR

GIMBAL/ACTUATOR DRIVE ASSEMBLY

FOR

BOEING SECOND GENERATION HELIOSTAT

JUNE 27, 1980

Reference: FACC TM20



Ford Aerospace &  
Communications Corporation

1.0 INTRODUCTION

The purpose of this appendix is to describe the procedures used in testing each azimuth drive/bearing assembly. These tests are established to verify that each assembly meets the performance specifications. \*

2.0 LIST OF TESTS

1. Dimensional verification - Interface dimensions
2. Gear ratio verification
3. Survival loads a) Operational b) Non-Operational
4. No backdriving under survival loads
5. No load breakloose friction torque
6. Input backlash
7. Torsional stiffness
8. Moment stiffness
9. Running torque and efficiency
10. Preload

3.0 TEST PROCEDURES

3.1 Dimensional Verification

- (a.) Interface dimensions to BEC pedestal
- (b.) Interface dimensions to gimbal housing
- (c.) Motor interface
- (d.) Overall dimensions
- (e.) Azimuth axis orthogonality to base mounting surface
- (f.) Orthogonality of gimbal housing mounting surface to azimuth axis.

3.2. Gear Ratio Verification

- (a.) Check number of teeth and calculate gear ratio
- (b.) (Alternate). Determine actual overall gear ratio by measuring the number of revolutions of the input shaft for one revolution of output shaft. Will review possibility of using a frequency counter on the input shaft triggered by a limit switch on the output shaft.

3.3 Survival Loads

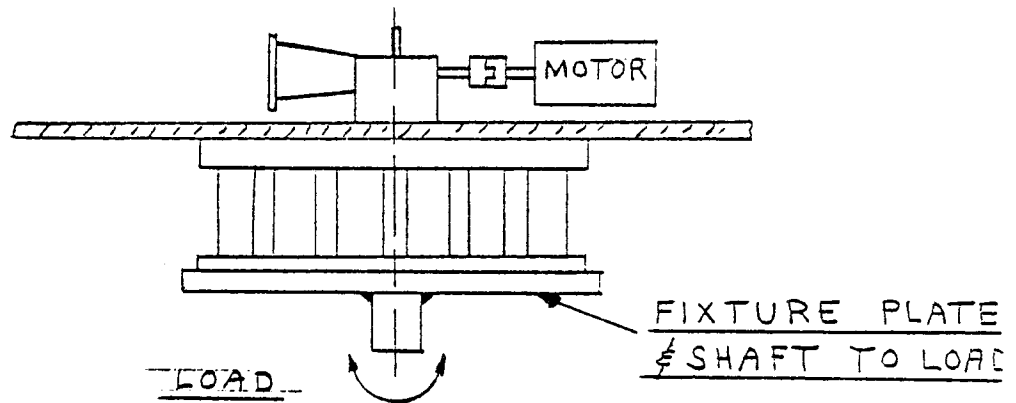
(a.) Operating

Under running conditions will apply maximum azimuth operating torque (3,900 ft. lbs.) and run the input against this load at a

---

\* The tests described are in conformance with the test plan (TM11).

motor speed of 1750 RPM until the output has rotated three revolutions. The direction will be reversed and the test repeated.



The load will be applied with a disk brake. A fixture plate will be fastened to the base (lower casting) to which the disk brake will be attached with a coupling. The entire reducer will be fastened to the test stand at the cover (upper casting).

An attempt will be made to repeat the test at a load of 7,800 ft. lbs. However, oil temperatures will be carefully monitored to prevent possible overheating. If this occurs, the actual load will be limited based on oil temperature rise.

(b.) Non-Operating

At three different orientations, the non-operating azimuth survival torque of 7,800 ft. lbs will be applied statically in both directions to the output. This will be accomplished by joggng the input with the disk brake applied to the output until load is reached.

3.4 Backdriving

The survival azimuth torque of 7,800 ft. lbs. will be applied to the output. Verification that the input shaft does not rotate will be made by using a dial indicator. Will repeat in opposite direction.

3.5 Break Loose Friction Torque

With no external torque, measurement of static break loose torque will be determined at the input shaft. A torque wrench will be used. Test to be performed in both directions (CW and CCW) and at 3 different azimuth orientations.

### 3.6 Input Backlash

The input shaft will be rotated in one direction until movement of the output is indicated by a dial indicator. The input shaft position will be recorded. The input shaft will then be rotated in the opposite direction until the output shows movement and that input shaft position recorded. The input backlash will be the difference in shaft positions expressed in degrees or radians. Measure input backlash in 3 different azimuth orientations.

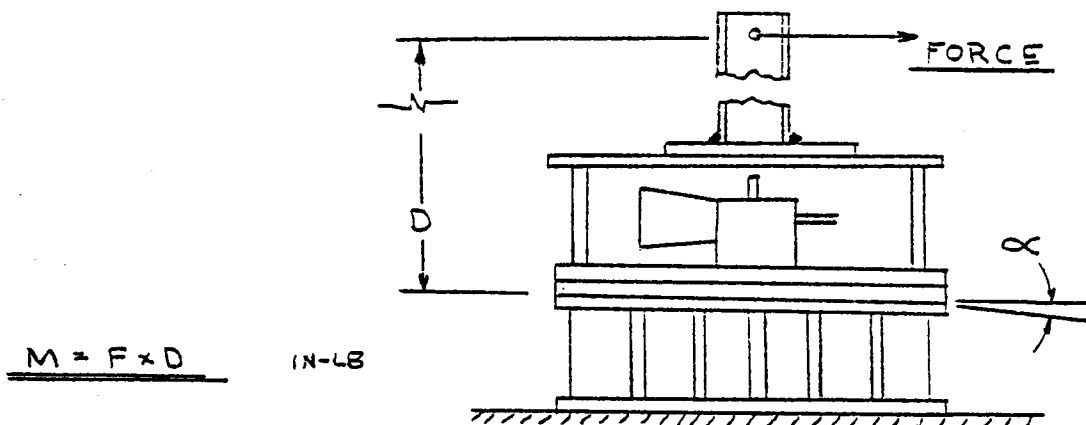
### 3.7 Torsional Stiffness

A maximum of 2,300 ft. lbs. will be applied statically to the output (base) in increments of 400 ft. lbs. and the output rotations will be recorded relative to the cover. The torque will then be reduced to zero in the same steps with a record of output rotation. The torque will be reversed and the procedure repeated. Two cycles at three azimuth orientations will be performed. This will be performed with an arm attached to the fixture plate located on the base. A hydraulic cylinder or other arrangement will be used to apply the torque. The effect of output backlash will be measured during this test.

### 3.8 Moment Stiffness

An elevation moment will be applied in increments of 400 ft. lbs. to a maximum of 2,000 ft. lb and the deflection or angular movement recorded. The moment will be similarly reduced to zero while recording angular deflection. The moment will be reversed and repeated. Four cycles will be performed.

For this test, the base will be secured and a moment applied evenly across the cover.





3.9 Running Torque and Efficiency

Measurement of starting torque and running torque will be made at four different levels of output torque up to a maximum of 3,900 ft. lbs. Efficiency will also be determined. Input speed will be 1750 RPM.

Determination of input torque will be made using a strain gage torque transducer on the input shaft. Input speed will be measured on a frequency counter. Output torque will be determined on the disk brake test stand. The reducer will be mounted similar to that shown in Step 3.3 (a). The operating survival load test described in 3.3 (a) may be performed as a part of this test.

3.10 Preload

Record required dimensions and calculate bearing preload.



REPORT E-12

GIMBAL/ACTUATOR DRIVE ASSEMBLY TEST PROCEDURES

FOR

GIMBAL/ACTUATOR DRIVE ASSEMBLY

FOR

BOEING SECOND GENERATION HELIOSTAT

JUNE 27, 1980

Reference: FACC TM22



Ford Aerospace &  
Communications Corporation

## 1.0 INTRODUCTION

The purpose of this appendix is to describe the procedures that will be used in testing the assembled Gimbal/Actuator Drive Assembly. These tests are established to verify that the assembly meets the performance specification.

## 2.0 LISTS OF TESTS

### 2.1 FACC ASSEMBLY TESTS

The following tests are performed at FACC on the assembled gimbal/actuator drive assembly:

- 1) Azimuth and elevation axes orthogonality.
- 2) Dimensional verification.
- 3) Azimuth survival load capability.
- 4) Azimuth drive motor capability under the maximum operational load.
- 5) Azimuth stiffness.
- 6) Travel limits of azimuth drive.
- 7) Emergency manual operation of elevation drive.
- 8) Elevation drive capability under the maximum operational load.
- 9) Elevation stiffness.
- 10) Elevation survival load capability.
- 11) Backdriving of elevation drive.
- 12) Travel limits of elevation drive.

### 2.2 RELATIONSHIP TO TEST PLAN

The tests described are in conformance with the test plan (TM10) except the following four tests were deleted:

- #4 - Azimuth axis wobble.
- #5 - Moisture intrusion.
- #8b - Elevation dead load unbalance input torque.
- #8e - Elevation running torque/efficiency,

### 2.3 AZIMUTH DRIVE/BEARING ASSEMBLY TESTS

The following azimuth drive/bearing assembly tests (appendix E-11) will have been performed by the azimuth drive vendor prior to performing the testing described herein:

- Azimuth axis orthogonality to base mounting surface.
- Azimuth drive backlash.
- Azimuth drive breakloose friction torque.
- Azimuth drive running torque/efficiency.
- Azimuth drive backdriving.

3.0 APPLICABLE DRAWINGS

The following FACC drawings describe the tested prototype gimbal/actuator drive assembly:

- #531146 Gimbal Housing
- #531147 Torque Tube/Arms Assembly
- #531148 Miscellaneous Details
- #531149 Gimbal/Actuator Drive Assembly
- #531150 Interface Control Drawing



3939 Fabian Way  
Palo Alto, California 94303

Code Ident. No. 11530

#### 4.0 TEST PROCEDURES

##### 4.1 Azimuth and Elevation Axis Orthogonality

###### 4.1.1 Object

Verify that the orthogonality of azimuth and elevation axes are within the specified value of  $\pm 0.25^\circ$ .

Record the measured value; this data is necessary for input to the control system software for the heliostat to which the gimbal is assigned.

###### 4.1.2 Procedure

See Figure 1.

This test shall be performed before installing the torque tube on the gimbal and azimuth gearbox.

1. Place the azimuth gearbox and gimbal assembly on flat surface.
2. Install long tooling pin through two elevation bushings such that it will extend outside by approximately one inch on each side. Clearance between the bushings and pin shall not exceed 0.001 inch.
3. Set up one dial indicator from ground to probe the tooling pin on one side in vertical direction and take dial indicator reading. Record in Section 5.1.
4. Rotate the assembly around azimuth axis until dial indicator probes against the other end of pin and again take dial indicator reading. Repeat for accuracy.
5. Non-orthogonality (radians) = Difference in readings for dial indicator divided by the distance between points on pin where dial indicator touches.
6. Record non-orthogonality in degrees to the accuracy of  $0.001^\circ$  for control system use.

##### 4.2 Dimensional Verification

###### 4.2.1 Object

Verify overall physical dimensions and dimensions of interfaces of the drive unit to the BEC pedestal and the torque tube flanges.

###### 4.2.2 Procedure

The gimbal drive unit shall be dimensionally checked to verify conformance to design control drawings. The verification shall include the following:



3939 Fabian Way  
Palo Alto, California 94303

Code Ident. No. 11530

- a. Overall dimensions
- b. Interface dimensions to pedestal
- c. Interface dimensions to torque tube flanges
- d. Parallelism of torque tube flanges and perpendicularity to elevation axis.
- e. Clearance and accessibility of azimuth and elevation motors and sensors.

See data section 5.2 for a list of the dimensions to be verified.

#### 4.3 Azimuth Survival Loading

##### 4.3.1 Object

Verify the ability of the unit to endure a survival, non-operating, azimuth torque. Also verify that no slippage occurs at the torque tube under this condition.

##### 4.3.2 Procedure

See figures 2 and 3.

1. Locate the torque tube to correspond to 0° elevation (vertical mirror).
2. Mount the flange plates to each side of the torque tube flanges using BEC supplied bolts. Torque to 17 lb. ft.
3. Clamp a displacement gauge (dial indicator) onto each flange plate so that the dial indicator probe touches the torque tube.
4. Mount the force inducing units.
5. Apply the tensile and load of 1560 lb to each flange plate (this force is equivalent to the survival load of 7800 lb-ft which occurs at 50 mph wind).
6. As the load is applied, verify that there is no slippage between the flange plate and the torque tube flange by observing for any sudden movement in the dial indicator. Also verify that there is no physical damage. Record findings.
7. Reverse the loading (i.e., direction of the torque) and repeat steps 4, 5, and 6.
8. Run the total travel capability test, see section 4.6, after this survival loading test to verify that functional operation is not impaired by survival loading; in specific, observe for any sudden locking or unusual and excessive noise while driving the unit.





Ford Aerospace &  
Communications Corporation  
Western Development  
Laboratories Division

Page 7

3939 Fabian Way  
Palo Alto, California 94303

Code Ident. No. 11530

#### 4.4 Azimuth Drive Motor Capability Under Maximum Operational Load

##### 4.4.1 Object

Verify that the azimuth drive motor meets its drive requirements. The azimuth drive performance parameters will be checked at the azimuth drive vendor. The drive motor capability under maximum operational loads corresponding to 35 and 50 mph wind with mirror in worst orientation will be calculated from the drive performance tests.

##### 4.4.2 Procedure

The running torque and efficiency test is performed as a part of the azimuth drive performance testing at the vendor's facility. The input torque is determined by driving against varying output torques from no-load up to simulated 50 mph wind load. Test procedures were described in Appendix E-11.

#### 4.5 Azimuth Stiffness

##### 4.5.1 Object

Verify that the total rotation of the torque tube flanges about the azimuth axis between clockwise operating torque and counterclockwise operating torque corresponding to 27 mph wind velocity is less than 6 mrad (2 x 3 mrad).

##### 4.5.2 Procedure

See figures 4 and 5. (Note: during this test, do not readjust the displacement gauges until the test is complete.)

1. Locate the torque tube to correspond to zero degree elevation (vertical mirror).
2. Set a displacement gauge to probe each torque tube flange in opposite horizontal directions.



3939 Fabian Way  
Palo Alto, California 94303

Code Ident. No. 11530

3. At each torque tube flange plate, apply equal and opposite horizontal loads. The loads shall be applied as to first induce counter clockwise torque, then clockwise torque for two complete cycles. See data section 5.5 for appropriate loads.
4. For each load listed in data section 5.5, take the dial indicator readings and record them in the data section.
5. Calculate the rotational angles by adding the dial indicator readings and dividing by the distance between the dial indicators.
6. Plot rotation vs torque.
7. The difference between maximum and minimum angle shall be less than 6 milliradians.

#### 4.6 Azimuth Drive Travel Limits

##### 4.6.1 Object

Determine the azimuth drive travel limits and verify that the drive unit is capable of rotating at least  $\pm 165$  degrees in azimuth.

##### 4.6.2 Procedure

See figure 6

1. Set the angular location of azimuth axis in a central position ( $0^\circ$ ) to the base.
2. Drive the unit in azimuth in both clockwise and counterclockwise directions.
3. Verify the angular travel limits.
4. Record the verification in data section 5.6

#### 4.7 Elevation Drive Emergency Operation

##### 4.7.1 Object

Verify the ability of the elevation drive assembly to be driven without the drive motor.

##### 4.7.2 Procedure

See figure 7.



3939 Fabian Way  
Palo Alto, California 94303

Code Ident. No. 11530

1. Put a  $\frac{1}{4}$  H.P. reversible drill motor directly on the worm extension opposite the actuator motor.
2. Turn the drill motor on and verify that the assembly can be driven in elevation.

Caution: Do not continuously run the drive motor if and when the travelling nut runs into either of the actuator stops.

#### 4.8 Elevation Drive Capability Under the Maximum Operational Loads

##### 4.8.1 Object

Verify that the actuator is capable of driving against the maximum operational loads at four elevation orientations.

##### 4.8.2 Procedure

See figure 8.

(Caution: Do not impose any compressive load on the screw beyond the specified test load limit).

1. Position the drive unit corresponding to zero degree elevation (vertical mirror).
2. With the flange plates in place, apply the maximum operation elevation torque to the torque tube flange. See data section 5.8 for appropriate loads.
3. Start the stopwatch, and at the same time, turn the elevation motor on as to drive the unit against the torque. Verify that the motor is able to drive against the torque without stalling for a minimum of 1 minute continuously.
4. Repeat steps 2 and 3 for elevation angles of  $30^{\circ}$ ,  $60^{\circ}$ , and  $90^{\circ}$ .

#### 4.9 Elevation Stiffness

##### 4.9.1 Object

Verify that the total rotation of the torque tube flanges about the elevation axis between clockwise operating torque and counterclockwise operating torque corresponding to 27 mph wind is less than 6 milliradians ( $2 \times 3$  mrad) at the elevation angle of  $0^{\circ}$  (vertical mirror) and  $90^{\circ}$  (horizontal mirror).



3939 Fabian Way  
Palo Alto, California 94303

Code Ident. No. 11530

#### 4.9.2 Procedure

See figure 9.

1. Locate the torque tube to correspond to  $0^{\circ}$  elevation.
2. With the flange plates in place, attach an electronic level or dial indicators securely to the torque tube.
3. At flange plate, apply equal and opposite horizontal loads to each side of the torque tube. See data section 5.9 for appropriate loads.
4. For each load listed in data section 5.9, take the instrument reading and record it in the data section.
5. Plot rotation vs. torque.
6. The difference between maximum and minimum angle shall be less than 6 milliradians.
7. Locate the torque tube to correspond to  $90^{\circ}$  elevation.
- 8 Repeat steps 2 through 7 for this elevation angle of  $90^{\circ}$ .
9. Determine the output backlash from the rotation vs. torque plot at  $90^{\circ}$  elevation.

#### 4.10 Elevation Survival Loading

##### 4.10.1 Object

Verify the ability of the unit to endure a survival, non-operating, elevation torque. Also verify that no slippage occurs at the torque tube under this condition.

Note: Test of next section 4.11 should be done simultaneously with this test. See section 4.11.

##### 4.10.2 Procedure

See figure 10.

1. Locate the torque tube to correspond to  $90^{\circ}$  elevation (horizontal mirror).
2. With flange plates in place, clamp a displacement gauge onto each side of torque tube so that the dial indicator probe touches the upper end of flange plate.



3939 Fabrian Way  
Palo Alto, California 94303

Code Ident. No. 11530

3. Apply the tensile load of 4000 lb to each of the four force inducing units (this force is equivalent to the survival load of 20,000 lb-ft which occurs at 90 mph wind).
4. As the load is applied, verify that there is no slippage between the flange plate and the torque tube flange by observing for any sudden movement in dial indicators. Also verify that there is no physical damage. Record findings.
5. Reverse the loading (i.e., the direction of the torque) and repeat steps 2, 3, and 4.
6. Run the total travel capability test, see section 4.12 after this survival loading test to verify that functional operation is not impaired by survival loading; in specific, observe for any sudden locking or unusual and excessive noise while driving the unit.

#### 4.11 Elevation Drive Backdriving

##### 4.11.1 Object

Verify that the drive unit cannot be backdriven in elevation.

##### 4.11.2 Procedure

See figure 11.

While testing the drive unit for survival against elevation survival torque of 20,000 ft-lb (see section 4.10), observe and verify that there is no input shaft rotation when output torque is applied.

#### 4.12 Elevation Drive Travel Limits.

##### 4.12.1 Objects

Verify that the drive unit is capable of rotating in the range of +93 degrees to -3 degrees in elevation.

##### 4.12.2 Procedure

See figure 12

1. Set the angular location of elevation axis in a neutral position ( $0^{\circ}$ ).



Ford Aerospace &  
Communications Corporation  
Western Development  
Laboratories Division

Page 12

3939 Fabian Way  
Palo Alto, California 94303

Code Ident. No. 11530

2. Drive the unit in elevation to the limits of +93 degrees and -3 degrees.
3. Verify the angular travel limits.
4. Record the verification.



Ford Aerospace &  
 Communications Corporation  
 Western Développement  
 Laboratories Division

3939 Fabian Way  
 Palo Alto, California 94303  
 Code Ident. No. 11530

5.0 DATA SHEETS

5.1 Azimuth and Elevation Axis Orthogonality

(a) Initial reading of dial indicator a = \_\_\_\_\_ inches

(b) Final reading of dial indicator b = \_\_\_\_\_ inches

(c) Distance between two points, where dial indicator touches,  $l$  } = \_\_\_\_\_ inches

(d) Axes non-orthogonality

$$= \frac{a-b}{l} \text{ Radians}$$

$$= \text{_____ Radians}$$

$$= \text{_____ Radian} * 57.296$$

$$= \text{_____ Degrees}$$



3939 Fabian Way  
 Palo Alto, California 94303

Code Ident. No. 11530

5.2 Dimensional Verification

Items (a.i) and (a.ii) shall be verified at FACC/WDL. Items (a.iii), (a.iv), (c), and (d) shall be verified at the torque tube subcontract facility. Items (a.v) shall be verified at the gimbal subcontract facility. Items of (b) shall be verified at the azimuth drive vendor facility. All items verified at subcontractor facilities shall be recorded in this section.

a. Overall dimensions

- i) Height of elevation axis over base flange =  
     (21.50 + 0.100)
- ii) Offset between elevation and azimuth axes =  
     (4.50 + 0.100)
- iii) Distance between elevation axis and torque  
     tube center line..... =
- iv) Distance between elevation axis and upper  
     pivot point of actuator..... =
- v) Distance between elevation axis and lower  
     pivot point of actuator..... =

b. Interface dimensions to pedestal

- i) Mounting hole diameter..... =
- ii) Distance between adjacent holes ..... =
- iii) Bolt circle diameter..... =

c. Interface dimension to torque tube flanges

- i) Mounting hole diameter ..... =
- ii) Distance between adjacent holes ..... =
- iii) Bolt circle diameter..... =
- iv) Location of bolt holes with respect to  
     elevation bearing and actuator pivot is  
     located correctly =





3939 Fabian Way  
Palo Alto, California 94303

Code Ident. No. 11530

d. Perpendicularity of torque tube flanges and parallelism of flange axis to the elevation axis.

i) Torque tube flanges are parallel within =

ii) Flanges are perpendicular to elevation axis within..... =

e. Clearance and accessibility (record findings)

i) Azimuth motor

ii) Azimuth motor revolution sensors

iii) Azimuth zero reference sensor

iv) Elevation motor



Ford Aerospace &  
Communications Corporation  
Western Development  
Laboratories Division

Page 16

3939 Fabian Way  
Palo Alto, California 94303

Code Ident. No. 11530

v) Elevation motor revolution sensors

vi) Elevation zero reference sensor

5.3 Azimuth Survival Loading

List here any abnormalities observed during or after the test.

5.4 Azimuth Drive Motor Capability Under Maximum Operational Loads

Can the motor drive against maximum operational torque without stalling?

(YES or NO) \_\_\_\_\_

Record comments or findings if any.



Ford Aerospace &  
Communications Corporation  
Western Development  
Laboratories Division

3939 Fabian Way  
Palo Alto, California 94303

Code Ident. No. 11530

5.5 Azimuth Stiffness

Torque Induced (ft-lb)	Force (lb)	Dial Indicator Reading (Inches)		Reading Sum <sup>(1)</sup> (Inches)	Rotational Angle <sup>(2)</sup> (Milliradians)
		#1	#2		
0	0				
400	80				
800	160				
1200	240				
1600	320				
2000	400				
2300	460				
2000	400				
1600	320				
1200	240				
800	160				
400	80				
0	0				
-400	-80				
-800	-160				
-1200	-240				
-1600	-320				
-2000	-400				
-2300	-460				
-2000	-400				
-1600	-320				
-1200	-240				
-800	-160				
-400	-80				
0	0				
400	80				
800	160				
1200	240				
1600	320				
2000	400				
2300	460				
2000	400				
1600	320				
1200	240				
800	160				
400	80				



Ford Aerospace &  
Communications Corporation  
Western Development  
Laboratories Division

3939 Fabian Way  
Palo Alto, California 94303

Code Ident. No. 11530

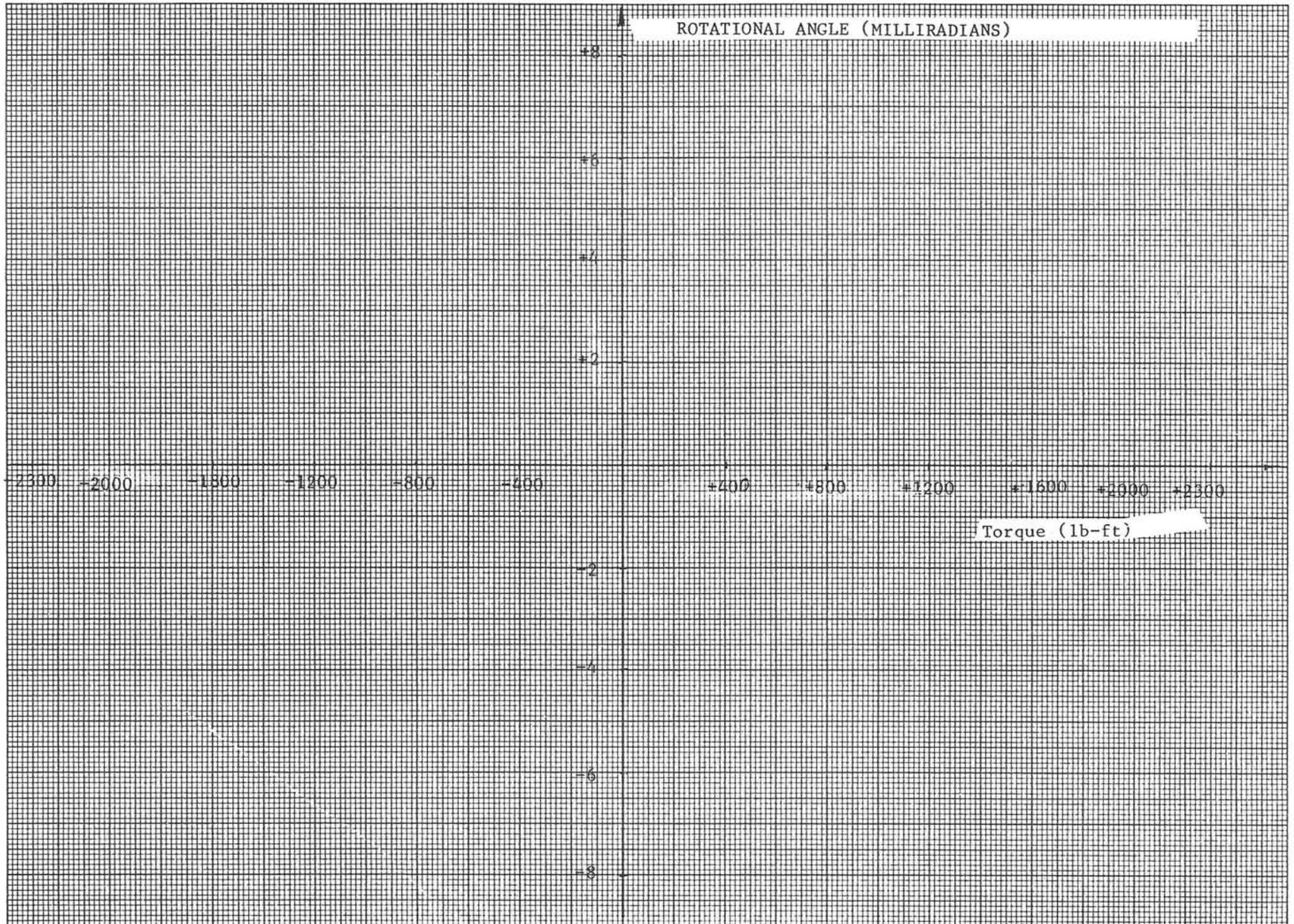
Torque Induced (ft-lb)	Force (lb)	Dial Indicator Reading (Inches)		Reading Sum <sup>(1)</sup> (inches)	Rotational Angle (Milliradians)
		#1	#2		
0	0				
-400	-80				
-800	-160				
-1200	-240				
-2000	-400				
-2300	-460				
-2000	-400				
-1600	-320				
-1200	-240				
-800	-160				
-400	-80				
0	0				

(Pointing error Angle = .5 X (Maximum Angle - Minimum Angle) = \_\_\_\_\_ Milliradians

(1) Reading Sum = Reading, Indicator #1 + Reading, Indicator #2

(2) Rotational Angle =  $\frac{\text{Reading Sum}}{\text{Distance between indicators}} \times 1000$   
 (in milliradians) (in inches)

AZIMUTH STIFFNESS: PLOT OF ROTATIONAL ANGLE VS TORQUE INDUCED





Ford Aerospace &  
Communications Corporation  
Western Development  
Laboratories Division

Page 20

3939 Fabian Way  
Palo Alto, California 94303

Code Ident. No. 11530

5.6 Azimuth Drive Travel Limits

Overall travel limits

+ \_\_\_\_\_ degrees to - \_\_\_\_\_ degrees

Record comments if any.

5.7 Elevation Drive Emergency Operation of Elevation Drive

Is it possible to drive elevation drive with drill motor? \_\_\_\_\_ (Yes or No)

Record comments if any.



Ford Aerospace &  
Communications Corporation  
Western Development  
Laboratories Division

Page 21

3939 Fabian Way  
Palo Alto, California 94303

Code Ident. No. 11530

5.8 Elevation Drive Capability Under Maximum Operational Loads

Output Torque Induced (lb-ft)	Elevation Angle (degrees)	Does the motor stall? (Yes or No)
7080	0°	
10920	30°	
11750	60°	
6330	90°	

Record comments, if any.



Ford Aerospace &  
Communications Corporation  
Western Development  
Laboratories Division

3939 Fabian Way  
Palo Alto, California 94303

Code Ident. No. 11530

5.9 Elevation Stiffness

NOTE: Include the unbalance  
effect of tooling fixture.

5.9.1 Elevation Angle 0° (Vertical Mirror)

Torque Induced Ft-lbs	Force (lb)	Instrument Readings	Rotational Angle (Milliradians)
3880	776		
4000	800		
4200	840		
4400	880		
4600	920		
4800	960		
5000	1000		
5200	1040		
5340	1068		
5200	1040		
5000	1000		
4800	960		
4600	920		
4400	880		
4200	840		
4000	800		
3880	776		
4000	800		
4200	840		
4400	880		
4600	920		
4800	960		
5000	1000		
5200	1040		
5340	1068		
5200	1040		
5000	1000		
4800	960		
4600	920		
4400	880		
4200	840		
4000	800		
3880	776		





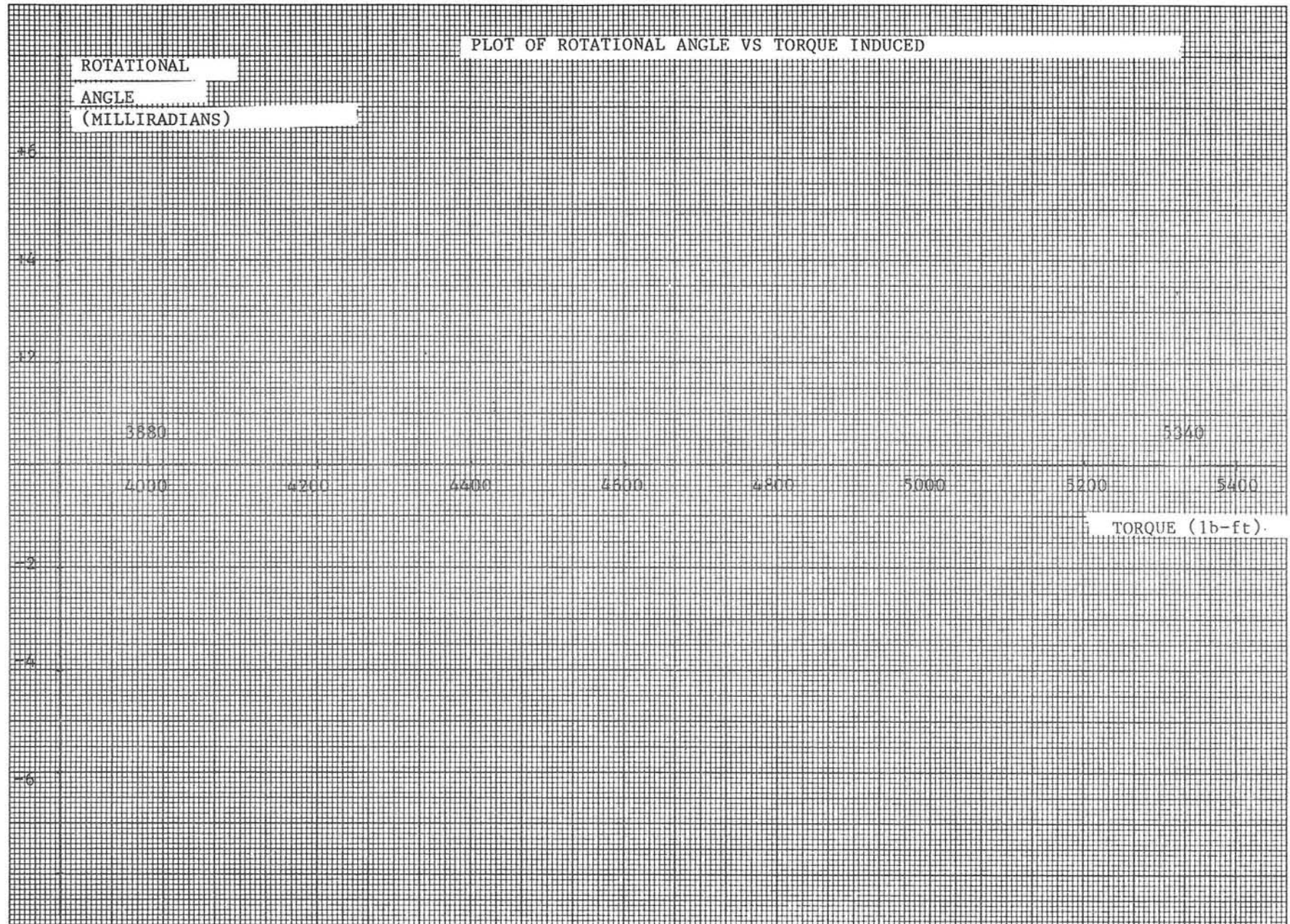
Ford Aerospace &  
Communications Corporation  
Western Development  
Laboratories Division

Page 23

3939 Fabian Way  
Palo Alto, California 94303  
Code Ident. No. 11530

Pointing Error Angle = .5 X (maximum angle - minimum angle) = \_\_\_\_\_ Milliradians.

ELEVATION STIFFNESS; & ELEVATION ANGLE, 0° (VERTICAL MIRROR)





Ford Aerospace &  
 Communications Corporation  
 Western Development  
 Laboratories Division

3939 Fabian Way  
 Palo Alto, California 94303

Code Ident. No. 11530

NOTE: Include the unbalance  
 effect of tooling  
 fixture.

5.9.2 Elevation Angle of 90° (horizontal mirror)

Torque Induced ft.-lb.	Force (lb)	Instrument Readings	Rotational Angle (milliradians)
0	0		
300	60		
600	120		
900	180		
1200	240		
1500	300		
1810	362		
1500	300		
1200	240		
900	180		
600	120		
300	60		
0	0		
-300	-60		
-600	-120		
-900	-180		
-1200	-240		
-1500	-300		
-1810	-362		
-1500	-300		
-1200	-240		
-900	-180		
-600	-120		
-300	-60		
0	0		
300	60		
900	180		
1200	240		
1500	300		
1810	362		
1500	300		
1200	240		
900	180		
600	120		
300	60		



Ford Aerospace &  
Communications Corporation  
Western Development  
Laboratories Division

Page 26

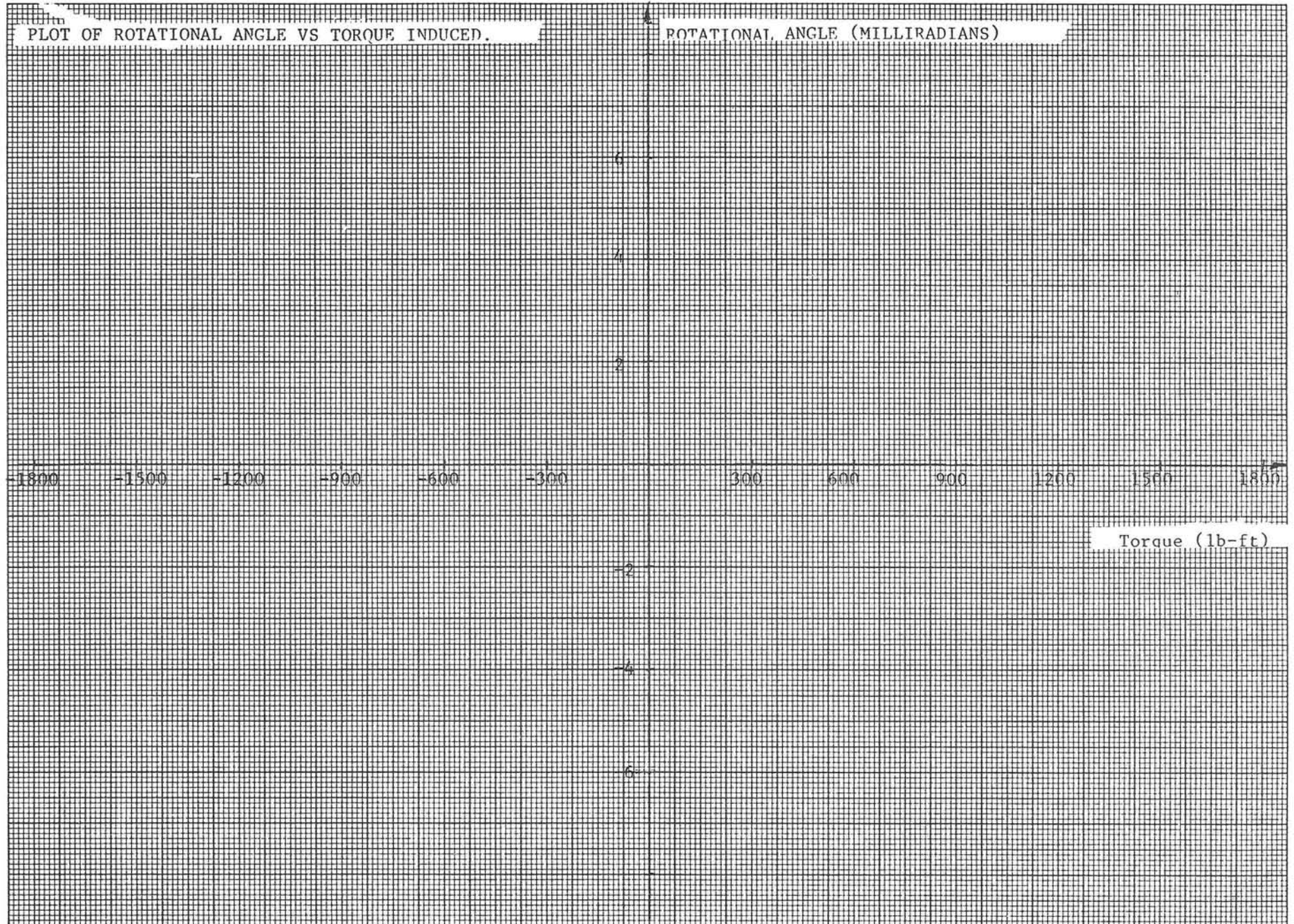
3939 Fabian Way  
Palo Alto, California 94303

Code Ident. No. 11530

Torque Induced (ft-lb)	Force (lb)	Instrument Readings	Rotational Angle
0	0		
-300	-60		
-600	-120		
-900	-180		
-1200	-240		
-1500	-300		
-1810	-362		

$$\begin{aligned} \text{Pointing Error Angle} &= .5 \times (\text{Maximum Angle} - \text{Minimum Angle}) \\ &= \underline{\hspace{2cm}} \text{ Milliradians} \end{aligned}$$

ELEVATION STIFFNESS: ELEVATION ANGLE,  $90^{\circ}$  (HORIZONTAL MIRROR)





Ford Aerospace &  
Communications Corporation  
Western Development  
Laboratories Division

Page 28

3939 Fabian Way  
Palo Alto, California 94303

Code Ident. No. 11530

5.10 Elevation Survival Loading

List here any abnormalities observed during or after the test.

5.11 Elevation Drive Backdriving

Is the input shaft rotation observed when survival output torque is applied at elevation axis: \_\_\_\_\_ (yes or no)

Record comments, if any.

5.12 Elevation Drive Travel Limits

+ \_\_\_\_\_ degrees to - \_\_\_\_\_ degrees

Record comments, if any.

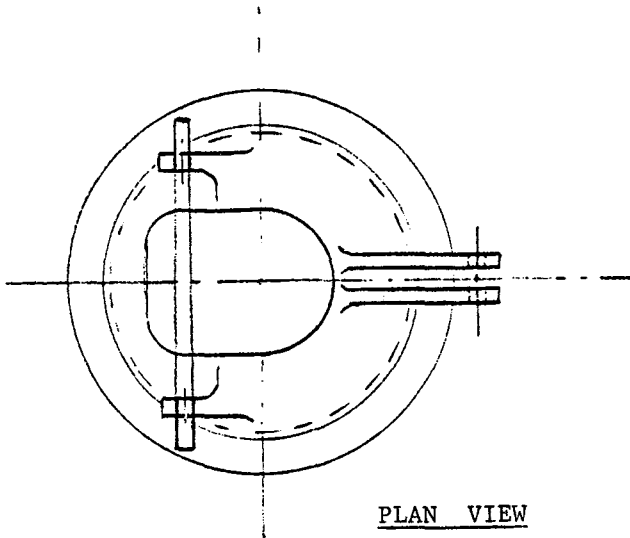




Ford Aerospace &  
Communications Corporation  
Western Development  
Laboratories Division

3939 Fabian Way  
Palo Alto, California 94303

Code Ident. No. 11530



PLAN VIEW

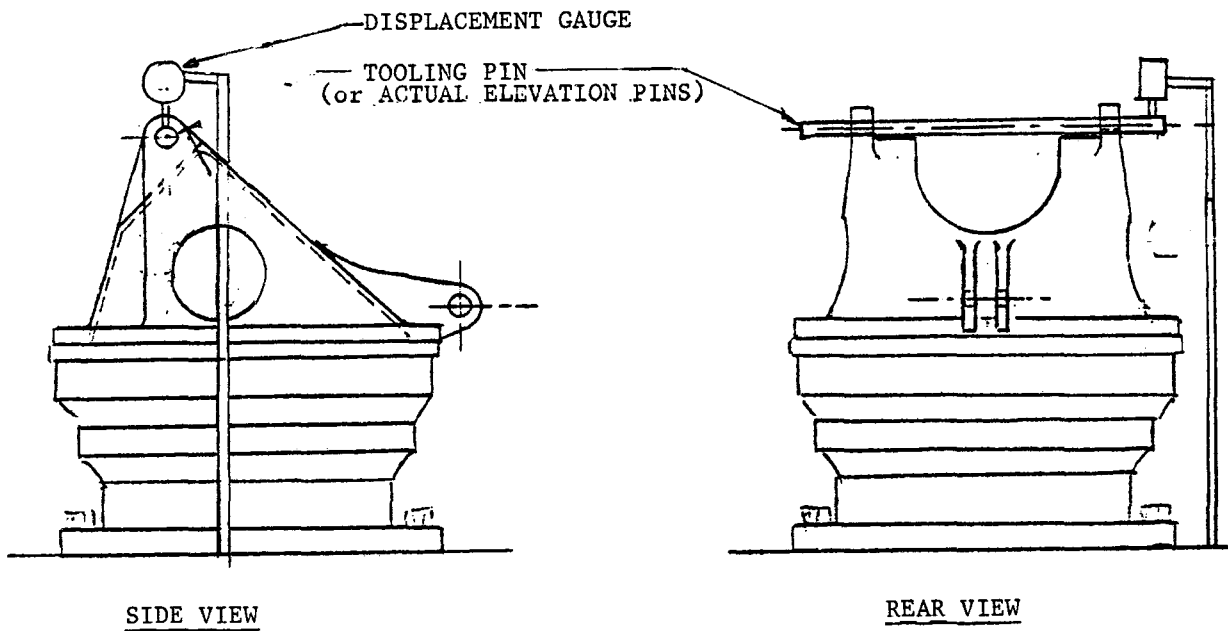


FIGURE 1: AZIMUTH AND ELEVATION AXIS ORTHOGONALITY



Ford Aerospace &  
Communications Corporation  
Western Development  
Laboratories Division

3939 Fabrian Way  
Palo Alto, California 94303

Code Ident. No. 11520

FLANGE PLATE

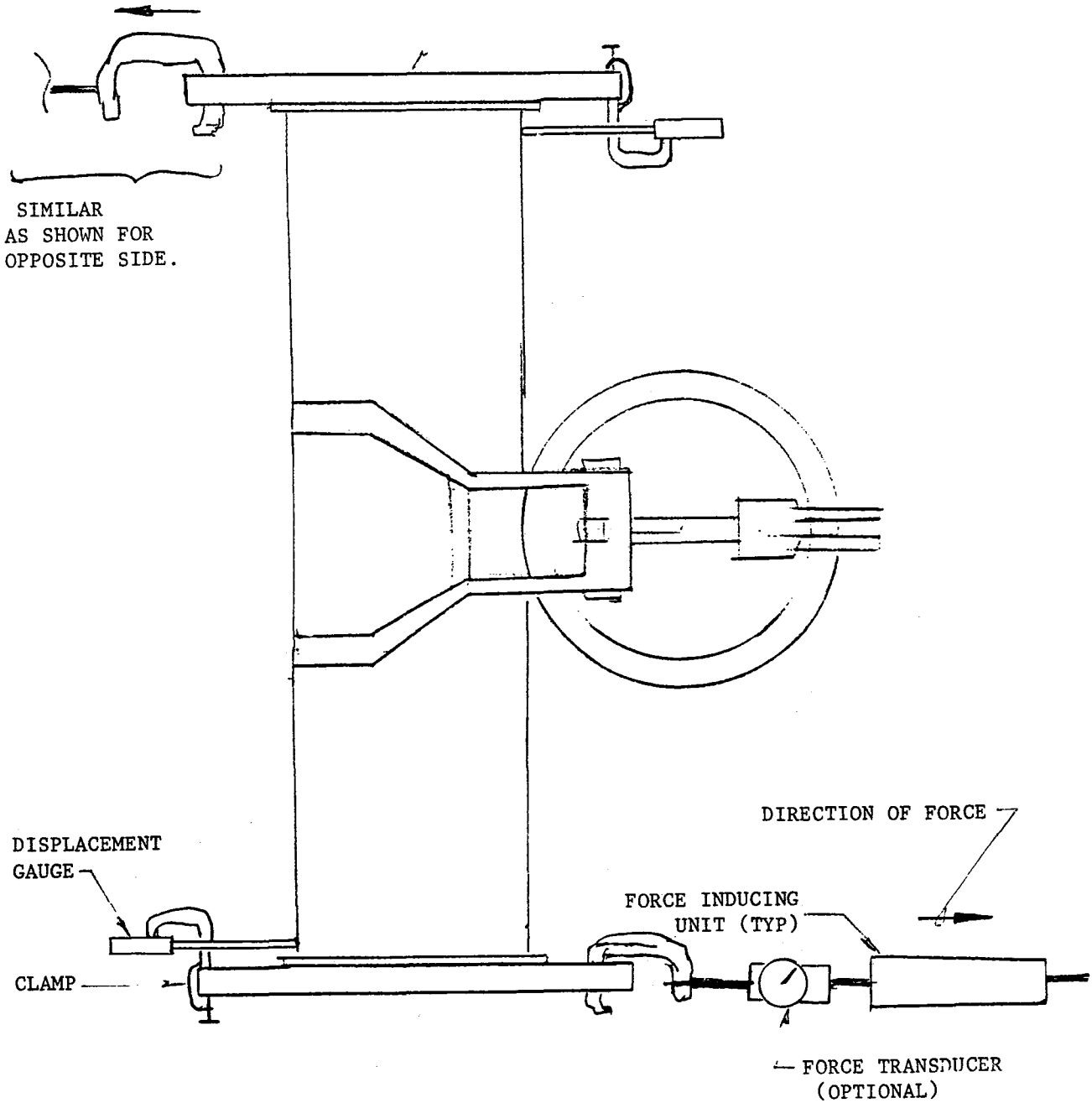


FIGURE 2: PLAN VIEW

AZIMUTH SURVIVAL LOADING





Ford Aerospace &  
Communications Corporation  
Western Development  
Laboratories Division

3939 Fabrian Way  
Palo Alto, California 94303

Code Ident. No. 11530

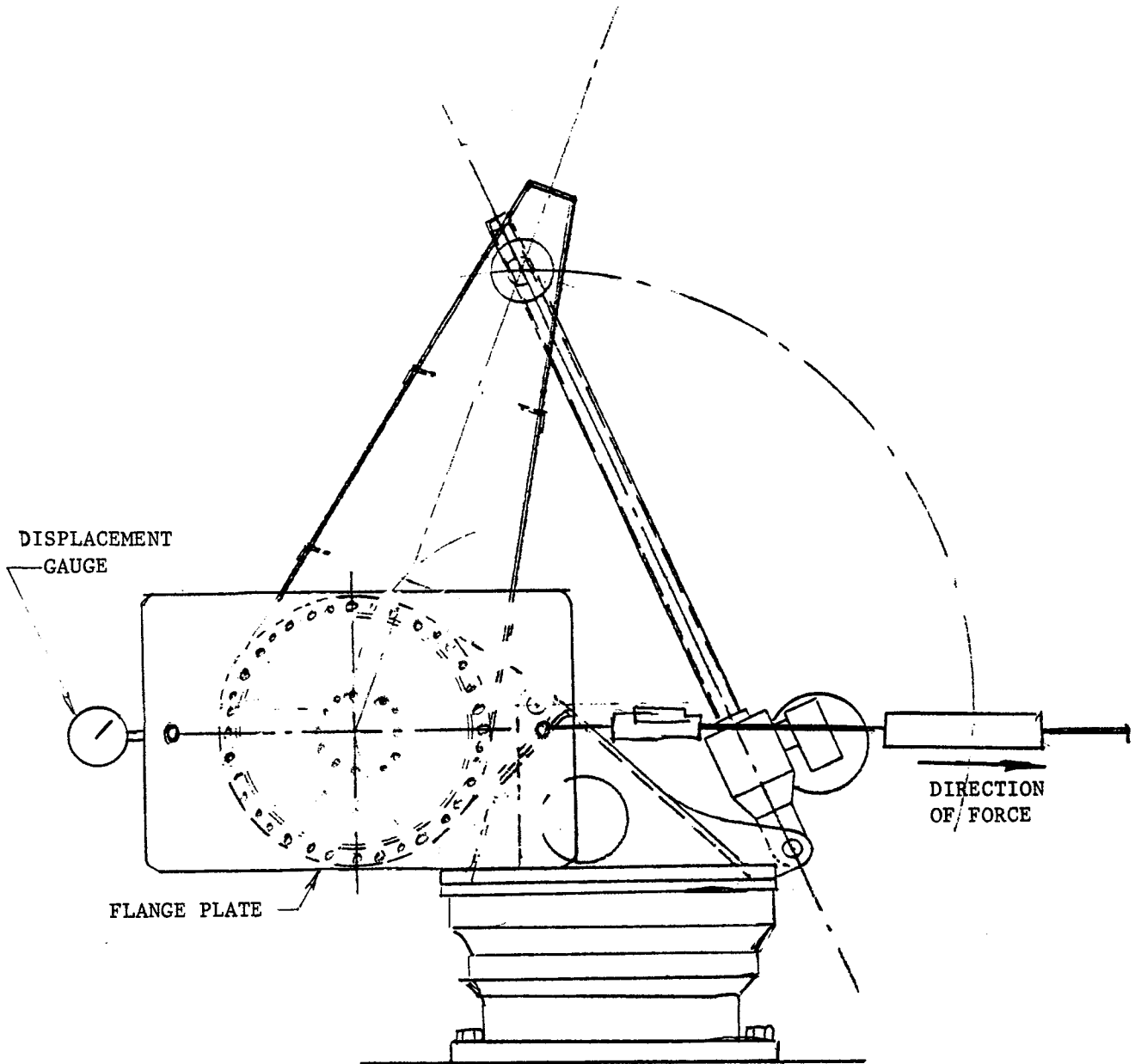


FIGURE 3: SIDE VIEW:  
AZIMUTH SURVIVAL LOADING

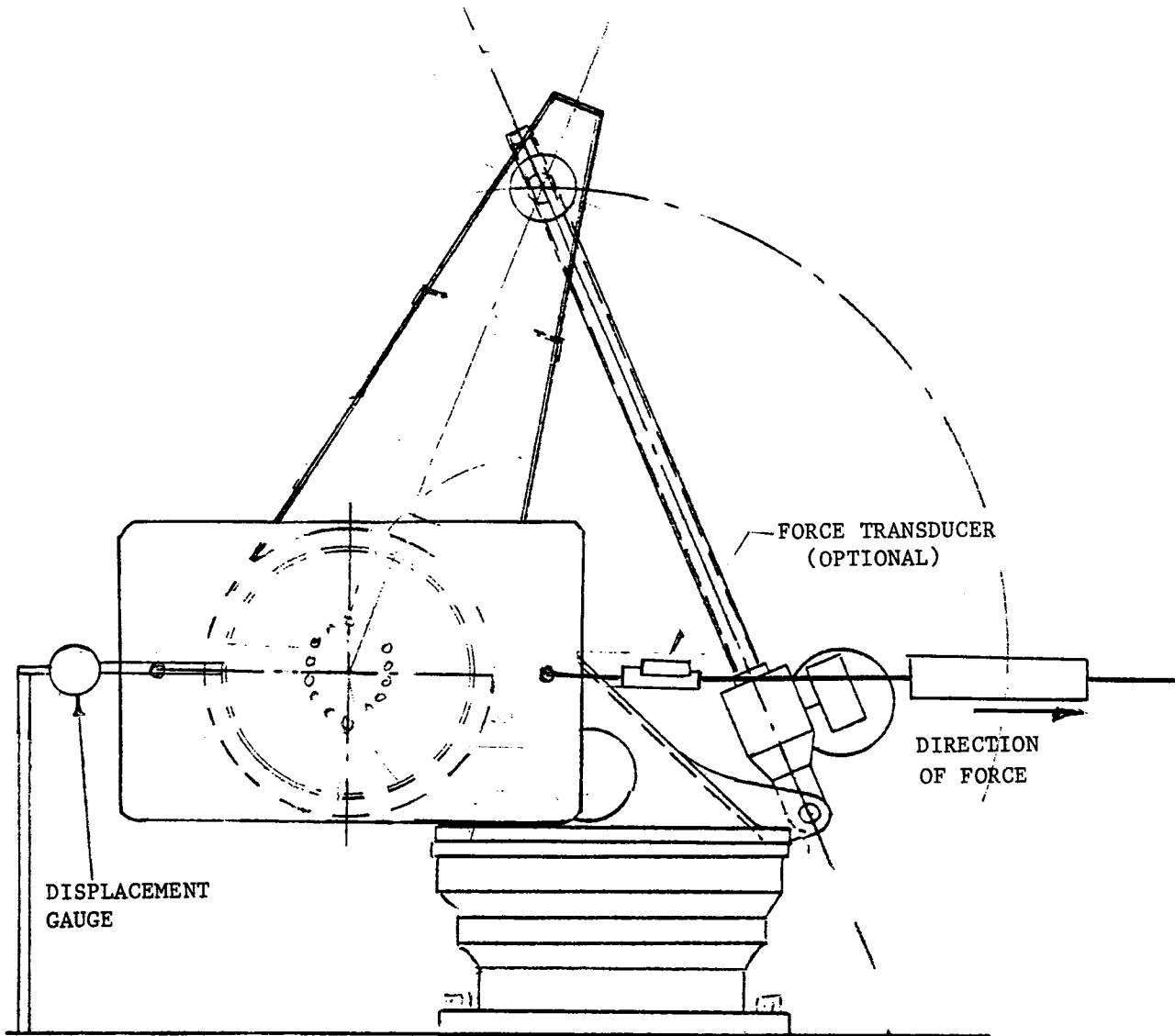


Ford Aerospace &  
Communications Corporation  
Western Development  
Laboratories Division

3939 Fabian Way  
Palo Alto, California 94303

Code Ident. No. 11530

Page 32



SIDE VIEW:

FIGURE 4: STIFFNESS OF AZIMUTH DRIVE



Ford Aerospace &  
Communications Corporation  
Western Development  
Laboratories Division

3939 Fabian Way  
Palo Alto, California 94303

Code Ident. No. 11530

Page 33

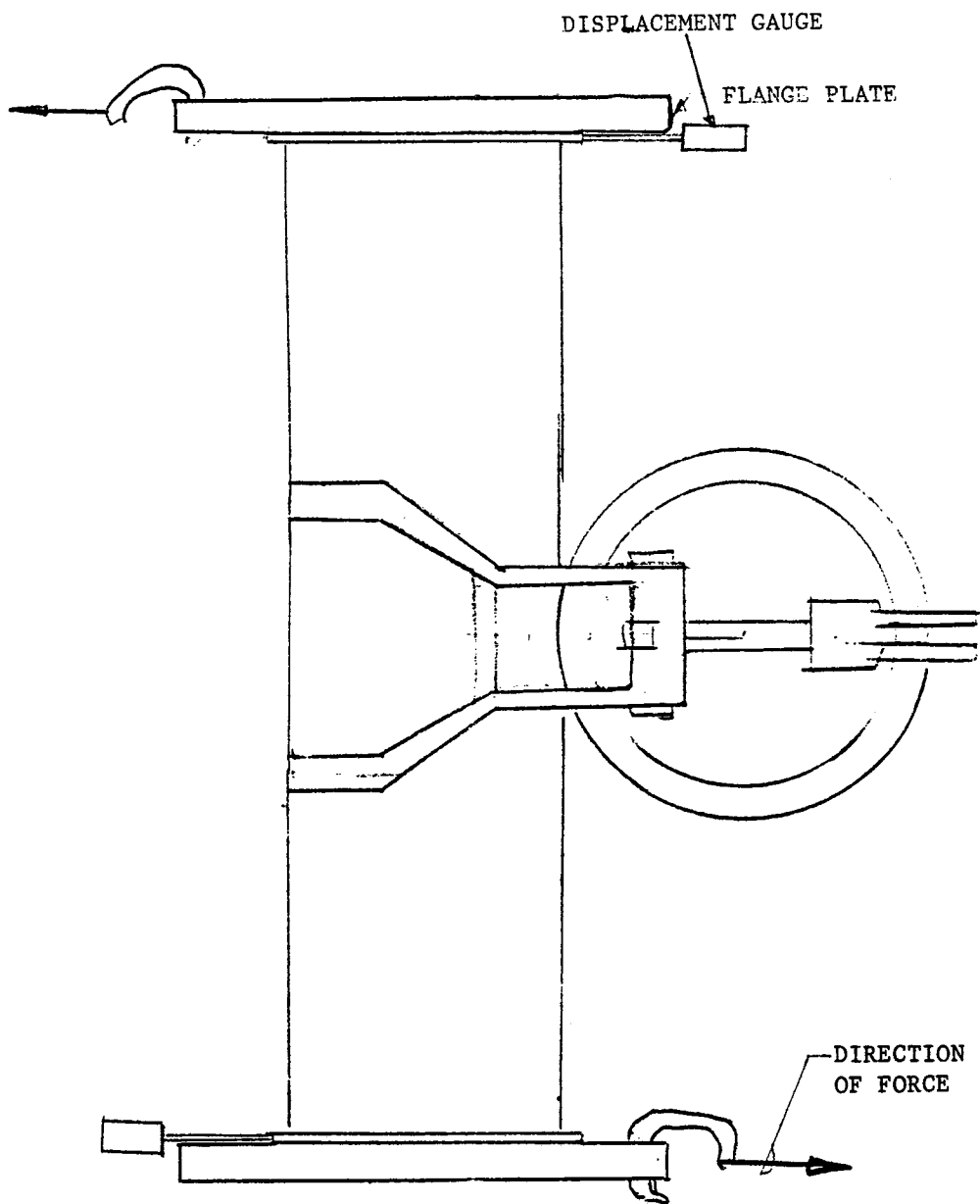


FIGURE 5: PLAN VIEW  
STIFFNESS OF AZIMUTE DRIVE



Ford Aerospace &  
Communications Corporation  
Western Development  
Laboratories Division

3939 Fabian Way  
Palo Alto, California 94303

Code Ident. No. 11530

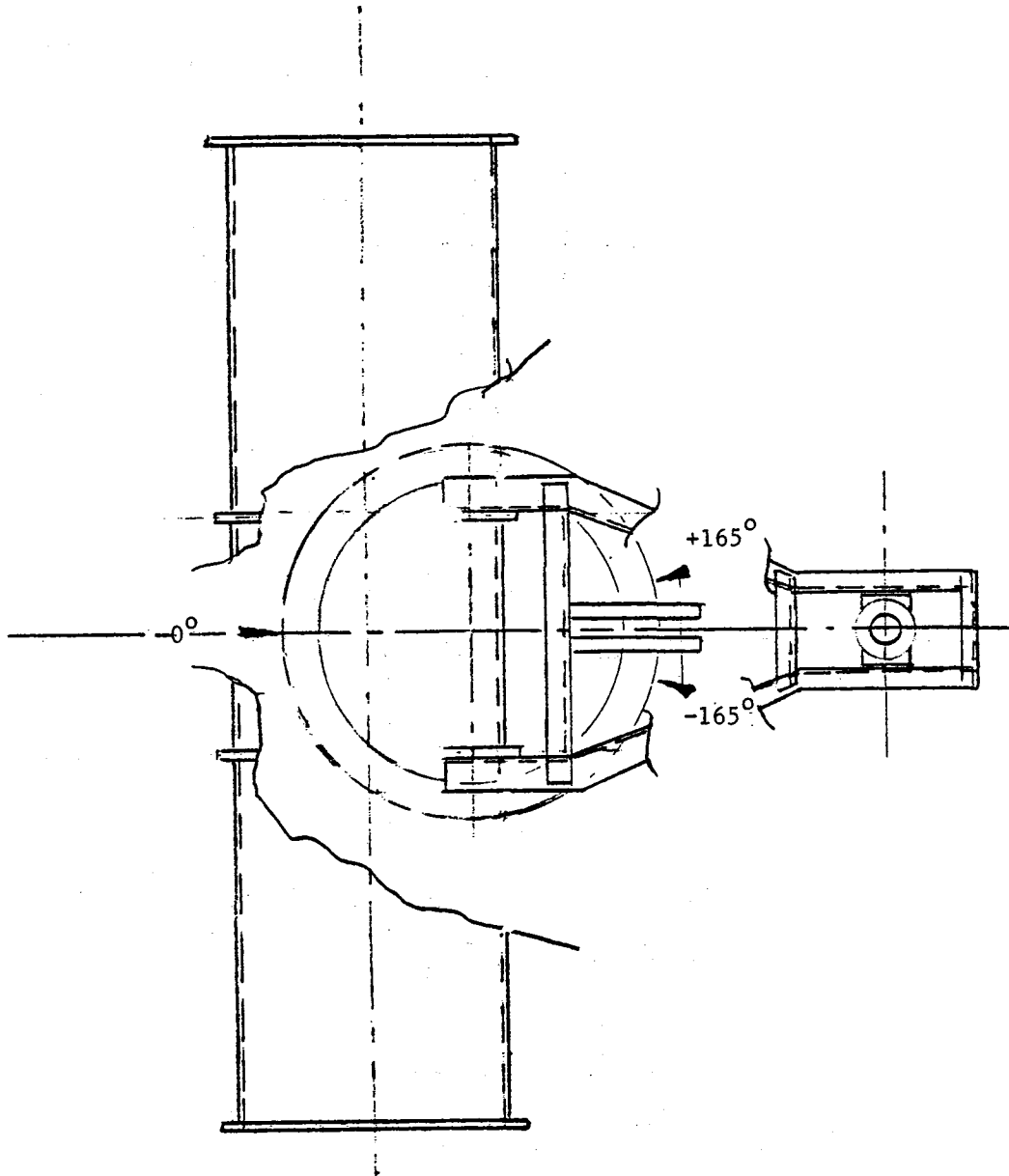


FIGURE 6: AZIMUTH DRIVE TRAVEL LIMITS



Ford Aerospace &  
Communications Corporation  
Western Development  
Laboratories Division

3939 Fabrian Way  
Palo Alto, California 94303

Code Ident. No. 11530

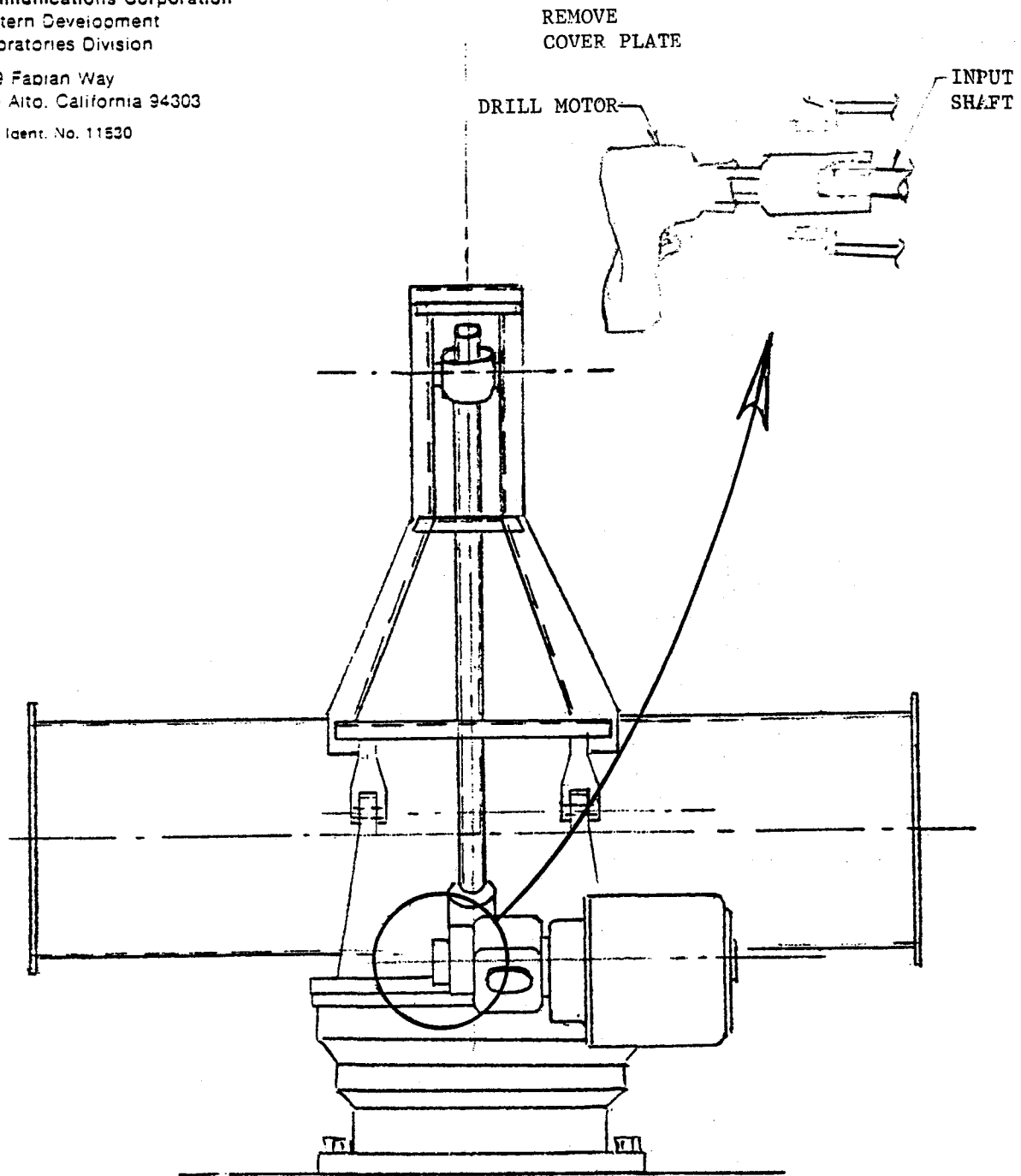


FIGURE 7: ELEVATION DRIVE EMERGENCY OPERATION



Ford Aerospace &  
Communications Corporation  
Western Development  
Laboratories Division

3939 Fabian Way  
Palo Alto, California 94303

Code Ident. No. 11530

NOTE: THE TORQUE IS POSITIVE  
WHEN THE SCREW IS IN TENSION,  
AND TORQUE IS NEGATIVE  
WHEN THE SCREW IS IN COMPRESSION.

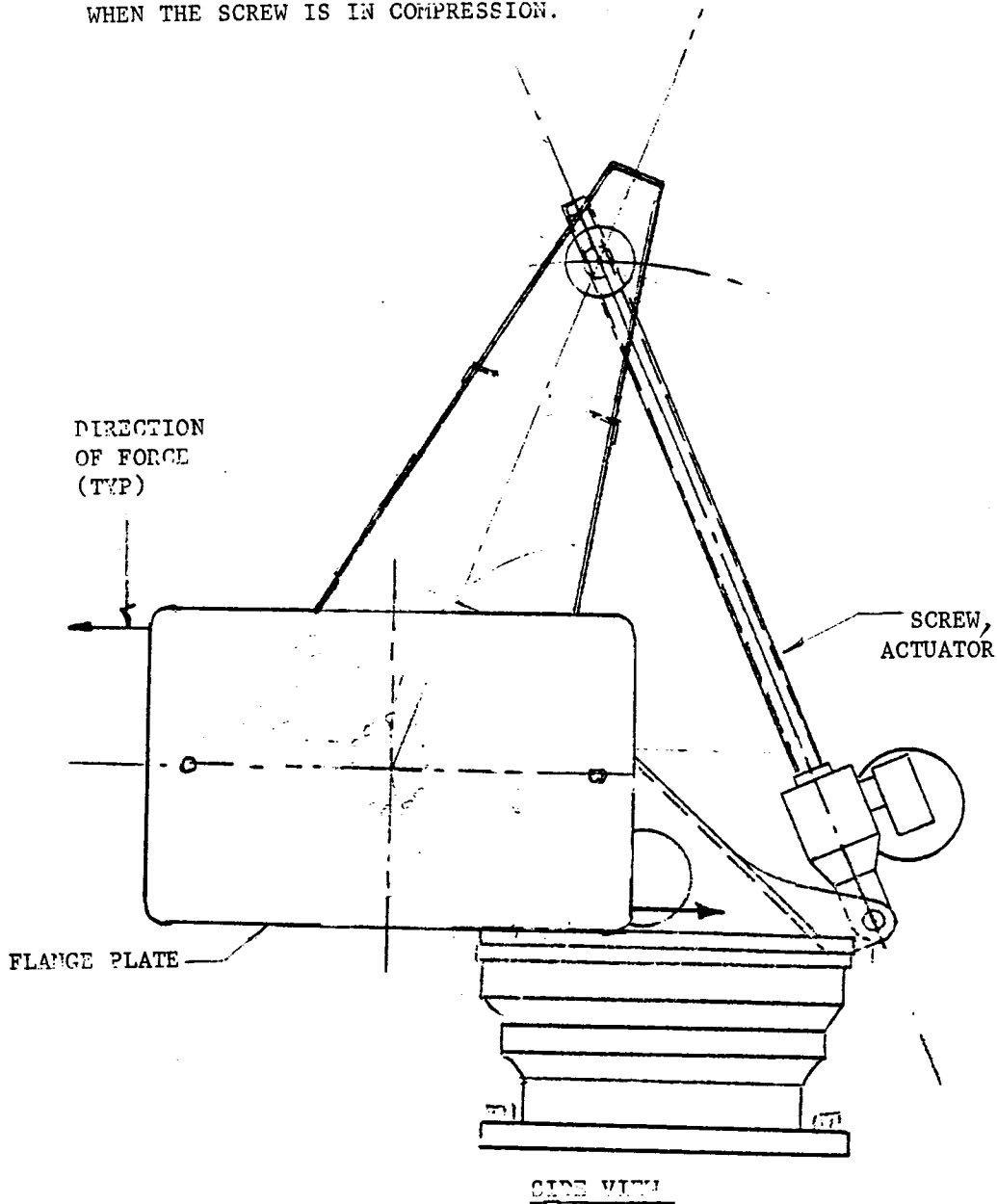


FIGURE 8: ELEVATION DRIVE CAPABILITY UNDER THE MAXIMUM OPERATIONAL LOADS



Ford Aerospace &  
Communications Corporation  
Western Development  
Laboratories Division

3939 Fabrian Way  
Palo Alto, California 94303

Code Ident. No. 11530

NOTE: LOAD SIMILARLY  
AS SHOWN IN  
FIGURE 8.

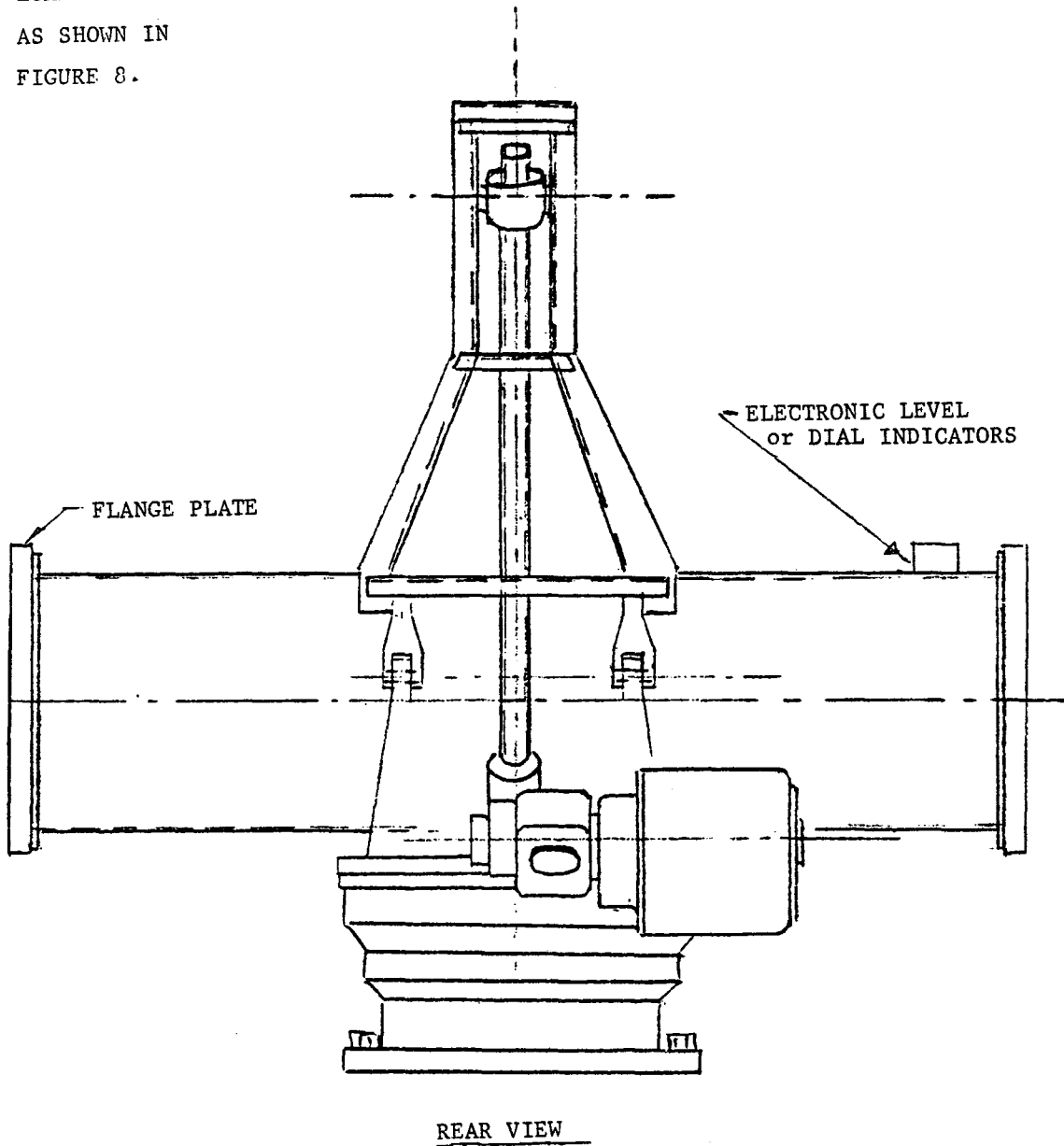


FIGURE 9: STIFFNESS OF ELEVATION



Ford Aerospace &  
Communications Corporation  
Western Development  
Laboratories Division

3939 Fabian Way  
Palo Alto, California 94303

Code Ident. No. 11530

Page 38

DIRECTION OF  
FORCE (TYP)

NOTE: LOAD SIMILARLY  
AS SHOWN IN  
FIGURE 8.

PLAN VIEW

DISPLACEMENT  
GAUGE

CLAMPS

FIGURE 10: ELEVATION SURVIVAL LOAD CAPABILITY

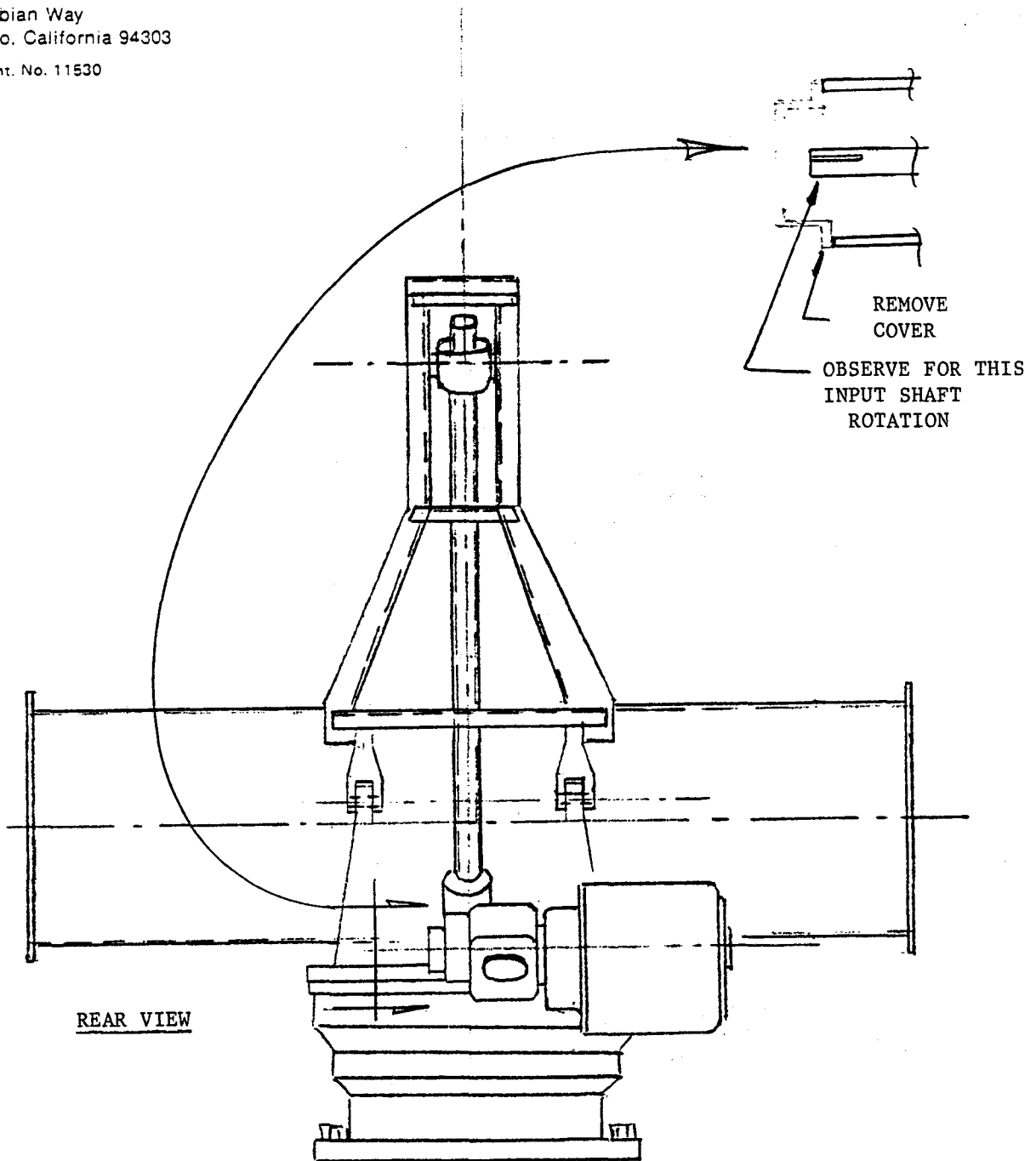




Ford Aerospace &  
Communications Corporation  
Western Development  
Laboratories Division

3939 Fabian Way  
Palo Alto, California 94303

Code Ident. No. 11530



REAR VIEW

FIGURE 11: ELEVATION DRIVE BACKDRIVING



Ford Aerospace &  
Communications Corporation  
Western Development  
Laboratories Division

3939 Fabian Way  
Palo Alto, California 94303

Code Ident. No. 11530

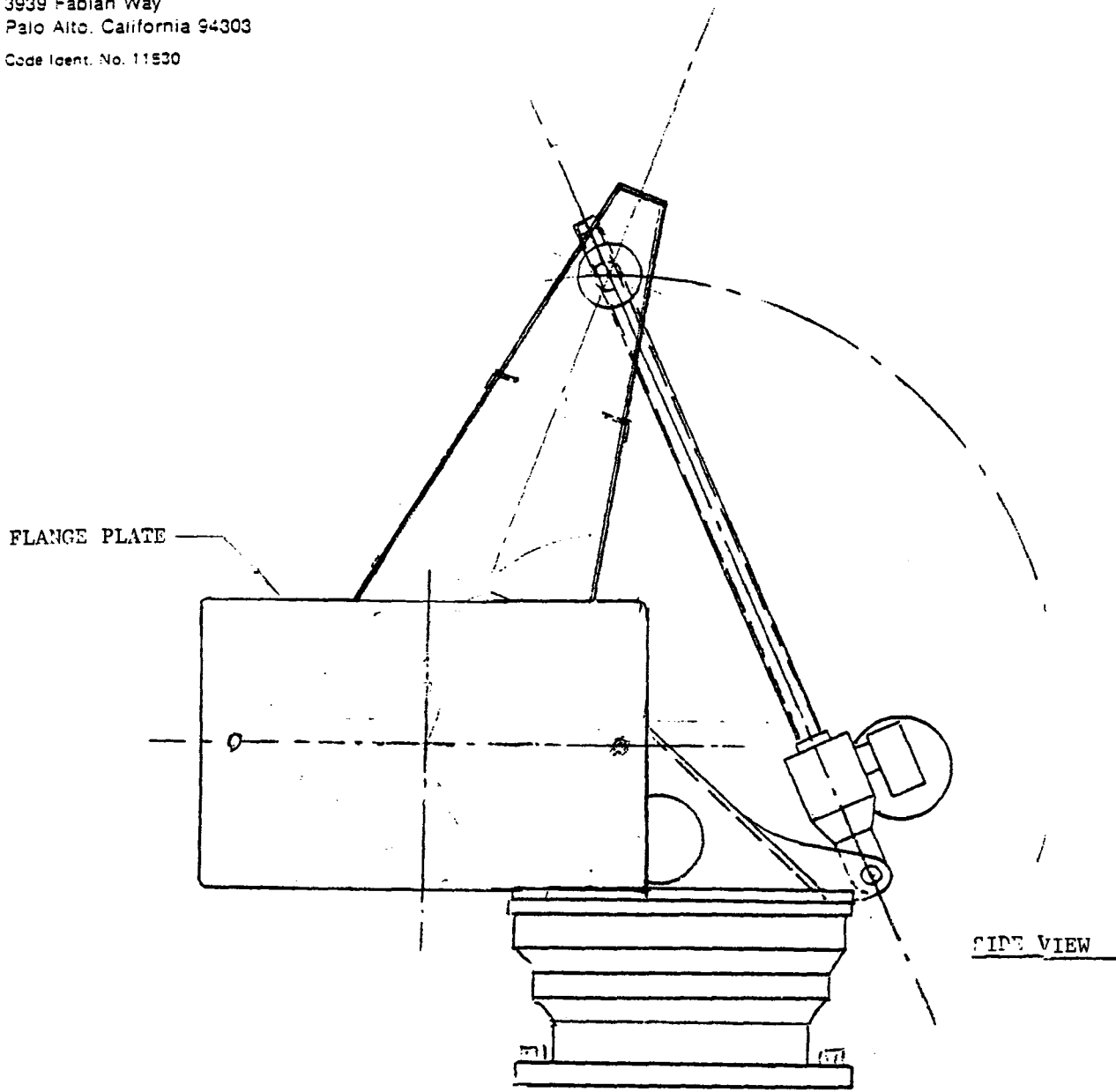


FIGURE 12: ELEVATION DRIVE TRAVEL LIMITS



REPORT E-13

DRIVE MOTOR TRADE STUDIES

FOR

GIMBAL/ACTUATOR DRIVE ASSEMBLY

FOR

BOEING SECOND GENERATION HELIOSTAT

JUNE 27, 1980

Reference: FACC TM08



Ford Aerospace &  
Communications Corporation

## DRIVE MOTOR TRADE STUDY

1.0 INTRODUCTION

The goal of this trade study was to establish the least costly category of motor that would be sufficient to position the azimuth and elevation heliostat axes and fulfill the Boeing performance requirements.

2.0 SUMMARY

Of the various types of motors considered, direct-acting motors such as linear motors and on-axis torquers were rejected as inherently incompatible with the requirements, and brush-type DC and AC motors were not acceptable in terms of life and maintenance. The following categories were considered to be the best candidates and are the subjects of this trade study:

- o Stepper Motors
- o Brushless DC Motors
- o Induction Motors

After initial contacts with motor manufacturers, it became apparent that the desired motor was not available as a standard item and that prices in quantities of 50,000 or more are not readily obtainable - especially on short notice and for a trade study for which no significant quantities would be ordered in the near future. In fact, one manufacturer stated flatly that they had been exercised with this program so frequently during the last several years that they would respond only by purchase order for engineering services at established rates. Therefore, the study had to be conducted with verbal inputs, and the manufacturers were found to be generally quite cooperative.

Extensive discussions with Warner Electric Company, who offers a large stepper motor, stated that they could supply a motor and controller that would fulfill our performance requirements, but with regard to the economy aspect they could not recommend any stepper motor. Their cost estimates for initial acquisition, together with the requisite power supply and 30 year power consumption, confirm their judgement.

Two brushless DC manufacturers responded. Magnetic Technology and PMI Motors both offered an acceptable motor with associated controller, but each required a separate DC power supply. Close correspondence of total acquisition cost, motor plus controller and power supply, was achieved.

The Magnetic Technology total cost was \$229 each and PMI was \$269. However, in order to achieve a valid comparison, the PMI motor would require additional gear reduction, for its shaft speed would be approximately three times that of the other motors; this element would raise the cost of the PMI offering to \$319.

Responses from several induction motor manufacturers indicate that such a motor, with its control elements, could be applied for the least initial cost. Two different manufacturers submitted very similar initial cost estimates, ranging from \$90 to \$99 depending upon the type of motor, including appropriate control elements.

Attempts to quantify the cost of power consumed by the motor and control equipment was only partially successful to date. However, when faced with the task of combining present acquisition costs with future costs for maintenance and power, it was concluded that the power consumption could be considered as a burden on the total energy produced by the heliostat and that the initial cost of the motors and controllers be included as a part of the total heliostat acquisition cost. By forming a ratio of each candidate motor, a measure of salable power per dollar of initial cost is obtained. Then by comparing these ratios, the relative merit of each motor type can be measured without having to project the cost of money over the 30 year period or the value of power consumed. This is particularly important because at high money rates, a small error in initial cost can easily mask the 10¢ per KWH average power cost; at 15% per annum, a one dollar initial cost looks like a sixty-six dollar element.

It should be mentioned that this trade study has utilized elevation axis parameters under the assumption that a motor category with sufficient capability to drive the elevation loads would be representative of the smaller motor required for azimuth as well, and that the category of motor selected would be minimum priced for both axes.

A tabulation of the study results to date is presented in Table I. This shows the initial acquisition price of components for each candidate motor, the estimated power consumption of each, and pertinent remarks. Within the induction motor category, it should be pointed out that the power consumption figures have been extrapolated from experimental data on motors of 5 HP and 1/12 HP ratings and that the large difference indicates an invalid extrapolation.

3.0 CONCLUSIONS

- o 3-phase induction motors were selected as having sufficient performance, moderate efficiency, low risk and low cost.
- o 1-phase PSC induction motors had sufficient performance, moderate efficiency and low cost, but were not selected due to their development risk.
- o Brushless DC motors probably have the best performance and efficiency, however, they are a high risk with insufficient development time and an unknown cost.
- o Stepper motors have low risk but high cost, low efficiency and marginal torque.
- o Brush-type DC and AC motors were not acceptable in terms of life and maintenance.
- o Direct-acting motors such as linear motors and on-axis torquers were rejected as inherently incompatible with the requirements.

TYPE	INITIAL ACQUISITION				PWR. CON. PER DAY	REMARKS
	MOTOR	CONT	PWR. SUPP.	OTHER		
<u>STEPPER:</u> 1. Warner Elec SM-080-0750- FB.	\$150	\$100	100V @ 18A \$200		1.52 KWH	750 RPM
<u>BRUSHLESS DC</u> 1. Mag Tech 2. PMI	\$114 \$120*		28V @ 15A \$110 60V @ 6A \$100	\$50	0.33 KWH 0.29 KWH	*Additional Hi Speed Spur Reduction Req'd ~ \$50
<u>3Ø INDUCTION:</u> 1. Robbins & Myers 289  2. DOERR	\$30-34* \$61	\$38			2.62 KWH	*Open Frame  TENV
<u>PSC INDUCTION</u> 1. Robbins & Myers 249  2. DOERR	\$23-25* \$72	\$18			0.27 KWH	* Open Frame  TENV

TABLE 1



## APPENDIX

1. Elevation and Azimuth Axis Drive Power
2. Motor Life Cycle
3. Vendor Contact
4. Induction Motor Controller

## APPENDIX 1

### Elevation and Azimuth Drive Power

BOEING HELIOSTATELEVATION AXIS DRIVE POWER

Estimate the axis torque required to drive the elevation axis to stow (90° Elev.) from the lowest angle (-3° Elev) as the wind speed increases from 35 MPH at a uniform rate of 0.02 MPH/Sec. Assume that the elevation axis rate is constant at 90°/15 min, that acceleration torque is zero, and that wind and gravity loads per Boeing Appendix pages A2, A25, Figures 3.2.1-1, 3.4.1-1 are only external disturbances (no snow & ice).

1. Use modified Figure 3.2.1-1 to extract wind only curves.
2. Calculate wind speed at each 10° elev. angle.
3. Scale wind torque @ 27 mph to torque at each higher speed.
4. Add gravity component

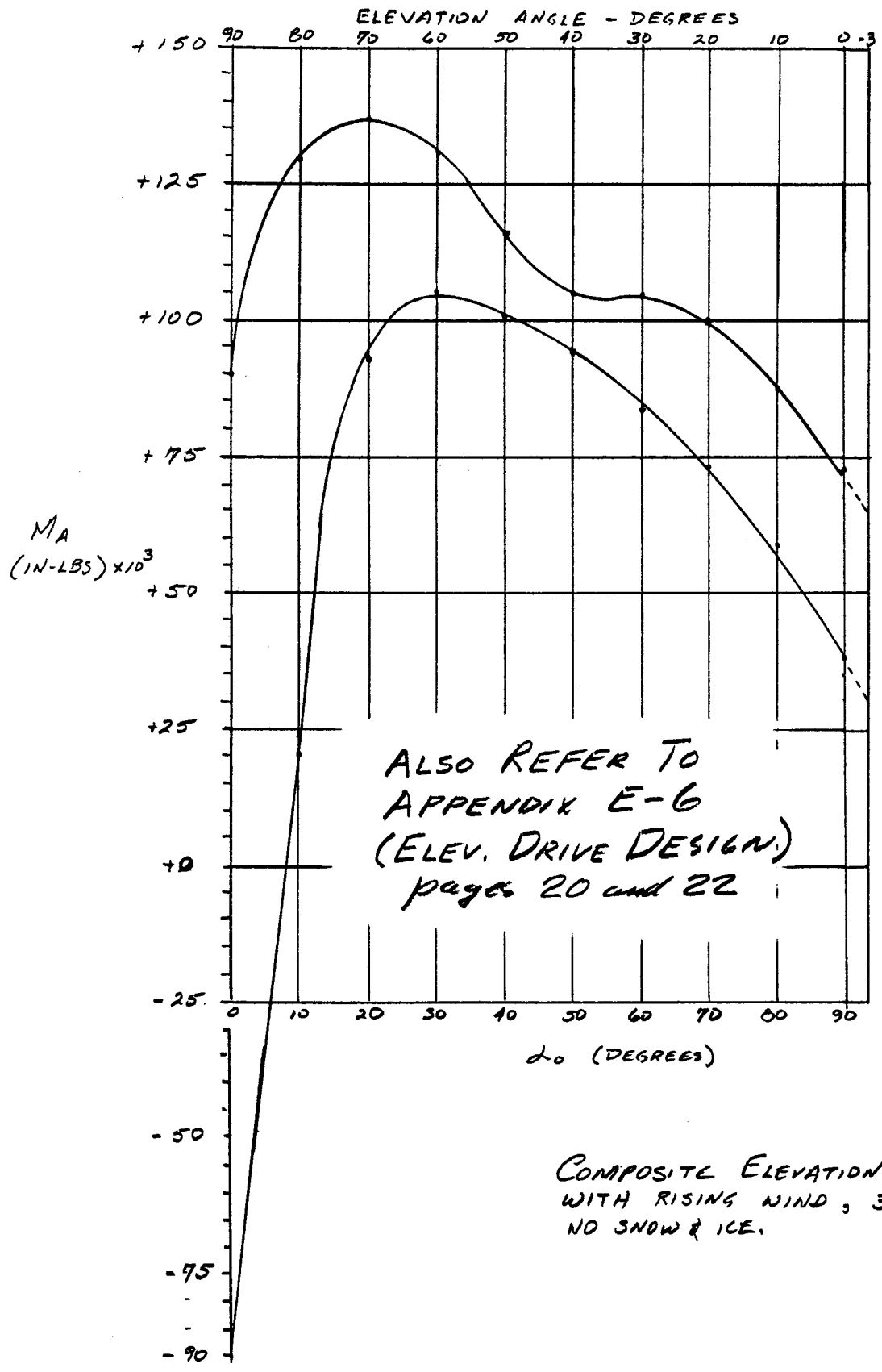
ELEV ANGLE	TIME (SEC)	WIND Δ (MPH)	WIND SPD.	27 MPH WIND RATIO	LO WIND ONLY IN-LB X 10 <sup>3</sup>	SCALED LO WIND IN-LB X 10 <sup>3</sup>	PLUS GRAVITY IN-LB X 10 <sup>3</sup>	HI WIND ONLY IN-LB X 10 <sup>3</sup>	SCALED HI WIND IN-LB X 10 <sup>3</sup>	PLUS GRAVITY IN-LB X 10 <sup>3</sup>
-3°	0	0	35	1.69						
0	30	0.6	35.6	1.71	-10	-17.4	38.0	+10	+17.4	72.8
+10	130	2.6	37.6	1.94	+2	+3.9	58.4	17	33.0	87.5
+20	230	4.6	39.6	2.15	+10	21.5	73.5	22	47.5	99.5
+30	330	6.6	41.6	2.37	+15	35.6	83.5	24	57.0	104.9
40	430	8.6	43.6	2.60	+20	52.0	94.4	24	62.6	105.0
50	530	10.6	45.6	2.85	+23	65.5	101.1	28	80.0	115.6
60	630	12.6	47.6	3.10	+25	77.6	105.3	33	103.0	130.7
70	730	14.6	49.6	3.37	+22	74.0	92.9	35	118.0	136.9
80	830	16.6	51.6	3.65	+3	10.9	20.5	33	120.0	129.6
90	930	18.6	53.6	3.93	-23	-90.0	-90.0	23	90.0	90.0

Plot "Plus Gravity" for both high wind and low wind against elevation; peak axis torque occurs at 70° elevation and is approximately  $137 \times 10^3$  in-lb.

Axis Horsepower is:

$$\frac{1}{60} \times \frac{137 \times 10^3}{12} = 0.0364 \text{ Horsepower}$$

Assuming elevation drive efficiency of 10.3% required motor horsepower is 0.354 H.P. (without acceleration).



AZIMUTH AXIS DRIVE POWER(1) Maximum 35 mph Operation

Since the present operational scenario dictates that azimuth will not be driven to stow in winds above 35 mph until elevation has reached zenith, azimuth wind torques in excess of 35 are not to be considered. In addition, pointing error specifications apply only to 27 mph winds. From Boeing figure 3.2.2-1, peak azimuth axis torque is 20,000 in-lbs. At 35 mph, the torque is  $(35/27)^2 \times 20,000 = 47,000$  in-lbs.

Azimuth rate is  $180^\circ/15$  min., or  $1/30$  rpm, so the peak azimuth horsepower is:

$$\frac{1/30 \times \frac{4700}{12}}{5250} = 0.0249 \text{ Horsepower}$$

If the azimuth drive efficiency is 15%, required motor horsepower is 0.167 H.P. (without acceleration).

(2) Operation Over 35 mph

Regarding the possibility of driving in azimuth at any elevation angle in winds up to 50 mph in order to resolve a possible beam safety scenario, the logic for not increasing the azimuth motor size to account for an "over 35 mph stow condition" follows:

(a) Motors are designed for full duty cycle max 35 mph wind at worst reflector elevation angle and worst wind orientation under step design (repeated on-off operation).

(b) The "over 35 mph stow condition" impacts the azimuth motor for only a short time, and even under the worst elevation and azimuth orientation, the motor should accommodate the increased load without overheating. The stow operation is continuous and not repeated on-off. The motor will drive out of the worst wind orientation if the motor even encounters it.

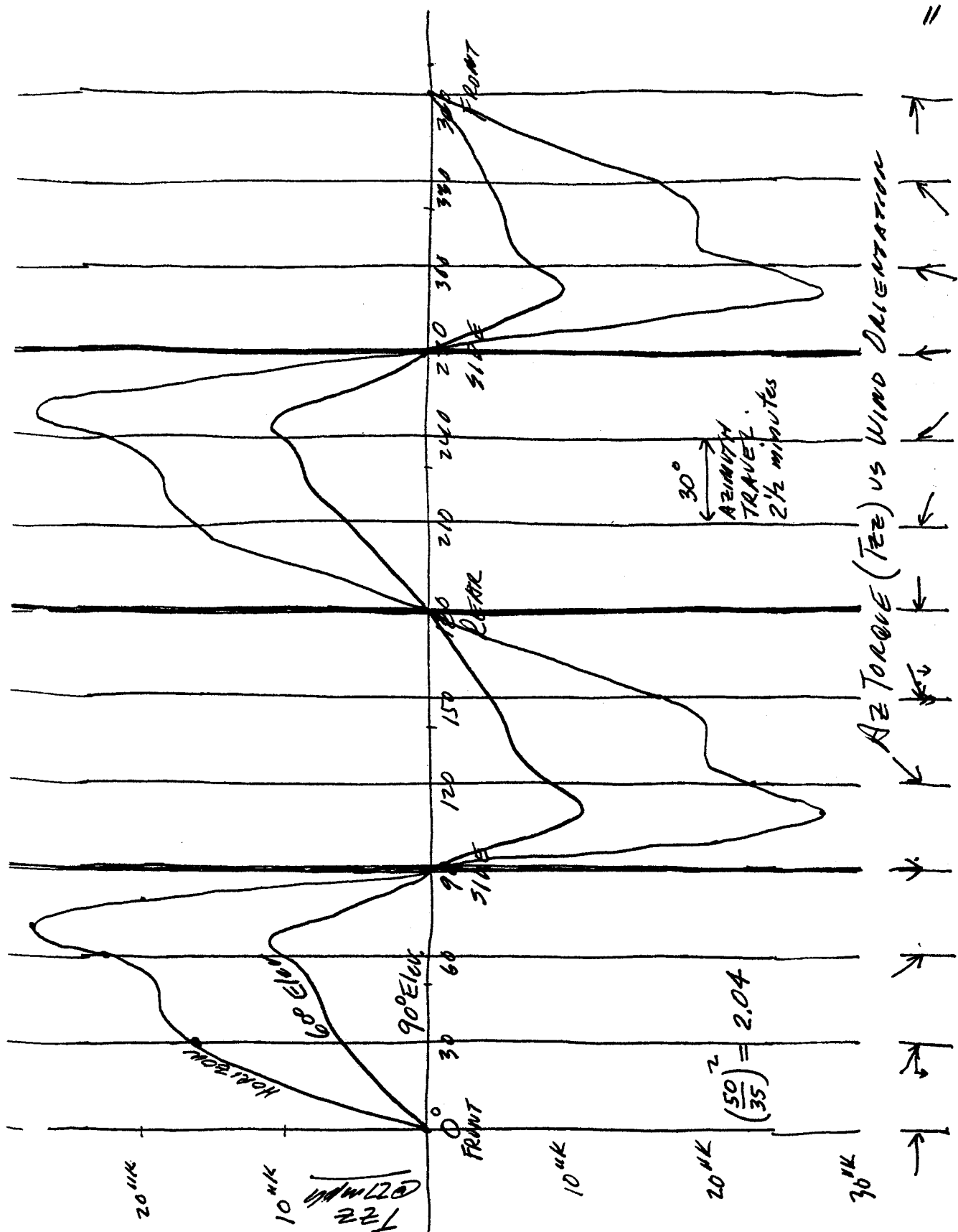
Azimuth torques vs. wind orientation and elevation angle are shown on the next page.

(c) The failure mode consists only of motor overheating, which trips the overheat temperature breaker, and stops the azimuth motion until the temperature reduces; at which time the drive will then continue. The impact on system operation might be an occasional heliostat driving in elevation to zenith stow without first proceeding to the "walk-the-wire" azimuth orientation.

(d) Increased motor size would result in a worst condition during basic "under 35 mph on-off" operation by producing greater heating.

(e) Increased motor size would result in a worst load condition on the azimuth gear system under normal operation.

(f) Increased motor size would increase cost unnecessarily (initial cost plus power consumption life-cycle cost).



APPENDIX 2

Motor Life Cycle

## MOTOR LIFE CYCLE

MOTOR LIFE IS SPECIFIED AS 30 DUTY CYCLES:

360 NORMAL CYCLES:

$$165^\circ \times 4 = 660^\circ = 1.83 \text{ AXIS REVOL EACH DAY}$$

→ 19800 AXIS REVOLUTIONS

72 ADVERSE TRACKING CYCLES:

$$165^\circ \times 4 = 660^\circ = 1.83 \text{ AXIS REVOL}$$

→ 3960 AXIS REVOLUTIONS

49 ALTERNATE STOW CYCLES:

$$165^\circ \times 2 = 330^\circ = 0.91 \text{ AXIS REVOL}$$

→ 1350 AXIS REVOLUTIONS

TOTAL AXIS REVOLUTIONS WILL BE 25,110 REV IN 30 YRS FOR AZIMUTH.

ELEVATION WILL EXPERIENCE THE SAME NUMBER OF CYCLES, BUT EACH CYCLE WILL CONSIST OF AN ANGULAR EXCURSION OF  $96^\circ \times 2$ , OR  $192^\circ$ .

THEREFORE, THE TOTAL ELEVATION AXIS REVOLUTIONS WILL BE:

$$25,110 \times \frac{192}{660} = 7304 \text{ REVOLUTIONS}$$



APPENDIX 3

Vendor Contact

WARNER OFFERS A 750 OZ-IN VARIABLE RELUCTANCE STEP MOTOR WHICH IS CAPABLE OF AN AVERAGE 265 OZ-IN TORQUE AT 750 RPM WITH ONE COIL ENERGIZED OR 530 OZ-IN WITH TWO COILS ENERGIZED. IT IS AN 80 STEP PER REVOLUTION MOTOR. THIS IS EQUIVALENT TO 0.39 HP, AND WOULD BE ADEQUATE FOR THE HELIOSTAT.

INITIAL COST IS ESTIMATED TO BE \$150 EACH MOTOR AND \$100 EACH CONTROLLER IN QUANTITY.

ELECTRICAL POWER CONSUMPTION IS 100 VOLTS @ 9 AMPS PER COIL. FOR A SINGLE REVOLUTION OF THE AXIS, THE TIME DURATION OF POWER CONSUMPTION IS ASSUMED TO BE THE SAME WITHOUT REGARD TO THE TOTAL ELAPSED TIME. THIS TIME IS SPECIFIED TO BE  $93 \frac{1}{15}$  MIN, OR 0.968 REV PER HOUR. DURING THIS TIME, THE MOTOR WILL CONSUME 1800VA, YIELDING A PER REVOLUTION POWER REQUIREMENT OF 1.74 KWH. (OVER THE 30 YEAR LIFE, THIS REPRESENTS 12,723 KWH, OR \$1272 AT 10¢ / KWH.)

SIMILARLY, THE CONTROLLER WILL CONSUME POWER AT A PRESUMED RATE OF  $1.8V \times 9A / COIL \times 2 COILS \times .968 HR$ , OR 31.4 WATT-HOURS/REV. OVER 30 YEARS, THIS IS:

$$31.4 \times 7304 = 229 \text{ KWH}$$

(AT 10¢ PER KWH, THE CONTROLLER WILL COST \$22.91 IN POWER.)

IF THE DC POWER SUPPLY AND LOW-LEVEL ELECTRONICS OPERATE AT 78% EFFICIENCY, THE TOTAL INPUT POWER CONSUMPTION WILL BE:

$$\frac{12,723 + 229}{0.78} = 16,605 \text{ KWH}$$

THUS THE TOTAL INPUT POWER, AT 10¢ PER KWH OVER 30 YEARS WILL COST \$1661.

IN ADDITION TO ACQUISITION COSTS, ROUTINE MAINTENANCE OF POWER SUPPLY AND CONTROLLER COMPONENTS WILL BE REQUIRED. PRIMARY ELEMENTS OF CONCERN ARE ELECTROLYTIC CAPACITORS AND POWER SEMICONDUCTORS. THE BEST ESTIMATE OF COMPONENT LIFE IS 10 YEARS, AT WHICH TIME, REPLACEMENT PARTS TOTALLING 40% OF ORIGINAL ACQUISITION COST WILL BE REQUIRED. SEE TABLE BELOW.

<u>ORIGINAL</u>	<u>ACQUISITION COST</u>	<u>10 YR MAINT</u>	<u>20 YR MAINT</u>	<u>TOTAL</u>
POWER SUPPLY	\$76.50 $\Delta$	\$30.00	\$30.60	\$137.10
CONTROLLER	100.00 $\ddagger$	40.00	40.00	180.00
MOTOR	150.00 $\S$	*	*	150.00
				<u>\$ 467.70</u>

\* 30-YEAR MAINTENANCE ELEMENTS FOR MOTOR IS REPLACEMENT OF BEARINGS EVERY 8000 TO 10,000 HOURS. SINCE THIS IS THE SAME FOR ALL MOTORS, IT IS NOT PART OF THIS COST TRADE.

ADDING POWER CONSUMPTION TO ACQUISITION & MAINTENANCE COSTS YIELDS THE 30 YEAR LIFE CYCLE COSTS:

\$ 467.70  
149.00  
 \$ 616.70

MAGNETIC TECHNOLOGY

By performing a ratio analysis on existing design, Magnetic Technology has projected a brushless DC motor that would satisfy the heliostat requirements. Although it is not an optimized design, it is envisioned as an integral package of motor plus electronics, 4 inches in diameter and  $4\frac{1}{2}$  inches long. Utilizing ceramic magnets, it would cost \$114 in quantity. In addition to the motor, it would require a separate DC power supply of 28V at 15 amperes per motor. Shaft speed would be 1750 RPM, input power is 410 watts and efficiency would be about 65%. (If the efficiency is 65% as stated, the input power for a 1/3 HP motor should be more like  $746/(3 \times .65)$ , or 380 watts). Maintenance costs for the motor, excluding electronics, would consist of bearing replacement at the same frequency as any other motor under the same service: other than this, they could not estimate a life cycle cost. (Power supply and controller will require maintenance). Cost of power over 30 years is estimated from the 7304 revolutions at  $.25 \text{ Hr}/96^{\circ}$  times  $360^{\circ}/\text{revolution}$ , and 410 watts. This yields a 30 year motor power consumption of 2807 KWH. Assuming the power supply efficiency to be 78%, the input line power would be 3599 KWH; at 10¢ per KWH, this yields a 30 year power cost of \$360.

PMI MOTORS, KOLLMORGEN CORPORATION

PMI has developed a brushless DC motor and associated power control electronics which they recommend for the heliostat drive. This motor is in component form; it is a 12 CM diameter pancake motor with printed circuit rotor. The stator is a separate metal shell housing ferrite magnets. Being a motor in component form, there are no bearings. The gearbox shaft would support the rotor and the gearbox case would support the stator. Control electronics would be packaged in two parts. Power switches would be mounted on a heat sink and logic level electronics would be mounted on a separate card. These electronics would accept a computer command to go or stop and a command for which way to go, with the motor responding with a full speed slew in the appropriate direction and dynamic braking to a stop (resistor sink of back EMF). Because this requirement is at the upper end of the PMI horsepower range, they offered a 60 oz-in motor at 6000 RPM. This necessitates a 3 or 4 to 1 gear ratio between the motor and the gimbal gearbox, and the associated cost must be included in the motor element. In addition, a DC power supply capable of 6 amperes at 60 volts is necessary.

Power consumption per motor would be 360 watts per motor. At the same axis rate and number of axis revolutions as the other motors, this would consume  $0.360 \text{ KW} \times .938 \text{ Hr/Rev} \times 7304 \text{ Rev}$ , or 2466 KWH. If the power supply is 78% efficiency, the input power will be 3162 KWH. Cost of the motor with control electronics is estimated to be \$120 in quantity, and they would be in stock (the basic design in standard form) at PMI by February 1980.

ACME ELECTRIC

Acme Electric manufactures ferroresonant power supplies and has a standard item that approximates the 28V at 15 amp rating for one of the brushless DC motors. It costs \$230 each and estimated to cost 50% of that in large quantities, or \$115. It operates at 78% efficiency and has a calculated MTBF of 200,000 hours, per MIL-HDBK-217. Output is inherently regulated but varies 1.3% per cycle. Maintenance over 30 years might require replacement of an AC capacitor at \$10 each. Price in quantity for the other supplies is a linear function of output power, so:

$$100V @ 18A = \frac{1800}{28 \times 15} \times \$115 = \$493$$

$$60V @ 6A = \frac{360}{28 \times 15} \times \$115 = \$99$$

At 78% efficiency, losses would increase the input power to 1.28 KVA for each KVA of output.

NSE

This company manufactures power supplies and responded with estimates for unregulated units for each of the candidate DC motors:

<u>Rating</u>	<u>Price</u>	<u>Efficiency</u>	<u>MTBF</u>	<u>Leakage</u>
100V @ 18A	\$200	80 - 85%	100,000 hrs	5% F.L.
28V @ 15A	\$100	75 - 80%	200,000 hrs	5% F.L.
60V @ 6A	\$100	75 - 79%	200,000 hrs	5% F.L.

BODINE ELECTRIC COMPANY

Bodine is a manufacturer of fractional and sub-fractional AC and DC motors. Data was not available initially for this trade study, but actual prototype units were procured per the developed 3Ø induction motor specification.

ROBBINS & MYERS

Robbins and Myers is a manufacturer of fractional horsepower motors for OEM markets. They exhibited considerable interest in this effort and offered a permanent - split - capacitor motor in their performance group 249 and a three-phase motor in performance group 289. These would be approximately \$35 each in quantity in open-house construction and twice that amount in TENV.

UNIVERSAL ELECTRIC COMPANY

This subsidiary of ESB Inc. manufactures induction motors for OEM customers exhibited considerable interest in the application. They offer the capability to produce these motors in the quantities required but were not able to establish a price within the time available. However, after telephone discussions of the heating, life, and power consumption aspects of this application, they suggested that we conduct experiments on a sample motor, for they had no comparable experience. They will supply the motor by the first week of January.

INTERNATIONAL RECTIFIER

Solid state switches for control of induction motors are available from I.R. For the permanent-split-capacitor motor with 115V at 9.2 amps locked rotor current, the D1210 should perform well without exceeding its PRV on half-wave plug stop. However, for the 230V three-phase motor, a D2410 would suffice only if it was specified to have a 600 volt PRV rating (avail at no extra cost).

These devices are estimated to cost in quantity:

D1210	\$7.00
D2410	\$9.50
D2425	\$10.00

For a 3-phase motor, four switches are necessary, and for a permanent-split-capacitor motor, only two switches are required.

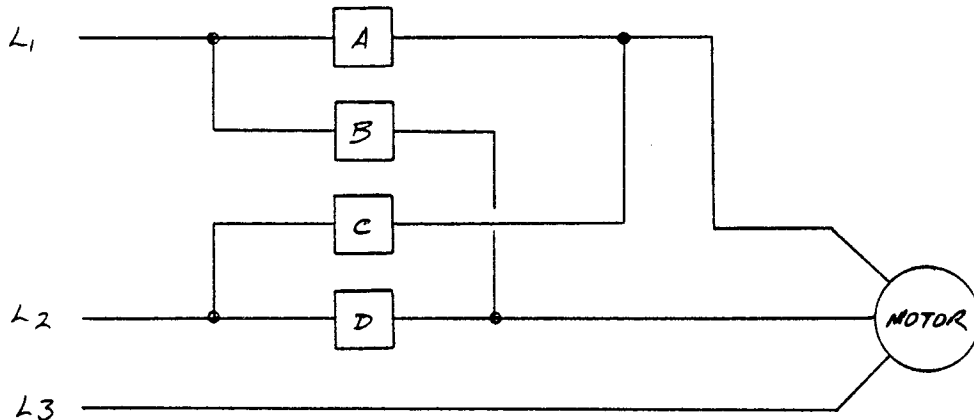


**APPENDIX 4****Induction Motor Controller**

INDUCTION MOTOR CONTROLLER

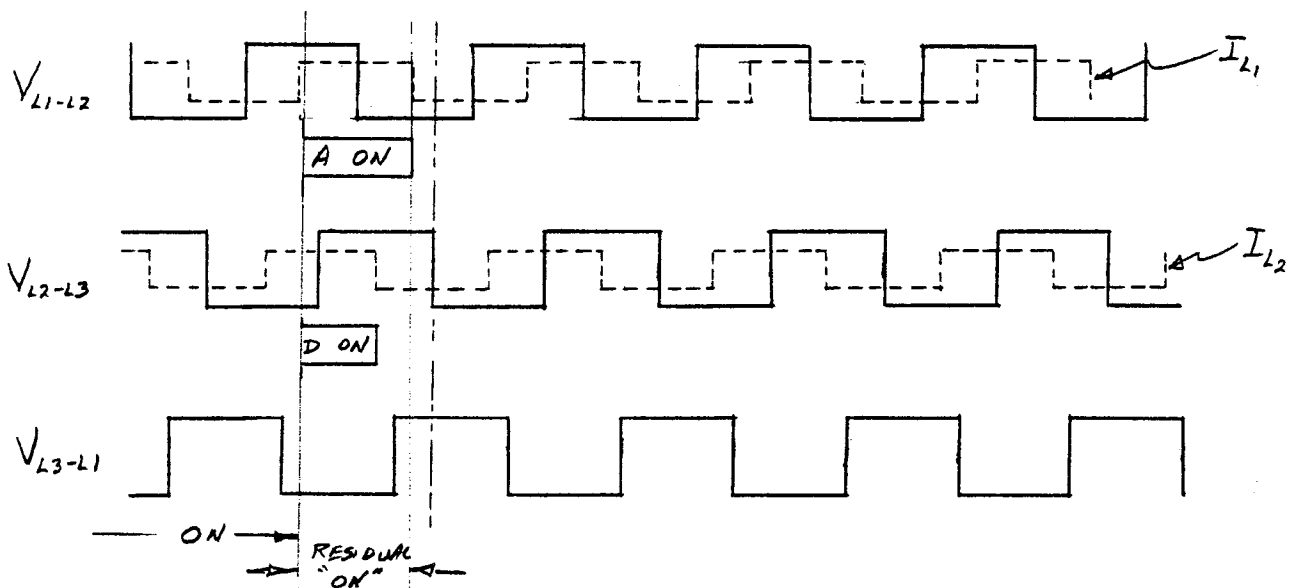
DETERMINE SMALLEST PRACTICAL GUARD BAND FOR THREE-PHASE ZERO-CROSSING CONTROLLER.

ZERO CROSSING, SOLID STATE SWITCHES TURN ON AS LINE VOLTAGE CROSSES ZERO & TURN OFF AS CURRENT CROSSES ZERO. THEREFORE, IT IS IMPERATIVE THAT A PARTICULAR SWITCH ASSUME ITS NON-CONDUCTIVE STATE BEFORE ITS COMPANION SWITCH IS ALLOWED TO TURN ON IF LINE-TO-LINE SHORTS ARE TO BE AVOIDED. SEE THE DIAGRAM BELOW.



IF THE MOTOR IS ROTATING IN RESPONSE TO S.S. SWITCHES A & D BEING "ON", WHAT IS THE EARLIEST TIME, AFTER REMOVING THE "ON" COMMAND TO A & D, THAT COMMANDS TO B & C CAN BE ISSUED?

SKETCH LINE-TO-LINE VOLTAGES AND ASSOCIATED LINE CURRENTS (ASSUMING WORST-CASE LAG):



D. McCauley 5 DEC 79

BOEING HELIOSTAT

24 24

### INDUCTION MOTOR CONTROLLER

THE SCHEMATIC DIAGRAM ILLUSTRATES POTENTIAL LINE-TO-LINE SHORT BETWEEN ONLY L1 AND L2, SO ONLY  $V_{L1-L2}$  IN THE TIMING DIAGRAM NEED BE CONSIDERED. THUS, IF A AND D ARE INITIALLY "ON" AND THE "ON" COMMAND IS REMOVED JUST AFTER VOLTAGE ZERO CROSSING, A WILL REMAIN ON  $1/2$  CYCLE PLUS THE CURRENT LAG ( $\cos^{-1}$  P.F.). THIS IS LIMITED TO A TOTAL OF  $3/4$  CYCLE FOR A POWER FACTOR OF ZERO. THUS, B AND C SHOULD NOT RECEIVE AN "ON" COMMAND UNTIL JUST BEFORE THE START OF THE NEXT CYCLE.



REPORT E-14

ELECTRICAL DRIVE CONTROL CONFIGURATION

FOR

GIMBAL/ACTUATOR DRIVE ASSEMBLY

FOR

BOEING SECOND GENERATION HELIOSTAT

JUNE 27, 1980

Reference: FACC TM14



**Ford Aerospace &  
Communications Corporation**

## 1.0 INTRODUCTION

The purpose of this appendix is to document the electrical drive motor and control configuration suggestions presented for the Boeing Heliostat. This configuration includes TTL dynamic braking logic, limit circuits, motor and motor control switches, and motor protective devices.

## 2.0 DISCUSSION

Pre-limit switches can be employed to stop the drive at travel ranges in excess of  $\pm 180$  degrees. To reduce the travel range to less than  $\pm 180$  degrees, the sector switch (S3) would be eliminated.

Optical isolators are employed to permit location of the logic electronics some distance from the pedestal and limit switches.

In addition (or alternate) to the pre-limits, a final limit arrangement can be devised which utilizes a cable-wrap lanyard terminated at the motor starter. With the lanyard properly adjusted and its upper end attached to the rotating part of the gimbal, excessive azimuth rotation will wrap the lanyard about the pedestal and pull the starter into the "off" position. If if is desired, a spring in the lanyard would permit operator override of the final limit.

Motor protection, line disconnect, and line protection is offered by the motor starter. It is recognized that this device, utilizing relatively slow thermal elements will not protect the solid-state relays from short-period, high current surges, the occasional loss of a relay is considered acceptable. Use of metaloxide varistors across the motor leads would mitigate the surge problem. The General Electric V250LA15A should be adequate for either motor.

The attached pages present the following data:

- o Prototype drive controls, single axis schematic, diagrams and notes.
- o Azimuth cable-wrap lanyard.
- o Parts list, prototype drive control.
- o Elevation drive motor specification.
- o Azimuth drive motor specification.

- o Azimuth drive inertia.
- o Reference PHC synchronization.
- o Alternate final limit.

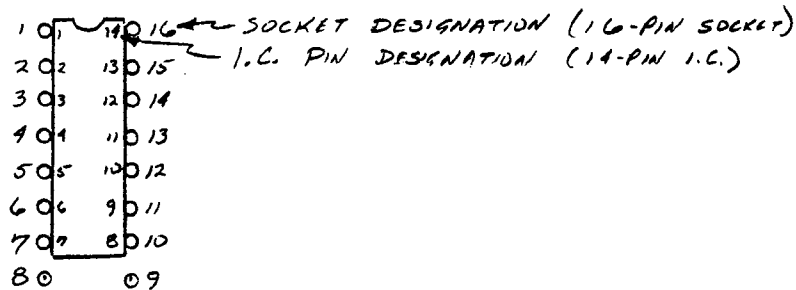
D.D. MCCAULEY 24 JAN 80

BOEING HELIOSTAT  
 PROTOTYPE DRIVE CONTROLS  
 SINGLE AXIS SCHEMATIC

REVISED 29 JAN 80

NOTES FOR MOTOR CONTROL DIAGRAM

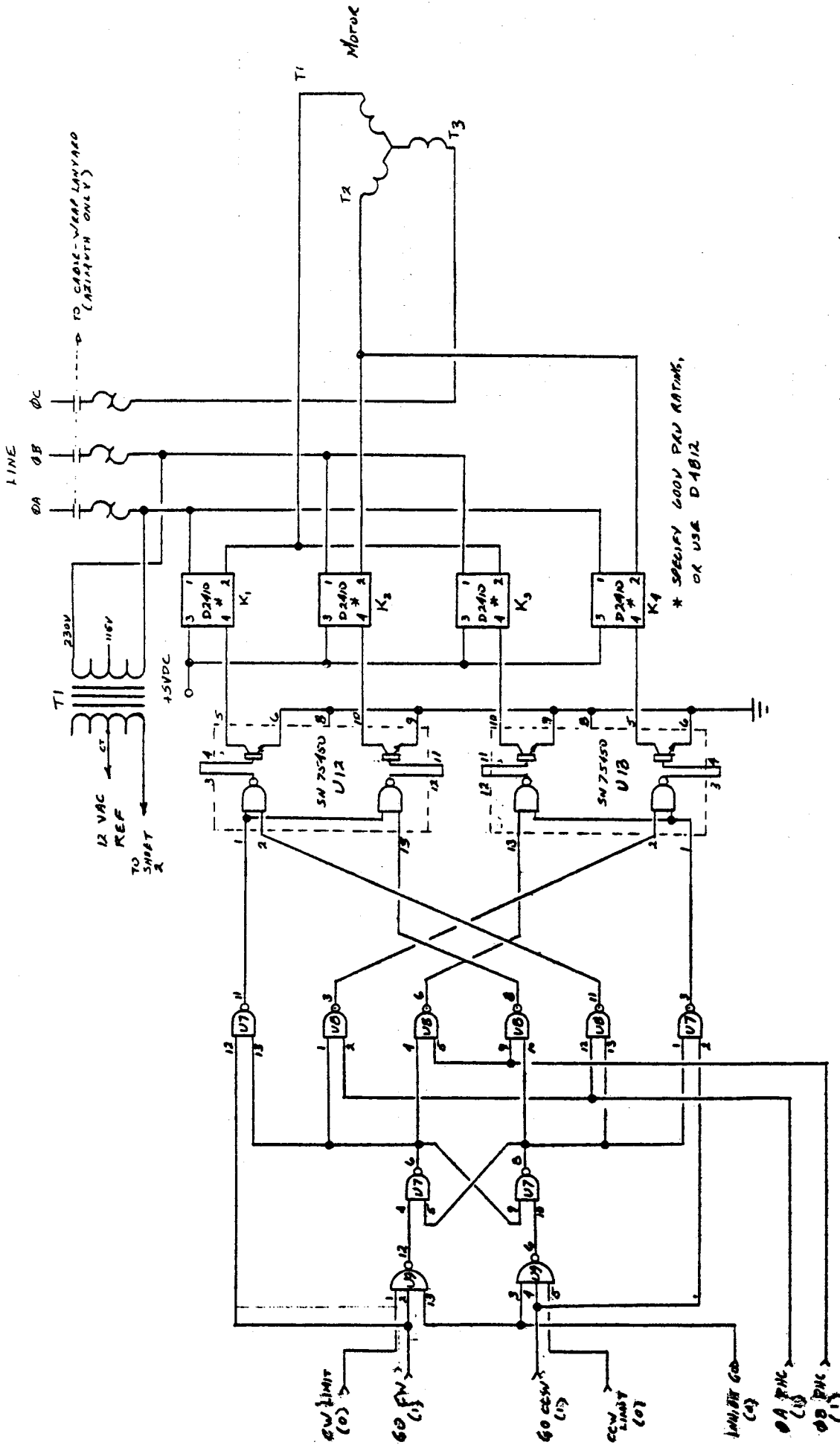
1. I.C. PIN DESIGNATIONS ARE FOR I.C. CHIP. WHERE 14-PIN CHIP OCCUPIES A 16-PIN SOCKET, INSERT CHIP WITH PIN 1 IN SOCKET 1 AND INCREMENT SOCKET NUMBERS BY 2 FOR ALL NUMBERS OF 2 THROUGH 14:



2. MOUNT SOLID STATE RELAYS ON HEAT SINKING SURFACE, USING THERMAL COMPOUND (WAKEFIELD TYPE 120 OR EQUIV.)
3. LIMIT CIRCUITS SHOWN ARE FOR AZIMUTH ONLY. FOR ELEVATION, DELETE SWITCHES  $S_1, S_2$  &  $S_3$ , RESISTORS  $R_1$  &  $R_2$ , OPTICAL LOGIC GATES  $U_{10}$  &  $U_{11}$ , AND TIE LIMIT INPUTS AT  $U_9-1$  &  $U_9-5$  TO +5VDC.
4. USE PRECAUTIONS OUTLINED IN NOTE 1 ABOVE WHEN WIRING 8-PIN I.C.'S  $U_{10}$  &  $U_{11}$ .
5. UNUSED SECTIONS OF I.C.'S:
- |      |               |               |
|------|---------------|---------------|
| 7400 | $U_6$         | ONE GATE      |
| 7410 | $U_1$ & $U_9$ | ONE GATE EACH |
| 7420 | $U_{11}$      | ONE GATE      |
6. DC POWER REQUIRED IS 5VDC  $\pm$  0.5V AT APPROXIMATELY 300 MA PER AXIS.
7. CONNECT SAFETY GROUND ACROSS CABLE-WRAP & BEARINGS
8. MODIFY AZIMUTH MOTOR STARTER TO PROVIDE TRAVEL LIMIT PROTECTION. SEE SEPARATE SKETCH.







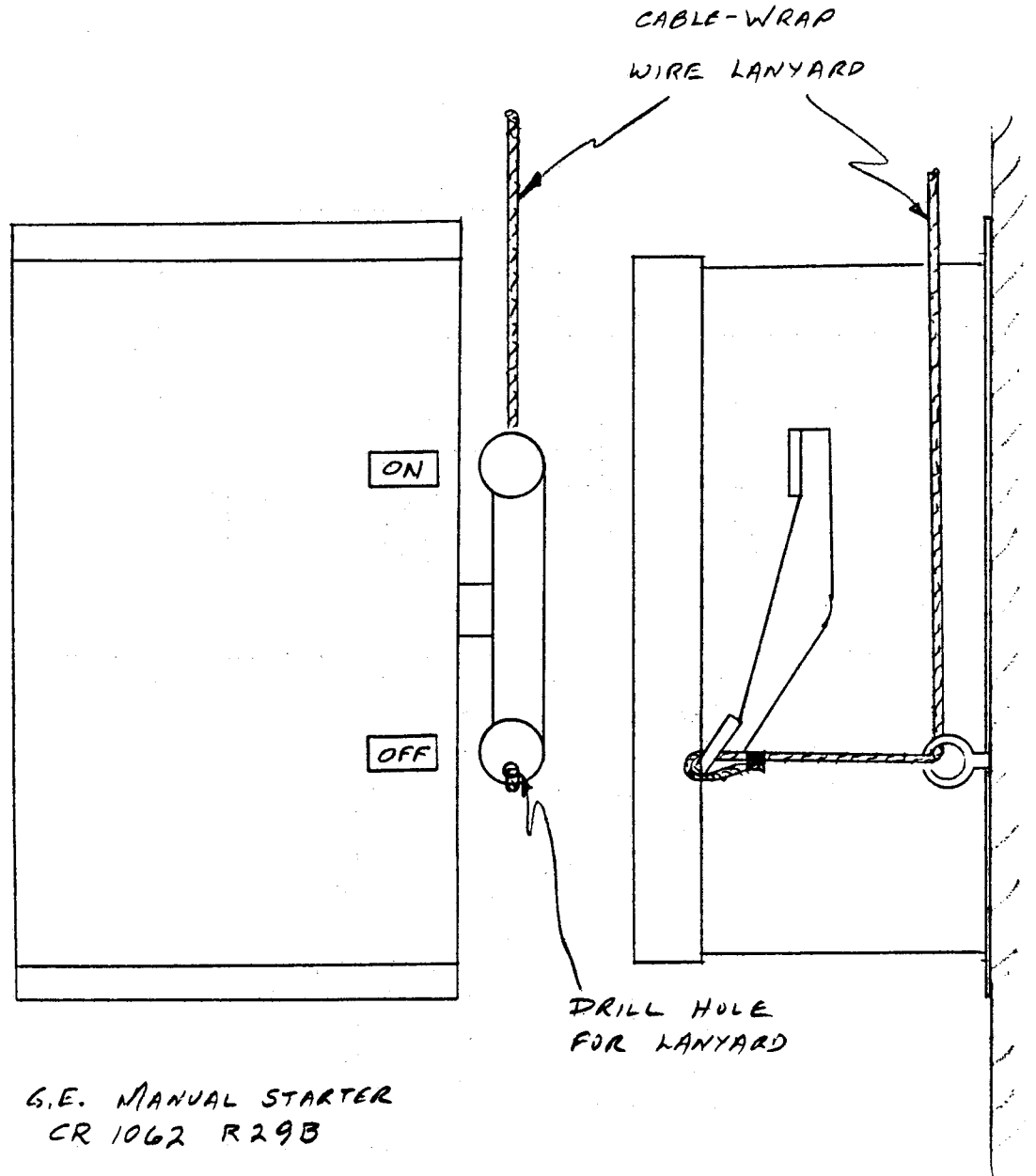
BOEING HELICOSTAT  
 PROTOTYPE DRIVE CONTROLS  
 SINGLE AXIS SCHEMATIC  
 D.D. MCCAWLEY 24 JAN 60  
 REVISED 29 JAN 60

\* SPECIFY 600V PIV RATINGS,  
 OR USE D1812

D. McCauley 28 JAN 80

BOEING HELIOSTAT  
PROTOTYPE DRIVE CONTROLS  
AZIMUTH LIMIT PROTECTION

DRAWING NO. 1062 R29B  
JOB NO. 1062 R29B



DRAWN BY DATE

PROTOTYPE DRIVE CONTROL  
PARTS LIST

SHEET NO. OF

JOB NO.

REVISED 29 JAN 80  
21 FEB 80

DESCRIPTION	AZIMUTH	QTY	ELEVATION	QTY
1. SOLID STATE SWITCH K <sub>1</sub> THRU K <sub>4</sub>	INT. RECT. D4B12	4	INT. RECT. D4B12	4
2. TRANSFORMER T <sub>1</sub>	TRIAD F3116X OR EQUIV.	1	TRIAD F3116X OR EQUIV.	1
3. MOTOR STARTER HEATERS	GENERAL ELECT. CR 1062 R293 TBD	1 3	GENERAL ELECT. CR 1062 R293 TBD	1 3
4. DRIVER U <sub>12</sub> , U <sub>13</sub>	75450	2	75450	2
5. 3-INPUT NAND GATE U <sub>1</sub> , U <sub>9</sub>	7410	2	7410	2
6. HEX INVERTER U <sub>2</sub> , U <sub>3</sub>	7404	2	7404	2
7. 2-INPUT NAND GATE U <sub>4</sub> , U <sub>5</sub> , U <sub>6</sub> , U <sub>7</sub> , U <sub>8</sub> ,	7400	5	7400	5
8. UP-DOWN COUNTER U <sub>10</sub>	74193	1	74193	1
9. 4-INPUT NAND GATE U <sub>11</sub>	7420	1	7420	1
10. RESISTOR R <sub>1</sub>	1200Ω 1/2W, 5%	1	1200Ω 1/2W, 5%	1
11. LIMIT SWITCH S <sub>1</sub> & S <sub>2</sub>	MICROSWITCH 1 LS1	2	-	0
12. LIMIT SWITCH S <sub>3</sub>	MICROSWITCH 6 LS1	1	-	0
13. DIODE, ZENER CR <sub>1</sub>	1N751	1	1N751	1
14. RESISTOR, 390Ω R <sub>2</sub> , R <sub>3</sub>	390Ω 1/2W, 5%	2	-	0
15. OPTICAL LOGIC GATE U <sub>10</sub> , U <sub>11</sub>	GENERAL INST. MCL 601	2	-	0
16. MOTOR	TBD	1	TBD	1
17. —	—	—	—	—
18. ADAPTOR PLUG	AUGAT G16-BG2 OR EQUIV.	1	AUGAT G16-BG2 OR EQUIV.	1
19. PACKAGING PANEL	AUGAT B136-PG 21 OR EQUIV.	1	SAME AS AZIMUTH	1





## AZIMUTH DRIVE

AXIS INERTIA REFLECTED THROUGH THE GEAR TRAIN IS:

$$100,000 \text{ LB-IN}^2 \div (108,000)^2 = 0.855 \times 10^{-3} \text{ LB-IN}^2$$

ESTIMATED MOTOR INERTIA FOR ROTOR:

$$J = \frac{1}{2} MR^2 = \frac{1}{2} D \pi R^4 L$$

$$D = .293 \text{ LB/IN}^3$$

$$R = 1" \quad (\text{EST MIN})$$

$$L = 2" \quad (\text{EST MIN})$$

$$J = \frac{1}{2} (.293) \pi (1)^4 \cdot 2$$

$$= 0.92 \text{ LB-IN}^2$$

THIS REPRESENTS THE SMALLEST ANTICIPATED MOTOR INERTIA, AND WHEN COMPARED TO THE REFLECTED LOAD INERTIA, IT IS FOUND TO BE OF THE ORDER OF  $10^3$  TIMES AS MUCH AS THE LOAD INERTIA. THUS, THE SYSTEM ACCELERATION TORQUE WILL BE PREDOMINANTLY THAT FOR THE MOTOR AND GEARBOX INPUT COMPONENTS.

ESTIMATE OF GEARBOX INPUT COMPONENT INERTIA IS:

SHAFT & WORM - 5/8" DIA X 6" LONG

$$J = 0.03 \text{ LB-IN}^2$$

COUPLING - 1.2" DIA X 1.5" LONG

$$J = 0.09$$

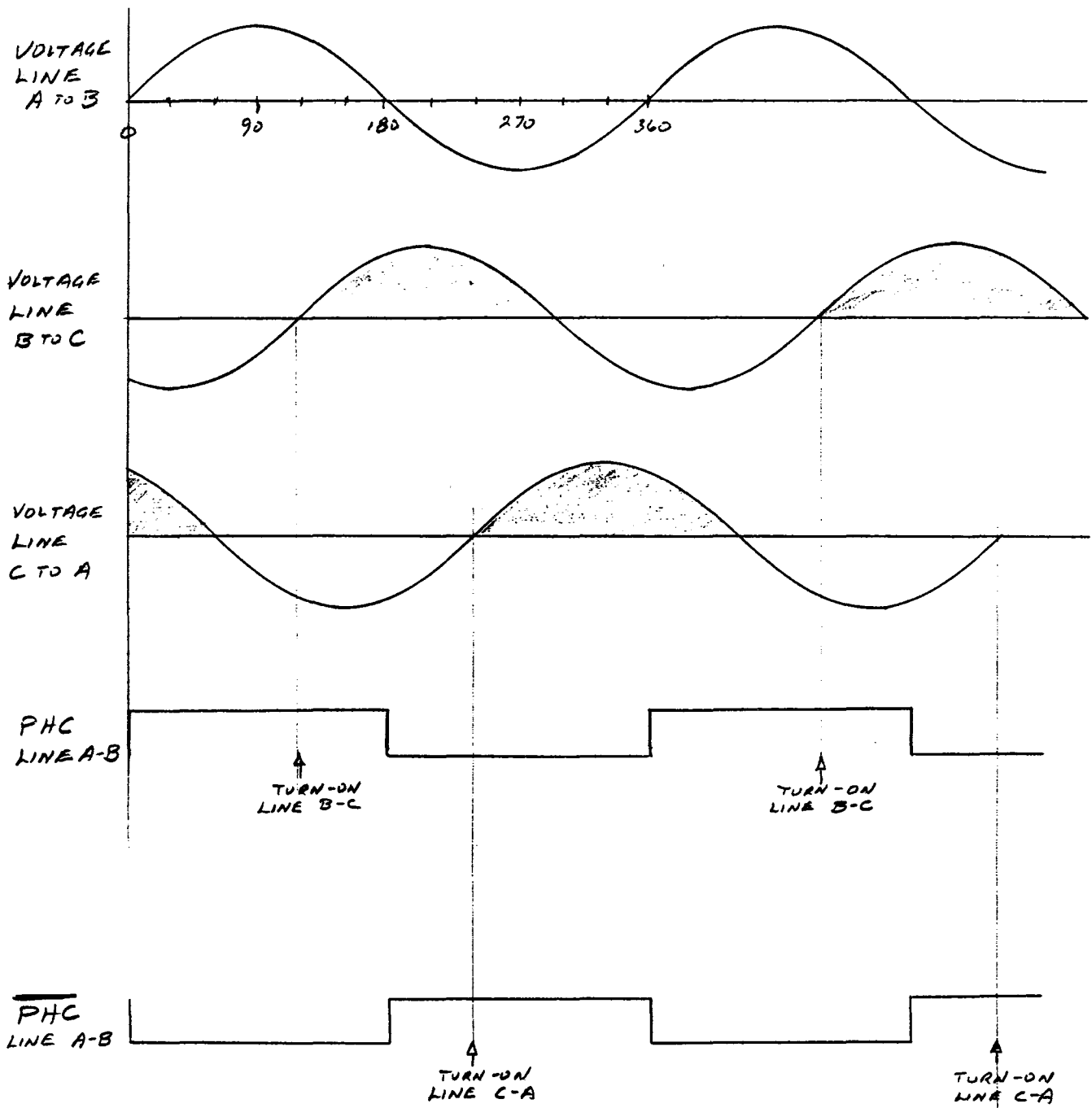
TOTAL

$$0.12 \text{ LB-IN}^2$$

THIS TOTAL, TOGETHER WITH THE REFLECTED LOAD INERTIA IS STILL  $0.12 \text{ LB-IN}^2$ , OR 13% OF THE MOTOR INERTIA.

D. McCauley 21 JAN 80 BOEING HELIOSTAT

REFERENCE PHC SYNCHRONIZATION

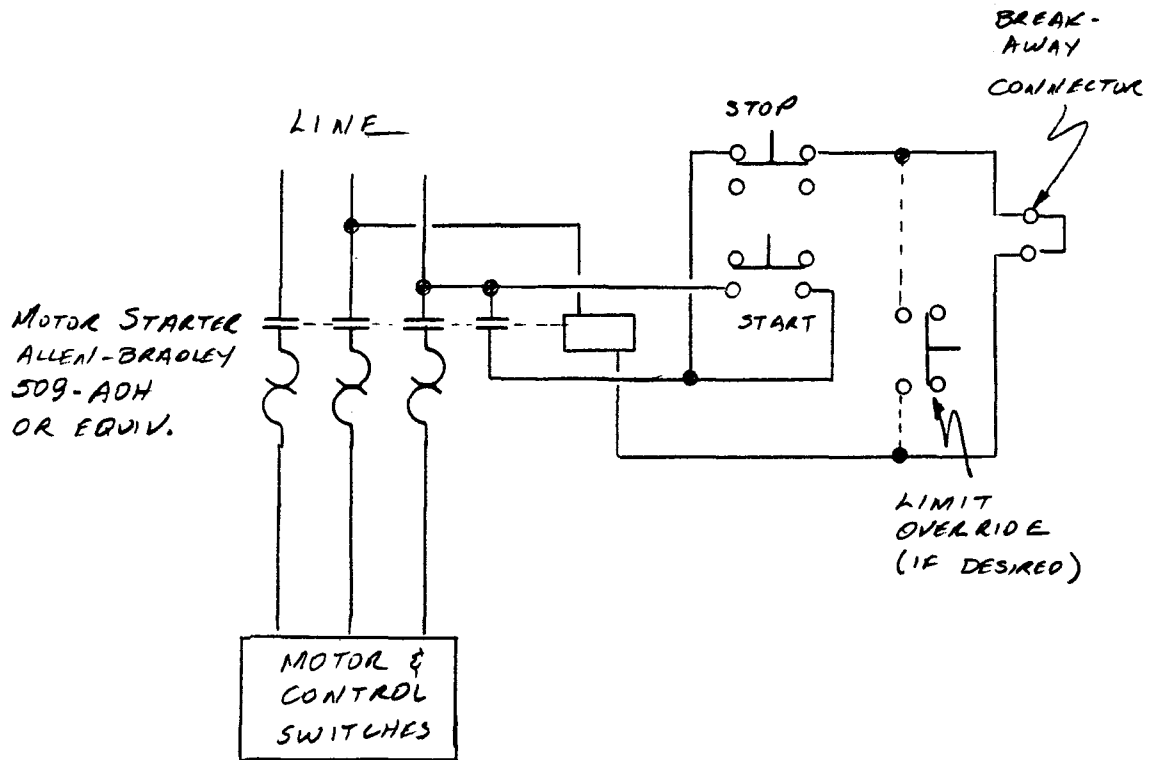


THE DIAGRAMS ABOVE ILLUSTRATE THE RELATIONSHIP BETWEEN REFERENCE PHC PULSES DERIVED FROM LINE A-B VOLTAGE AND DYNAMIC BRAKING PULSES. ZERO CROSSING OF LINE B-C OCCURS WHILE PHC IS HIGH (60° BEFORE THE TRAILING EDGE OF PHC). SIMILARLY, THE INVERSE OF PHC RISES 60° BEFORE ZERO CROSSING OF LINE C-A. THEREFORE, A SINGLE TRANSFORMER CONNECTED ACROSS LINES A & B CAN BE UTILIZED TO GENERATE THE REQUISITE PHC PULSES AND IT HAS AN INHERENT PHASE SHIFT TOLERANCE OF ± 60° OF LINE CYCLE.



D. McCawley BOEING HELIOSTAT  
PROTOTYPE  
ALTERNATE FINAL LIMIT

AS AN ALTERNATE TO THE EXPENSIVE WEATHER PROOF  
MANUAL MOTOR STARTER, AN OPEN TYPE MAGNETIC  
MOTOR STARTER AND BREAK-AWAY CABLE COULD BE  
EMPLOYED:





REPORT E-15

SENSOR SELECTION

FOR

GIMBAL/ACTUATOR DRIVE ASSEMBLY

FOR

BOEING SECOND GENERATION HELIOSTAT

JUNE 27, 1980

Reference: FACC TM12



Ford Aerospace &  
Communications Corporation

CONTENTS

1.0	Introduction and Summary
2.0	Requirements
3.0	Sensor Categories
4.0	Magnets
5.0	Hall Effect Sensors
6.0	Revolution Count Sensor Arrangement
7.0	Sprague/Microswitch Sensors
8.0	Mounting the Hall Effect Sensors and Magnet
9.0	Warning Time
10.0	Incremental Pulse Width
Appendix I	Microswitch Sensor Data
Appendix II	Sprague Sensor Data
Appendix III	Hicorex Magnet Data (Hitachi Magnetics Corp.)

## 1.0 INTRODUCTION AND SUMMARY

This study is intended to find a suitable sensor for zero reference and for revolution count measurements. Various devices available in the market are explored. They are analyzed as regards to their measurement accuracy, applicability and cost.

The sensor categories are investigated with the following conclusions:

- o The Hall Effect sensors responding to a magnetic field were selected as the least costly, and further analyzed and tested for performance.
- o Optical encoders are the most accurate devices in the market today, but not considered further for heliostat application due to their huge cost.
- o The manufacturers and specifications of various proximity switches were investigated, but due to cost constraint, these devices also were not considered further.

Various Hall Effect devices from four manufacturers were analyzed for the revolution and zero reference sensors. The Sprague and Microswitch types were selected for testing over the F.W. Bell and Xolox Corp. Sensor arrangements, sensor/magnet mounting tolerances, warning time, incremental pulse width, sensitivity to drift due to age and temperature variation, and supply voltage were investigated.

Rare earth samarium cobalt target magnets from Hitachi Magnetics Corps and Indiana General were analyzed.

Two Hall Effect sensors (Microswitch #513SS16 and Sprague #UGN 3020T) were tested in conjunction with a Hitachi samarium cobalt permanent magnet (.08 inch square X .04 inch thick). The change in the operate and release points due to the change in power supply voltage, distance between sensor and magnet, and lateral offset distance between sensor and magnet were studied. The magnet was moved via a jig bore machine past each fixed Hall Effect sensor. All test methods, equipment, data results and recommendations are reported in Appendix E-16, Hall Effect Sensors Evaluation Report.

Since resolution and repeatability are only secondary considerations for the incremental revolution sensors, the studies and test results indicate that the Sprague sensors can be effectively employed and benefits of their lower cost and compact package can be realized.

It is also clear from the curves of the Sensors Evaluation Report that the Microswitch sensors are preferable for the zero reference sensors.

## 2.0 REQUIREMENTS:

2.1 Zero Reference Sensor:

Max. shaft speed	12°/min for AZ	6.2°/min for EL
Shaft dia.	app. 20"	
Accuracy	.1m rad (1 mil at 10")	
Repeatability	.01m rad	
Approx. cost	\$20.00	
Life	30 years with exposure to outdoor environment	
Temperature		
Operating	0°C to +50°C	
Non Operating	-30°C to +50°C	

2.2 Revolution Count Sensor:

Max. shaft speed	1750 rpm
Accuracy	+ 1 rev.
Approx. cost	\$10.00
Life	30 years with exposure to outdoor environment
Temperature	
Operating	0°C to +50°C
Non Operating	-30°C to +50°C

## 3.0 SENSOR CATEGORIES:

3.1 Optical Encoders: These are most accurate devices in the market today, but beyond our range as far as the cost is concerned. The prices for these encoders range from \$200.00 to \$1000.00. Due to cost constraint these devices are not considered for our application. The error due to the speed of the shaft will be none.

3.2 Proximity Switches: These use eddy current principle and can be operated by any type of metal target, although sensitivity to non-ferrous metals is approximately one-third that of ferrous metals. Their sensitivity depends on temperature, mass of the target, sensor to sensor isolation and distance to nearby non-target

metal. These sensors come with electronics to give digital current sinking output along with a repeatability up to .002". Price for these units ranges from \$30.00 to \$150.00. In case of Turck Model No. B1 1-MO8-AN7 the maximum switching distance can be .039" but .02" is advisable.

These and other various proximity switches are listed in Table I indicating their manufacturers and brief specifications. The worst switching frequency is 100 Hz, as can be seen from the Table I, which is well above the shaft speed. Due to cost constraint these devices also are not considered further.

- 3.3 Hall Effect Sensors: These sensors respond to a magnetic field. They can be operated by an electromagnet or a permanent magnet. These sensors give a digital source or sink output compatible with bipolar or MOS logic circuits. These are the least expensive devices of all in the market today which can give an accuracy of the order of .001".

They can be used for both the zero reference as well as for the revolution count. In order to give direction sense two of these sensors shall have to be used, ~~and to resolve count accuracy up to  $\pm 1/2$  revolution two magnets shall be used~~ (for revolution count). The shaft speed will not introduce any measurement error due to these sensors. But they shall be mounted away from the metal (in case of revolution counter) in order to avoid eddy current effect at higher shaft speed.

3.3.1 Manufacturers:

- 1) F. W. Bell, Inc.: They manufacture only hall effect generators which gives an analog output in millivolts. We will have to provide amplifier and switching electronics for these generators Also their prices are \$20.00 in quantity. Hence, they are not considered further.
- 2) Microswitch: Their prices are in the range of \$5.00 to \$50.00 depending on the package. Their rugged sealed package 103SR has a wide variation of release point with temperature. The other package 513SS16 has a flux concentrator with quick disconnect terminals which provides less variation of release point with temperature. Hence, only 513SS16 is considered further in our analysis. Detailed specifications are given in Appendix I. Microswitch is also exploring to give a thermoplastic custom housing for 513SS16. Their devices can be used to give a repeatability of the order of .001 inch. For a 50,000 quantity, their unit price for 513SS16 is \$1.91 and with plastic housing is expected to be around \$4.00 to \$5.00.

Contact Mr. Robert Eliason

408) 998-3131

Mr. Norm Wheelock

815) 235-5975

TABLE I

MANUFACTURER.	TYPE	MODEL NO.	SWITCHING FREQ.	RESOLUTION	REPEATABILITY	COST	REMARKS	
1. AUTOMATION INDUSTRIES	OPTICAL	S 25	25,400 c/s/rev.	2000 cycles/rev.		\$ 340.00	Too EXPENSIVE	
		L 25.		5000 cycles/rev.		\$ 200.00		
2. TRANS TET INC.	OPTICAL	SERIES 600		INFINITE	.102"	\$ 400.00	Too EXPENSIVE	
3. ELMI SYSTEMS	OPTICAL	1125 EM	500 KHZ/CR.	5080 Kcycles/Turn		\$ 350.00	Too EXPENSIVE	
4. F.L. BELL INC.	HALL GENERATOR	BHT 910				\$ 260.00	WILL NEED AMPLIFIER AND SWITCHING ELECTRONICS	
5. TUNCK.	MAGNETIC PROXIMITY SWITCH	NIGA 20/EX	200 HZ		.0008"	\$ 97.00		
		N125-G17-Y0	100 HZ		.0008"	\$ 93.00		
		N150-K90SR-UM.7	100 HZ		.0002"	\$ 148.00		
	MAGNETIC DC. PROXIMITY SWITCH	N150-K90SR-Y0	200 HZ			.0002"	\$ 128.00	
		MP SERIES	300 HZ			.008"	\$ 67.00	
		B11-M08-AN7	5 KHZ			.0002"	\$ 58.00	
6. MICRO SWITCH	PROXIMITY	FY	25,000/SEC.			\$ 30.00		
		HALL EFFECT DIGITAL SW.	513 SS 16			\$ 4.50	Flux Concentrator with quick connect terminals.	
			103 SR			\$ 35.00	Rugged sealed package. Temp. Change has pronounced effect on Release Point.	
7. SPRAGUE	HALL EFFECT DIGITAL SW.	UGN-3019T				\$ -	Large differential between Operate and Release Point. Small variation of Operate Point with temp.	
		UGN-3020T				\$ 0.75	Small differential between Operate and Release Point. Large variation of Operate Point with temp.	
		UGC-3020T				\$ -	Better Operating Temp. Range -40°C to +150°C	
		UGN-3020H				\$ 20.00	Hermetically sealed.	
8. KOLOX CORP.	HALL EFFECT DIGITAL SW.					\$ 3.90	Uses Sprague chip in epoxy sealed plastic enclosure.	
9. KAMAN SCIENCES CORP.	PROXIMITY SW.	KS-1001	10,000/SEC.		.00001" ± .016 mil/2	\$ 146.00	Target should be about .5" dia. & .01" thickness. Quantity priced \$ 120.00 Too EXPENSIVE	
10. R. B. DENISON	MAGNETIC PROXIMITY SW.	NJ 20TU	100 HZ		.002"			



- 3) Sprague: Their UGN 3020T hall effect digital switches are the least expensive sensors which can be used to repeat within .001 inch. Their unit price for a 50,000 quantity is \$0.75. Detailed specification for UGN 3020T is given in Appendix II.

Sprague also makes the following packages:

- i) UGS 3020T - with an extended operating temperature range of  $-40^{\circ}\text{C}$  to  $+150^{\circ}\text{C}$ .
- ii) UGN 3020H - an environmental proof hermetically sealed dual in line 8 pin package which meets MIL Spec 881. The cost is approximately \$15.00 in quantity.

Contact Mr. John Haussler 603) 224-1961

- 4) Xolox Corp.: They make an epoxy sealed plastic enclosure containing Sprague UGN 3030T hall effect sensor switch. They can make the enclosure to our requirements. Their unit price for a 50,000 quantity is \$3.90. This is a fairly new and a small company. With no product history and higher price they are not considered further.

3.3.2 Based on data received by manufacturers, our recommendation at this stage will be for Sprague UGN 3020T and Microswitch 513 SS16 over other manufacturers. The sensitivity drift due to age and temperature variation data are not readily available. The sensitivity drift can affect our zero reference point. Manufacturers claim to expect a 30 year life without any problem and do not expect an appreciable sensitivity drift within our operating temperature range of 0 to  $50^{\circ}\text{C}$ .

The Sprague and Microswitch hall effect devices will be studied further as regards to change in operate and release point due to change in supply voltage, change in the air gap between sensor and the magnet, and due to offset between sensor and the magnet. After comparing the test result, a device will be selected.

#### 4.0 MAGNETS

A rare earth samarium cobalt magnet shall be used for target magnet. These magnets give very high flux density in a very small piece. For example, a .100 inch square X .040 inch thick piece of samarium cobalt magnet will give approximately 1200 gauss at its surface.



When the sensor approaches the magnet, it will give a logic '0' output (voltage  $V_0$ ). When the sensor moves further and leaves the magnet, it will give a logic '1' output (voltage  $V_1$ ).

### 5.1 Zero Reference Sensors:

The falling edge (OP) at time  $t_0$  of this output voltage, can be used for warning signal to indicate that zero reference point is approaching within time 't' seconds. Then the rising edge (RP) at time  $t_R$  can be used for the zero reference point. When the magnet is moving at maximum slew rate for that axis, the output voltage pulse width time 't' can be adjusted for desired  $3.5 \pm 0.5$  sec. by varying the size of the magnet, its flux density or using a flux concentrator.

### 5.2 Revolution Counter Sensors:

These sensors will be used to count the number of revolutions made by the motor shaft and also to sense the direction of rotation. Operate point will be used to indicate a shaft count. Two sensors shall be used in order to sense the direction of rotation and ~~two~~ <sup>one</sup> magnet shall be used in order to give a count accuracy up to ~~± 1~~ <sup>± 2</sup> motor shaft revolution. The sensors will be mounted radially along the motor shaft within a very short distance and the magnet will be glued on to the rotating motor shaft, ~~180° apart~~. The set up shall be the same for both AZ and EL axis.

### 6.0 REVOLUTION COUNT SENSOR ARRANGEMENT

- 1) The sensors A and B are located radially along the shaft as shown in Figure 3. The sensors are mounted on a printed circuit card. The magnets are glued to the motor shaft and placed in an epoxy.

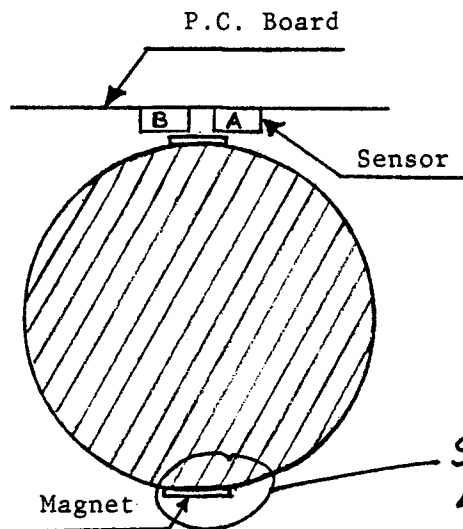


Figure 3

- 2) Each time the magnet passes in front of the sensor, the corresponding sensor will give a voltage pulse output. Both magnets are long enough to get a pulse from the other sensor at half way of the first sensor pulse. Hence, the output pulses from sensors A and B will overlap.
- 3) The sensors will give a logic state '0' output approaching the magnet and will give a logic state '1' output while leaving the magnet.
- 4) Depending upon which sensor output comes first will determine the direction of rotation. This in turn will determine whether the present count is to be incremented or decremented.

As per Figure 3, Sensor A output going to state '0' when Sensor B output is already in '0' state will establish a clockwise sense of rotation of the motor shaft. In the same way, Sensor B output going to state '0' when Sensor A output is already in '0' state will establish a counter-clockwise sense of rotation of the motor shaft.

- 5) A falling edge of the output pulse of any sensor when the output of the other sensor is already low will give ~~half~~ the revolution count for the motor shaft. The maximum count error in this case can be  $\pm \frac{1}{2}$  motor shaft revolution.

If only one magnet is used, the maximum count error will be  $\pm 1$  motor shaft revolution.

- 6) The sensor outputs will be as under:

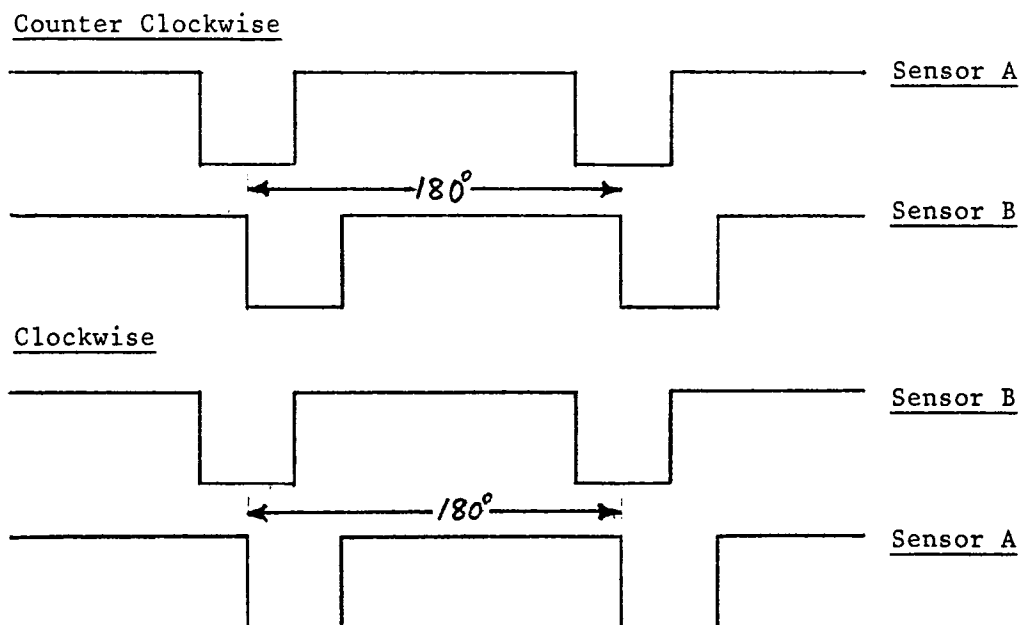


Figure 4

-8-

## 7.0 Sprague/Microswitch Sensors

Since resolution and repeatability are only secondary considerations for the incremental sensors, the Sprague UGN 3020T may be effectively employed and benefits of their lower cost and compact package may be realized. Refer to the Hall effect sensor evaluation report, Appendix E-16, and page 18 for the device characteristics.

It is also clear from the curves of the Sensors Evaluation Report, that for Microswitch sensors the desired supply voltage ' $V_{cc}$ ' is +10 Volts and the switching distance 'SD' is .015 inches. The same voltage but larger 'SD' may be used for Sprague sensors since in case of revolution count the repeatability is not that important.

## 8.0 MOUNTING THE HALL EFFECT SENSORS AND MAGNET

### 8.1 AZ Axis Zero Reference

The sensor shall be mounted on rotating upper casting using an angle bracket as shown in Figure 5 . There is another hole in the bracket to get the wires from the sensor. The magnet is glued in a 1/4" diameter hole in the other bracket with epoxy around it and top surface flush with the bracket. This bracket shall be mounted on stationary gear underneath the sensor as shown in Figure 5 . One of these brackets shall have slotted mounting holes in order to adjust the gap between sensor and the magnet.

After soldering the wires to the sensor, but before mounting, both sensor and the magnet are dipped into weatherproofing compound "Ucarsil", manufactured by Hughson Chemicals. After mounting, the sensor and the magnet are aligned parallel to each other with an air gap of .015 inch between them. The wires from the sensor pass through a strain relief connector before going to the cable wrap.

### 8.2 EL Axis Zero Reference

The sensor shall be mounted on the round surface of the rotating AZ axis drum using a bracket coming out as shown in Figure 5 so as to be about 10 inches from the EL axis. The magnet shall be mounted on the EL axis arm flange so as to be 10 inches away from the EL axis when the heliostat is at 5° EL. The magnet is glued in a 1/4" diameter hole with epoxy around it and top surface flush with the metal as shown in Figure 5.

After soldering the wires to the sensor, but before mounting, both sensor and the magnet are dipped into weatherproofing compound "Ucarsil". After mounting, the sensor and the magnet are aligned parallel to each other with an air gap of .015 inch between them. The wires from the sensor are from a three conductor cable which comes from the cable wrap.

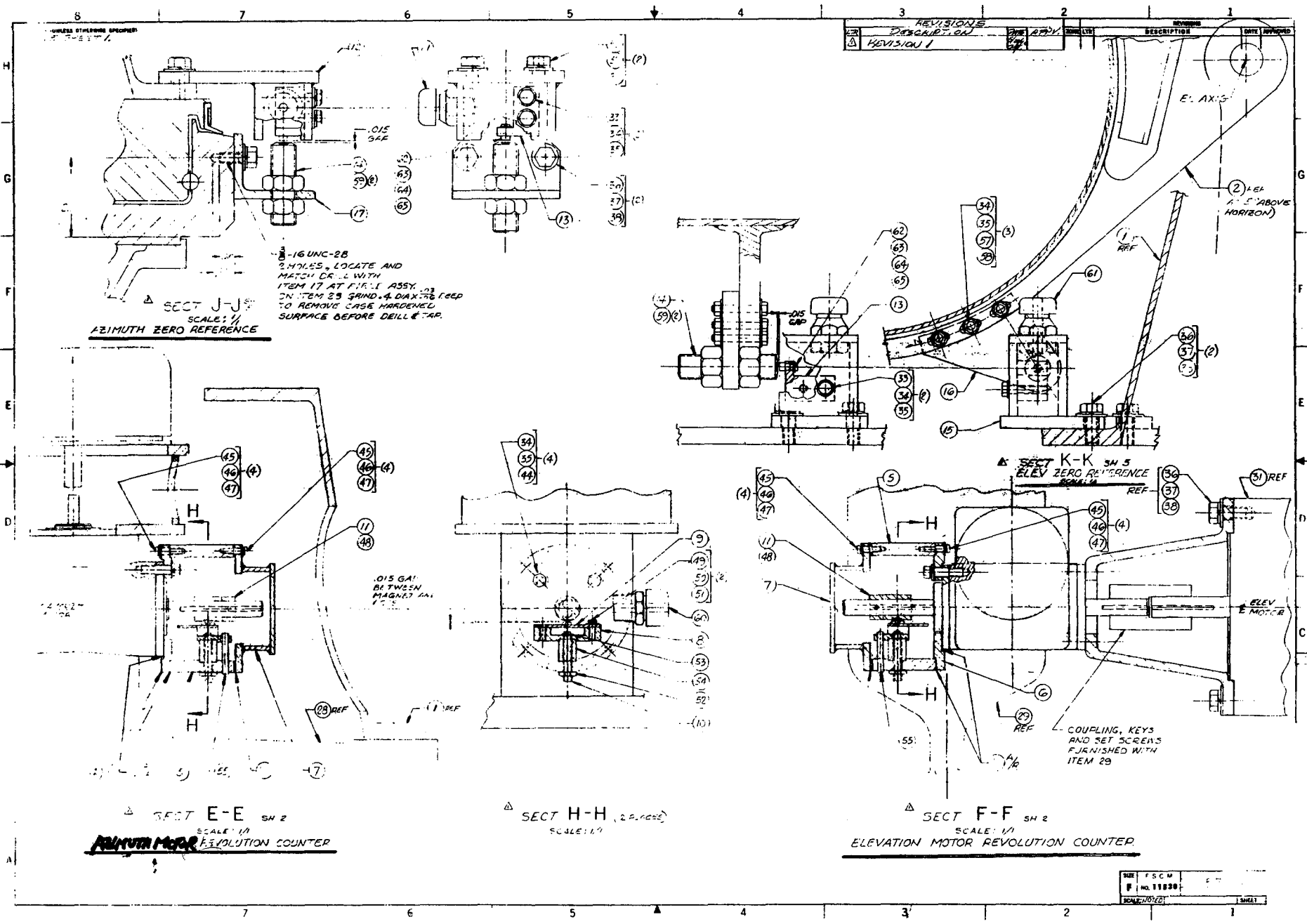


Figure 5

REV	FSCN	DATE
1	F	NO. 11838
DRAWN/NOTED		SHEET

### 8.3 Revolution Count

In this case, the Sprague UGN 3020T sensors shall be used. The scheme will be the same for both AZ and EL axis.

Two Sprague UGN 3020T sensors are mounted on a  $1\frac{1}{2}$ " X 2" printed circuit card as shown in Figure 5. The printed circuit card is supported over the coupling by two threaded rods and nuts as shown in Figure 5. The nuts are adjusted so as to keep sensor surface .030 inch away from the coupling. ~~Two magnets~~ **ONE** are glued on the coupling, ~~180°~~ **apart.**

After soldering the wires to the printed circuit card, before mounting, both sensor and the magnet are dipped into weatherproofing compound "Ucarsil". The wires from the sensors are from two three conductor cables coming from the cable wrap.

### 9.0 WARNING TIME

From the test results, it is clear that Microswitch hall effect sensor 513SS16 is a better choice over Sprague UGN 3020T. Based on the desired supply voltage  $V_{CC}$  of +10 Volts and a switching distance 'SD' of .015 inches, the output pulse width is .13078 inch.

#### 9.1 For AZ Axis

Output shaft diameter = 23.25 inches.

Maximum slew rate at the output shaft =  $\frac{180^\circ}{15 \text{ min}} = 0.2^\circ/\text{sec.}$

For an output voltage pulse width of .13078 inches, the output shaft travel at maximum slew rate =  $\frac{.13078}{23.25/2} = 11.25 \text{ m rad.}$

This corresponds to an angular shaft travel of  $11.25 \times 10^{-3} \times \frac{180}{\pi}$   
= .645°.

The corresponding warning time =  $\frac{.645^\circ}{.2^\circ} = \underline{3.23 \text{ sec.}}$

#### 9.2 For EL Axis

The sensor and magnet are located at 10 inches from the EL axis.

Maximum slew rate at the output shaft =  $\frac{93^\circ}{15 \text{ min}} = 0.1033^\circ/\text{sec.}$

For an output voltage pulse width of .13078 inches, the output shaft travel at maximum slew rate =  $\frac{.13078}{10} = 13.08 \text{ m rad.}$

This corresponds to an angular shaft travel of  $13.08 \times 10^{-3} \times \frac{180}{\pi}$   
 $= .749^\circ.$

The corresponding warning time =  $\frac{.749}{.1033} = \underline{7.25 \text{ sec.}}$

#### 10.0 INCREMENTAL PULSE WIDTH

Using a Sprague hall effect device for each incremental sensor, an output pulse will be produced as the magnet passes beneath. From the curves of Appendix E-16, Figure 8, the width of the output pulse will correspond to the distance between the operate point and release point, or about 0.10 inches, in this case.

Assuming that the shaft speed is 1750 RPM and that the coupling diameter is 1", the surface speed will be:

$$\frac{1750}{60} \times \pi = 91.63 \text{ in/sec}$$

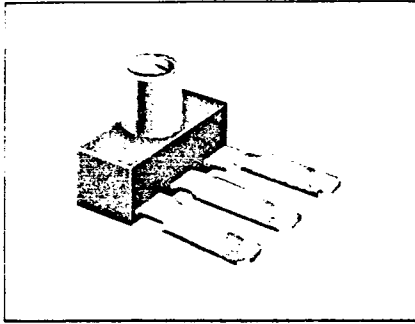
At this surface speed, the magnet will transit the 0.10 inch distance in:

$$\frac{0.10}{91.63} = 1.09 \text{ milliseconds}$$

Thus, the incremental sensor pulse width will be 1.09 milliseconds for one inch of coupling (magnet support) diameter.



# Magnetically operated position sensors

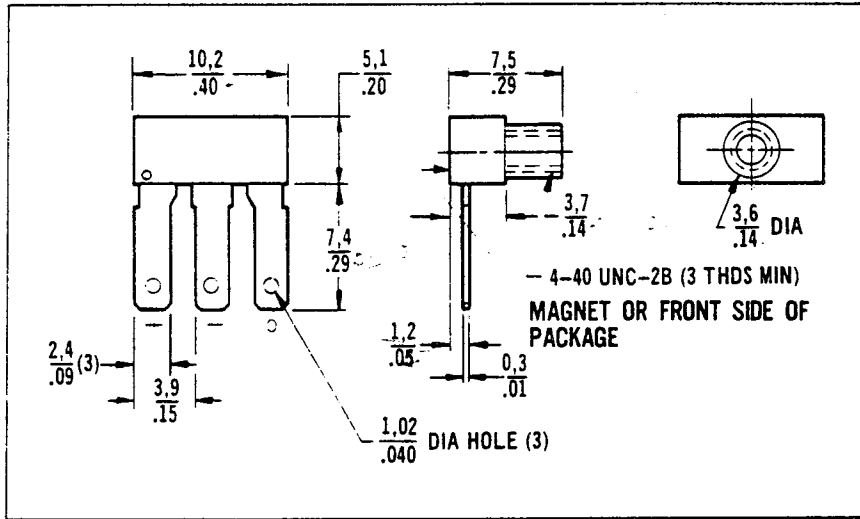


*Hall effect sensing*  
 Single digital output ... current sinking or current sourcing  
 3 pin solder quick-connect terminals ... easy wiring as remote sensor  
 Internally threaded flux concentrator ... channels more of available flux density from magnet into sensor. Also used as mounting means  
 4.5 to 5.5 VDC or 6 to 16 VDC supply voltages

Connectors for solderless installation may be ordered from your local AMP distributor. AMP catalog number for 1 000 piece roll is 62041-1.

Absolute Maximum Ratings Calibrated Hall Element information, actuation, interfacing, sinking and sourcing information: see pages 16 thru 18.

## MOUNTING DIMENSIONS

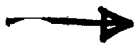


Supply Voltage (VDC)	Supply Current (mA max.)	Type	Current per Output	Catalog Listings
4.5 to 5.5	4.0	Source	20mA	5SS16
		Sink	8mA	55SS16
6 to 16	13.0	Source	20mA	512SS16
		Sink		513SS16
				517SS16

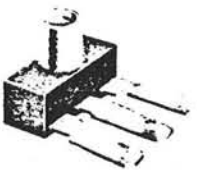









## 5SS MAGNETIC CHARACTERISTICS

Catalog Listing	Magnetic Characteristics & Temperature											
	0 to 70°C			- 40 to 100°C			- 40 to 150°C			25°C Typical		
	Max. Op.	Min. Rel.	Min. Dif.	Max. Op.	Min. Rel.	Min. Dif.	Max. Op.	Min. Rel.	Min. Dif.	Typ. Op.	Typ. Rel.	Typ. Dif.
5SS16	500	30	25	—	—	—	—	—	—	245	150	95
55SS16	370	70	25	370	30	55	—	—	—	245	150	95
512SS16	320	105	25	330	85	25	340	30	25	230	170	60
513SS16	320	105	25	330	85	25	340	30	25	230	170	60
517SS16	115	-115	25	125	-125	25	140	-140	25	35	-35	70



# Hall effect sensor selection guide

	 10 Series	 13 Series	 10S Series	 10T Series
Sensor Type, Actuation	Hall effect, magnetically operated			
Supply Voltage	4.5 to 5.5 VDC and 6 to 16 VDC			
Supply Current	2 mA typ. (4.5 to 5.5 VDC), 6 mA typ. (6 to 16 VDC)			
Output Type	Sink or Source, 4 to 20 mA		Sink, 4 to 20 mA	
Terminals	Solder quick-connect		Printed circuit board	
Features	Large flux concentrator for tightest magnetic range		Optional flux concentrator	Standard or precision magnetics
	Miniature sensor for remote mounting		Printed circuit board mounting	
	Single output	Dual outputs	Dual outputs	Single output

	 30SR Series	 400SR Series	 1AV Series	 4AV Series
Sensor Type, Actuation	Hall effect, magnetically operated		Hall effect, ferrous vane operated	
Supply Voltage	4.5 to 5.5 VDC and 6 to 16 VDC	6 to 16 VDC		4.5 to 5.5 VDC and 6 to 16 VDC
Supply Current	2 mA typ. (4.5 to 5.5 VDC) 6 mA typ. (6 to 16 VDC)	6 mA typical		2 mA typ. (4.5 to 5.5 VDC) 6 mA typ. (6 to 16 VDC)
Output Type	Sink or Source, 20 mA	Sink, 4 to 20 mA		
Terminals	Leadwires	Solder/quick-connect connector	Leadwires, solder/quick-connect	PC board, leadwires, connector block
Features	Threaded aluminum bushing	Thermoplastic housing	Magnet and sensor in same rugged package	
	Sealing meets NEMA 3, 3R, 3S, 4, 4X, 6, 12, 13	Locating boss	UL recognized housing and leadwires	
	Single output	Single output	Single output	Single output — leadwires Dual outputs — others

**ABSOLUTE MAXIMUM RATINGS (HALL EFFECT SENSORS)\***

Parameters	Type	4.5 to 5.5 VDC Circuit		6 To 16 VDC Circuit	
Supply Voltage	N/A	- 1.2 to + 10 VDC		- 1.2 to + 20 VDC	
Voltage Externally Applied to Output	Sink	+ 10 VDC max. (OFF only) - 0.5 VDC min. (ON or OFF)		+ 20 VDC max. (OFF only) - 0.5 VDC min. (ON or OFF)	
	Source	+ 6.5 VDC max. (ON or OFF) - 0.5 VDC min. (ON)		+ 6.5 VDC max. (OFF only) (Vs + 4) VDC (ON)	
Output Current	Sink	Single	Dual	Single	Dual
		20mA	10mA/output	40mA	20mA output
	Source	40mA	20mA/output	20mA	20mA/output
Switching Time ( $\mu$ sec max.)	Sink	Rise	Fall	Rise	Fall
		2.0	1.0	1.5	0.5
	Source	1.0	1.0	0.5	2.0
Temperature	N/A	- 40°C to + 100°C		- 40°C to + 150°C	
Magnetic Flux	N/A	No limit. Circuit cannot be damaged by magnetic overdrive.			

\* Hall effect sensors will not be damaged unless these ratings are exceeded  
Preferred operating characteristics are included in product Order Guide.



**INTEGRATED CIRCUIT  
ENGINEERING BULLETIN**

**TYPE UGN-3020T and UGS-3020T SOLID-STATE  
LOW-COST 'HALL EFFECT' DIGITAL SWITCHES**

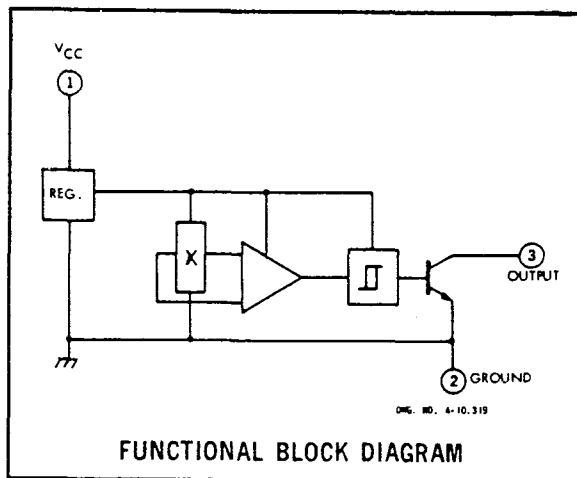
**TYPE UGN-3020T and UGS-3020T SOLID-STATE  
LOW-COST 'HALL EFFECT' DIGITAL SWITCHES**

**Features:**

- Operate from 4.5 V to 24 V d-c power supply
- Operable with a small permanent magnet
- High Reliability - eliminates contact wear, contact bounce; no moving parts.
- Small size.
- Constant amplitude output - independent of frequency

DESIGNED to provide contactless switching or position sensing, the Type UGN-3020T and UGS-3020T solid-state sensors utilize the Hall effect for determining the presence of a magnetic field. The increased sensitivity of these devices allows them to be used with smaller magnets or with increased magnet-to-sensor spacing. The UGN-3020T device is intended for operation over the temperature range of 0°C to +70°C. The UGS-3020T is designed for use over an extended temperature range of -40°C to +150°C. Both devices will typically operate up to a 100 kHz repetition rate.

Each circuit is a silicon monolithic integrated circuit incorporating a Hall cell, differential amplifier, trigger, output stage, and voltage regulator. The



regulator permits circuit operation over a wide range of supply voltages. The output stage can be easily interfaced with bipolar or MOS logic circuits.

The UGN-3020T and UGS-3020T Hall effect digital switches are supplied in a low-cost 3-pin single output plastic package.

**ELECTRICAL CHARACTERISTICS;  $V_{CC} = 4.5 V$  to 24 VDC,  $T_A = 25^\circ C$**

Characteristic	Symbol	Test Conditions	Limits			Units
			Min.	Typ.	Max.	
Magnetic Flux Density "Operate Point" "Release Point"	$B_{OP}$		—	300	350	Gauss
	$B_{RP}$		50	210	—	Gauss
Hysteresis	$B_H$		20	90	—	Gauss
"0" Output Voltage	$V_{OUT(0)}$	$B \geq 350$ Gauss, $I_{OUT} = 15$ mA	—	85	400	mV
"1" Output Current	$I_{OUT(1)}$	$B \leq 50$ Gauss, $V_{OUT} = 24$ V	—	0.1	20	$\mu A$
Supply Current	$I_{CC}$	$V_{CC} = 4.5$ V, output open	—	4.5	9	mA
		$V_{CC} = 24$ V, output open	—	7	14	mA
Output Rise Time	$t_r$	$V_{CC} = 12$ V, $R_L = 820 \Omega$ , $C_L = 20$ pF	—	15	—	ns
Output Fall Time	$t_f$	$V_{CC} = 12$ V, $R_L = 820 \Omega$ , $C_L = 20$ pF	—	100	—	ns

Note: Magnetic flux density is measured at most sensitive area of device. This area is located 0.042"  $\pm$  0.001" (1.07  $\pm$  0.03 mm) below the front surface of package.

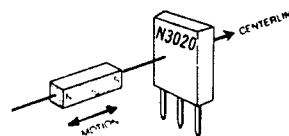
**ABSOLUTE MAXIMUM RATINGS**

Power Supply, $V_{CC}$ .....	25 V
Magnetic Flux Density, $B$ .....	Unlimited
Output "Off" Voltage, $V_{OUT(1)}$ .....	25 V
Output "On" Current, $I_{OUT(O)}$ .....	50 mA
Storage Temperature Range, $T_s$ .....	-65°C to +150°C
Operating Temperature Range, $T_A$	
UGS-3020T.....	-40°C to +150°C
UGN-3020T.....	0°C to +70°C

**OPERATION**

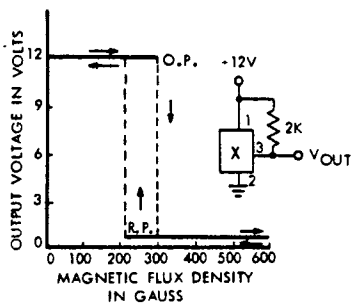
The output transistor is normally "off" when the magnetic field perpendicular to the surface of the chip is below the threshold or "operate point." When the field exceeds the "operate point," the output transistor switches "on" and will sink 15 mA.

The output transistor switches "off" when the magnetic field is reduced below the "release point" which is less than the "operate point." This is illustrated graphically in the transfer characteristic curve. The hysteresis characteristic provides for unambiguous or non-oscillatory switching.



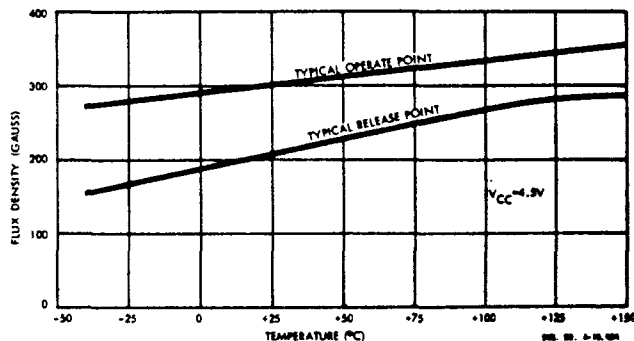
DWG. NO. A-9762

Note: In the illustration, the magnet's axis is on the center line of the packaged device and the magnet is moved toward and away from the device. Also, note the orientation of the magnet's south pole in relation to the side of the package which is marked with the part number.



DWG. NO. A-10,320

The simplest form of magnet which will operate the Hall effect digital sensor is a bar magnet as shown. Other methods are possible. Design information covering these methods is found in Sprague Engineering Bulletin No. 27404.1.

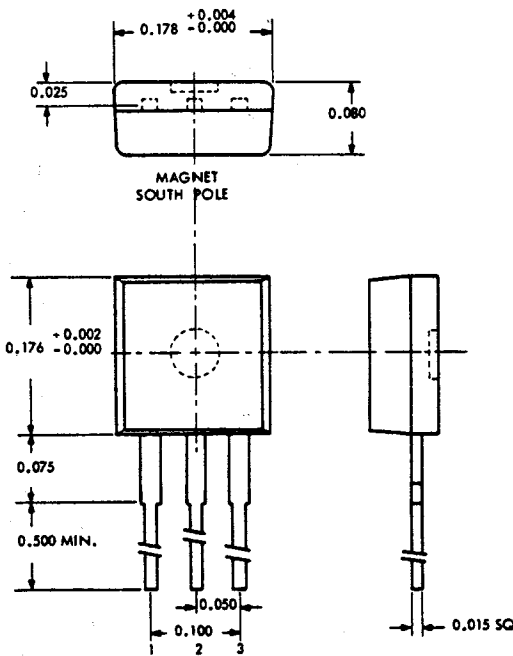


DWG. NO. A-10,320

### GUIDE TO INSTALLATION

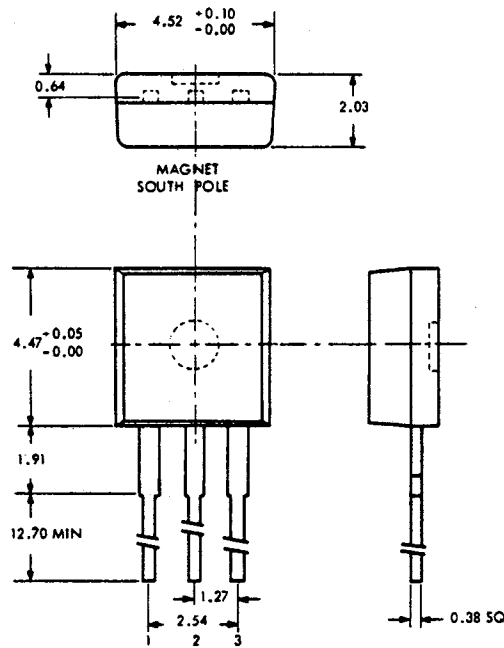
1. All Hall effect integrated circuits are susceptible to mechanical stress effects. Caution should be exercised to minimize the application of stress to the leads or the epoxy package.
2. To prevent permanent damage to the Hall cell I.C., heat sink the leads during hand soldering. For wave soldering, the part should not experience more than 230°C for more than 5 seconds and no closer than 0.125" to the epoxy package.

### PACKAGE INFORMATION



NOTES: 1. All dimensions are in inches.  
 2. Hall cell is centrally located.

DWG. NO. 4-9761 1R



NOTES: 1. All dimensions are in millimetres  
 2. Hall cell is centrally located.

DWG. NO. 4-9761 1R

In the construction of the components described, but full intent of the specification will be met. The Sprague Electric Company however, reserve the right to make from time to time such departure from the detail specifications as may be required to permit improvements in the design of its products. Component made under military approvals will be in accordance with the approval requirements. The information included herein is believed to be accurate and reliable. However, the Sprague Electric Company assumes no responsibility for use; nor for any infringements of patents or other rights of third parties which may result from its use.

## APPENDIX III

HICOREX

Hicorex is the Hitachi Magnetics Corp. trade name for a new family of rare earth cobalt high energy permanent magnets. Hicorex magnets are fabricated by pressing small particle rare earth cobalt powder properly aligned by the influence of a magnetic field, then sintering to high densities and heat treating to optimize properties. These magnets have a preferred direction of magnetization. Powder preparation using high purity materials assures magnetic and physical quality of the finished magnets. They can be pressed to size for many shapes, thereby reducing the amount of finish grinding.

## Typical Room Temperature Properties

Property	Hicorex 90A	Hicorex 90B
Residual induction ( $B_r$ ), gauss	8200	8700
Coercive Force ( $H_c$ ), oersteds	7500	8200
Intrinsic Coercive Force ( $H_{ci}$ ), oersteds	30000	15000
Energy Product (B·H) Max, mgo	16	18
Recoil Permeability	1.05	1.05
Required Magnetization Field ( $H_s$ ), oersteds	20000*	15000*
Hardness, Vickers D.P.H.	500	500
Density grams/cm <sup>3</sup>	8.2	8.3
Tensile Strength, p.s.i.	5000	5000
Resistivity, p, micro ohm-cm @ 25°C	50	50
Thermal Conductivity, K, (Cal·cm)/(°C·sec·cm <sup>2</sup> )	0.025	0.025
Thermal Expansion // to Orientation, cm/cm, °C	5X10 <sup>-6</sup>	NA
Thermal Expansion ⊥ to Orientation, cm/cm, °C	13X10 <sup>-6</sup>	NA

\* Magnetization requirement based on having a magnet that has been thermally demagnetized. Higher fields are required if demagnetized state was achieved by a magnetic field.

Temperature Effects**Reversible Losses**

Stabilized magnets change properties with temperature, but these changes are completely reversible, and the properties return to the initial values when the magnet is back at room temperature. Temperature changes cause a reversible displacement of the Hicorex demagnetization curve, producing a slight decrease in properties at elevated temperatures, and conversely, a slight increase in properties at low temperatures.

**Reversible Temperature Coefficient, Percent per °C**

Hicorex Grade	Temp Range	20 °C to -100 °C	20 °C to 50 °C	20 °C to 100 °C	20 °C to 150 °C	20 °C to 200 °C	20 °C to 250 °C
	90A & 90B		+ .033	-.040	-.042	-.045	-.046

**Irreversible Losses**

Hicorex exhibits a permanent or irreversible loss in properties when exposed to high temperatures. The magnitude of the loss depends upon the temperature and permeance coefficient (B/H) of the magnet. Prior exposure to high temperature for several hours stabilizes the magnet, and recycling does not produce additional irreversible loss. Stabilization at a few degrees above the expected service temperature is effective. We recommend that a service temperature of 250°C not be exceeded for Hicorex materials.

**Irreversible Loss, Percent**

Hicorex Grade	Temp. °C	B/H = ¼	B/H = ½	B/H = 1	B/H = 2	B/H = 10
90A 90B	50	-0.9 -0.9	-0.4 -0.4	-0.4 -0.4	0.0 0.0	0.0 0.0
90A 90B	100	-1.8 -1.8	-0.9 -0.9	-0.8 -0.8	-0.1 -0.1	0.0 0.0
90A 90B	150	-2.7 -	-1.6 -3.0	-1.4 -1.4	-0.25 -0.25	0.0 0.0
90A 90B	200	-5.5 -	-2.5 -7.0	-2.0 -2.0	-0.5 -0.5	-0.2 -0.2
90A 90B	250	-10.0 -	-4.0 -	-3.0 -	-1.5 -	-0.7 -

These are typical values. Changes in geometry, weight and composition cause some variation in irreversible losses.



To eliminate irreversible loss in service due to temperature change, it is recommended that the magnet be cycled in the magnetized condition through a temperature range somewhat greater than that expected in service.

If variations with temperature cannot be tolerated, and it is not possible to maintain constant temperature, compensation can be made. The most practical method employs a temperature-sensitive shunt adjacent and parallel to the permanent magnet. At low temperatures the shunt permeability increases, enabling the shunt to carry or direct more flux from the air gap. At higher temperatures, the reverse condition exists; the shunt permeability decreases and less air-gap flux is diverted. For these applications, the most widely-used materials are 30-32% nickel-iron alloys, often referred to as Curie alloys.



REPORT E-16

HALL EFFECT SENSOR EVALUATION

FOR

GIMBAL/ACTUATOR DRIVE ASSEMBLY

FOR

BOEING SECOND GENERATION HELIOSTAT

JUNE 27, 1980

Reference: FACC TM09



Ford Aerospace &  
Communications Corporation

HALL EFFECT SENSORS EVALUATION REPORT

1.0 INTRODUCTION:

The purpose of this effort is to determine the locus of trip and release points for a Hall effect absolute position sensor.

Two hall effect sensors, one manufactured by Microswitch 513SS16 and the other for Sprague UGN3020T, are used in conjunction with a Hitachi Samarium Cobalt permanent magnet (.08 inch square X .04 inch thick) for this test. The change in the operate and release points due to the change in power supply voltage ' $V_{CC}$ ', distance between sensor and magnet 'SD' and offset distance between sensor and magnet 'D' are studied.

2.0

A Mitsui Seiki Jig boring machine model No. 4B was used for this test. This machine is of double column planer type construction as shown in Fig. 1. Coordinate measuring and positioning are obtained by an Elm Systems Readout. Standard scales are mounted on the table and spindle saddle.

2.1 Jig Boring Specifications

2.1.1 Measuring Capacity

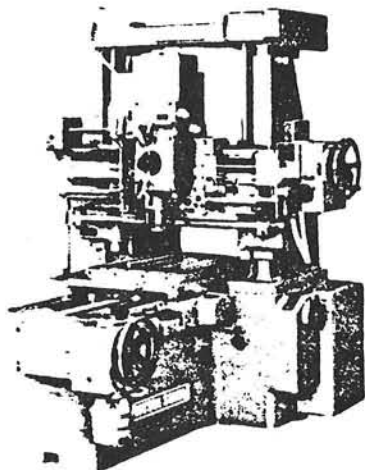
a)	Standard scale graduations	1 div.	0.05	in.
b)	Auxiliary scale graduations	1 div.	0.05	in.
c)	Screen graduations	1 div.	0.005	in.
d)	Minimum reading on micro-drum		0.00005	in.
e)	Displacement accuracy		0.00012	in.

2.1.2 Machine Size

a)	Length		74	in.
b)	Width		67	in.
c)	Height		83	in.
		Maximum height	90	in.
d)	Height of table surface from floor		50 3/4	in.
e)	Net weight		5500	lbs.

**mitsui seiki**

JIG BORERS; MODEL NOS. 0, 1, 3, 4, 5, 6, 7



Jig Boring Machine  
Model: 4B

FIG. 1

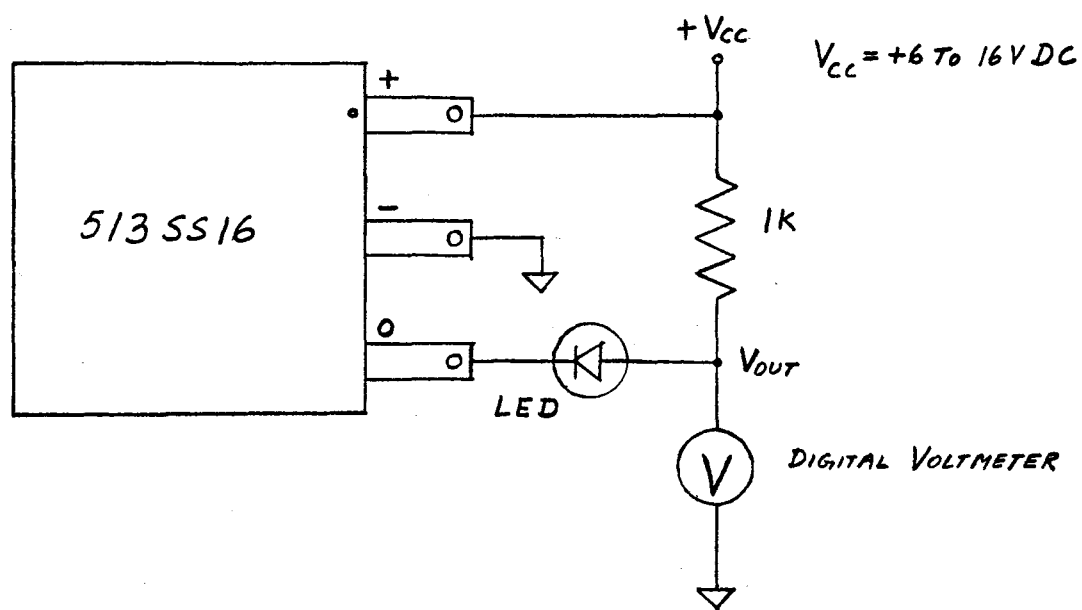
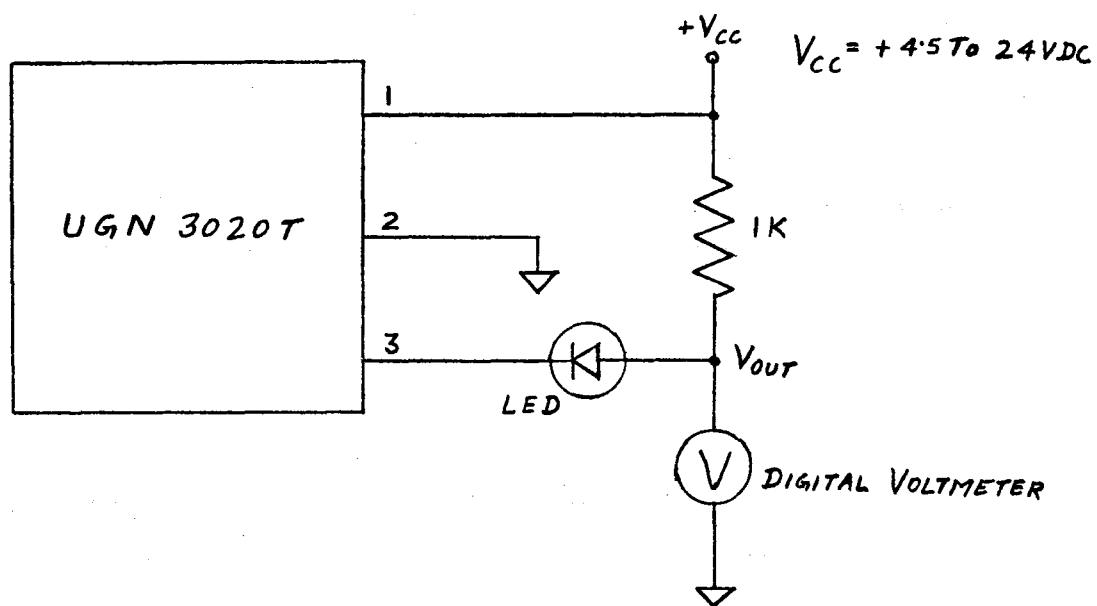
TEST SET UP FOR MICROSWITCH HALL EFFECT SENSORTEST SET UP FOR SPRAGUE HALL EFFECT SENSOR

FIG. 2

TEST SET UP

NOTE:

Magnet's south pole should be in front of the sensor side marked with the part number.

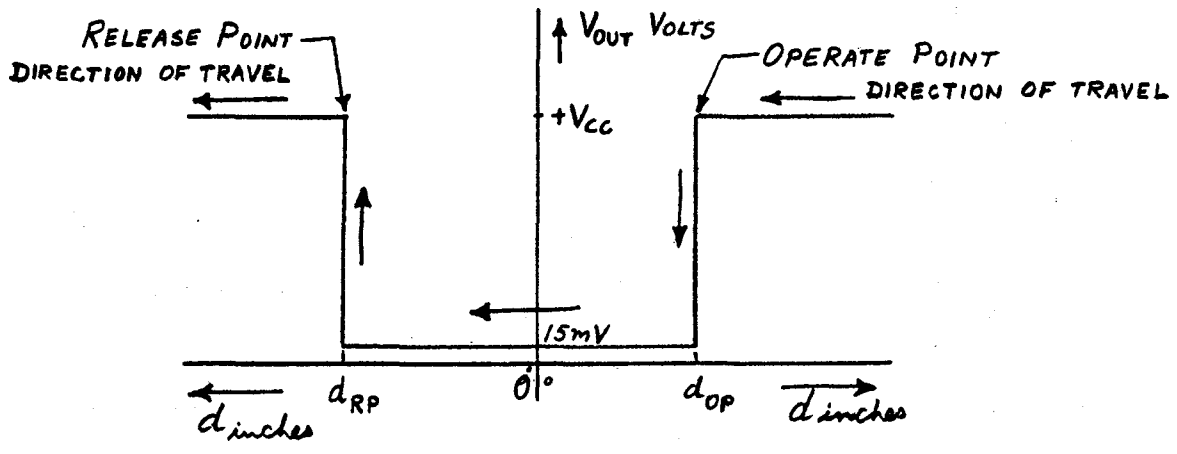
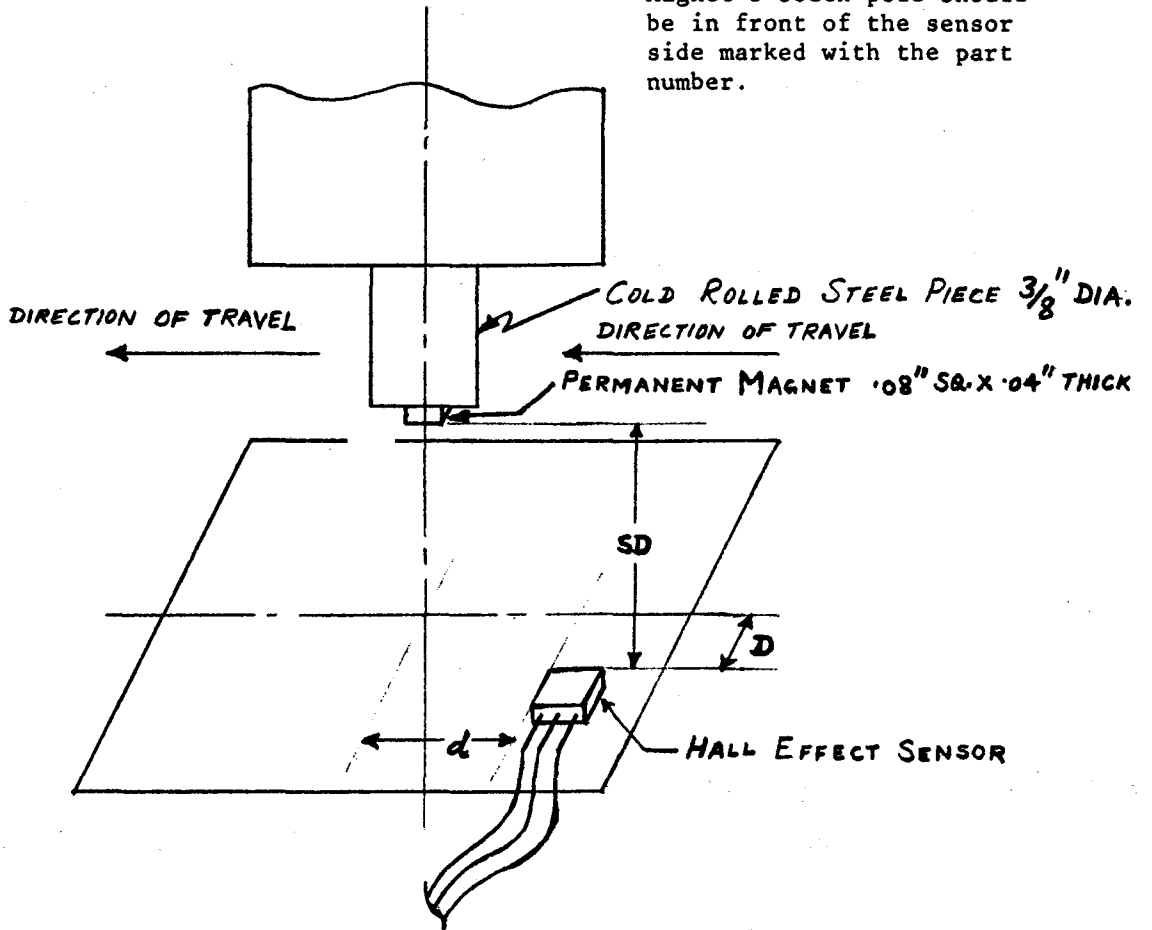


FIG. 3

## 2.2 Elm Systems Readout

The Elm Systems Readout is designed for use in machine tool and process control applications. This system can be used in any application where accurate, reliable measurement and display of position is required, such as, milling machines, jig bores and lathes.

Total System accuracy .00005" per foot @ 68°F

Resolutions available .0001" and .00005"

Repeatability .000025"

Traverse Speed 1200"/min.

Alignment Elm glass scale and head have a unique optical system which removes all first order effects of contamination and misalignment between scale and reading head.

## 3.0 TEST SETUP

- 3.1 The magnet is held by a 3/8 inch diameter cylindrical piece of cold rolled steel in a Jig Borer Chuck and, the sensor is mounted on the Jig Borer bed and held by two-sided tape on a plastic piece (for Sprague Sensor) or by a screw through the plastic piece (for Microswitch Sensor). A picture of the Jig Bore machine used is shown in Fig. 1 and the test setup is as shown in Figs 2 and 3.
- 3.2 The Microswitch 513SS16 sensor is mounted as per para 3.1 then the magnet is moved over the sensor from right to left at various switching distances 'SD' (distance between sensor and magnet) with no offset distance between sensor and magnet 'D' (i.e., magnet and sensor centers are aligned) and at a constant supply voltage ' $V_{cc}$ '. For each switching distance 'SD', ten readings for operate and release points are taken as per Table I.
- 3.3 All the readings taken in 3.2 are repeated for various supply voltages ' $V_{cc}$ ' as per Table I.
- 3.4 For a fixed supply voltage ' $V_{cc}$ ' of +10 Volts and Switching distance 'SD' of .015 inch, the operate and release points are recorded for various offset distances 'D' between sensor and the magnet on either side as per Table I.



FOR MICRO SWITCH HALL EFFECT SENSOR  
 SAMARIUM COBALT MAGNET .08 INCH SQ. X .04 INCH THICK

CHANGE IN OPERATE AND RELEASE POINT DUE TO CHANGE IN SUPPLY VOLTAGE

AMBIENT TEMP. = 68°F

SWITCHING DISTANCE SD = .015 INCH  
 OFFSET BETWEEN SENSOR AND MAGNET D = 0

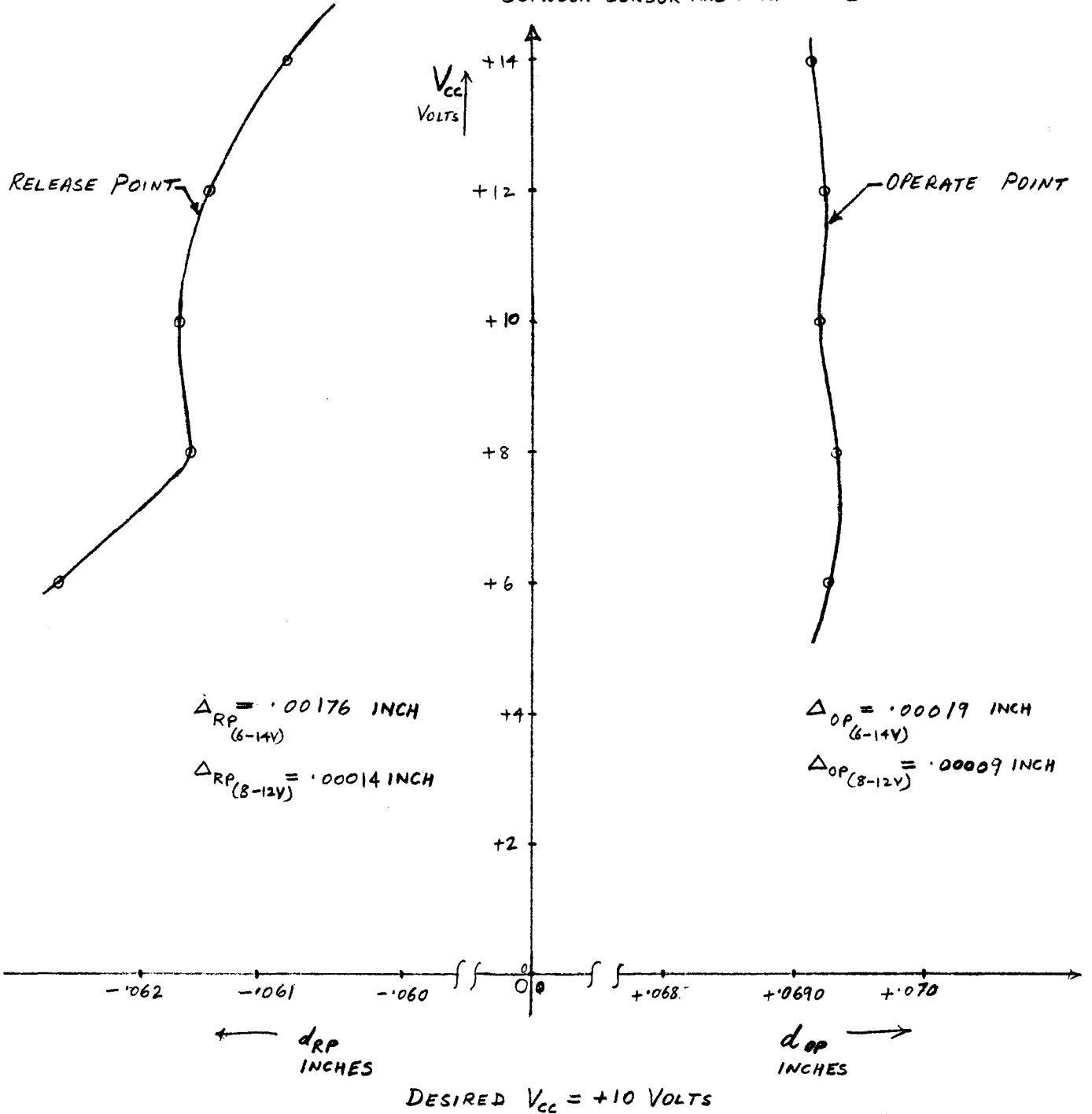


Figure 4

FOR MICRO SWITCH HALL EFFECT SENSOR  
 SAMARIUM COBALT MAGNET .08 INCH SQ X .04 INCH THICK

CHANGE IN OPERATE AND RELEASE POINT DUE TO CHANGE IN SWITCHING DISTANCE

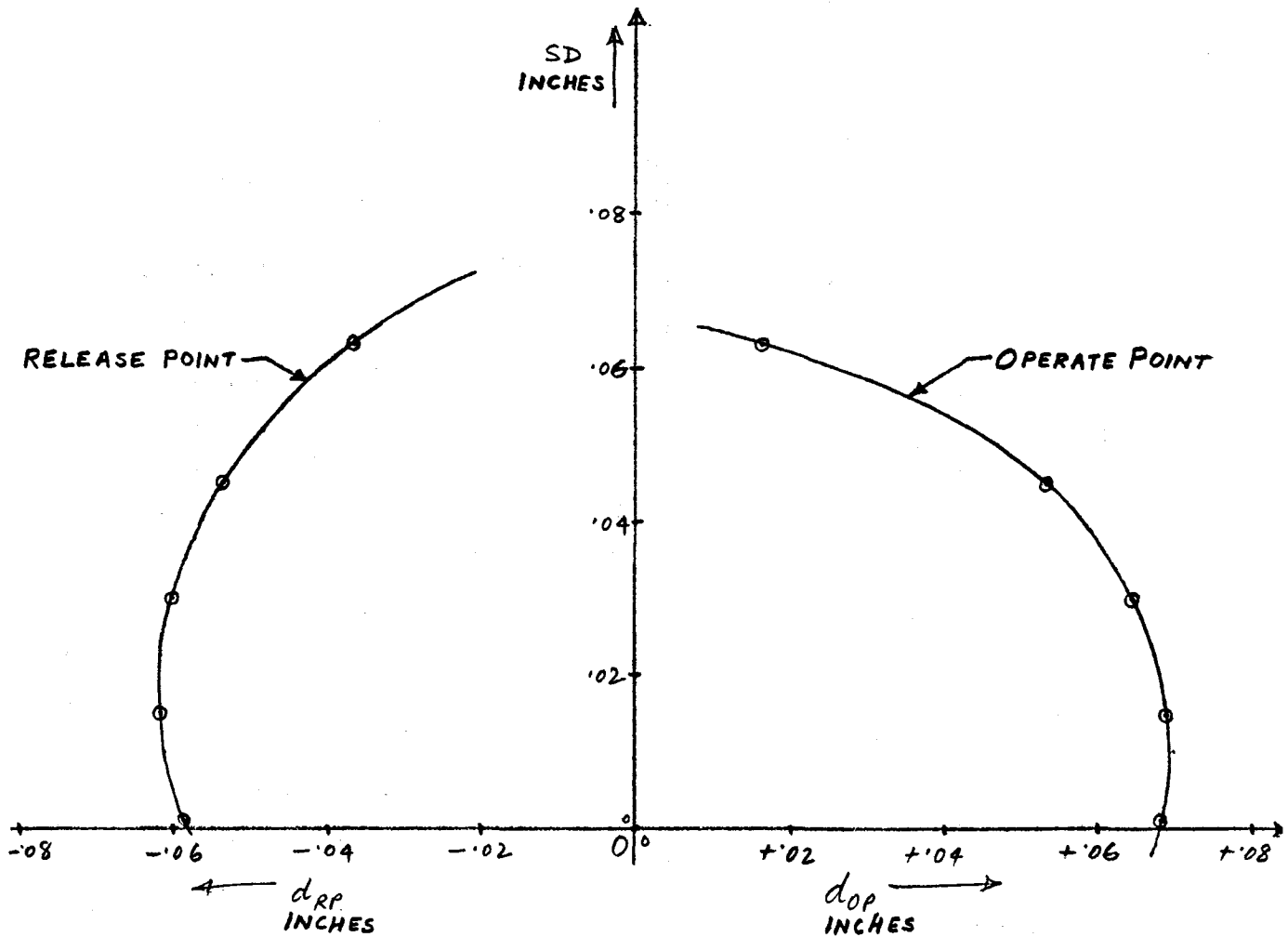
AMBIENT TEMP. = 68°F

SUPPLY VOLTAGE  $V_{CC} = +10$  VOLTS

OFFSET BETWEEN SENSOR AND MAGNET  $D=0$

$$\Delta_{RP(.01-.03)} = .001 \text{ INCH}$$

$$\Delta_{OP(.01-.03)} = .005 \text{ INCH}$$



DESIRED SD = .015 inch

Figure 5

FOR MICRO SWITCH HALL EFFECT SENSOR  
SAMARIUM COBALT MAGNET .08 INCH SQ. X .04 INCH THICK

RANGE IN OPERATE AND RELEASE POINT DUE TO OFFSET OF MAGNET AND SENSOR

AMBIENT TEMP. = 68° F

SWITCHING DISTANCE  $SD = .015$  INCHES

SUPPLY VOLTAGE  $V_{CC} = +10$  VOLTS

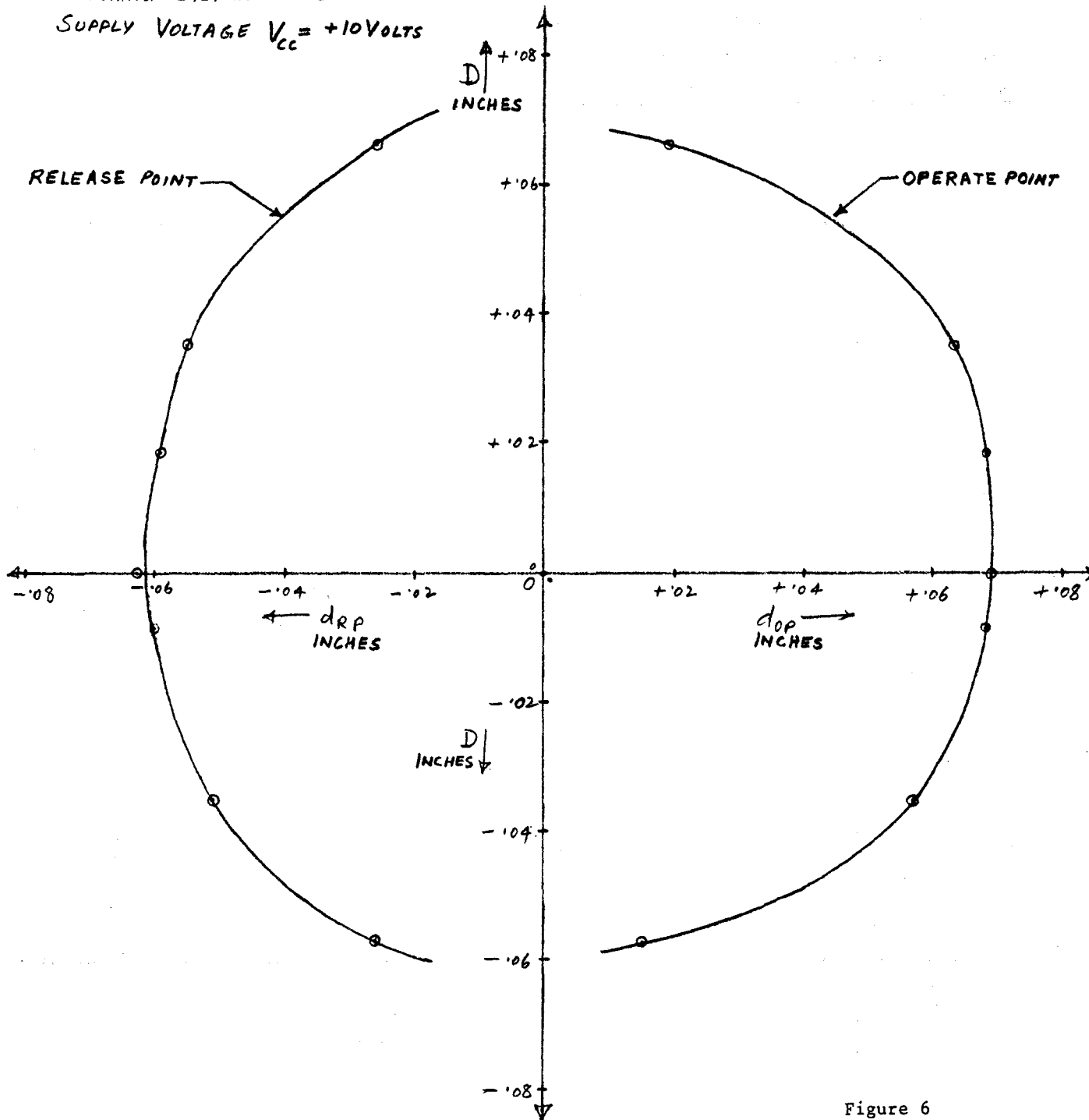


Figure 6

FOR MICROSWITCH HALL EFFECT SENSOR  
 SAMARIUM COBALT MAGNET .08 INCH SQ. X .04 INCH THICK

REPEATABILITY SPAN FOR OPERATE AND RELEASE POINTS

AMBIENT TEMP. = 68° F.

SWITCHING DISTANCE  $SD = .015$  INCH

OFFSET BETWEEN SENSOR AND MAGNET  $D = 0$

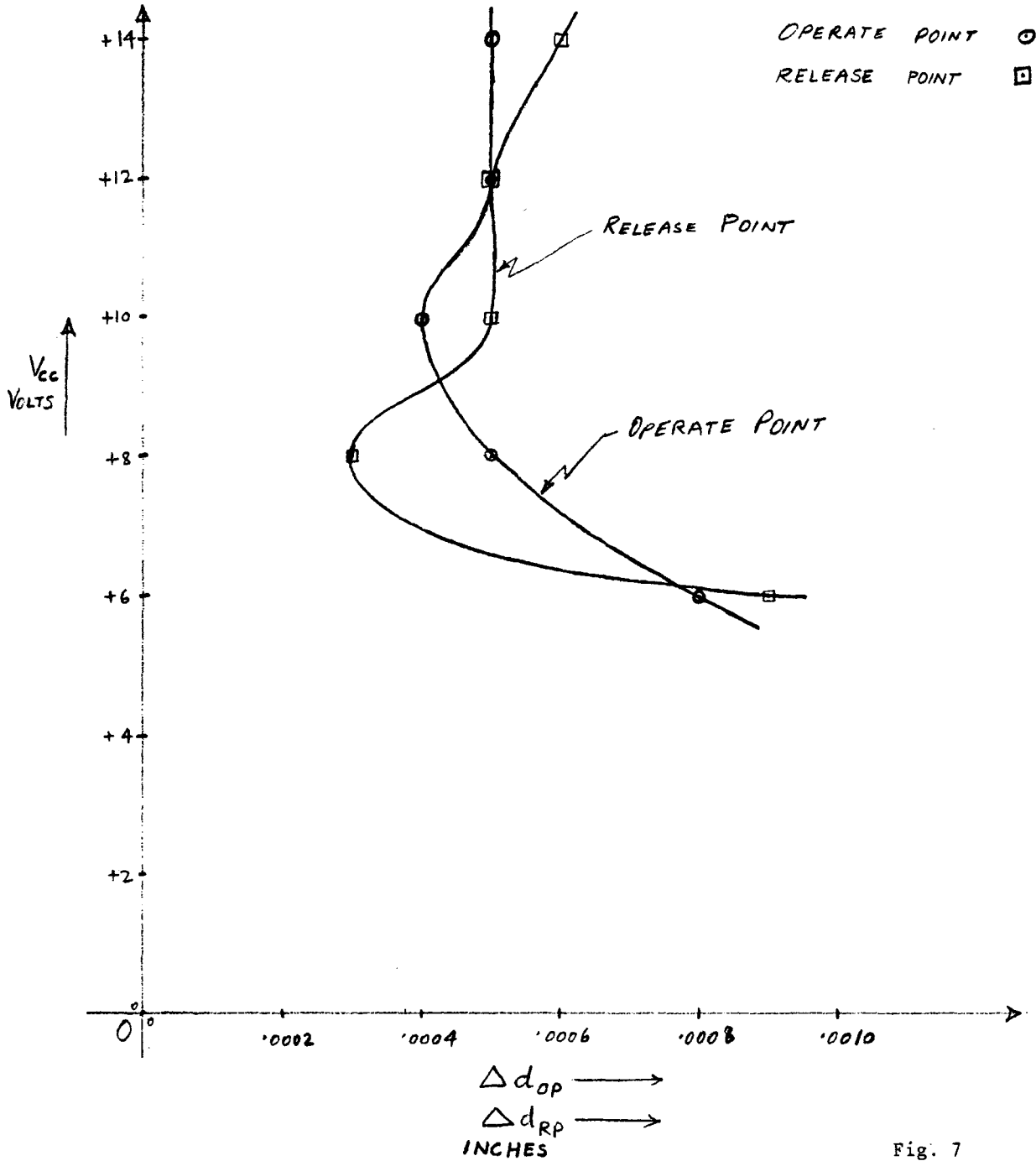


Fig. 7

FOR SPRAGUE HALL EFFECT SENSOR  
 SAMARIUM COBALT MAGNET .08 INCH SQ. X .04 INCH THICK

CHANGE IN OPERATE AND RELEASE POINT DUE TO CHANGE IN SWITCHING DISTANCE

AMBIENT TEMP. = 68°F

SUPPLY VOLTAGE  $V_{CC} = +10$  VOLTS

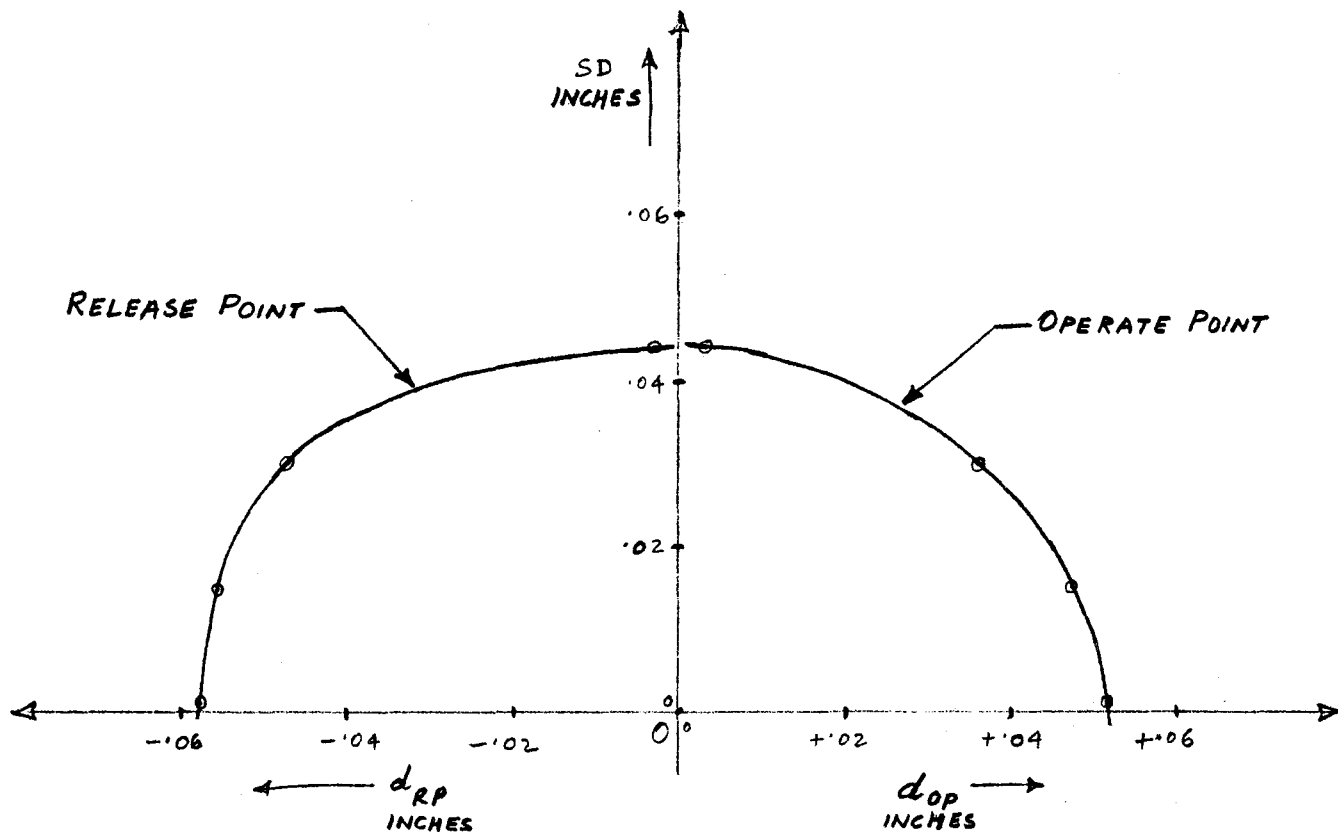
OFFSET BETWEEN SENSOR AND MAGNET  $D = 0$

$$\Delta_{RP}(.01-.03) = .010 \text{ INCH}$$

$$\Delta_{RP}(0-.02) = .004 \text{ INCH}$$

$$\Delta_{OP}(.01-.03) = .015 \text{ INCH}$$

$$\Delta_{OP}(0-.02) = .006 \text{ INCH}$$



DESIRED  $SD = .010$  INCH

Fig. 8

FOR SPRAGUE HALL EFFECT SENSOR  
 SAMARIUM COBALT MAGNET .08 INCH SQ. X .04 INCH THICK

CHANGE IN OPERATE AND RELEASE POINT DUE TO CHANGE IN SUPPLY VOLTAGE

AMBIENT TEMP. = 68°F

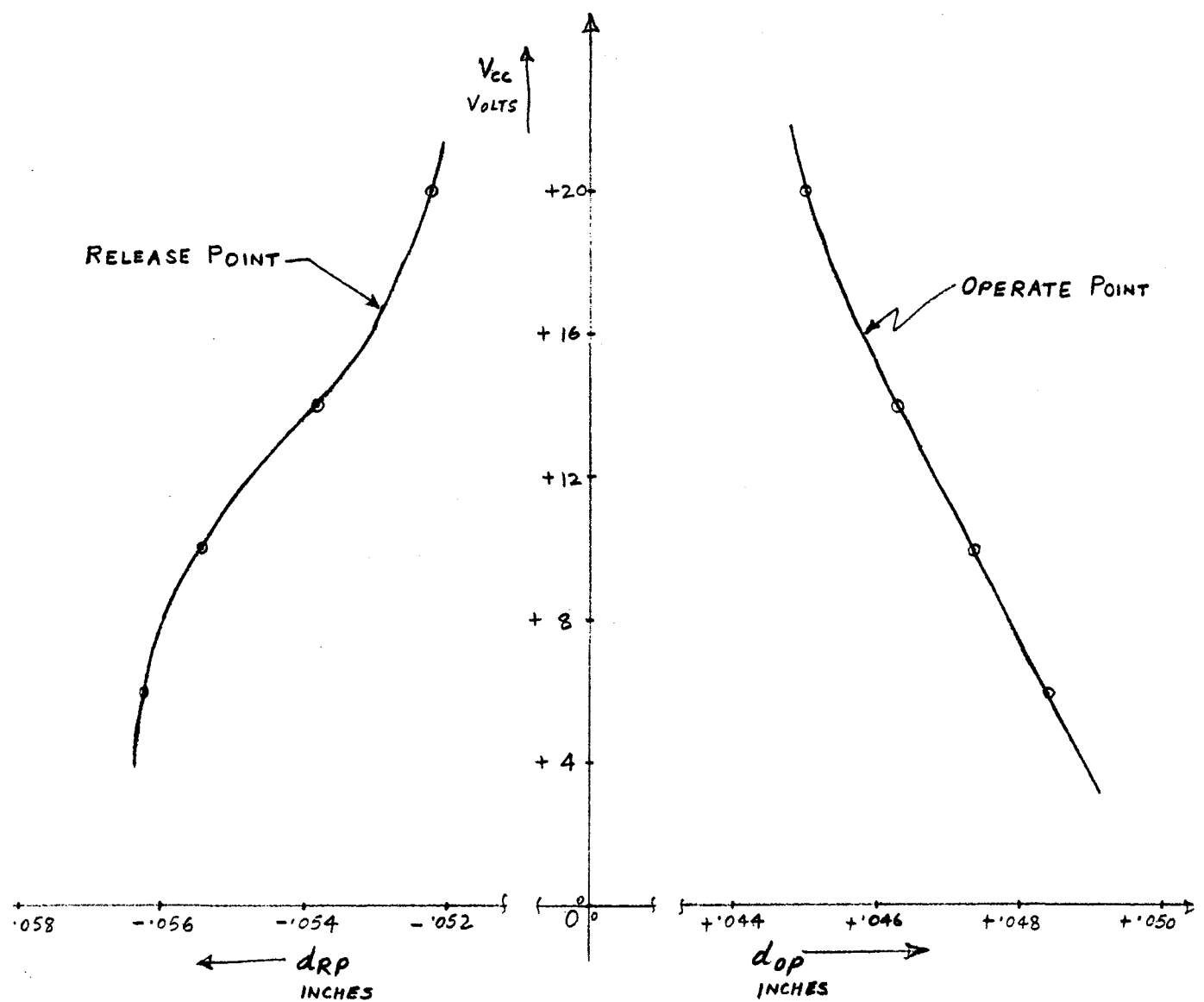
SWITCHING DISTANCE  $SD = .015$  inches  
 OFFSET BETWEEN SENSOR AND MAGNET  $D = 0$

$\Delta_{RP(6-20V)} = .004$  INCH

$\Delta_{OP(6-20V)} = .0034$  INCH

$\Delta_{RP(4-8V)} = .0004$  INCH

$\Delta_{OP(4-8V)} = .0010$  INCH



Desired Voltage = +20 V

Fig. 9

FOR SPRAGUE HALL EFFECT SENSOR  
SMARIUM COBALT MAGNET .08 INCH SQ. X .04 INCH THICK  
CHANGE IN OPERATE AND RELEASE POINT DUE TO OFFSET OF MAGNET AND SENSOR

AMBIENT TEMP. = 68°F

ITCHING DISTANCE SD = .015 INCH

SUPPLY VOLTAGE  $V_{CC} = +10V$

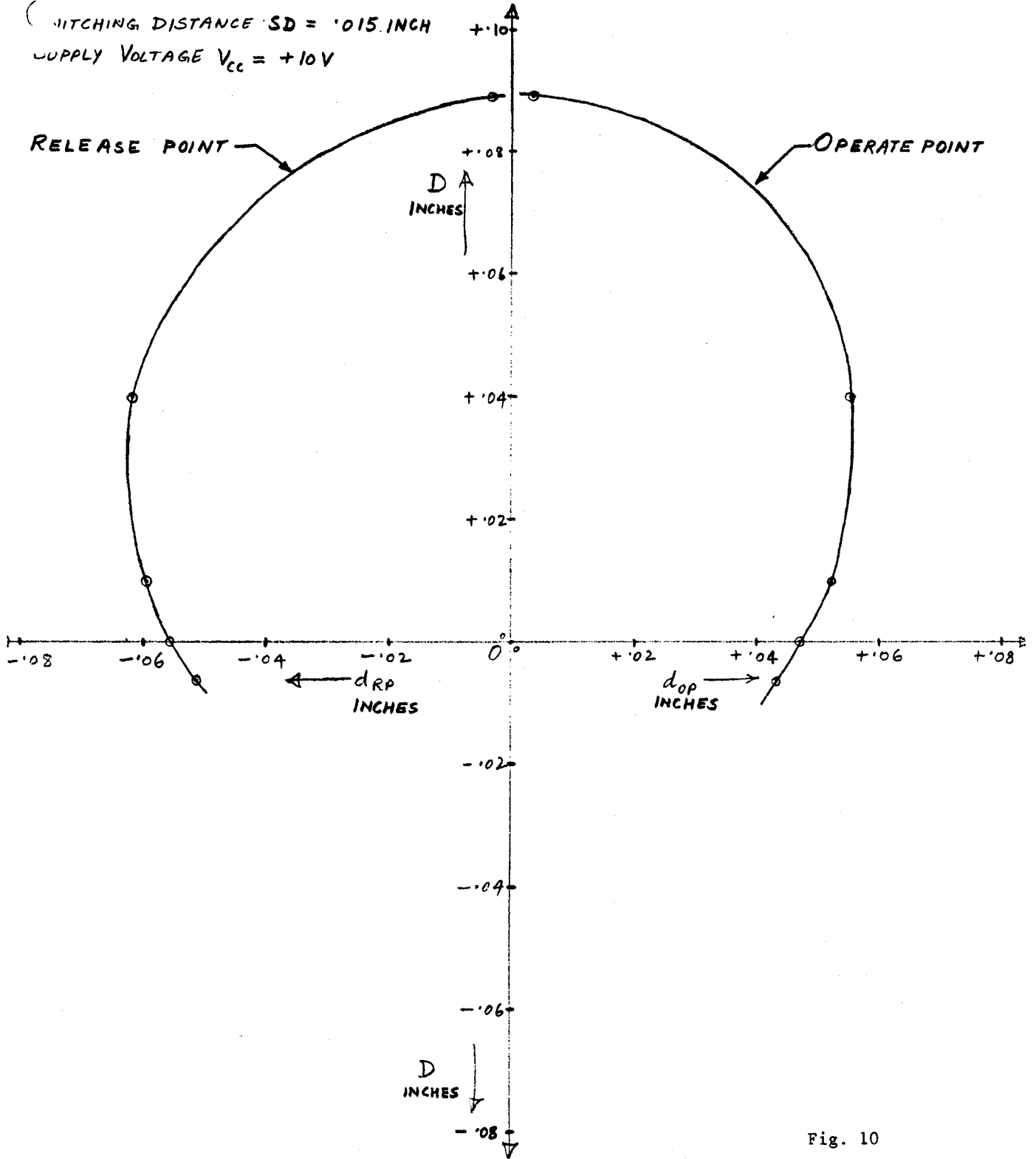


Fig. 10

FOR SPRAGUE HALL EFFECT SENSOR  
SAMARIUM COBALT MAGNET .08 INCH SQ. X .04 INCH THICK

REPEATABILITY SPAN FOR OPERATE AND RELEASE POINTS

AMBIENT TEMP. = 68°F

SWITCHING DISTANCE SD = .015 inches

OFFSET BETWEEN SENSOR AND MAGNET D = 0

OPERATE POINT ○  
RELEASE POINT □

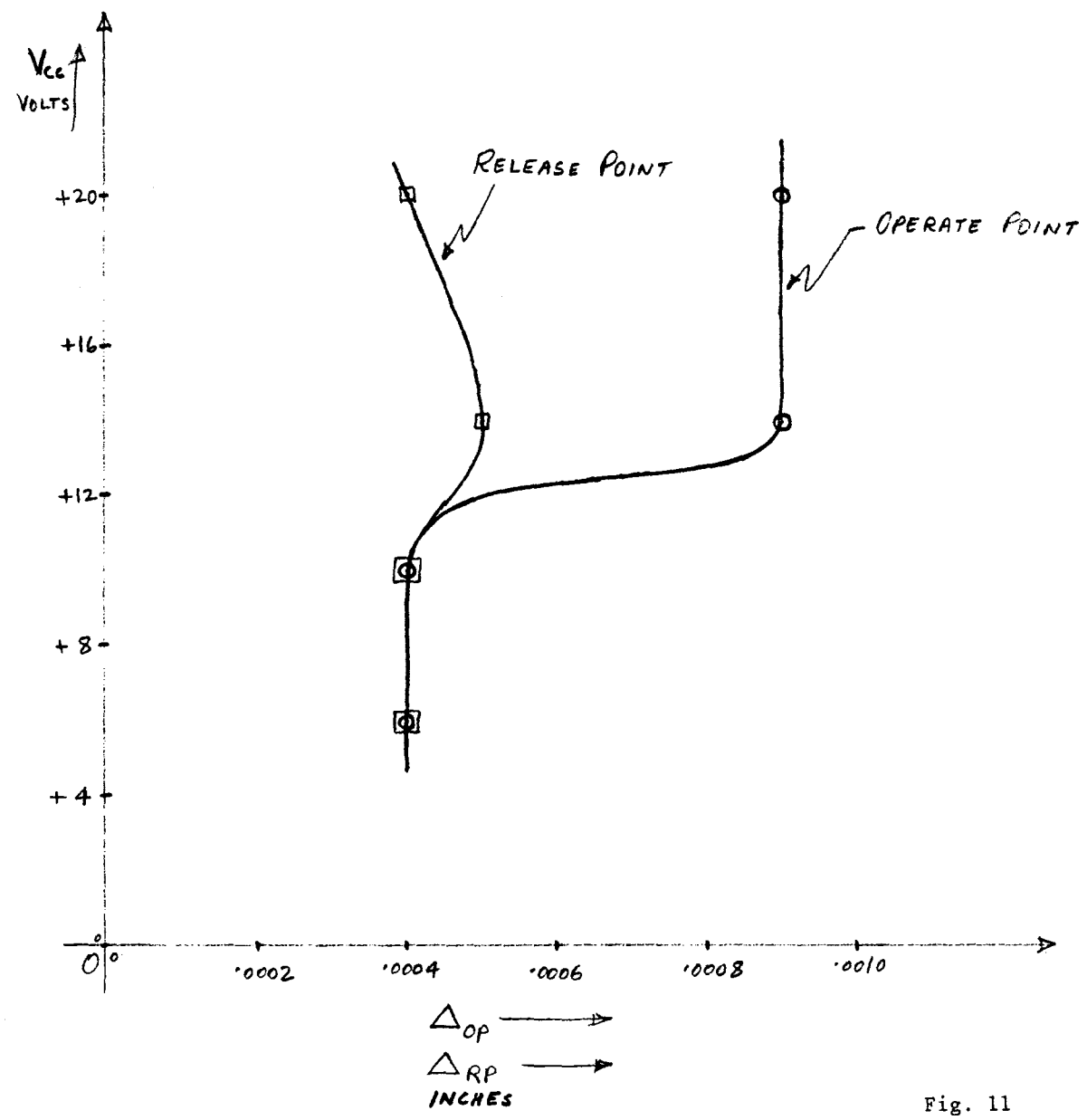


Fig. 11



- 3.5 All the readings are tabulated per Table I. The average operate point, release point and distance between operate and release points are calculated as shown in Table I.
- 3.6 Various curves showing the effect on operate and release points due to a change in supply voltage ' $V_{CC}$ ', switching distance ' $SD$ ' and offset distance ' $D$ ' between sensor and magnet are plotted as shown in Figures 4 through 6. Also a repeatability span curve is plotted as shown in Fig. 7.
- 3.7 The Sprague UGN 3020T sensor is mounted as per para 3.1. Repeat the whole procedure of para 3.2 through 3.6 for this sensor. Results of these tests are shown in Figures 8 through 11.
- 4.0 Comparing the results of curves for both Microswitch and Sprague Sensors, the Microswitch sensor gives better performance for operate and release points.

The desired supply voltage ' $V_{CC}$ ' and the switching distance ' $SD$ ' for Microswitch sensor shall be +10V and .015 inch respectively as can be seen from the curves.

APPENDIX

## TEST DATA

TABLE

- I For Microswitch Hall Effect Sensor 513SS16 and Hitachi Samarium Cobalt Permanent Magnet .08 inch square X .04 inch thick. Following tables show the test results like Offset distance 'D', Supply voltage 'V<sub>cc</sub>', Switching distance 'SD', Operate point 'd<sub>op</sub>', and Release point 'd<sub>RP</sub>'. The average operate, release and the distance between operate and release points are also shown in the table.
- II For Sprague Hall Effect Sensor UGN 3020T and Hitachi Samarium Cobalt Permanent Magnet .08 inch square X .04 inch thick. One of the magnet corners broke during this part of the test and hence this part is repeated and continued in Table III, using new magnet.
- III For Sprague Hall Effect Sensor UGN 3020T and Hitachi Samarium Cobalt Paermanent Magnet .08 inch square X .04 inch thick. New target magnet was used for this part of the test.
- IV To find if there are more than one Operate and Release Points, Sprague Sensor and new magnet were used.
- V To find if there are more than one Operate and Release Points, after orienting the magnet by 45<sup>o</sup>, Sprague Sensor and new magnet were used.
- VI To find if there are more than one Operate and Release Points, Microswitch Sensor and new magnet were used.

12/17/89

Ambient Temp. = 68°F.

Micro Switch ~~S~~ Hall Effect Sensor  
 Samarium Cobalt magnet .08 in. dia x .04 in. thick

TABLE I

OFFSET DISTANCE "D" INCHES	SUPPLY VOLTAGE Vcc VOLTS	SWITCHING DISTANCE "SD" INCHES	OPERATE POINT dop INCHES	RELEASE POINT dRp INCHES	(dRp - dop) INCHES	
D=0	+6V	.001	1. .0683	.06876	1. .0596	.12847
			2. .0687		2. .0602	
			3. .0686		3. .0595	
			4. .0689		4. .0594	
			5. .0686		5. .0595	
			6. .0690		6. .0599	
			7. .0690		7. .0598	
			8. .0689		8. .0596	
			9. .0687		9. .0597	
			10. .0689		10. .0599	
.018		.018	1. .0694	.06927	1. .0632	.13197
			2. .0693		2. .0629	
			3. .0692		3. .0623	
			4. .0694		4. .0623	
			5. .0694		5. .0627	
			6. .0697		6. .0628	
			7. .0693		7. .0623	
			8. .0691		8. .0624	
			9. .0690		9. .0629	
			10. .0689		10. .0624	
.032		.032	1. .0641	.06454	1. .0607	.12563
			2. .0644		2. .0608	
			3. .0648		3. .0615	
			4. .0645		4. .0618	
			5. .0645		5. .0609	
			6. .0645		6. .0613	
			7. .0646		7. .0611	
			8. .0648		8. .0606	
			9. .0646		9. .0614	
			10. .0646		10. .0608	
.047		.047	1. .0542	.05425	1. .0549	.10891
			2. .0542		2. .0547	
			3. .0544		3. .0548	
			4. .0542		4. .0545	
			5. .0542		5. .0547	
			6. .0544		6. .0546	
			7. .0543		7. .0544	
			8. .0541		8. .0547	
			9. .0543		9. .0547	
			10. .0541		10. .0546	
<del>.066</del> .062		<del>.066</del> .062	1. .0303	.03042	1. .0426	.07293
			2. .0302		2. .0427	
			3. .0305		3. .0429	
			4. .0303		4. .0426	
			5. .0305		5. .0425	
			6. .0305		6. .0425	
			7. .0305		7. .0423	
			8. .0307		8. .0423	
			9. .0305		9. .0423	
			10. .0302		10. .0424	
.066		.066	1. .0098	.00949	1. .0378	.04699
			2. .0098		2. .0376	
			3. .0096		3. .0375	
			4. .0097		4. .0372	
			5. .0098		5. .0375	
			6. .0093		6. .0373	
			7. .0093		7. .0373	
			8. .0094		8. .0374	
			9. .0094		9. .0374	
			10. .0095		10. .0374	







17  $\left( \begin{matrix} .030 \\ .041 \end{matrix} \right) \rightarrow$  Horizontal Line:

1-⑤

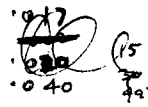


TABLE I

Group	Distance	Top Index	Bottom Index	Top Index	Bottom Index
D = -.0083 +6 ✓	.001	1. .0520	.05206	+.0732	.1252
		2. .0522		.0732	.1254
		3. .0520		.0731	.1251
		4. .0523		.0720	.1253
		5. .0528		.0720	.1248
	.015	1. .0533	.05338	.0768	.1294
		2. .0534		.0760	.1294
		3. .0533		.0761	.1294
		4. .0534		.0762	.1296
		5. .0535		.0762	.1297
	.030	1. .0491	.04912	.0750	.1241
		2. .0492		.0746	.1238
		3. .0491		.0747	.1238
		4. .0492		.0746	.1238
		5. .0490		.0747	.1237
	.045	1. +.0542	.05392	-.0538	.1080
		2. .0536		.0536	.1072
		3. .0537		.0534	.1071
		4. .0541		.0534	.1080
		5. .0540		.0536	.1076
	.064	1. .0110	.0111	.0371	.0481
		2. .0113		.0367	.0480
		3. .0110		.0365	.0475
		4. .0111		.0367	.0478
		5. .0112		.0365	.0477
+10V	.001	1. .0676	.06732	.0571	.1247
		2. .0672		.0576	.1248
		3. .0672		.0575	.1247
		4. .0674		.0574	.1248
		5. .0672		.0578	.1250
	.015	1. .0678	.06828	.0602	.1280
		2. .0682		.0602	.1284
		3. .0685		.0600	.1285
		4. .0685		.0600	.1285
		5. .0684		.0605	.1289
	.030	1. .0640	.06404	.0590	.1230
		2. .0642		.0592	.1234
		3. .0640		.0587	.1227
		4. .0640		.0588	.1228
		5. .0640		.0584	.1224
	.045	1. .0533	.05344	.0523	.1056
		2. .0536		.0521	.1057
		3. .0534		.0520	.1054
		4. .0536		.0522	.1058
		5. .0533		.0522	.1055
	.063	1. .0192	.01902	.0365	.0557
		2. .0190		.0364	.0554
		3. .0189		.0361	.0550
		4. .0189		.0360	.0549
		5. .0191		.0365	.0556

TABLE I

						OP - RP:	23
D = +0186	+ 10V	.001	1. +00677	-00575	.1252	.12450	
			2. 00674	00569	.1243		
			3. 00673	00569	.1242		
			4. 00676	00570	.1246		
			5. 00673	00569	.1242		
.015		.015	1. 00685	00598	.1283	.12846	
			2. 00685	00600	.1285		
			3. 00685	00599	.1284		
			4. 00686	00598	.1284		
			5. 00687	00600	.1287		
.030		.030	1. 00640	00587	.1227	.12268	
			2. 00640	00587	.1227		
			3. 00640	00585	.1225		
			4. 00639	00588	.1227		
			5. 00641	00587	.1228		
.045		.045	1. 00531	00522	.1053	.10556	
			2. 00535	00520	.1055		
			3. 00536	00519	.1055		
			4. 00533	00526	.1059		
			5. 00533	00523	.1056		
.063		.063	1. 00154	00358	.0509	.05078	
			2. 00150	00357	.0507		
			3. 00150	00357	.0507		
			4. 00155	00353	.0508		
			5. 00156	00352	.0508		
D = +0350	+ 10V	.015	1. 00637	00550	.1187	.11874	
			2. 00637	00550	.1187		
			3. 00639	00551	.1190		
			4. 00638	00552	.1190		
			5. 00630	00553	.1183		
D = +0661	+ 10V	.015	1. 00202	00258	.0460	.04504	
			2. 00188	00260	.0448		
			3. 00188	00259	.0447		
			4. 00190	00262	.0452		
			5. 00188	00257	.0445		
D = -0350	+ 10V	.015	1. 00570	00510	.1080	.10820	
			2. 00573	00509	.1082		
			3. 00573	00512	.1085		
			4. 00570	00511	.1081		
			5. 00573	00509	.1082		
D = -0573	+ 10V	.015	1. +00151	-00260	.0411	.04146	
			2. +00155	00262	.0417		
			3. 00154	00262	.0416		
			4. 00151	00261	.0412		
			5. 00155	00262	.0417		



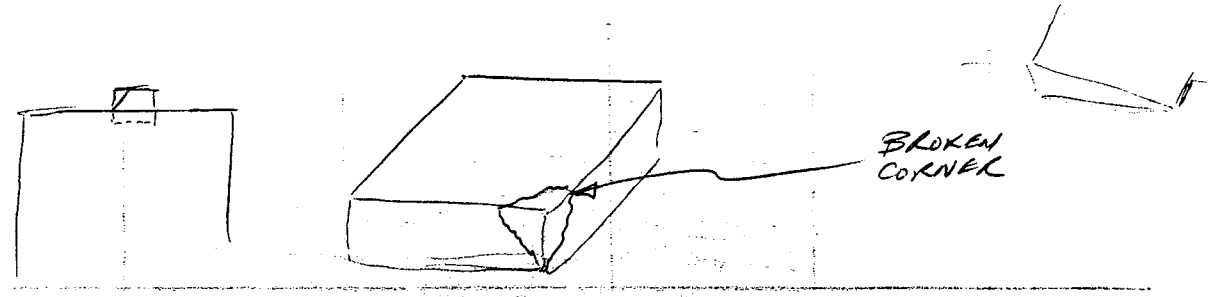
Sprague

Small Magnet

TABLE II

D=0	+6	.001					
			1. .0448	.0457	.0638	.0637	.1086
			2. .0447		.0640		.1087
			3. .0449		.0638		.1087
			4. .0450		.0639		.1089
			5. .0455		.0636		.1091
			6. .0448		.0643		.1091
			7. .0451		.0637		.1088
			8. .0451		.0638		.1089
			9. .0453		.0640		.1093
			10. .0455		.0638		.1093
			-----				
		.015	1. .0447	.04091	.0620	.0617	.1067
			2. .0403		.0616		.1019
			3. .0403		.0618		.1021
			4. .0406		.0618		.1024
			5. .0406		.0622	.0617	.1028
			6. .0405		.0619		.1024
			7. .0404		.0623		.1027
			8. .0404		.0623		.1022
			9. .0403		.0619		.1030
			10. .0408		.0622		.1026
			-----				
		.030	1. .0293	.0300	.0551	.05520	.0844
			2. .0294		.0551		.0845
			3. .0295		.0554		.0849
			4. .0292		.0552		.0844
			5. .0292		.0551		.0843
			6. .0296		.0551		.0847
			7. .0349		.0552		.0845
			8. .0297		.0551		.0846
			9. .0302		.0553		.0846
			10. .0300				

Note:  
 The corner piece of the target magnet ~~is~~ found broken. New magnet will be used here on.



12/19

1-9

Sprague Hall Effect Sensor

Ambient Temp. = 68°F

New Small ~~As~~ magnet.  
New Samarium Cobalt magnet, .08" dia Sq. X .04" in thick.

TABLE III

Sample ID	Reading	Average	Standard Deviation	Final Value
D20 +6V .001	1. + .0522	.05224	.0590	.1112
	2. .0522			
	3. .0523			
	4. .0522			
	5. .0523			
	6. .0523			
	7. .0523			
	8. .0522			
	9. .0523			
	10. .0524			
.015	1. .0485	.04840	.0560	.1045
	2. .0485			
	3. .0484			
	4. .0482			
	5. .0484			
	6. .0482			
	7. .0484			
	8. .0486			
	9. .0484			
	10. .0484			
.030	1. .0381	.03802	.0490	.0871
	2. .0381			
	3. .0381			
	4. .0378			
	5. .0381			
	6. .0380			
	7. .0379			
	8. .0380			
	9. .0379			
	10. .0380			
.045	1. + .0043	.00409	.0340	.0383
	2. .0039			
	3. .0038			
	4. .0038			
	5. .0043			
	6. .0047			
	7. .0039			
	8. .0043			
	9. .0038			
	10. .0039			
+10V .001	1. .0520	.05184	.0578	.1098
	2. .0518			
	3. .0519			
	4. .0519			
	5. .0518			
	6. .0519			
	7. .0519			
	8. .0516			
	9. .0518			
	10. .0518			
.015	1. .0474	.04739	.0552	.1026
	2. .0472			
	3. .0471			
	4. .0475			
	5. .0475			
	6. .0472			
	7. .0475			
	8. .0475			
	9. .0475			
	10. .0475			
.030	1. .0355	.03602	.0475	.0828
	2. .0361			
	3. .0360			
	4. .0258			
	5. .0361			
	6. .0360			
	7. .0366			
	8. .0360			
	9. .0361			
	10. .0362			

TABLE III

D=0	+ 10V	.044	1. + .0005	.0289	.0328	.0320	.0333		
			2. .0047					.0332	.0353
			3. .0021					.0332	.0363
			4. .0032					.0331	.0345
			5. .0020					.0325	.0364
			6. .0034					.0330	.0358
			7. .0030					.0328	.0352
			8. .0019					.0333	.0359
			9. .0031					.0328	.0372
			10. .0050					.0322	
	+ 14V	.001	1. .0512	.0511	.0578	.0570	.1090		
			2. .0512					.0569	.1081
			3. .0511					.0570	.1031
			4. .0511					.0568	.1079
			5. .0511					.0572	.1083
			6. .0510					.0568	.1078
			7. .0509					.0568	.1077
			8. .0512					.0569	.1081
			9. .0513					.0570	.1083
			10. .0510					.0568	.1078
		.015	1. .0466	.04630	.0537	.0530	.1003		
			2. .0465					.0541	.1006
			3. .0463					.0537	.1000
			4. .0459					.0538	.0997
			5. .0463					.0536	.0999
			6. .0464					.0538	.1002
			7. .0466					.0537	.1003
			8. .0458					.0541	.1009
			9. .0466					.0537	.1003
			10. .0457					.0538	.0995
		.030	1. .0342	.03398	.0452	.04483	.0794		
			2. .0339					.0449	.0788
			3. .0343					.0451	.0794
			4. .0338					.0449	.0787
			5. .0335					.0449	.0784
			6. .0342					.0445	.0787
			7. .0340					.0450	.0790
			8. .0335					.0450	.0785
			9. .0341					.0448	.0787
			10. .0343					.0440	.0783
		.042	1. + .0085	.00778	.0318	.0320	.0403		
			2. .0086					.0317	.0403
			3. .0067					.0321	.0388
			4. .0071					.0320	.0391
			5. .0092					.0325	.0417
			6. .0075					.0318	.0393
			7. .0094					.0324	.0408
			8. .0067					.0316	.0383
			9. .0078					.0322	.0400
			10. .0073					.0321	.0394
	+ 20V	.001	1. .0507	.05060	.0538	.056598	.1065		
			2. .0508					.0557	.1065
			3. .0507					.0561	.1068
			4. .0507					.0558	.1068
			5. .0505					.0560	.1065
			6. .0505					.0560	.1065
			7. .0506					.0563	.1065
			8. .0504					.0561	.1069
			9. .0505					.0560	.1067
			10. .0505					.0560	.1065
		.015	1. .0456	.04505	.0525	.05223	.0981		
			2. .0451					.0523	.0974
			3. .0450					.0521	.0971
			4. .0447					.0522	.0969
			5. .0447					.0522	.0969
			6. .0454					.0521	.0975
			7. .0451					.0521	.0972
			8. .0451					.0522	.0973
			9. .0451					.0524	.0975
			10. .0447					.0522	.0979

TABLE III

D	V	Group	Item	Value 1	Value 2	Value 3	Value 4
D=0	+20V	.030	1.	.0327	.0426	.0753	.07458
			2.	.0318	.0433	.0751	
			3.	.0322	.0433	.0755	
			4.	.0313	.0429	.0742	
			5.	.0322	.0425	.0745	
			6.	.0310	.0428	.0738	
			7.	.0319	.0425	.0744	
			8.	.0311	.0424	.0735	
			9.	.0323	.0427	.0750	
			10.	.0320	.0425	.0745	
		.040	1.	.0105	.0308	.0413	.04143
			2.	.0107	.0308	.0415	
			3.	.0104	.0305	.0396	
			4.	.0100	.0300	.0400	
			5.	.0106	.0315	.0421	
			6.	.0112	.0312	.0424	
			7.	.0100	.0312	.0412	
			8.	.0100	.0306	.0406	
			9.	.0116	.0315	.0431	
			10.	.0110	.0315	.0425	
D = -.0065	+10V	.001	1.	.0478	.0545	.1023	.10148
			2.	.0476	.0542	.1028	
			3.	.0472	.0542	.1024	
			4.	.0473	.0544	.1017	
			5.	.0479	.0543	.1022	
		.015	1.	.0427	.0516	.0943	.09458
			2.	.0435	.0513	.0948	
			3.	.0438	.0512	.0950	
			4.	.0431	.0513	.0944	
			5.	.0431	.0513	.0944	
.030	1.	.0297	.0428	.0725	.07232		
	2.	.0296	.0424	.0720			
	3.	.0291	.0427	.0718			
	4.	.0292	.0420	.0712			
	5.	.0295	.0426	.0721			
.040	1.	.0033	.0317	.0350	.03512		
	2.	.0030	.0319	.0349			
	3.	.0042	.0321	.0353			
	4.	.0030	.0323	.0353			
	5.	.0030	.0321	.0351			

TABLE III

D	SIGNAL STABLE	SIGNAL STABLE	OPERATE POINT		RELOAD POINT (Rea - 400)				
			Top Inches	Top Inches	Top Inches	Top Inches			
D = +0100	+10V	001	1. +0555	05556	0614	0614	1167		
			2. 0555					0620	1175
			3. 0554					0613	1167
			4. 0552					0613	1165
			5. 0562					0614	1176
015			1. 0523	05214	0594	05944	1119		
			2. 0519					0594	1113
			3. 0524					0592	1116
			4. 0521					0595	1116
			5. 0520					0595	1115
030			1. 0420	04220	0529	05304	0959		
			2. 0424					0529	0953
			3. 0420					0529	0947
			4. 0426					0528	0954
			5. 0420					0529	0949
048			1. 0082	00826	0335	03388	0417		
			2. 0079					0334	0413
			3. 0085					0338	0423
			4. 0085					0344	0429
			5. 0082					0343	0425
<del>001</del>	+10V	001	1. 0587	05862	0633	06318	1220		
			2. 0586					0633	1219
			3. 0580					0630	1210
			4. 0587					0632	1219
			5. 0591					0631	1222
015			1. 0556	05558	0620	0619	1176		
			2. 0557					0618	1175
			3. 0557					0620	1177
			4. 0555					0618	1173
			5. 0554					0619	1173
030			1. 0466	04686	0557	0559	1023		
			2. 0471					0560	1031
			3. 0471					0561	1032
			4. 0467					0558	1025
			5. 0468					0559	1027
048			1. 0207	02014	0399	03780	0606		
			2. 0299					0394	0593
			3. 0194					0399	0593
			4. 0204					0401	0605
			5. 0203					0397	0600

$D = 0$        $+10V$        $.015$

TABLE III

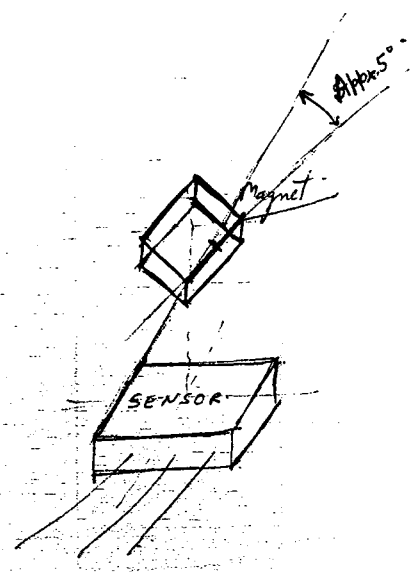
OFFSET DISTANCE "D" INCHES	SUPPLY VOLTAGE "V <sub>cc</sub> " VOLTS	SWITCHING DISTANCE "SD" INCHES	OPERATE POINT "dop" INCHES	RELEASE POINT "drp" INCHES	(drp - dop) INCHES	
D = +.0918	+10V	.001	1. .0063	.0272 .0266 .0264 .0269 .0269	.0335 .0327 .0316 .0319 .0329	.03246
			2. .0058			
			3. .0052			
			4. .0050			
			5. .0060			
D = +.0890	+10V	.015	1. .0037	.0287 .0283 .0285 .0284 .0280	.0324 .0318 .0316 .0323 .0316	.03194
			2. .0035			
			3. .0031			
			4. .0039			
			5. .0036			
D = +.0800	+10V	.030	1. .0047	.0315 .0315 .0309 .0312 .0309	.0362 .0368 .0363 .0369 .0366	.03456
			2. .0053			
			3. .0054			
			4. .0057			
			5. .0057			
D = +.0687	+10V	.040	1. .0034	.0325 .0313 .0316 .0318 .0323	.0359 .0368 .0381 .0380 .0385	.03746
			2. .0055			
			3. .0065			
			4. .0062			
			5. .0062			

To find if there are more than one Operate and Release Points.

TABLE IV

TRIP POINT	OPERATE POINT	RELEASE POINT	OPERATE POINT	RELEASE POINT
For Travel from +.5" to -.5"			From .500	
D = 0	+10V	.015	+ 0.0472	+ 0.0570
				From .500
			- 0.0485	+ 0.0550
				.1035

TRIP POINT	OPERATE POINT	RELEASE POINT	OPERATE POINT	RELEASE POINT
For Travel from +.25" to -.25"			From .250	
d = 0	+10V	.015	D = - 0.0245	D = + 0.0960
				.1205
				From .250
			+ 0.0886	- 0.0376
				.1204



To find if there are more than one Operate and Release Points 1-17

After orientating the magnet approx.  $45^\circ$

TABLE V

Direction	Switching Voltage	Switching Distance (100 Inches)	Operate Point (100 Inches)	Release Point (100 Inches)	(See notes)
For travel from $+15^\circ$ to $-15^\circ$	$D=0$	$+10V$	$0.500$		
		$.015$	$d = +.0448$	$-.0515$	$.0963$
			$d = -.0437$	$+ .0520$	$.0957$
For travel from $+25^\circ$ to $-25^\circ$	$d=0$	$+10V$			
		$.015$	$D = -.0231$	$D = +.0985$	$.1216$
			$D = +.0917$	$D = -.0300$	$.1217$



Repeat reading on Micro Sw. Sensor with new magnet.

TABLE VII. Also to verify <sup>and</sup> there is only one Operate and Release Point.

Distance	Supply Voltage	Distance to Magnet	Operate Point (to Inhibit)	Release Point (to Inhibit)	Mean Value
D=0	+10V	.015"	+ .0608	- .0665	.1273
			+ .0608	- .0666	.1274
D=0	+10V	.015"	.0597	+ .0673	.1270
d=0	+10V	.015"	D <sub>2</sub> + .0798	D <sub>1</sub> - .0559	.1357
			D <sub>2</sub> - .0454	D <sub>1</sub> + .0870	.1324

.1275

.1270

.1305

UNLIMITED RELEASE  
INITIAL DISTRIBUTION

UC-62d (350)

U.S. Department of Energy  
600 E Street NW  
Washington, D. C. 20585  
Attn: W. W. Auer  
G. W. Braun  
K. Cherian  
M. U. Gutstein  
L. Melamed  
J. E. Rannels

U.S. Department of Energy  
San Francisco Operations Office  
1333 Broadway  
Oakland, CA 94612  
Attn: S. D. Elliott  
S. Fisk  
R. W. Hughey  
W. Nettleton

U.S. Department of Energy  
Solar Ten Megawatt Project Office  
P. O. Box 1449  
Canoga Park, CA 91304  
Attn: M. Slaminski

U.S. Department of Energy  
Solar Ten Megawatt Project Office  
5301 Bolsa Ave. MS14-1  
Huntington Beach, CA 92649  
Attn: R. N. Schweinberg

USAF Logistics Command  
P. O. Box 33140  
Wright-Patterson AFB  
Ohio 45433  
Attn: G. Kastanos

UCLA  
900 Veteran Avenue  
Los Angeles, CA 90024  
Attn: F. Turner

Georgia Institute of Technology  
Engineering Experiment St.  
Atlanta, GA 30332  
Attn: S. H. Bomar, Jr.

University of Houston  
Houston  
Solar Energy Laboratory  
4800 Calhoun  
Houston, TX 77004  
Attn: A. F. Hildebrandt  
L. L. Vant-Hull

U.S. Department of Interior  
Water & Power Res. Service  
P.O. Box 427  
Boulder City, NV 89005  
Attn: J. Sundberg

Acurex  
485 Clyde Avenue  
Mountain View, CA 94042  
Attn: J. Hull

Aerospace Corporation  
Solar Thermal Projects  
Energy Systems Group, D-5  
Room 1110  
P.O. Box 92957  
El Segundo, CA 90009  
Attn: P. deRienzo  
P. Mathur

Airesearch Manufacturing Co.  
2525 West 190th Street  
Torrance, CA 90509  
Attn: M. G. Coombs  
For: P. F. Connelly

AMFAC  
700 Bishop Street  
Honolulu, HI 96801  
Attn: G. St. John

ARCO  
911 Wilshire Blvd  
Los Angeles, CA 90017  
Attn: J. H. Caldwell, Jr.

Arizona Public Service  
P. O. Box 21666  
Phoenix, AZ 85036  
Attn: D. L. Barnes  
For: E. Weber

Arizona Solar Energy Commission  
1700 W. Washington - 502  
Phoenix, AZ 85007  
Attn: R. Sears

Babcock & Wilcox  
91 Stirling Avenue  
Barberton, OH 44203  
Attn: G. Grant  
For: J. Pletcher  
M. Seale

Babcock & Wilcox  
P. O. Box 1260  
Lynchburg, VA 24505  
Attn: W. Smith

Babcock & Wilcox  
20 S. VanBuren Avenue  
Barberton, OH 44203  
Attn: M. Wiener

Badger Energy, Inc.  
One Broadway  
Cambridge, MA 02142  
Attn: F. D. Gardner

Battelle Pacific Northwest Labs  
P. O. Box 999  
Richland, WA 99352  
Attn: M. A. Lind

Bechtel National, Inc.  
P. O. Box 3965  
San Francisco, CA 94119  
Attn: E. Lam  
For: J. B. Darnell  
R. L. Lessley

Black & Veatch  
P. O. Box 8405  
Kansas City, MO 64114  
Attn: C. Grosskreutz  
For: J. E. Harder  
S. Levy

Boeing Engineering & Construction  
P. O. Box 3707  
Seattle, WA 98124  
Attn: R. L. Campbell  
R. Gillette  
J. R. Gintz

Booz, Allen & Hamilton, Inc.  
8801 E. Pleasant Valley Road  
Cleveland, OH 44131  
Attn: W. Hahn

Brookhaven National Laboratory  
Upton, NY 11973  
Attn: G. Cottingham

Burns and Roe, Inc.  
550 Kinderkamack Rd.  
Oradell, NJ 07649  
Attn: J. Willson

Burns and Roe, Inc.  
185 Crossways Park Drive  
Woodbury, NY 11797  
Attn: R. Vondrasek

Busche Energy Systems  
7288 Murdy Circle  
Huntington Beach, CA 92647  
Attn: K. Busche

California Public Utilities Commission  
350 McAllister St., Room 5024  
San Francisco, CA 94102  
Attn: B. Barkovich  
For: C. Waddell

Chevron Research  
P. O. Box 1627  
Richmond, CA 94804  
Attn: L. Fraas

Chevron Oil Research  
P. O. Box 446  
La Habra, CA 90631  
Attn: W. Peake  
For: J. Ploeg  
W. Stiles

Colt Industries  
Trent Tube Division  
East Troy, WI 53170  
Attn: J. Thackray

Corning Glass Works  
Advanced Products Dept.  
M/S 25  
Corning, NY 14830  
Attn: W. M. Baldwin  
A. Shoemaker

Custom Metals Enterprises, Inc.  
3288 Main Street  
Chula Vista, CA 92011  
Attn: T. J. Bauer

Data Science Corp.  
1189 Oddstad Drive  
Redwood City, CA 94063  
Attn: M. Liang

Electric Power Research Institute  
P. O. Box 10412  
Palo Alto, CA 93403  
Attn: J. Bigger

El Paso Electric Company  
P. O. Box 982  
El Paso, TX 79946  
Attn: J. E. Brown

Energy, Inc.  
P. O. Box 736  
Idaho Falls, ID 83401  
Attn: G. Meredith

Exxon Enterprises-Solar Thermal Systems  
P. O. Box 592  
Florham Park, NJ 07932  
Attn: P. Joy  
For: D. Nelson  
G. Yenetchi

Ford Aerospace  
3939 Fabian Way, T33  
Palo Alto, CA 94303  
Attn: I. E. Lewis  
For: H. Sund

Foster-Miller Associates  
135 Second Avenue  
Waltham, MA 02154  
Attn: E. Poulin

Foster Wheeler Dev. Corp.  
12 Peach Tree Hill Road  
Livingston, NJ 07039  
Attn: A. C. Gangadharan  
For: R. Zoschak

GAI Consultants, Inc.  
570 Beatty Rd.  
Monroeville, PA 15146  
Attn: H. Davidson

General Atomic Company  
P. O. Box 81608  
San Diego, CA 92138  
Attn: H. A. Chiger

General Electric Company  
Advanced Energy Programs  
P. O. Box 8661  
Philadelphia, PA 19101  
Attn: A. A. Koenig

General Electric Company  
1 River Road  
Schenectady, NY 12345  
tric Company  
1 River Road  
Schenectady, NY 12345  
Attn: J. A. Elsner  
For: R. N. Griffin  
R. Horton

GM Transportation System Center  
GM Technical Center  
Warren, MI 48090  
Attn: J. Britt

GM Corp. Harrison Rad. Division  
A and E Building  
Lockport, NY 14094  
Attn: A. Stocker

Houston Lighting and Power  
P. O. Box 1700  
Houston, TX 77001  
Attn: J. Ridgway

Institute of Gas Technology  
Suite 218  
1825 K Street, NW  
Washington, D. C. 25006  
Attn: D. R. Glenn

Jet Propulsion Laboratory  
Building 520-201  
4800 Oak Grove Drive  
Pasadena, CA 91103  
Attn: M. Adams  
H. Bank  
W. Carley  
E. Cuddihy  
J. Sheldon  
J. Swan  
V. Truscello

Kaiser Engineers, Inc.  
300 Lakeside Drive  
Oakland, CA 94612  
Attn: I. Kornyey

Lawrence Berkeley National Laboratory  
University of California  
Berkeley, CA 94720  
Attn: A. J. Hunt

*[Faint, illegible text, possibly bleed-through from the reverse side of the page]*

Los Alamos National Laboratory  
P. O. Box 1663  
Los Alamos, NM 87545  
Attn: S. W. Moore

Los Angeles Water and Power  
111 North Hope Street  
Los Angeles, CA 90051  
Attn: B. M. Tuller  
R. Radmacher

Martin Marietta Corporation  
P. O. Box 179  
Denver, CO 80201  
Attn: P. R. Brown  
A. E. Hawkins  
T. Heaton  
L. Oldham  
H. C. Wroton

McDonnell Douglas Astronautics Co.  
5301 Bolsa Avenue  
Huntington Beach, CA 92647  
Attn: P. Drummond  
R. L. Gervais  
D. A. Steinmeyer  
L. Weinstein

Meridian Corporation  
5515 Cherokee Avenue  
Alexandria, VA 22312  
Attn: B. S. Macazeer

Nielsen Engineering. & Research  
510 Clyde Avenue  
Mt. View, CA 94043  
Attn: R. Schwind

Northrup, Inc.  
302 Nichols Drive  
Hutchins, TX 75141  
Attn: J. A. Pietsch

ARCO Power Systems  
Suite 301  
7061 S. University Boulevard  
Littleton, CO 80122  
Attn: J. Anderson  
F. Blake

Olin Corporation  
275 Winchester Avenue  
New Haven, CT 06511  
Attn: S. L. Goldstein



OSC Department of Commerce  
341 West 2d Street  
San Bernardino, CA 92401  
Attn: M. G. Heaviside

Pacific Gas and Electric Co.  
77 Beale Street  
San Francisco, CA 94105  
Attn: P. D. Hindley  
For: J. F. Doyle  
A. Lam

Pacific Gas and Electric Co.  
3400 Crow Canyon Road  
San Ramon, CA 9426  
Attn: H. Seielstad  
For: J. Raggio

Phillips Chemical Co.  
13-D2 Phillips Building  
Bartlesville, OK 74004  
Attn: M. Bowman

Pittsburgh Corning  
800 Presque Isle Drive  
Pittsburgh, PA 15239  
Attn: W. F. Lynsavage

Pittsburgh Corning  
723 N. Main Street  
Port Allegany, PA 16743  
Attn: W. J. Binder  
For: R. Greene

PPG Industries, Inc.  
One Gateway Center  
Pittsburgh, PA 15222  
Attn: C. R. Frownfelter

Public Service Co. of New Mexico  
P. O. Box 2267  
Albuquerque, NM 87103  
Attn: A. Akhil

Research and Development  
Public Service Co. of Oklahoma  
P. O. Box 201  
Tulsa, OK 74102  
Attn: F. Meyer

Rockwell International  
Energy Systems Group  
8900 De Soto Avenue  
Canoga Park, CA 91304  
Attn: T. Springer

*[Faint, illegible text, likely bleed-through from the reverse side of the page]*

S. C. Plotkin & Associates  
6451 West 83rd Street  
Los Angeles, CA 90045  
Attn: W. Raser

Safeguard Power Transmission Co.  
Hub City Division  
P. O. Box 1089  
Aberdeen, SD 57401  
Attn: R. E. Feldges

Sargent and Lundy  
55 East Monroe  
Chicago, IL 60603  
Attn: N. Weber

Schumacher & Associates  
2550 Fair Oaks Blvd., Suite 120  
Sacramento, CA 95825  
Attn: J. C. Schumacher

Sierra Pacific Power Co.  
P. O. Box 10100  
Reno, NV 89510  
Attn: W. K. Branch

Solar Energy Research Institute  
1617 Cole Boulevard  
Golden, CO 80401  
Attn: L. Duhham, TID  
G. Gross  
B. Gupta  
D. W. Kearney  
L. M. Murphy  
R. Ortiz, SEIDB  
J. Thornton

Solar Thermal Test Facility  
User Association  
Suite 1205  
First National Bank East  
Albuquerque, NM 87112  
Attn: F. Smith

Solar Turbines International  
P. O. Box 80966  
San Diego, CA 92138  
Attn: P. Roberts

Southern California Edison  
2244 Walnut Grove Road  
Rosemead, CA 91770  
Attn: J. Reeves  
For: C. Winarski

Southwestern Public Service Co.  
P. O. Box 1261  
Amarillo, TX 78170  
Attn: A. Higgins

Standard Oil of California  
555 Market Street  
San Francisco, CA 94105  
Attn: S. Kleespies

Stanford Research Institute  
333 Ravenswood Avenue  
Menlo Park, CA 94025  
Attn: A. Slemmons

Stearns-Roger  
P. O. Box 5888  
Denver, CO 80217  
Attn: W. Lang  
For: J. Hopson

Stone & Webster Engineering Corp.  
245 Summer Street  
P. O. Box 2325  
Boston, MA 02107  
Attn: R. Kuhr

Townsend and Bottum  
9550 Flair Drive  
El Monte, CA 91731  
Attn: R. Schwing

US Gypsum  
101 S. Wacker Drive  
Chicago, IL 60606  
Attn: Ray McCleary

US Water & Power Resources Service  
Bureau of Reclamation  
Code 1500 E  
Denver Federal Center  
P. O. Box 25007  
Denver, CO 80225  
Attn: S. J. Hightower

Van Leer Plastics  
15581 Computer Lane  
Huntington Beach, CA 92649  
Attn: Larry Nelson

Veda, Inc.  
400 N. Mobile, Building D  
Camarillo, CA 90310  
Attn: L. E. Ehrhardt  
For: W. Moore

Westinghouse Corporation  
 Box 10864  
 Pittsburgh, PA 15236  
 Attn: J. J. Buggy  
 For: R. W. Devlin  
 W. Parker

Winsmith  
 Division of UMC Industries  
 Springville, NY 14141  
 Attn: W. H. Heller

K. R. Miller, 3153  
 G. E. Brandvold, 4710; Attn: J. F. Banas, 4716  
 J. A. Leonard, 4717  
 B. W. Marshall, 4713; Attn: D. L. King  
 A. B. Maish, 4724  
 R. G. Kepler, 5810; Attn: L. A. Harrah, 5811  
 J. G. Curro, 5813  
 F. P. Gerstle, 5814  
 J. N. Sweet, 5824; Attn: R. B. Pettit and E. P. Roth  
 T. B. Cook, 8000; Attn: A. N. Blackwell, 8200  
 B. F. Murphey, 8300  
 C. S. Hoyle, 8122; Attn: V. D. Dunder  
 R. J. Gallagher, 8124; Attn: B. A. Meyer  
 D. M. Schuster, 8310; Attn: R. E. Stoltz, 8312, for M. D. Skibo  
 A. J. West, 8314  
 W. R. Even, 8315  
 R. L. Rinne, 8320  
 C. T. Yokomizo, 8326; Attn: L. D. Brandt  
 P. L. Mattern, 8342  
 L. Gutierrez, 8400; Attn: R. A. Baroody, 8410  
 D. E. Gregson, 8440  
 C. M. Tapp, 8460  
 C. S. Selvage, 8420  
 V. Burolla, 8424; Attn: C. B. Frost  
 R. C. Wayne, 8450  
 T. D. Brumleve, 8451  
 W. R. Delameter, 8451  
 P. J. Eicker, 8451 (5)  
 R. M. Houser, 8451  
 C. L. Mavis, 8451  
 W. L. Morehouse, 8451  
 H. F. Norris, Jr., 8451  
 W. S. Rorke, Jr., 8451  
 D. N. Tanner, 8451  
 S. S. White, 8451  
 A. C. Skinrod, 8452  
 W. G. Wilson, 8453  
 Publications Division, 8265/Technical Library Processes Division, 3141  
 Technical Library Processes Division, 3141 (2)  
 M. A. Pound, 8214, for Central Technical Files (3)